

# **Characterization of Upstream Regulators Controlling Light-Mediated Alternative Splicing During Photomorphogenesis**

## **Dissertation**

der Mathematisch-Naturwissenschaftlichen Fakultät  
der Eberhard Karls Universität Tübingen  
zur Erlangung des Grades eines  
Doktors der Naturwissenschaften  
(Dr. rer. nat.)

vorgelegt von  
Jennifer Saile  
aus Reutlingen

Tübingen  
2022

Gedruckt mit Genehmigung der Mathematisch-Naturwissenschaftlichen Fakultät der  
Eberhard Karls Universität Tübingen.

Tag der mündlichen Qualifikation:

04.10.2022

Dekan:

Prof. Dr. Thilo Stehle

1. Berichterstatter/-in:

Prof. Dr. Andreas Wachter

2. Berichterstatter/-in:

Prof. Dr. Klaus Harter

*Für meinen Opa*





## Danksagung

An erster Stelle möchte ich meinem Doktorvater, Prof. Dr. Andreas Wachter, danken. Lieber Andreas, vielen Dank, dass Du mich auf diese aufregende Reise mitgenommen und mir die Arbeit an diesem vielseitigen und großartigen Projekt ermöglicht hast. Besonders dankbar bin ich Dir für die gute Zusammenarbeit, Deine jahrelange Unterstützung, Dein Interesse an meiner Forschung und Dein Vertrauen, welches mir ermöglicht hat, meine eigenen Forschungsideen zu entwickeln und über mich hinauszuwachsen.

Ein großer Dank gilt außerdem Prof. Dr. Klaus Harter, der das Zweitgutachten übernimmt und zusammen mit Prof. Dr. Claudia Oecking mein TAC Komitee gebildet hat. Liebe Claudia, lieber Klaus, ich danke Euch herzlich, dass Ihr trotz der örtlichen Distanz immer Zeit für meine Anliegen gefunden habt. Ihr seid zwei wunderbare Wissenschaftler und ich habe unsere kritischen Diskussionen und Euren hilfreichen Input sehr geschätzt.

Ganz besonders danke ich meiner Vorgängerin, Dr. Theresa Wießner-Kroh, die mir durch Ihre herzliche Art den Einstieg in die Gruppe und das Projekt erleichtert hat. Liebe Theresa, vielen Dank für die exzellente Zusammenarbeit und Deine Freundschaft. Wir waren ein unschlagbares Team, egal ob im Labor oder auf Konferenzen – gemeinsam haben wir alles geschafft. Ich danke Dir für diese unvergessliche Zeit.

Ein ganz großes Dankeschön an meine lieben Studenten, die mich während meiner Promotion begleitet haben: Moritz Denecke, Katarina Erbstein und Laura Schütz. Ihr Lieben, vielen Dank für Eure großartige Unterstützung, ohne die ein Teil meiner Arbeit nicht möglich gewesen wäre. Es hat mir eine sehr große Freude bereitet mit Euch zusammenzuarbeiten und mein Wissen an Euch weiterzugeben. Gleichzeitig habe ich aber auch sehr viel von Euch gelernt.

Lieber Moritz, ich danke Dir von ganzem Herzen, dass Du so viel Arbeit und Zeit in mein PhD Projekt gesteckt hast. Besonders in den letzten Monaten warst Du eine sehr große Hilfe und hast während meiner Schreibphase die Stellung gehalten und dadurch meine Projekte weiter vorgebracht – Danke dafür! Außerdem bist Du ein sehr angenehmer lab mate, ein super DJ und ein ausgezeichneter Barkeeper.

Liebe Katarina, ich bin Dir sehr dankbar, dass wir zusammen das Kinasen Projekt voranbringen konnten und gleichzeitig durch unsere schönen Frühstückspausen und Gesangseinlagen eine super schöne Zeit im Lab hatten. Danke, dass Du mir die besten Cafés in Mainz und Umgebung gezeigt hast. Tack för din vänskap.

Liebe Laura, vielen Dank, dass Du mit Deiner positiven Art in jeden meiner rainy days ganz viel sunshine gebracht hast. Vor allem im Endspurt meiner Doktorarbeit hast Du mich mit Deiner unfassbaren Produktivität und Zuverlässigkeit auf die Zielgerade gebracht. Danke!

Ganz besonders danke ich auch Cornelia Braun für die gute Zusammenarbeit. Liebe Conny, danke, dass Du mich zum Lachen bringst, mir durch unsere Schokoladen-Pausen viel Energie gibst, immer ein offenes Ohr für mich hast und auch immer eine Lösung für meine Probleme findest. Danke, dass Du unsere Bay komplett machst und zu einer angenehmen Arbeitsatmosphäre beiträgst.

Weiterhin möchte ich mich bei allen ehemaligen und aktuellen Wachter Lab members für die schöne Zeit in Tübingen und Mainz bedanken.

Ich danke auch dem SFB1101 für die finanzielle Unterstützung während meiner Promotion. Die wöchentlichen SFB talks, sowie die jährlichen SFB retreats in Heidelberg werden mir stets als bereichernd in Erinnerung bleiben.

Ein großer Dank gilt auch meinen Freunden, die zu vielen schönen und unvergesslichen Momenten in den letzten Jahren beigetragen haben. An dieser Stelle möchte ich mich auch bei meiner Koch-Crew bedanken, durch die jeder Mittwochabend zu einem vollen Genuss wurde.

Zu guter Letzt gilt mein größter Dank meiner Familie. Liebe Mama, lieber Papa, liebe Svenja, danke, dass Ihr mich immer unterstützt und an mich glaubt. Danke, dass Ihr mich aufmuntert, wenn ich einen schlechten Tag habe und motiviert weiterzumachen, wenn ich am liebsten aufgeben würde. Ohne Eure Unterstützung hätte ich das alles nicht geschafft. Danke Svenja, für unsere kritischen Diskussion zu jeder Tages- und Nachtzeit, Deinen Input und Deine Hilfe, die zum Gelingen dieser Arbeit beigetragen haben.

# Table of content

<b>List of abbreviations</b> .....	<b>I</b>
<b>Zusammenfassung</b> .....	<b>V</b>
<b>Summary</b> .....	<b>VII</b>
<b>Chapter I: Introduction</b> .....	<b>1</b>
Pre-mRNA splicing – A crucial mechanism controlling gene expression.....	2
Regulation of AS in response to light.....	6
Splicing regulators .....	8
Serine/arginine-rich (SR) proteins.....	8
Heterogenous nuclear ribonucleoproteins (hnRNPs) .....	12
Skoto- and photomorphogenesis .....	13
Dark and light signaling.....	13
Phytochrome signaling.....	14
Crosstalk between light- and hormone signaling .....	14
Master regulators of energy signaling.....	16
Sucrose-Non-Fermenting-Related Kinase-1 (SnRK1) .....	16
Target of Rapamycin (TOR).....	18
Aim of this work.....	20
References.....	22
<b>Chapter II: Draft manuscript 1</b> .....	<b>43</b>
Contributions .....	45
Abstract .....	46
Introduction .....	47
Results and Discussion .....	48
Methods.....	56
References.....	62
Main figures .....	68
Supplemental information .....	73

<b>Chapter III: Draft manuscript 2</b> .....	<b>94</b>
Contributions .....	95
Abstract .....	97
Introduction .....	98
Results .....	101
Light and sugar specifically induce phosphorylation of RS proteins .....	101
Generation of <i>rs</i> loss-of function mutants .....	101
Loss of all <i>RS</i> genes results in reduced fertility .....	102
Generation and characterization of <i>RS</i> OE lines .....	103
Light regulates transcript levels of <i>RS31</i> and <i>RS40</i> .....	104
RS41 and RS31 protein abundance is regulated by light .....	105
RS proteins act as positive regulators in red light signaling .....	106
Loss of <i>RRC1</i> enhances red light hyposensitivity in <i>rs</i> mutants.....	108
RS41 does not co-localize with phyB in <i>N. benthamiana</i> .....	109
<i>RS41</i> overexpression induces cotyledon opening in darkness .....	110
RS proteins play a positive role in light-induced cotyledon opening .....	111
Sucrose does not induce cotyledon opening in darkness.....	112
COP, PIFs and auxin are not the major players controlling <i>RS</i> -induced cotyledon opening .....	113
RS-induced cotyledon opening involves BR signaling .....	114
Inhibition of BR-signaling induces AS changes .....	115
RS proteins control alternative splicing in darkness.....	116
Overexpression of <i>RS41</i> affects <i>SR30</i> and <i>PPD2</i> splicing in darkness.....	118
Discussion .....	120
RS proteins are novel regulators of AS during the early seedling stage .....	120
Light affects <i>RS31</i> and <i>RS40</i> transcript abundance .....	123
Light affects RS31 and RS41 protein stability that might involve post-translational modifications .....	124

RS41 positively controls cotyledon opening that involves BR signaling.....	126
RS proteins are involved in reproductive development .....	128
Materials and Methods.....	130
References.....	137
Main figures .....	151
Supplemental information.....	159
<b>Chapter IV: Draft manuscript 3.....</b>	<b>211</b>
Contributions .....	212
Introduction .....	213
Results .....	214
RS proteins show a light-dependent localization in cotyledons .....	214
RS proteins localize in the nucleoplasm and nuclear speckles .....	215
RS-TbID <sub>NLS</sub> fusion proteins can biotinylate proteins in Arabidopsis seedlings..	216
Discussion .....	217
Material and Methods.....	219
References.....	222
Main figures .....	227
Supplemental information.....	232
<b>Chapter V: Conclusion and perspectives .....</b>	<b>239</b>
References.....	243

**List of abbreviations**

<b>A</b>	ABA	Abscisic acid
	amiR	Artificial micro-RNA
	AMP	Adenosine monophosphate
	AMPK	AMP-activated protein kinase
	AS	Alternative splicing
	ATP	Adenosine triphosphate
<b>B</b>	BES1	Brassinazole-resistant 2
	bHLH	Basic helix-loop-helix
	BL	Blue light
	bp	base pair
	BRs	Brassinosteroids
	BRZ	Brassinazole
	BZR1	Brassinazole-resistant 1
<b>C</b>	c	continuous
	Cds	Coding sequence
	Col-0	Columbia-0
	COP	Constitutive photomorphogenic
	CRISPR	Clustered regularly interspaced short palindromic repeats
	CRY	Cryptochrome
	CS	Constitutive splicing
<b>D</b>	DIN	Dark induced
	Dk	Dark
	DMSO	Dimethyl sulfoxide
	DNA	Deoxyribonucleic acid
<b>E</b>	EGFP	Enhanced green fluorescent protein
	ESEs	Exonic splicing enhancer
	ESS	Exonic splicing silencer
<b>F</b>	F	Forward
	FRL	Far-red light
<b>H</b>	HA	Human influenza hemagglutinin
	hnRNPs	Heterogeneous nuclear ribonucleoproteins

	HY5	Elongated hypocotyl 5
<b>I</b>	IAA	Indole-3-acetic acid
	i-amiR	inducible amiR
	IDRs	Intrinsically disordered regions
	ISE	Intronic splicing enhancer
	ISS	Intronic splicing silencer
<b>K</b>	kDa	Kilo Dalton
<b>L</b>	LLPS	Liquid liquid phase separation
	LST8	Lethal with Sec Thirteen 8
	LUC	Luciferase
<b>M</b>	Man	Mannitol
	MS	Murashige and Skoog
<b>N</b>	NLS	Nuclear localization signal
	NMD	Nonsense-mediated mRNA decay
<b>O</b>	OD	Optical density
	OE	Overexpression
<b>P</b>	PCR	Polymerase chain reaction
	PHOT	Phototropin
	PHY	Phytochrome
	PIF	Phytochrome interacting factor
	PL	Proximity labeling
	Pre-mRNA	Precursor messenger RNA
	PTB	Polypyrimidine tract-binding
	PTC	Premature termination codon
	PTT	Polypyrimidine tract
<b>Q</b>	qPCR	Quantitative PCR
<b>R</b>	R	Reverse
	RAPTOR	Regulatory-associated protein of TOR
	RL	Red light
	RNA	Ribonucleic acid
	RPS6	Ribosomal protein S6
	RRC1	Reduced red light responses in cry1 cry2 background 1
	RRM	RNA recognition motif

	rsQ <sub>c</sub>	CRISPR rs quadruple mutant
	rsT <sub>c</sub>	CRISPR rs triple mutant
	rsT <sub>t</sub>	T-DNA rs triple mutant
	RT-PCR	Reverse transcription-PCR
<b>S</b>	SAUR	Small auxin upregulated RNA
	SFPS	Splicing factor for phytochrome signaling
	sgRNA	Single guide RNA
	SNF1	Sucrose-non-fermenting 1
	SnRK1	SNF1-related protein kinase
	snRNA	Small nuclear RNA
	SPA	Suppressor of phytochrome A-105
	SR	Serine/Arginine
	SS	Splice site
	Suc	Sucrose
	SWAP1	Suppressor-of-white-apricot/surp RNA-binding domain-containing protein1
<b>T</b>	TbID	TurbID
	T-DNA	Transfer-DNA
	TF	Transcription factor
	TOR	Target of rapamycin
	TORC1	Tor complex1
	tRFP	Tag red fluorescent protein
<b>U</b>	uORF	Upstream open reading frame
	UTR	Untranslated region
	UV	Ultraviolet
<b>W</b>	WL	White light
	WT	Wildtype
<b>Y</b>	YFP	Yellow fluorescent protein





## Zusammenfassung

Es wird zunehmend erkannt, dass alternatives Spleißen (AS) eine Rolle bei der Pflanzenentwicklung, einschließlich der Photomorphogenese, spielt. Die Photomorphogenese geht mit einer massiven Umprogrammierung der Genexpression einher, die durch Veränderungen der Gesamttranskriptionsmenge, der Transkriptionsstartstelle, der Translationskontrolle und des AS erfolgt. Zuvor wurde gezeigt, dass die Zufuhr von externem Zucker und die Hemmung von Kinase-Signalwegen in dunkel gewachsenen *Arabidopsis thaliana* Keimlingen ähnliche AS-Änderungen hervorrufen, wie sie bei Belichtung beobachtet werden. Diese Ergebnisse deuten darauf hin, dass das lichtvermittelte AS mit Stoffwechsel- und Kinase-Signalen zusammenhängt. Um die vorgelagerten Regulationsmechanismen weiter zu entschlüsseln, analysierten wir zunächst die Rolle der beiden wichtigsten Energiesensorkinasen ‚SNF1-related kinase1‘ (SnRK1) und ‚target of rapamycin‘ (TOR) während der Skoto- und Photomorphogenese. Unter Verwendung induzierbarer künstlicher microRNAs fanden wir ähnliche AS-Veränderungen in etiolierten Keimlingen nach Ausschaltung von SnRK1 und TOR, wie sie als Reaktion auf Licht- oder Zuckerbehandlung beobachtet wurden. Darüber hinaus ergaben phänotypische Analysen, dass beide Kinase-Mutanten bei Dunkelheit verkürzte Hypokotyle aufweisen, aber auch eine verzögerte Keimblattöffnung während der Deetiolierung bei Licht zeigen. Diese Ergebnisse zeigen, dass sowohl SnRK1 als auch TOR für ein ordnungsgemäßes skoto- und photomorphogenetisches Wachstum unerlässlich sind.

Angesichts der Rolle von SnRK1 und TOR bei der lichtabhängigen AS-Regulierung schlugen wir vor, dass eine veränderte Kinase-Signalübertragung phosphorylierungsabhängige Veränderungen in der Aktivität von Spleißregulatoren und damit die AS-Reaktion auslösen könnte. Mithilfe der Phosphoproteomik identifizierten wir Spleißregulatoren aus der RS-Unterfamilie der Serin/Arginin-reichen (SR) Proteine, die bei Zucker- und Lichtbehandlung spezifisch phosphoryliert werden. Die RS-Unterfamilie ist spezifisch für Pflanzen und umfasst vier Mitglieder in *Arabidopsis*: RS31, RS31a, RS40 und RS41. Das Ausschalten aller vier *RS*-Gene führte zu fast vollständiger männlicher Sterilität, was darauf hindeutet, dass *RS*-Proteine für die Fortpflanzung unerlässlich sind. Darüber hinaus stellten wir fest, dass *RS*-Proteine für das skoto- und photomorphogenetische Wachstum von entscheidender Bedeutung sind, da sie die Hypokotyllänge und die Öffnung der Keimblätter kontrollieren. Wir konnten nachweisen, dass die *RS*-induzierte

Keimblattöffnung mit Brassinosteroid-Signalen zusammenhängt und fanden außerdem heraus, dass *rs* Mutanten eine veränderte Rotlichtempfindlichkeit aufweisen. Spleißmusteranalysen zeigten, dass RS-Proteine zur Regulierung der lichtvermittelten AS-Ereignisse in der Dunkelheit beitragen. Darüber hinaus konnten wir zeigen, dass RS-Proteine im Zellkern lokalisiert sind und als Reaktion auf Licht und Zucker aus dem Nukleoplasma in biomolekulare Kondensate re-lokalisieren.

Zusammengefasst bieten unsere Ergebnisse neue Einblicke in die Mechanismen und biologischen Funktionen von SnRK1-, TOR- und RS-Proteinen in der lichtabhängigen Pflanzenentwicklung.

## Summary

Alternative splicing (AS) is increasingly recognized to play a role in plant development, including photomorphogenesis. Photomorphogenesis is accompanied by massive reprogramming of gene expression via changes in total transcript levels, transcription start sites, translational control, and AS. Previously, it has been shown that external sugar supply and the inhibition of kinase signaling cause similar AS changes in dark grown *Arabidopsis thaliana* seedlings as observed upon illumination. These findings suggested that light-mediated AS involves metabolic and kinase signaling. To further dissect the upstream regulatory mechanisms, we first analyzed the role of the two major energy sensor kinases ‘SNF1-related kinase1’ (SnRK1) and ‘target of rapamycin’ (TOR) during skoto- and photomorphogenesis. Using inducible artificial microRNAs, we found similar AS changes in etiolated seedlings upon SnRK1 and TOR knockdown, as observed in response to light or sugar treatment. Furthermore, phenotypical analyses revealed that both kinase mutants display shortened hypocotyls in darkness, but also exhibit delayed cotyledon opening during de-etiolation in light. These findings demonstrate that both SnRK1 and TOR are indispensable for proper skoto- and photomorphogenic growth.

Given the role of SnRK1 and TOR in light-responsive AS regulation, we proposed that an altered kinase signaling might trigger phosphorylation-dependent changes in the activity of splicing regulators and hence, the AS response. Using phosphoproteomics, we identified splicing regulators from the RS subfamily of serine/arginine-rich (SR) proteins that are specifically phosphorylated upon sugar and light treatment. The RS subfamily is specific to plants and comprises four members in *Arabidopsis*: RS31, RS31a, RS40 and RS41. Knocking out all four *RS* genes resulted in almost complete male sterility, suggesting that RS proteins are essential for reproductive processes. In addition, we found that RS proteins are crucial for skoto- and photomorphogenic growth, as they control hypocotyl elongation and cotyledon opening. We could demonstrate that RS-induced cotyledon opening involves brassinosteroid signaling and further found that *rs* mutants display an altered red-light sensitivity. Splicing pattern studies revealed that RS proteins contribute to the regulation of light-mediated AS events in darkness. Furthermore, we showed that RS proteins localize to the nucleus and undergo a re-localization from the nucleoplasm into biomolecular condensates in response to light and sugar.

Together, our results provide novel insights into mechanisms and biological functions of SnRK1, TOR and RS proteins in light-dependent plant development.

## Chapter I: Introduction



## **Pre-mRNA splicing – A crucial mechanism controlling gene expression**

Precursor messenger ribonucleic acid (pre-mRNA) splicing is an important regulatory mechanism to control gene expression that occurs either co- or post-transcriptionally (Chaudhary, Khokhar et al., 2019; Reddy et al., 2013; Shukla & Oberdoerffer, 2012). It involves the removal of typically non-coding intervening regions (introns) from pre-mRNAs and the subsequent ligation of the exonic regions to produce mature mRNAs. Pre-mRNA splicing is catalysed by the spliceosome, a large RNA-protein machinery (Will & Lührmann, 2011). In eukaryotes, two types of spliceosomes are present, a major and a minor spliceosome (Will & Lührmann, 2011). The major spliceosome is required for the removal of U2-type introns, whereas the minor one is needed for releasing U12 introns (Patel et al., 2002; Will & Lührmann, 2005). Interestingly, only 0.5% of the eukaryotic introns are U12-type introns (Burge et al., 1998; Levine & Durbin, 2001) that are absent from some eukaryotes, such as *Drosophila* and yeast (Burge et al., 1998; Patel et al., 2002; Will & Lührmann, 2005).

The U2-dependent spliceosome is composed of five small nuclear ribonucleoprotein complexes (U1, U2, U4/U6, U5 snRNPs) (Koncz et al., 2012; Will & Lührmann, 2011; Zhou et al., 2002), whereas, the U12-dependent spliceosome is formed by the U11, U12, U5, and U4atac/U6atac snRNPs (Patel & Steitz, 2003). Each snRNP consists of one small nuclear RNA (snRNA) (or two in case of U4/U6), a heptameric protein ring of Sm proteins (or Sm-like (LSm) proteins in case of U6), and specific core proteins as well as additional splicing related proteins (Kastner et al., 2019).

Pre-mRNA splicing in eukaryotes is specified by core splicing signals that are conserved sequences defining introns. U2-type introns are flanked by the 5' splice site (SS) and the 3' SS that are characterized by GU or AG sequences, respectively (Reddy et al., 2013; Will & Lührmann, 2005). The branch point is another consensus sequence with a conserved adenine residue that is typically located 18 to 40 nucleotides upstream of the 3' SS, and followed by a polypyrimidine tract (PPT) in higher eukaryotes (Reddy et al., 2013; Will & Lührmann, 2005, 2011). The branch point is required for the nucleophilic attack on the 5' SS which is the first catalytic step of the splicing reaction (Kastner et al., 2019; Will & Lührmann, 2011). Apart from these core splice site motifs, there are additional features within the pre-mRNA that control splicing decisions: *Cis*-regulatory elements include exonic and intronic splicing enhancers (ESEs and ISEs) or silencers (ESSs and ISSs) (Chen & Manley, 2009;

Reddy et al., 2013). These sequences serve as binding sites for *trans*-acting factors such as serine/arginine-rich (SR) splicing regulators or heterogeneous nuclear ribonucleoproteins (hnRNPs) (Chen & Manley, 2009; Reddy et al., 2013). SR proteins are extensively recognized as positive *trans*-acting factors, recruiting U1 snRNP and U2 auxiliary factor (U2AF) to the 5' SS and 3' SS by binding to exonic and purine-rich sequences (Chen & Manley, 2009; Fu & Ares, 2014). However, other modes of action exist that depend either on the pre-mRNA binding site or the interaction with splicing-related proteins (Wachter et al., 2012).

In contrast, hnRNPs are often described as spliceosomal repressors by binding to splicing silencers (Fu & Ares, 2014; Wachter et al., 2012). A well-studied member of the hnRNP family is the polypyrimidine tract-binding protein (PTB) that functions in splicing regulation (Wachter et al., 2012). In plants it was shown that PTB proteins have a binding preference for pyrimidine-rich sequences that can be found between the intronic branch point and the 3' SS (Ruehl et al., 2012, Wachter et al., 2012). On the one hand, PTB proteins repress the splicing reaction by e.g., masking binding sites for spliceosomal proteins which interferes with the recognition of splice sites (Fu & Ares, 2014; Wachter et al., 2012). On the other hand, it was reported that PTB can reduce the binding of SRp30c in the *hnRNPA1* pre-mRNA in HeLa cells, demonstrating that PTB in some instances also functions as an anti-repressor by neutralizing the repressor activity of SRp30c (Paradis et al., 2007). Hence, repressing or activating functions of *trans*-acting factors depend on their binding position within the pre-mRNA and the suite of regulatory factors. Consequently, the interplay between these specific sequences and those regulatory proteins promotes or represses the assembly of spliceosomal complexes and thus, influences pre-mRNA splicing (Fu & Ares, 2014; Wachter et al., 2012; Wang & Burge, 2008).

In contrast to constitutive splicing (CS) where only specific splice sites are used to generate one major mRNA transcript, alternative splicing (AS) utilizes alternative splice sites within one pre-mRNA, thereby producing multiple mRNA isoforms from a single pre-mRNA (Figure 1) (Reddy, 2007). AS can lead to exon skipping or inclusion, the usage of alternative 5' and 3' SSs, or to intron retention (Reddy et al., 2013). In general, exon skipping events are the most frequent type in mammals (Sugnet et al., 2004), whereas intron retention events and the usage of alternative 3' SS are the most common types in plants (Hartmann et al., 2016; Marquez et al., 2012). A recent study



reported the contribution of non-intron retention events in environmental responses, indicating that other types of AS may take a major role in modulating gene expression (Martín et al., 2021).

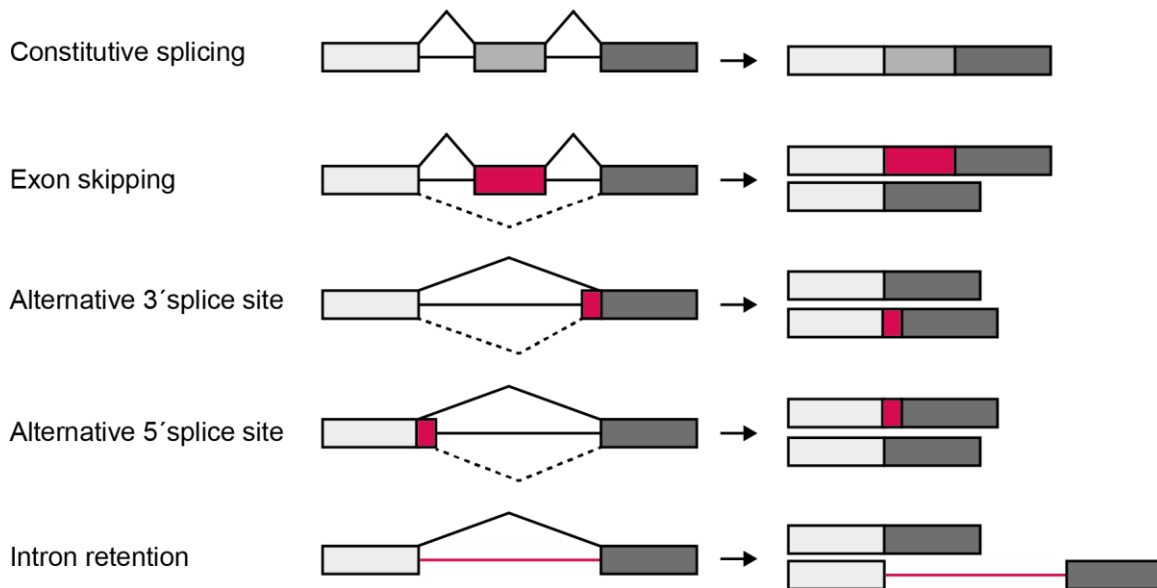


**Figure 1: Different types of (alternative) splicing events.** Pre-mRNAs are depicted with exons shown as boxes and introns as lines. Red coloured boxes indicate the alternative splicing event and solid and dashed lines show constitutive and alternative splice site choice, respectively. The figure is based on (Laloum et al., 2018).

In humans, 95% of all intron-containing genes are giving rise to AS variants (Pan et al., 2008) and defects in AS are associated with a wide range of human diseases (Jiang & Chen, 2020). Analyses of *Arabidopsis thaliana* plants grown under normal conditions revealed that at least 61% of intron-containing genes produce splice variants (Marquez et al. 2012). However, it is likely that different growth conditions, and also different developmental stages may further increase the known AS frequencies in plants (Martín et al., 2021; Staiger & Brown, 2013).

AS is a crucial mechanism to control gene expression (Nasif et al., 2018). On the one hand, AS can affect transcript abundance by producing unstable mRNA isoforms that are e.g. degraded via the RNA surveillance mechanism nonsense-mediated decay (NMD) (Drechsel et al., 2013; Kalyna et al., 2012). NMD recognizes aberrant mRNA isoforms that show different types on unusual translation termination, e.g. a premature termination codon (PTC) and hence, avoids the generation of truncated protein isoforms (Kurihara et al., 2009; Palusa & Reddy, 2010; Rebbapragada & Lykke-Andersen, 2009). In addition to PTCs, long 3'UTRs and introns within 3'UTRs as well

as upstream open reading frames (uORFs) are classical features of NMD (Lykke-Andersen & Jensen, 2015). Using a high-resolution RT-PCR system, Kalyna and co-workers predicted that around 13% of intron-containing genes in *Arabidopsis* are targeted by NMD (Kalyna et al., 2012). A genome-wide study confirmed these estimations (Drechsel et al., 2013). Remarkably, some transcripts containing retained introns or introns within long 3'UTRs, are, however, NMD-insensitive due to nuclear retention (Goehring et al., 2014; Hartmann et al., 2018).

On the other hand, AS can affect gene expression by generating different protein isoforms. However, the impact of AS on protein diversity in plants is largely unclear due to limited proteomic data (Chaudhary, Jabre et al., 2019). Recently, it was demonstrated that 35% of AS events in 10 d-old *Arabidopsis* seedlings and inflorescences are represented in polysome-associated mRNAs, suggesting that these isoforms can be translated into proteins (Yu et al., 2016). Truncated proteins derived from AS often act in a regulatory feedback loop to control the function and abundance of their full-length counterparts, thereby acting as a dominant negative inhibitor (Aprile et al., 2018; Seo et al., 2012). Intriguingly, exitrons (cryptic introns) are exon-like introns within protein-coding exons that were identified as a subgroup of retained introns. However, unlike transcripts exhibiting retained introns, isoforms harbouring retained exitrons are translated into protein isoforms with different protein features. Hence, exitrons contribute to proteome complexity by affecting protein domains and disordered regions as well as post-translational modification sites (Marquez et al., 2015; Yu et al., 2016). Thus, protein isoforms can differ in their activity, function and subcellular localization as well as in their stability (Reddy, 2004).

## Regulation of AS in response to light

Light is one of the most crucial factors that serves as an important energy source for plants and as a regulator of plant development, including photomorphogenesis (Kami et al., 2010). Strikingly, gene expression studies revealed that light induces massive transcriptome-wide reprogramming (Ma et al., 2001). In rice and *Arabidopsis*, 20% of all genes have been found to be differentially expressed in response to light (Jiao et al., 2005; Jiao et al., 2007).

Previous work demonstrated that changing light conditions also affects AS, suggesting a major role of AS in the regulation of light signaling (Hartmann et al., 2016; Mancini et al., 2016; Shikata et al., 2014; Wu et al., 2014). Early studies in pumpkins showed light-regulated AS of a hydroxypyruvate reductase and a peroxidase gene (Mano et al., 1997; Mano et al., 1999). More recently, several studies reported that light-regulated AS is dependent on red light photoreceptors in etiolated *Arabidopsis* seedlings (Shikata et al., 2014), *Arabidopsis* seeds (Soledad Tognacca et al., 2019) and *Physcomitrella patens* (Wu et al., 2014). Light-regulated AS affected a subset of genes encoding splicing regulators (Petrillo et al., 2014; Shikata et al., 2014; Shikata, Shibata et al., 2012; Soledad Tognacca et al., 2019), highlighting the complexity of AS regulation. The observation that light-regulated AS depends on phytochromes hints towards a major role of photoreceptors in light-triggered AS. However, contradictory findings reported that light-regulated AS in *Arabidopsis* is independent of photoreceptors, and rather involves chloroplast retrograde signaling which senses and communicates light signals to the nucleus (Hartmann et al., 2016; Mancini et al., 2016; Petrillo et al., 2014; Riegler et al., 2021). These contradictory findings can be attributed to the co-existence of separate signaling pathways in light-regulated AS.

Further connections between light signaling and AS was provided by the identification of RRC1 (reduced red-light responses in *cry1cry2* background1) (Shikata, Nakashima et al., 2012; Shikata, Shibata et al., 2012), SFPS (splicing factor for phytochrome signaling) (Xin et al., 2017; Xin et al., 2019) and SWAP1 (suppressor-of-white-apricot/surp RNA-binding domain-containing protein1) (Kathare et al., 2022). All three splicing regulators are involved in phytochrome signaling. The mutants *rrc1*, *sfps* and *swap1* show a reduced red light sensitivity and additionally, AS changes in many light- and circadian clock-related genes (Shikata et al., 2014; Shikata, Nakashima et al., 2012; Xin et al., 2017; Xin et al., 2019; Kathare et al., 2022).

To gain more insights into the upstream regulatory mechanisms of light-regulated AS, Hartmann et al. (2016) compared transcriptomes of etiolated *Arabidopsis* seedlings exposed to red, blue, and white light. AS patterns were changed in response to all three light qualities, with strongly overlapping patterns of AS changes under all three light conditions. This indicates that signaling does not depend on a particular light quality and photoreceptor type (Hartmann et al., 2016). Indeed, analysing the upstream signaling mechanism of light-regulated AS revealed that phytochromes and cryptochromes play only a minor role in white light-modulated AS changes. On the contrary, phytochromes are required for AS changes under far-red light, which is photosynthetically inactive (Hartmann et al., 2016). Moreover, Hartmann et al. (2016) revealed that sugar feeding triggers similar AS changes in etiolated *Arabidopsis* seedlings as induced by light exposure. Together, these observations suggest that photosynthesis-supporting light-regulated AS is mainly controlled by metabolic signaling, and not by photoreceptor signaling. Furthermore, the inhibition of kinase signaling caused similar AS changes as observed by light or sugar exposure, suggesting that kinase signaling contributes to the regulation of light-controlled AS (Hartmann et al., 2016).

Interestingly, Hartmann et al. also analysed the consequence of light-regulated AS: Approximately 80% of all splicing variants corresponding to light-regulated AS events contained NDM-triggering features and were relatively more abundant in dark than in light. Strikingly, 61% of the light-regulated AS events displayed a relative increase in the ratio of the presumably unproductive transcript produced in darkness to a protein-coding variant generated in light (Hartmann et al., 2016). Previous work demonstrated that the pre-mRNA encoding the splicing regulator SR30 undergoes light-regulated AS (Hartmann et al., 2016; Hartmann et al., 2018). The unproductive splicing variant *SR30.2* is mainly generated in darkness, whereas the protein coding isoform *SR30.1* is generated upon illumination. Although, *SR30.2* contains NMD triggering features, it is mainly kept in the nucleus and hence, escapes from NMD (Hartmann et al., 2018).

To date, the exact mechanism controlling light-regulated AS remains largely elusive. However, several reports suggested that different pathways might co-exist. Just recently, it was revealed that the splicing regulators RRC1, SFPS and SWAP1 as well as the kinase TOR (target of rapamycin) control light-regulated AS in *Arabidopsis* seedlings (Kathare et al., 2022; Xin et al., 2017; Xin et al., 2019) and roots (Riegler et

al., 2021), respectively. Identifying additional upstream regulators might help to shed more light on the molecular mechanism of AS regulation during photomorphogenesis.

## **Splicing regulators**

### **Serine/arginine-rich (SR) proteins**







#### Identification and characterization of SR proteins

Serine/arginine-rich (SR) proteins are a highly conserved family of RNA binding proteins (RBPs), involved in constitutive and alternative pre-mRNA splicing (Palusa & Reddy, 2010; Reddy, 2004). SR proteins were first identified in metazoans (Ge et al., 1991; Krainer et al., 1991) and later also detected in plants using the human mAb104 antibody, raised against the phosphoserine epitope of SR proteins (Lazar et al., 1995). First studies demonstrated that plant SR proteins can affect splice site selection in nuclear HeLa extracts (Lazar et al., 1995) and complemented a SR-deficient HeLa cell cytosolic extract (S100) to catalyse the splicing reaction (Lopato, Mayeda et al., 1996; Lopato, Waigmann et al., 1996). All these observations suggested that these proteins are evolutionary conserved (Reddy & Shad Ali, 2011).

SR proteins have a distinct domain structure, characterized by one or two RNA recognition motifs (RRMs) at the N-terminus, with a conserved SWQDLKD sequence in the second RRM, and a C-terminal arginine/serine-rich (RS) or serine/arginine-rich (SR) domain (Barta et al., 2010). The RRM can recognize and bind to specific sequences within the pre-mRNA that can either enhance or suppress splicing. SR proteins were previously identified to bind to AG-rich motifs that were described to function as splicing enhancer sequences (Fairbrother et al., 2002; Thomas et al., 2012; Yan et al., 2017). In contrast, the RS domain is important for protein-protein interactions and hence, allows the recruitment and interaction with other spliceosomal proteins (Reddy and Shad Ali 2011). As several SR proteins have been identified to interact with the U1 core component U1-70K as well as the U2 auxiliary factor U2AF, it is proposed that SR proteins recruit the U1 snRNP to the 5' SS and the U2AF to the 3' SS, respectively (Golovkin & Reddy, 1998, 1999; Lorković et al., 2004; Yan et al., 2017). Furthermore, the RS domain contains localization signals that are essential for the nuclear or nucleocytoplasmic shuttling of SR proteins (Cazalla et al., 2002; Mori et al., 2012; Reddy & Shad Ali, 2011; Tillemans et al., 2005; Tillemans et al., 2006).

The number of SR proteins varies greatly between different organisms. Plants encode almost twice as many as humans (12 SR proteins), due to whole genome duplications (Kalyna & Barta, 2004). Therefore, 18 and 22 SR proteins were identified in *Arabidopsis* and the crop plant *Oryza sativa*, respectively (Barta et al., 2010). However, during the last years, SR proteins were also found and characterized in early land and crop plants. For instance *Chlamydomonas reinhardtii* encodes 9 SR proteins (Bowman et al., 2017), and 9 were also found in *Chara braunii* (Nishiyama et al., 2018), whereas 6 were identified in *Marchantia polymorpha* (Bowman et al., 2017), 16 in *Physcomitrella patens* (Melo et al., 2020) and 17 in *Solanum lycopersicum* (Rosenkranz et al., 2021).

Plant SR proteins can be grouped into 6 subfamilies (Figure 2): SR (ASF/SF2-like: SR30, SR34, SR34a and SR34b), RSZ (9G8-like: RSZ21, RSZ22, RSZ22a), SC (ortholog of SC35: SC35), SCL (SC35-like: SCL28, SCL30, SCL30a and SCL33), RS2Z (RS2Z32 and RS2Z33), and RS (RS31, RS31a, RS40 and RS41). The latter three subfamilies exhibit unique features and are specific to plants (Barta et al., 2010).

Subfamily	Domain structure	<i>Arabidopsis thaliana</i> proteins
SR		At-SR30, At-SR34, At-SR34a, At-SR34b
RSZ		At-RSZ21, At-RSZ22, At-RSZ22a
SC		At-SC35
SCL		At-SCL28, At-SCL30, At-SCL30a, At-SCL33
RS2Z		At-RS2Z32, At-RS2Z33
RS		At-RS31, At-RS31a, At-RS40, At-RS41

**Figure 2: Domain structures of SR proteins and corresponding *Arabidopsis* proteins.** SR proteins harbor one or two RNA recognition motifs (RRMs). Furthermore, all SR proteins are characterized by a C-terminal SR or RS domain, consisting of either SR or RS dipeptides. RSZ and RS2Z proteins additionally contain a zinc binding domain (Zn) and RS2Z further possesses a serine-proline (SP)-rich extended region at the C-terminus. On the contrary, SCL proteins contain a N-terminal arginine, proline, serin, glycine, tyrosine-rich extension. The SCL, RS2Z and RS subfamilies are specific to plants. This figure is based on Melo et al., 2020.

### *SR* genes are targets of AS and regulators of plant development

Most of the *SR* genes show overlapping expression patterns and interestingly, undergo AS themselves. In *Arabidopsis*, 13 *SR* genes produce in total 75 splicing variants, including 53 PTC-containing isoforms (Palusa et al., 2007; Palusa & Reddy, 2010). Studies using the *upf3* mutant revealed that about half the PTC-containing *SR* mRNA isoforms accumulated in the NMD mutant. These results suggest that AS of *SR* genes is coupled to NMD, which affects *SR* protein abundance and hence, the regulation of several genes (Palusa et al., 2007; Palusa & Reddy, 2010). In this regard it was shown that some *SR* proteins undergo autoregulation, providing powerful means to control gene expression (Hartmann et al., 2018; Kalyna et al., 2003; Thomas et al., 2012). Furthermore, AS of different *SR* genes was reported to be controlled in a developmental and tissue-specific manner. Moreover, abiotic stress conditions including cold and heat significantly alter AS of almost all *SR* genes, except of *RSZ21*, *RSZ22*, *RSZ22a* and *SCL28* (Palusa et al., 2007). On the contrary, the hormones ABA and IAA affect the AS pattern of only three *SR* genes (*SR34*, *SR34b* and *SCL33*) (Palusa et al., 2007).

*SR* proteins have been assigned to be regulators of plant development. This is probably caused by the mis-splicing of a variety of *SR* genes that cross-regulate each other and further regulate downstream targets. Overexpression of *SR30* changed AS of its own pre-mRNA and additionally, of *RS31* and *SR34* (Lopato et al., 1999). These splicing abnormalities were accompanied with a delayed flowering and larger flowers as well as rosette leaves in transgenic plants (Lopato et al., 1999). Similar studies overexpressing *RSZ33* revealed altered splicing patterns of *SR30* and *SR34* and its own pre-mRNA (Kalyna et al., 2003). Associated with splicing changes, *RSZ33* OE lines showed also changes in plant morphology and development, including shorter but thicker hypocotyls and also thicker cotyledons as well as root hairs and trichomes with more branching (Kalyna et al., 2003). These phenotypes are caused by altered cell expansion and cell shape (Kalyna et al., 2003).

Studies analysing the loss-of-function mutant *sr45* (the *SR*-related protein *SR45* is according to the current nomenclature no longer included in the *SR* family due to an atypical domain structure) showed different splicing pattern of *SR30*, *RS31*, *RS31a*, *SR34*, and *SR34b*, and displayed a delayed flowering phenotype, with elongated and curly leaves and an altered number of petals and stamens, as well as reduced root

growth (Ali et al. 2007). A recent study used the CRISPR/Cas9 technology to knockout several SR subfamilies (Yan et al., 2017). Knocking out SC35 and SC35-like proteins caused morphological abnormalities, such as serrated leaves, delayed flowering, shortened roots and abnormal siliques phyllotaxy (Yan et al., 2017). All these examples indicate that there might be a cross-regulation between different SR proteins, that (co)-regulate downstream targets involved in e.g., plant growth and development. However, overall, the functions of plant SR proteins and their targets remain only poorly understood.

#### Post-translational modifications of SR proteins

SR proteins get post-translationally modified by acetylation, methylation and phosphorylation (Zhou & Fu, 2013). SR protein phosphorylation was studied most by using MS-based phosphoproteomic approaches (van Fuente Bentem et al., 2006; van Fuente Bentem et al., 2008). RS domains of SR proteins are reversibly and extensively phosphorylated by two major kinases, referred to as SRPK (SR-specific protein kinase) (Gui et al., 1994) and Cdc-2 like kinase (cyclin-dependent like kinase or also known as LAMMER-type kinase) family (Colwill et al., 1996), (Jeong, 2017). Recent studies revealed that MAPKs (mitogen-activated protein kinases) (Feilner et al., 2005), as well as SnRK2 (Wang et al., 2013) can also phosphorylate SR proteins, providing a link between stresses and the regulation of splicing. Phosphorylation was identified to alter protein stability, function and localization (Zhou & Fu, 2013). In this context, *SR45* was identified to undergo AS, resulting in the generation of two protein-coding isoforms with distinct roles in plant development (Zhang & Mount, 2009). Remarkably, the two isoforms differ by an eight amino acid insertion, harbouring two specific phosphorylation sites. Using phospho-mutants it was revealed that these two phosphorylation sites are critical for the isoform-specific functions in plant development (Zhang & Mount, 2009). Phosphoproteome analyses also identified a specific phosphorylation site in RS41 isoforms that only differ in the presence/absence of one serine (van Fuente Bentem et al., 2006). These findings suggest functional differences between several variants.

Phosphorylation is also linked to protein localization. SR proteins localize to the nucleus, where they are diffusely distributed within the nucleoplasm or aggregated in nuclear speckles (Lorković et al., 2004). Some SR proteins also shuttle between the nucleus and the cytoplasm (Mori et al., 2012; Tillemans et al., 2005; Tillemans et al.,



2006). Several studies reported a redistribution of SR proteins in the response to changing temperatures (cold, heat shock) (Ali et al., 2003; Docquier et al., 2004). This redistribution was shown to be phosphorylation dependent, as treatments with phosphatase or kinase inhibitors affected SR localization accordingly (Ali et al., 2003; Docquier et al., 2004; Mori et al., 2012; Rausin et al., 2010; Tillemans et al., 2005; Tillemans et al., 2006).

Taken together, SR proteins can be extensively post-translationally modified that impacts their activity as well as subcellular localization. Whether SR proteins are also post-translationally modified in response to light remains elusive.

### **Heterogenous nuclear ribonucleoproteins (hnRNPs)**

hnRNPs are multifunctional proteins, controlling mRNA splicing, stability, and transport (Han et al., 2010; Martinez-Contreras et al., 2007). hnRNPs are composed of several domains, including an RRM or the quasi-RRM, a glycine-rich auxiliary domain comprising an RGG box and a KH domain that are required for the interaction with RNAs and proteins, respectively (Wachter et al., 2012). As hnRNPs bind to splicing silencers, they can act as antagonistic counterpart to SR proteins (Wachter et al., 2012). One of the best studied hnRNP are PTB (polypyrimidine tract-binding) proteins that are localized to the nucleus, cytosol and P-bodies in plants (Stauffer et al., 2010). Arabidopsis encodes three PTB proteins (PTB1, PTB2 and PTB3), of which PTB1 and PTB2 are subjected to auto- and cross-regulation via AS-coupled NMD (Stauffer et al., 2010). A transcriptome-wide RNA-seq study revealed that Arabidopsis PTB1 and PTB2 have specific but also redundant functions and regulate the AS of genes involved in e.g., seed germination and flowering (Ruehl et al., 2012).

## Skoto- and photomorphogenesis

### Dark and light signaling

Emerging seedlings grow heterotrophically in darkness, by mobilizing seed storage reserves (e.g., oil, carbohydrates) that fuel plant growth (Gommers & Monte, 2018). Etiolated seedlings aim at rapidly reaching the soil surface which allows switching to a photoautotrophic lifestyle by using photosynthesis. Therefore, etiolated seedlings induce hypocotyl elongation during skotomorphogenesis. Furthermore, skotomorphogenic growth is characterized by a closed apical hook that protects the shoot apical meristem during the emergence through the soil, and tiny closed cotyledons that contain etioplasts (Gommers & Monte, 2018; Seluzicki et al., 2017). Following the perception of the first light signals, seedlings rapidly switch to photomorphogenic growth that is accompanied by a reduction of hypocotyl elongation, opening of the apical hook, and greening and expansion of cotyledons as well as induced root development (Gommers & Monte, 2018). Since plants encode several photoreceptors, they are able to sense a broad spectrum of light (280 – 750 nm) (Briggs & Olney, 2001; Galvão & Fankhauser, 2015; Lariguet & Dunand, 2005). Phytochromes (phyA-phyE in *Arabidopsis*) are required for red and far-red light perception, whereas cryptochromes (cry1, cry2), phototropins (phot1, phot2) and members of the Zeitlupe family (ztl (zeitlupe), fkf1 (flavin-binding, kelch-repeat, f-box), and lkp2 (lov kelch protein2)) sense blue/UV-A light. In contrast, UV-B light is perceived by the UVR8 (UV resistance locus 8) photoreceptor (Briggs & Olney, 2001; Galvão & Fankhauser, 2015; Lariguet & Dunand, 2005; Paik & Huq, 2019; Rizzini et al., 2011).

Skoto- and photomorphogenesis are controlled by several key regulators, including PIFs (phytochrome interacting factors), COP1/SPA (constitutive photomorphogenic 1/suppressor of phytochrome A-105) and HY5 (elongated hypocotyl5) (Galvão & Fankhauser, 2015; Hoecker, 2017; Paik & Huq, 2019). In darkness, the PIF bHLH transcription factors (TFs) function as repressors of de-etiolation. PIF proteins as well as the E3 ubiquitin ligase complex COP1/SPA trigger the degradation of photomorphogenesis promoting factors by the 26S proteasome. Accordingly, *pifQ* quadruple (*pif1*, *pif3*, *pif4*, *pif5*) (Leivar et al., 2008) as well as *cop1* (Deng & Quail, 1992) and the *spa4* quadruple (*spa1*, *spa2*, *spa3*, *spa4*) mutants (Laubinger et al., 2004) exhibit strong constitutive photomorphogenic phenotypes and hence, resemble light grown seedlings.

Upon illumination, the COP1/SPA complex and PIFs are inhibited or degraded, respectively, which results in the stabilization of positive regulators of photomorphogenic growth, including HY5, LAF1 (long after far-red light1) and HFR1 (long hypocotyl in far-red1). Consequently, this results in the induction of gene expression that controls light-dependent development (Galvão & Fankhauser, 2015; Legris et al., 2019). Consistent with the promoting role of HY5 during photomorphogenesis, the *hy5* mutant exhibit severely elongated hypocotyl in light (Oyama et al., 1997).

### **Phytochrome signaling**

PhyA and phyB are the major red light photoreceptors in plants that are present in two forms, the inactive Pr and the active Pfr form. Upon red light illumination, Pr is converted into Pfr and transformed back by far-red light or prolonged darkness (Galvão & Fankhauser, 2015; Klose, Venezia et al., 2015; Legris et al., 2019). The Pr form localizes in the cytosol, however, upon red light exposure Pfr rapidly re-localizes into the nucleus. It is striking that phytochromes do not contain an NLS, suggesting that their translocation to the nucleus requires additional proteins. Indeed, it was shown that phyA uses FHY1 (far-red elongated hypocotyl1) and FHL (FHY1-like) for the nuclear import (Klose, Viczián et al., 2015). Nuclear localized Pfr interacts with PIF proteins. Pfr-PIF interaction was demonstrated to inhibit the DNA-binding capability of several PIF proteins (PIF1, PIF3, PIF4) and to trigger their phosphorylation that can result in ubiquitination and proteasomal degradation (Legris et al., 2019). Furthermore, Pfr of phyA and phyB inhibits COP1/SPA complex formation, resulting in the accumulation of its target HY5 and hence, photomorphogenic development (Sheerin et al., 2015).

### **Crosstalk between light- and hormone signaling**

Plant development during skoto- and photomorphogenesis involves the interplay between hormones and light. Brassinosteroids and gibberellins were identified to promote skotomorphogenesis, whereas cytokine, jasmonic acid and ethylene induce photomorphogenic growth (Kusnetsov et al., 2020).

As light- and hormone signaling result in many similar downstream processes, it was proposed that both signaling pathways might converge at components upstream of the final responses. Indeed, previous studies reported several key components to be

involved in light and hormone signaling suggesting that these factors could mechanistically link light- and hormone signaling pathways.

#### Brassinosteroids (BRs)

BRs are key regulators of skotomorphogenesis, as demonstrated by a de-etiolated phenotype of the BR biosynthesis mutant *det2* (*de-etiolated 2*) (Chory et al., 1991) and the BR signaling mutants *bri1* (*BR-insensitive 1*) (Clouse et al., 1996) and *bin2* (*BR-insensitive 2*) (Li & Nam, 2002) in darkness. Previous studies reported a major role of BRs in hypocotyl elongation. Under dark conditions, the TF BZR1 (Brassinazole-resistant 1) is present in its dephosphorylated and active form, where it is stabilized by COP1, thereby promoting BR signaling (Kim et al., 2014). Dephosphorylated BZR1 can interact with PIF4 to co-regulate gene expression of common genes, that are required for cell elongation during etiolation (Li & He, 2016; Oh et al., 2012). Furthermore, BRs were linked to cotyledon closure in darkness which also involves HY5 (Li & He, 2016; Wang et al., 2012). HY5 can interact with de-BZR1, resulting in its sequestration and hence, reduced expression of cotyledon closure genes (Li & He, 2016).

#### Auxin

Auxin plays a major role in apical hook formation and hypocotyl elongation, as demonstrated by the lack of an apical hook and shortened hypocotyls in auxin response mutants, such as *axr1* (*auxin resistant 1*) (Lehman et al., 1996; Lincoln et al., 1990). Apical hook formation is caused by asymmetrical distribution of auxin that triggers differential division and expansion of cells at the apical part of the hypocotyl. Upon illumination, auxin levels decline, and the apical hook opens up. Apart from auxin, ethylene and gibberellins also participate in the formation and maintenance of the apical hook (Abbas et al., 2013).

Recently, auxin has been linked to cotyledon opening, thereby involving *SAUR* (*small auxin upregulated RNA*) genes (Dong et al., 2019). The expression of *SAUR* genes is light-dependent and organ-specific (Sun et al., 2016). In darkness, *SAUR* expression is repressed in cotyledons through the binding of PIF3 to their promoter regions. In contrast, high auxin levels in the hypocotyl induce *SAUR* expression, followed by hypocotyl elongation in darkness (Dong et al., 2019). Illumination triggers PIF degradation and a decline of the auxin level in hypocotyls. Subsequently, hypocotyl elongation slows down, whereas TCP4 (teosinte branched1/cycloidea/proliferating cell

factor4) binding to *SAUR* promoters induces their expression and hence, cotyledon opening (Dong et al., 2019).

Altogether, these are some examples of light and hormone signal integration that regulates plant growth and development during skoto- and photomorphogenesis. However, future research is expected to uncover additional regulators that couple light and hormone cascades.

### **Master regulators of energy signaling**

Under diurnal conditions, photosynthesis typically produces an excess of energy-rich carbohydrates during the day, which are then reutilized for metabolism and growth during the night. The resulting sugars are distributed within the plant and can be broken down, e.g., to release energy through respiration. Apart from the role of sugar as energy source, it was also described that sucrose functions as signaling molecule (Wind et al., 2010).

As carbohydrates affect plant growth and development, it is of utmost importance that plants sense and integrate different signals in order to maintain the cellular homeostasis. To do so, plants have evolved two master regulators of energy signaling: Sucrose-non-fermenting-related kinase-1 (SnRK1) and target of rapamycin (TOR) (Rodriguez et al., 2019; Sheen, 2014). SnRK1 gets activated under low-energy and low-nutrient conditions and activates catabolic pathways to generate ATP, paralleled by the repression of anabolic processes to prevent energy consumption (Hardie, 2007; Sheen, 2014). In contrast to SnRK1, TOR is activated under favourable and nutrient-rich conditions, and promotes anabolic processes, including protein synthesis and cell proliferation (Rodriguez et al., 2019; Sheen, 2014).

#### **Sucrose-Non-Fermenting-Related Kinase-1 (SnRK1)**

SnRK1 is a conserved serine/threonine kinase that possesses a high sequence identity to its yeast and mammalian orthologs, SNF1 (sucrose-non-fermenting 1) and AMPK (AMP-activated protein kinase), respectively (Crozet et al., 2014). Arabidopsis SnRK1 encodes three catalytic  $\alpha$  subunits: SnRK1.1 (KIN10), SnRK1.2 (KIN11) and SnRK1.3 (KIN12) (Baena-González et al., 2007), where SnRK1.1 and SnRK1.2 were identified to complement the yeast *snf1* mutant (Alderson et al., 1991). *SnRK1.1* and *SnRK1.2* are ubiquitously expressed (Schmid et al., 2005), and a double knockout is lethal

(Baena-González et al., 2007), whereas *SnRK1.3* displays a very low expression and is only detected in pollen and seeds (Broeckx et al., 2016; Schmid et al., 2005).

Apart from the catalytic  $\alpha$  subunits, plants possess two regulatory subunits, a  $\beta$  and a plant specific  $\beta\gamma$  subunit, that form together with the  $\alpha$  subunit a heterotrimeric complex (Emanuelle et al., 2015). Under energy-consuming conditions, the catalytic  $\alpha$  subunit SnRK1.1 translocates into the nucleus, where it induces target gene expression (Ramon et al., 2019). On the contrary, the myristoylated  $\beta$  subunit can restrict SnRK1.1 translocation into the nucleus and hence, the induction of the target gene expression. The inhibitory effect of the  $\beta$  subunit is, however, abolished by the  $\beta\gamma$  subunit (Ramon et al., 2019).

Under starvation conditions, SnRK1 aims at downregulating energy-consuming processes, while energy-producing pathways are upregulated. Using transcriptome-wide studies it was demonstrated that SnRK1 causes massive transcriptional changes in protoplasts, adult plants and during seedling establishment (Baena-González et al., 2007; Henninger et al., 2022; Pedrotti et al., 2018). SnRK1 functions by either directly phosphorylating key enzymes involved in nitrogen, carbon or fatty acid metabolism or by regulating TFs to induce transcriptional reprogramming (Nukarinen et al., 2016; Wurzinger et al., 2018). Mair et al. identified bZIP63 as first TF that gets phosphorylated by SnRK1 under energy deprivation, resulting in bZIP63 homo- and heterodimerization and hence, transcriptional reprogramming of metabolism (Mair et al., 2015). Altered phosphorylation of bZIP63 was independently confirmed using phosphoproteomics in a *snrk1.1 snrk1.2* double mutant (Nukarinen et al., 2016). Moreover, SnRK1.1 phosphorylates the TF Wrinkled1 (WRI1) that is a master regulator of fatty acid biosynthesis (Zhai et al., 2017). SnRK1.1 induced phosphorylation of WRI1 triggers its proteasomal degradation which results in a reduced glycolysis and lipid biosynthesis (Zhai et al., 2017). These findings show that SnRK1 represses anabolic processes in order to maintain cellular homeostasis.

To date, little is known about the mechanism that regulates SnRK1 activity in plants. Studies in mammals and yeast reported that SnRK1 activation requires the phosphorylation of a conserved threonine residue in the T-loop of the catalytic  $\alpha$  subunit (McCartney & Schmidt, 2001; Stein et al., 2000). However, in plants SnRK1 activity seems not to correlate with this phosphorylation which is why the *DARK INDUCED6 (DIN6)* transcript is commonly used to monitor SnRK1.1 and SnRK1.2

activity *in planta* (Baena-González et al., 2007). Apart from phosphorylation, active SnRK1 triggers its own SUMOylation and ubiquitination which results in its proteasomal degradation (Crozet et al., 2016). This negative feedback loop is important to diminish SnRK1 signaling and hence, to avoid a persistent activation of stress responses.

Studies in *Arabidopsis* revealed that SnRK1.1 and SnRK1.2 affect plant growth, flowering and senescence, suggesting that SnRK1 functions in vegetative and reproductive growth (Baena-González et al., 2007; Ramon et al., 2019). A recent study reported a role of SnRK1 in seedling establishment and the mobilization of seed storage compounds in *Arabidopsis* under day/night regime (Henninger et al., 2022). Whether SnRK1 plays a role in skoto- and photomorphogenesis, as well as the regulation of splicing, remains to be determined.

### **Target of Rapamycin (TOR)**

TOR is a serine/threonine kinase that belongs to the phosphoinositide 3-kinase (PI3K)-related kinase family (Mahfouz et al., 2006; Menand et al., 2002; Wullschleger et al., 2006). Back in 1991 TOR was first identified in *Saccharomyces cerevisiae* through a genetic mutant screen of rapamycin resistant yeast cells (Heitman et al., 1991) and later also in mammals (Sabatini et al., 1994) and plants (Menand et al., 2002). In contrast to the other eukaryotes, plants contain only one TOR complex (TORC1) that consists of TOR, and the subunits RAPTOR (Regulatory-Associated Protein of TOR) and LST8 (Lethal with Sec Thirteen 8 protein) (Dobrenel et al., 2016). TOR is expressed in the endosperm, embryo and primary meristem of *Arabidopsis* plants (Menand et al., 2002). Studies in *Arabidopsis* identified *tor* null mutants to be embryo lethal, probably as TOR affects cell division and growth rates in embryos (Menand et al., 2002; Ren et al., 2011). To overcome embryo lethality, several groups generated inducible *tor* knockdown lines (Caldana et al., 2013; Deprost et al., 2007). *tor* knockdown mutants are characterized by a reduced growth of leaves and roots, caused by smaller cells, as well as early senescence (Caldana et al., 2013; Deprost et al., 2007). On the contrary, plants overexpressing *TOR* exhibit enhanced shoot and root growth, caused by increased cell size, and delayed senescence (Deprost et al., 2007; Ren et al., 2011). Metabolic and transcriptomic analyses in *tor* and *lst8* mutants revealed a crucial role of both proteins in the regulation of amino acid accumulation and secondary metabolism (Caldana et al., 2013; Moreau et al., 2012; Xiong et al.,

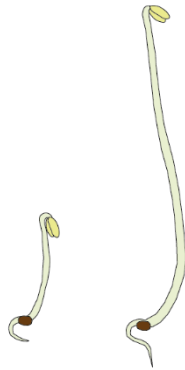
2013). The altered metabolism is caused by the inhibition of anabolic activities, paralleled by the upregulation of catabolic processes in *tor* mutants.

TOR was found to be activated by photosynthesis-derived glucose and induces then the phosphorylation of key substrates including S6K1 and S6K2 (Mahfouz et al., 2006; Xiong & Sheen, 2012). Corresponding phosphorylated versions of S6K are commonly used to monitor TOR activity (Xiong & Sheen, 2012). S6K proteins target RPS6 (Ribosomal Protein S6) and trigger the phosphorylation-induced activation of RPS6 that regulates protein synthesis (Mahfouz et al., 2006). Recently it was reported that light activates the TOR-RPS6 pathway which enhances protein synthesis in de-etiolated *Arabidopsis* seedlings (Chen et al., 2018). Hence, TOR plays an important role during photomorphogenesis (Chen et al., 2018; Pfeiffer et al., 2016). TOR was also linked to skotomorphogenic growth by the interaction with EIN2 (ethylene-insensitive protein 2). EIN2 suppresses hypocotyl elongation, however, glucose activated TOR induces EIN2 phosphorylation which prevents its nuclear localization and downstream signaling in dark grown *Arabidopsis* seedlings. As a consequence, hypocotyl elongation is promoted (Fu et al., 2021). Just recently, TOR was found to participate in light-and sugar-controlled AS in *Arabidopsis* roots under light/dark transitions (Riegler et al., 2021). However, whether TOR plays a role light- and sugar-controlled AS in etiolated *Arabidopsis* seedlings remains elusive.

Previous studies showed that TOR and RAPTOR interact with SnRK1.1, which is crucial for the inhibition of TOR under suboptimal conditions (Belda-Palazon et al., 2020; Nukarinen et al., 2016; van Leene et al., 2019). However, under favourable conditions, SnRK1 gets sequestered by SnRK2, which induces TOR activity and hence, growth (Belda-Palazon et al., 2020). Interestingly, Ling et al. found that mTORC1 inhibits AMPK through a direct phosphorylation of its catalytic subunit during starvation (Ling et al., 2020). Whether a similar regulatory mechanism exist in plants needs to be determined.



## Aim of this work



Photomorphogenesis is accompanied by alternative splicing (AS) changes, which can contribute to the rapid adaptation of plants to changing environmental conditions. Previous studies have shown that light-mediated AS in etiolated *Arabidopsis* seedlings involves metabolic and kinase signaling, but little is known about the upstream regulators involved in these processes. Therefore, this work aimed at identifying and characterizing novel upstream regulators of light-controlled AS during photomorphogenesis.

The first part of this work focused on the role of two major energy sensor kinases 'SNF1-related kinase1' (SnRK1) and 'target of rapamycin' (TOR) during skoto- and photomorphogenesis. Inducible artificial microRNAs targeting *SnRK1* and *TOR*, respectively, were used to study the splicing responses as well as skoto- and photomorphogenic growth parameters in the mutant lines.

Given the involvement of SnRK1 and TOR in light-mediated AS, we proposed that an altered kinase signaling might trigger phosphorylation-dependent changes in the activity of splicing regulators, which impacts the AS response. Therefore, the aim of the second part of this work was to identify splicing regulators that contribute to light-mediated AS and skoto- and photomorphogenic growth. Candidate splicing regulators were identified in a phosphoproteome-wide approach. Among the RNA binding proteins showing light- and sugar-induced changes in phosphorylation, I focused on the RS subfamily of serine/arginine-rich (SR) proteins and examined their function in light-mediated AS and seedling morphogenesis.

## References

- Abbas, M., Alabadí, D., & Blázquez, M. A. (2013). Differential growth at the apical hook: All roads lead to auxin. *Frontiers in Plant Science*, 4, 441. <https://doi.org/10.3389/fpls.2013.00441>
- Alderson, A., Sabelli, P. A., Dickinson, J. R., Cole, D., Richardson, M., Kreis, M., Shewry, P. R., & Halford, N. G. (1991). Complementation of *snf1*, a mutation affecting global regulation of carbon metabolism in yeast, by a plant protein kinase cDNA. *PROCEEDINGS of the NATIONAL ACADEMY of SCIENCES of the UNITED STATES of AMERICA*, 88(19), 8602–8605. <https://doi.org/10.1073/pnas.88.19.8602>
- Ali, G. S., Golovkin, M., & Reddy, A. S. N. (2003). Nuclear localization and in vivo dynamics of a plant-specific serine/arginine-rich protein. *The Plant Journal : For Cell and Molecular Biology*, 36(6), 883–893. <https://doi.org/10.1046/j.1365-313x.2003.01932.x>
- Aprile, M., Cataldi, S., Ambrosio, M. R., D'Esposito, V., Lim, K., Dietrich, A., Blueher, M., Savage, D. B., Formisano, P., Ciccodicola, A., & Costa, V. (2018). PPAR gamma Delta 5, a Naturally Occurring Dominant-Negative Splice Isoform, Impairs PPAR gamma Function and Adipocyte Differentiation. *CELL REPORTS*, 25(6), 1577-+. <https://doi.org/10.1016/j.celrep.2018.10.035>
- Baena-González, E., Rolland, F., Thevelein, J. M., & Sheen, J. (2007). A central integrator of transcription networks in plant stress and energy signalling. *NATURE*, 448(7156), 938–942. <https://doi.org/10.1038/nature06069>
- Barta, A., Kalyna, M., & Reddy, A. S. N. (2010). Implementing a rational and consistent nomenclature for serine/arginine-rich protein splicing factors (SR proteins) in plants. *The Plant Cell*, 22(9), 2926–2929. <https://doi.org/10.1105/tpc.110.078352>
- Belda-Palazon, B., Adamo, M., Valerio, C., Ferreira, L. J., Confraria, A., Reis-Barata, D., Rodrigues, A., Meyer, C., Rodriguez, P. L., & Baena-Gonzalez, E. (2020). A dual function of SnRK2 kinases in the regulation of SnRK1 and plant growth.

- NATURE PLANTS*, 6(11), 1345–1353. <https://doi.org/10.1038/s41477-020-00778-w>
- Bowman, J. L., Kohchi, T., Yamato, K. T., Jenkins, J., Shu, S., Ishizaki, K., Yamaoka, S., Nishihama, R., Nakamura, Y., Berger, F., Adam, C., Aki, S. S., Althoff, F., Araki, T., Arteaga-Vazquez, M. A., Balasubramanian, S., Barry, K., Bauer, D., Boehm, C. R., . . . Schmutz, J. (2017). Insights into Land Plant Evolution Garnered from the *Marchantia polymorpha* Genome. *Cell*, 171(2), 287–304.e15. <https://doi.org/10.1016/j.cell.2017.09.030>
- Briggs, W. R., & Olney, M. A. (2001). Photoreceptors in plant photomorphogenesis to date. Five phytochromes, two cryptochromes, one phototropin, and one superchrome. *Plant Physiology*, 125(1), 85–88.
- Broeckx, T., Hulsmans, S., & Rolland, F. (2016). The plant energy sensor: Evolutionary conservation and divergence of SnRK1 structure, regulation, and function. *Journal of Experimental Botany*, 67(22), 6215–6252. <https://doi.org/10.1093/jxb/erw416>
- Burge, C. B., Padgett, R. A., & Sharp, P. A. (1998). Evolutionary fates and origins of U12-type introns. *MOLECULAR CELL*, 2(6), 773–785.
- Caldana, C., Li, Y., Leisse, A., Zhang, Y., Bartholomaeus, L., Fernie, A. R., Willmitzer, L., & Giavalisco, P. (2013). Systemic analysis of inducible target of rapamycin mutants reveal a general metabolic switch controlling growth in *Arabidopsis thaliana*. *The Plant Journal : For Cell and Molecular Biology*, 73(6), 897–909. <https://doi.org/10.1111/tpj.12080>
- Cazalla, D., Zhu, J., Manche, L., Huber, E., Krainer, A. R., & Cáceres, J. F. (2002). Nuclear export and retention signals in the RS domain of SR proteins. *Molecular and Cellular Biology*, 22(19), 6871–6882. <https://doi.org/10.1128/MCB.22.19.6871-6882.2002>
- Chaudhary, S., Jabre, I., Reddy, A. S. N., Staiger, D., & Syed, N. H. (2019). Perspective on Alternative Splicing and Proteome Complexity in Plants. *Trends in Plant Science*, 24(6), 496–506. <https://doi.org/10.1016/j.tplants.2019.02.006>
- Chaudhary, S., Khokhar, W., Jabre, I., Reddy, A. S. N., Byrne, L. J., Wilson, C. M., & Syed, N. H. (2019). Alternative Splicing and Protein Diversity: Plants Versus

- Animals. *Frontiers in Plant Science*, 10, 708. <https://doi.org/10.3389/fpls.2019.00708>
- Chen, G.-H., Liu, M.-J., Xiong, Y., Sheen, J., & Wu, S.-H. (2018). Tor and RPS6 transmit light signals to enhance protein translation in deetioliating Arabidopsis seedlings. *PROCEEDINGS of the NATIONAL ACADEMY of SCIENCES of the UNITED STATES of AMERICA*, 115(50), 12823–12828. <https://doi.org/10.1073/pnas.1809526115>
- Chen, M., & Manley, J. L. (2009). Mechanisms of alternative splicing regulation: Insights from molecular and genomics approaches. *Nature Reviews. Molecular Cell Biology*, 10(11), 741–754. <https://doi.org/10.1038/nrm2777>
- Chory, J., Nagpal, P., & Peto, C. A. (1991). Phenotypic and Genetic Analysis of det2, a New Mutant That Affects Light-Regulated Seedling Development in Arabidopsis. *PLANT CELL*, 3(5), 445–459. <https://doi.org/10.1105/tpc.3.5.445>
- Clouse, S. D., Langford, M., & McMorris, T. C. (1996). A brassinosteroid-insensitive mutant in Arabidopsis thaliana exhibits multiple defects in growth and development. *Plant Physiology*, 111(3), 671–678. <https://doi.org/10.1104/pp.111.3.671>
- Colwill, K., Pawson, T., Andrews, B., Prasad, J., Manley, J. L., Bell, J. C., & Duncan, P. I. (1996). The Clk/Sty protein kinase phosphorylates SR splicing factors and regulates their intranuclear distribution. *The EMBO Journal*, 15(2), 265–275.
- Crozet, P., Margalha, L., Butowt, R., Fernandes, N., Elias, C. A., Orosa, B., Tomanov, K., Teige, M., Bachmair, A., Sadanandom, A., & Baena-Gonzalez, E. (2016). SUMOylation represses SnRK1 signaling in Arabidopsis. *PLANT JOURNAL*, 85(1), 120–133. <https://doi.org/10.1111/tpj.13096>
- Crozet, P., Margalha, L., Confraria, A., Rodrigues, A., Martinho, C., Adamo, M., Elias, C. A., & Baena-González, E. (2014). Mechanisms of regulation of SNF1/AMPK/SnRK1 protein kinases. *Frontiers in Plant Science*, 5, 190. <https://doi.org/10.3389/fpls.2014.00190>
- Deng, X.-W., & Quail, P. H. (1992). Genetic and phenotypic characterization of cop1 mutants of Arabidopsis thaliana. *The Plant Journal : For Cell and Molecular Biology*, 2(1), 83–95. <https://doi.org/10.1111/j.1365-313X.1992.00083.x>

- Deprost, D., Yao, L., Sormani, R., Moreau, M., Leterreux, G., Nicolaï, M., Bedu, M., Robaglia, C., & Meyer, C. (2007). The Arabidopsis TOR kinase links plant growth, yield, stress resistance and mRNA translation. *EMBO Reports*, 8(9), 864–870. <https://doi.org/10.1038/sj.embor.7401043>
- Dobrenel, T., Caldana, C., Hanson, J., Robaglia, C., Vincentz, M., Veit, B., & Meyer, C. (2016). Tor Signaling and Nutrient Sensing. *ANNUAL REVIEW of PLANT BIOLOGY*, 67, 261–285. <https://doi.org/10.1146/annurev-arplant-043014-114648>
- Docquier, S., Tillemans, V., Deltour, R., & Motte, P. (2004). Nuclear bodies and compartmentalization of pre-mRNA splicing factors in higher plants. *CHROMOSOMA*, 112(5), 255–266. <https://doi.org/10.1007/s00412-003-0271-3>
- Dong, J., Sun, N., Yang, J., Deng, Z., Lan, J., Qin, G., He, H., Deng, X. W., Irish, V. F., Chen, H., & Wei, N. (2019). The Transcription Factors TCP4 and PIF3 Antagonistically Regulate Organ-Specific Light Induction of SAUR Genes to Modulate Cotyledon Opening during De-Etiolation in Arabidopsis. *PLANT CELL*, 31(5), 1155–1170. <https://doi.org/10.1105/tpc.18.00803>
- Drechsel, G., Kahles, A., Kesarwani, A. K., Stauffer, E., Behr, J., Drewe, P., Rättsch, G., & Wachter, A. (2013). Nonsense-mediated decay of alternative precursor mRNA splicing variants is a major determinant of the Arabidopsis steady state transcriptome. *PLANT CELL*, 25(10), 3726–3742. <https://doi.org/10.1105/tpc.113.115485>
- Emanuelle, S., Hossain, M. I., Moller, I. E., Pedersen, H. L., van de Meene, A. M. L., Doblin, M. S., Koay, A., Oakhill, J. S., Scott, J. W., Willats, W. G. T., Kemp, B. E., Bacic, A., Gooley, P. R., & Stapleton, D. I. (2015). Snrk1 from Arabidopsis thaliana is an atypical AMPK. *The Plant Journal : For Cell and Molecular Biology*, 82(2), 183–192. <https://doi.org/10.1111/tpj.12813>
- Fairbrother, W. G., Yeh, R.-F., Sharp, P. A., & Burge, C. B. (2002). Predictive identification of exonic splicing enhancers in human genes. *Science (New York, N.Y.)*, 297(5583), 1007–1013. <https://doi.org/10.1126/science.1073774>
- Feilner, T., Hultschig, C., Lee, J., Meyer, S., Immink, R. G. H., Koenig, A., Possling, A., Seitz, H., Beveridge, A., Scheel, D., Cahill, D. J., Lehrach, H., Kreuzberger, J., & Kersten, B. (2005). High throughput identification of potential Arabidopsis

- mitogen-activated protein kinases substrates. *Molecular & Cellular Proteomics* : *MCP*, 4(10), 1558–1568. <https://doi.org/10.1074/mcp.M500007-MCP200>
- Fu, L., Liu, Y., Qin, G., Wu, P., Zi, H., Xu, Z., Zhao, X., Wang, Y., Li, Y., Yang, S., Peng, C., Wong, C. C. L., Yoo, S.-D., Zuo, Z., Liu, R., Cho, Y.-H., & Xiong, Y. (2021). The TOR-EIN2 axis mediates nuclear signalling to modulate plant growth. *NATURE*. Advance online publication. <https://doi.org/10.1038/s41586-021-03310-y>
- Fu, X.-D., & Ares, M., JR. (2014). Context-dependent control of alternative splicing by RNA-binding proteins. *NATURE REVIEWS GENETICS*, 15(10), 689–701. <https://doi.org/10.1038/nrg3778>
- Galvão, V. C., & Fankhauser, C. (2015). Sensing the light environment in plants: Photoreceptors and early signaling steps. *Current Opinion in Neurobiology*, 34, 46–53. <https://doi.org/10.1016/j.conb.2015.01.013>
- Ge, H., Zuo, P., & Manley, J. L. (1991). Primary structure of the human splicing factor ASF reveals similarities with Drosophila regulators. *Cell*, 66(2), 373–382. [https://doi.org/10.1016/0092-8674\(91\)90626-a](https://doi.org/10.1016/0092-8674(91)90626-a)
- Goehring, J., Jacak, J., & Barta, A. (2014). Imaging of Endogenous Messenger RNA Splice Variants in Living Cells Reveals Nuclear Retention of Transcripts Inaccessible to Nonsense-Mediated Decay in Arabidopsis. *PLANT CELL*, 26(2), 754–764. <https://doi.org/10.1105/tpc.113.118075>
- Golovkin, M., & Reddy, A. S. (1998). The plant U1 small nuclear ribonucleoprotein particle 70K protein interacts with two novel serine/arginine-rich proteins. *The Plant Cell*, 10(10), 1637–1648. <https://doi.org/10.1105/tpc.10.10.1637>
- Golovkin, M., & Reddy, A. S. (1999). An SC35-like protein and a novel serine/arginine-rich protein interact with Arabidopsis U1-70K protein. *The Journal of Biological Chemistry*, 274(51), 36428–36438. <https://doi.org/10.1074/jbc.274.51.36428>
- Gommers, C. M. M., & Monte, E. (2018). Seedling Establishment: A Dimmer Switch-Regulated Process between Dark and Light Signaling. *Plant Physiology*, 176(2), 1061–1074. <https://doi.org/10.1104/pp.17.01460>
- Gui, J. F., Tronchère, H., Chandler, S. D., & Fu, X. D. (1994). Purification and characterization of a kinase specific for the serine- and arginine-rich pre-mRNA

- splicing factors. *PROCEEDINGS of the NATIONAL ACADEMY of SCIENCES of the UNITED STATES of AMERICA*, 91(23), 10824–10828. <https://doi.org/10.1073/pnas.91.23.10824>
- Han, S. P., Tang, Y. H., & Smith, R. (2010). Functional diversity of the hnRNPs: Past, present and perspectives. *The Biochemical Journal*, 430(3), 379–392. <https://doi.org/10.1042/BJ20100396>
- Hardie, D. G. (2007). AMP-activated/SNF1 protein kinases: conserved guardians of cellular energy. *NATURE REVIEWS MOLECULAR CELL BIOLOGY*, 8(10), 774–785. <https://doi.org/10.1038/nrm2249>
- Hartmann, L., Drewe-Boß, P., Wießner, T., Wagner, G., Geue, S., Lee, H.-C., Obermüller, D. M., Kahles, A., Behr, J., Sinz, F. H., Rättsch, G., & Wachter, A. (2016). Alternative Splicing Substantially Diversifies the Transcriptome during Early Photomorphogenesis and Correlates with the Energy Availability in Arabidopsis. *PLANT CELL*, 28(11), 2715–2734. <https://doi.org/10.1105/tpc.16.00508>
- Hartmann, L., Wießner, T., & Wachter, A. (2018). Subcellular Compartmentation of Alternatively Spliced Transcripts Defines SERINE/ARGININE-RICH PROTEIN30 Expression. *Plant Physiology*, 176(4), 2886–2903. <https://doi.org/10.1104/pp.17.01260>
- Heitman, J., Movva, N. R., & Hall, M. N. (1991). Targets for cell cycle arrest by the immunosuppressant rapamycin in yeast. *Science (New York, N.Y.)*, 253(5022), 905–909. <https://doi.org/10.1126/science.1715094>
- Henninger, M., Pedrotti, L., Kruschke, M., Draken, J., Wildenhain, T., Fekete, A., Rolland, F., Mueller, M. J., Froeschel, C., Weiste, C., & Droege-Laser, W. (2022). The evolutionarily conserved kinase SnRK1 orchestrates resource mobilization during Arabidopsis seedling establishment. *The Plant Cell*, 34(1), 616–632. <https://doi.org/10.1093/plcell/koab270>
- Hoecker, U. (2017). The activities of the E3 ubiquitin ligase COP1/SPA, a key repressor in light signaling. *Current Opinion in Plant Biology*, 37, 63–69. <https://doi.org/10.1016/j.pbi.2017.03.015>



- Jeong, S. (2017). Sr Proteins: Binders, Regulators, and Connectors of RNA. *Molecules and Cells*, 40(1), 1–9. <https://doi.org/10.14348/molcells.2017.2319>
- Jiang, W., & Chen, L. (2020). Alternative splicing: Human disease and quantitative analysis from high-throughput sequencing. *COMPUTATIONAL and STRUCTURAL BIOTECHNOLOGY JOURNAL*, 19, 183–195. <https://doi.org/10.1016/j.csbj.2020.12.009>
- Jiao, Y. L., Ma, L. G., Strickland, E., & Deng, X. W. (2005). Conservation and divergence of light-regulated genome expression patterns during seedling development in rice and Arabidopsis. *PLANT CELL*, 17(12), 3239–3256. <https://doi.org/10.1105/tpc.105.035840>
- Jiao, Y., Lau, O. S., & Deng, X. W. (2007). Light-regulated transcriptional networks in higher plants. *NATURE REVIEWS GENETICS*, 8(3), 217–230. <https://doi.org/10.1038/nrg2049>
- Kalyna, M., & Barta, A. (2004). A plethora of plant serine/arginine-rich proteins: redundancy or evolution of novel gene functions? *Biochemical Society Transactions*, 32, 561–564.
- Kalyna, M., Lopato, S., & Barta, A. (2003). Ectopic expression of atRSZ33 reveals its function in splicing and causes pleiotropic changes in development. *Molecular Biology of the Cell*, 14(9), 3565–3577. <https://doi.org/10.1091/mbc.e03-02-0109>
- Kalyna, M., Simpson, C. G., Syed, N. H., Lewandowska, D., Marquez, Y., Kusenda, B., Marshall, J., Fuller, J., Cardle, L., McNicol, J., Dinh, H. Q., Barta, A., & Brown, J. W. S. (2012). Alternative splicing and nonsense-mediated decay modulate expression of important regulatory genes in Arabidopsis. *NUCLEIC ACIDS RESEARCH*, 40(6), 2454–2469. <https://doi.org/10.1093/nar/gkr932>
- Kami, C., Lorrain, S., Hornitschek, P., & Fankhauser, C. (2010). Light-regulated plant growth and development. *Current Topics in Developmental Biology*, 91, 29–66. [https://doi.org/10.1016/S0070-2153\(10\)91002-8](https://doi.org/10.1016/S0070-2153(10)91002-8)
- Kastner, B., Will, C. L., Stark, H., & Lührmann, R. (2019). Structural Insights into Nuclear pre-mRNA Splicing in Higher Eukaryotes. *Cold Spring Harbor Perspectives in Biology*, 11(11). <https://doi.org/10.1101/cshperspect.a032417>

- Kathare, P. K., Xin, R., Ganesan, A. S., June, V. M., Reddy, A. S. N., & Huq, E. (2022). SWAP1-SFPS-RRC1 splicing factor complex modulates pre-mRNA splicing to promote photomorphogenesis in *Arabidopsis*. *BioRxiv*, 2022.04.26.489584. <https://doi.org/10.1101/2022.04.26.489584>
- Kim, B., Jeong, Y. J., Corvalán, C., Fujioka, S., Cho, S., Park, T., & Choe, S. (2014). Darkness and gulliver2/phyB mutation decrease the abundance of phosphorylated BZR1 to activate brassinosteroid signaling in *Arabidopsis*. *The Plant Journal : For Cell and Molecular Biology*, 77(5), 737–747. <https://doi.org/10.1111/tpj.12423>
- Klose, C., Venezia, F., Hussong, A., Kircher, S., Schaefer, E., & Fleck, C. (2015). Systematic analysis of how phytochrome B dimerization determines its specificity. *NATURE PLANTS*, 1(7), 1–8. <https://doi.org/10.1038/NPLANTS.2015.90>
- Klose, C., Viczián, A., Kircher, S., Schäfer, E., & Nagy, F. (2015). Molecular mechanisms for mediating light-dependent nucleocytoplasmic partitioning of phytochrome photoreceptors. *The New Phytologist*, 206(3), 965–971. <https://doi.org/10.1111/nph.13207>
- Koncz, C., deJong, F., Villacorta, N., Szakonyi, D., & Koncz, Z. (2012). The spliceosome-activating complex: molecular mechanisms underlying the function of a pleiotropic regulator. *Frontiers in Plant Science*, 3. <https://doi.org/10.3389/fpls.2012.00009>
- Krainer, A. R., Mayeda, A., Kozak, D., & Binns, G. (1991). Functional expression of cloned human splicing factor SF2: Homology to RNA-binding proteins, U1 70K, and *Drosophila* splicing regulators. *Cell*, 66(2), 383–394. [https://doi.org/10.1016/0092-8674\(91\)90627-b](https://doi.org/10.1016/0092-8674(91)90627-b)
- Kurihara, Y., Matsui, A., Hanada, K., Kawashima, M., Ishida, J., Morosawa, T., Tanaka, M., Kaminuma, E., Mochizuki, Y., Matsushima, A., Toyoda, T., Shinozaki, K., & Seki, M. (2009). Genome-wide suppression of aberrant mRNA-like noncoding RNAs by NMD in *Arabidopsis*. *PROCEEDINGS of the NATIONAL ACADEMY of SCIENCES of the UNITED STATES of AMERICA*, 106(7), 2453–2458. <https://doi.org/10.1073/pnas.0808902106>

- Kusnetsov, V. V., Doroshenko, A. S., Kudryakova, N. V., & Danilova, M. N. (2020). Role of Phytohormones and Light in De-etiolation. *Russian Journal of Plant Physiology*, 67(6), 971–984. <https://doi.org/10.1134/S1021443720060102>
- Laloum, T., Martín, G., & Duque, P. (2018). Alternative Splicing Control of Abiotic Stress Responses. *Trends in Plant Science*, 23(2), 140–150. <https://doi.org/10.1016/j.tplants.2017.09.019>
- Lariguet, P., & Dunand, C. (2005). Plant photoreceptors: Phylogenetic overview. *JOURNAL of MOLECULAR EVOLUTION*, 61(4), 559–U59. <https://doi.org/10.1007/s00239-004-0294-2>
- Laubinger, S., Fittinghoff, K., & Hoecker, U. (2004). The SPA quartet: A family of WD-repeat proteins with a central role in suppression of photomorphogenesis in arabidopsis. *PLANT CELL*, 16(9), 2293–2306. <https://doi.org/10.1105/tpc.104.024216>
- Lazar, G., Schaal, T., Maniatis, T., & Goodman, H. M. (1995). Identification of a plant serine-arginine-rich protein similar to the mammalian splicing factor SF2/ASF. *PROCEEDINGS of the NATIONAL ACADEMY of SCIENCES of the UNITED STATES of AMERICA*, 92(17), 7672–7676. <https://doi.org/10.1073/pnas.92.17.7672>
- Legris, M., Ince, Y. Ç., & Fankhauser, C. (2019). Molecular mechanisms underlying phytochrome-controlled morphogenesis in plants. *Nature Communications*, 10(1), 5219. <https://doi.org/10.1038/s41467-019-13045-0>
- Lehman, A., Black, R., & Ecker, J. R. (1996). Hookless1, an ethylene response gene, is required for differential cell elongation in the Arabidopsis hypocotyl. *Cell*, 85(2), 183–194. [https://doi.org/10.1016/s0092-8674\(00\)81095-8](https://doi.org/10.1016/s0092-8674(00)81095-8)
- Leivar, P., Monte, E., Oka, Y., Liu, T., Carle, C., Castillon, A., Huq, E., & Quail, P. H. (2008). Multiple phytochrome-interacting bHLH transcription factors repress premature seedling photomorphogenesis in darkness. *Current Biology : CB*, 18(23), 1815–1823. <https://doi.org/10.1016/j.cub.2008.10.058>
- Levine, A., & Durbin, R. (2001). A computational scan for U12-dependent introns in the human genome sequence. *NUCLEIC ACIDS RESEARCH*, 29(19), 4006–4013.

- Li, J., & Nam, K. H. (2002). Regulation of brassinosteroid signaling by a GSK3/SHAGGY-like kinase. *SCIENCE*, *295*(5558), 1299–1301. <https://doi.org/10.1126/science.1065769>
- Li, Q.-F., & He, J.-X. (2016). Bzr1 Interacts with HY5 to Mediate Brassinosteroid- and Light-Regulated Cotyledon Opening in Arabidopsis in Darkness. *MOLECULAR PLANT*, *9*(1), 113–125. <https://doi.org/10.1016/j.molp.2015.08.014>
- Lincoln, C., Britton, J. H., & Estelle, M. (1990). Growth and development of the axr1 mutants of Arabidopsis. *PLANT CELL*, *2*(11), 1071–1080. <https://doi.org/10.1105/tpc.2.11.1071>
- Ling, N. X. Y., Kaczmarek, A., Hoque, A., Davie, E., Ngoei, K. R. W., Morrison, K. R., Smiles, W. J., Forte, G. M., Wang, T., Lie, S., Dite, T. A., Langendorf, C. G., Scott, J. W., Oakhill, J. S., & Petersen, J. (2020). mTORC1 directly inhibits AMPK to promote cell proliferation under nutrient stress. *NATURE METABOLISM*, *2*(1), 41-+. <https://doi.org/10.1038/s42255-019-0157-1>
- Lopato, S., Kalyna, M., Dorner, S., Kobayashi, R., Krainer, A. R., & Barta, A. (1999). Atsrp30, one of two SF2/ASF-like proteins from Arabidopsis thaliana, regulates splicing of specific plant genes. *Genes & Development*, *13*(8), 987–1001. <https://doi.org/10.1101/gad.13.8.987>
- Lopato, S., Mayeda, A., Krainer, A. R., & Barta, A. (1996). Pre-mRNA splicing in plants: Characterization of Ser/Arg splicing factors. *PROCEEDINGS of the NATIONAL ACADEMY of SCIENCES of the UNITED STATES of AMERICA*, *93*(7), 3074–3079. <https://doi.org/10.1073/pnas.93.7.3074>
- Lopato, S., Waigmann, E., & Barta, A. (1996). Characterization of a novel arginine/serine-rich splicing factor in Arabidopsis. *The Plant Cell*, *8*(12), 2255–2264. <https://doi.org/10.1105/tpc.8.12.2255>
- Lorković, Z. J., Hilscher, J., & Barta, A. (2004). Use of fluorescent protein tags to study nuclear organization of the spliceosomal machinery in transiently transformed living plant cells. *Molecular Biology of the Cell*, *15*(7), 3233–3243. <https://doi.org/10.1091/mbc.e04-01-0055>
- Lykke-Andersen, S., & Jensen, T. H. (2015). Nonsense-mediated mRNA decay: an intricate machinery that shapes transcriptomes. *NATURE REVIEWS*

*MOLECULAR CELL BIOLOGY*, 16(11), 665–677.  
<https://doi.org/10.1038/nrm4063>

- Mahfouz, M. M., Kim, S., Delauney, A. J., & Verma, D. P. S. (2006). Arabidopsis TARGET OF RAPAMYCIN interacts with RAPTOR, which regulates the activity of S6 kinase in response to osmotic stress signals. *The Plant Cell*, 18(2), 477–490. <https://doi.org/10.1105/tpc.105.035931>
- Mair, A., Pedrotti, L., Wurzinger, B., Anrather, D., Simeunovic, A., Weiste, C., Valerio, C., Dietrich, K., Kirchler, T., Nägele, T., Vicente Carbajosa, J., Hanson, J., Baena-González, E., Chaban, C., Weckwerth, W., Dröge-Laser, W., & Teige, M. (2015). Snrk1-triggered switch of bZIP63 dimerization mediates the low-energy response in plants. *ELife*, 4. <https://doi.org/10.7554/eLife.05828>
- Mancini, E., Sanchez, S. E., Romanowski, A., Schlaen, R. G., Sanchez-Lamas, M., Cerdan, P. D., & Yanovsky, M. J. (2016). Acute Effects of Light on Alternative Splicing in Light-Grown Plants. *PHOTOCHEMISTRY and PHOTOBIOLOGY*, 92(1), 126–133. <https://doi.org/10.1111/php.12550>
- Mano, S., Hayashi, M., & Nishimura, M. (1999). Light regulates alternative splicing of hydroxypyruvate reductase in pumpkin. *The Plant Journal : For Cell and Molecular Biology*, 17(3), 309–320. <https://doi.org/10.1046/j.1365-313x.1999.00378.x>
- Mano, S., Yamaguchi, K., Hayashi, M., & Nishimura, M. (1997). Stromal and thylakoid-bound ascorbate peroxidases are produced by alternative splicing in pumpkin. *FEBS Letters*, 413(1), 21–26. [https://doi.org/10.1016/s0014-5793\(97\)00862-4](https://doi.org/10.1016/s0014-5793(97)00862-4)
- Marquez, Y., Brown, J. W. S., Simpson, C., Barta, A., & Kalyna, M. (2012). Transcriptome survey reveals increased complexity of the alternative splicing landscape in Arabidopsis. *GENOME RESEARCH*, 22(6), 1184–1195. <https://doi.org/10.1101/gr.134106.111>
- Marquez, Y., Hoepfler, M., Ayatollahi, Z., Barta, A., & Kalyna, M. (2015). Unmasking alternative splicing inside Protein-coding exons defines exitrons and their role in proteome plasticity. *GENOME RESEARCH*, 25(7), 995–1007. <https://doi.org/10.1101/gr.186585.114>

- Martín, G., Márquez, Y., Mantica, F., Duque, P., & Irimia, M. (2021). Alternative splicing landscapes in *Arabidopsis thaliana* across tissues and stress conditions highlight major functional differences with animals. *Genome Biology*, *22*(1), 35. <https://doi.org/10.1186/s13059-020-02258-y>
- Martinez-Contreras, R., Cloutier, P., Shkreta, L., Fiset, J.-F., Revil, T., & Chabot, B. (2007). Hnrnp proteins and splicing control. *Advances in Experimental Medicine and Biology*, *623*, 123–147. [https://doi.org/10.1007/978-0-387-77374-2\\_8](https://doi.org/10.1007/978-0-387-77374-2_8)
- McCartney, R. R., & Schmidt, M. C. (2001). Regulation of Snf1 kinase - Activation requires phosphorylation of threonine 210 by an upstream kinase as well as a distinct step mediated by the Snf4 subunit. *JOURNAL of BIOLOGICAL CHEMISTRY*, *276*(39), 36460–36466.
- Melo, J. P., Kalyna, M., & Duque, P. (2020). Current Challenges in Studying Alternative Splicing in Plants: The Case of *Physcomitrella patens* SR Proteins. *Frontiers in Plant Science*, *11*, 286. <https://doi.org/10.3389/fpls.2020.00286>
- Menand, B., Desnos, T., Nussaume, L., Berger, F., Bouchez, D., Meyer, C., & Robaglia, C. (2002). Expression and disruption of the *Arabidopsis* TOR (target of rapamycin) gene. *PROCEEDINGS of the NATIONAL ACADEMY of SCIENCES of the UNITED STATES of AMERICA*, *99*(9), 6422–6427. <https://doi.org/10.1073/pnas.092141899>
- Moreau, M., Azzopardi, M., Clément, G., Dobrenel, T., Marchive, C., Renne, C., Martin-Magniette, M.-L., Taconnat, L., Renou, J.-P., Robaglia, C., & Meyer, C. (2012). Mutations in the *Arabidopsis* homolog of LST8/G $\beta$ L, a partner of the target of Rapamycin kinase, impair plant growth, flowering, and metabolic adaptation to long days. *The Plant Cell*, *24*(2), 463–481. <https://doi.org/10.1105/tpc.111.091306>
- Mori, T., Yoshimura, K., Nosaka, R., Sakuyama, H., Koike, Y., Tanabe, N., Maruta, T., Tamoi, M., & Shigeoka, S. (2012). Subcellular and subnuclear distribution of high-light responsive serine/arginine-rich proteins, atSR45a and atSR30, in *Arabidopsis thaliana*. *Bioscience, Biotechnology, and Biochemistry*, *76*(11), 2075–2081. <https://doi.org/10.1271/bbb.120425>
- Nasif, S., Contu, L., & Muhlemann, O. (2018). Beyond quality control: The role of nonsense-mediated mRNA decay (NMD) in regulating gene expression.

*SEMINARS in CELL & DEVELOPMENTAL BIOLOGY*, 75, 78–87.  
<https://doi.org/10.1016/j.semcdb.2017.08.053>

Nishiyama, T., Sakayama, H., Vries, J. de, Buschmann, H., Saint-Marcoux, D., Ullrich, K. K., Haas, F. B., Vanderstraeten, L., Becker, D., Lang, D., Vosolsobě, S., Rombauts, S., Wilhelmsson, P. K. I., Janitza, P., Kern, R., Heyl, A., Rümpler, F., Villalobos, L. I. A. C., Clay, J. M., . . . Rensing, S. A. (2018). The Chara Genome: Secondary Complexity and Implications for Plant Terrestrialization. *Cell*, 174(2), 448-464.e24. <https://doi.org/10.1016/j.cell.2018.06.033>

Nukarinen, E., Nägele, T., Pedrotti, L., Wurzinger, B., Mair, A., Landgraf, R., Börnke, F., Hanson, J., Teige, M., Baena-Gonzalez, E., Dröge-Laser, W., & Weckwerth, W. (2016). Quantitative phosphoproteomics reveals the role of the AMPK plant ortholog SnRK1 as a metabolic master regulator under energy deprivation. *Scientific Reports*, 6, 31697. <https://doi.org/10.1038/srep31697>

Oh, E., Zhu, J.-Y., & Wang, Z.-Y. (2012). Interaction between BZR1 and PIF4 integrates brassinosteroid and environmental responses. *Nature Cell Biology*, 14(8), 802–809. <https://doi.org/10.1038/ncb2545>

Oyama, T., Shimura, Y., & Okada, K. (1997). The Arabidopsis HY5 gene encodes a bZIP protein that regulates stimulus-induced development of root and hypocotyl. *Genes & Development*, 11(22), 2983–2995. <https://doi.org/10.1101/gad.11.22.2983>

Paik, I., & Huq, E. (2019). Plant photoreceptors: Multi-functional sensory proteins and their signaling networks. *SEMINARS in CELL & DEVELOPMENTAL BIOLOGY*, 92, 114–121. <https://doi.org/10.1016/j.semcdb.2019.03.007>

Palusa, S. G., & Reddy, A. S. N. (2010). Extensive coupling of alternative splicing of pre-mRNAs of serine/arginine (SR) genes with nonsense-mediated decay. *NEW PHYTOLOGIST*, 185(1), 83–89. <https://doi.org/10.1111/j.1469-8137.2009.03065.x>

Palusa, S. G., Ali, G. S., & Reddy, A. S. N. (2007). Alternative splicing of pre-mRNAs of Arabidopsis serine/arginine-rich proteins: Regulation by hormones and stresses. *The Plant Journal : For Cell and Molecular Biology*, 49(6), 1091–1107. <https://doi.org/10.1111/j.1365-313X.2006.03020.x>

- Pan, Q., Shai, O., Lee, L. J., Frey, J., & Blencowe, B. J. (2008). Deep surveying of alternative splicing complexity in the human transcriptome by high-throughput sequencing. *NATURE GENETICS*, *40*(12), 1413–1415. <https://doi.org/10.1038/ng.259>
- Paradis, C., Cloutier, P., Shkreta, L., Toutant, J., Klarskov, K., & Chabot, B. (2007). Hnrnp I/PTB can antagonize the splicing repressor activity of SRp30c. *RNA (New York, N. Y.)*, *13*(8), 1287–1300. <https://doi.org/10.1261/rna.403607>
- Patel, A. A., McCarthy, M., & Steitz, J. A. (2002). The splicing of U12-type introns can be a rate-limiting step in gene expression. *EMBO JOURNAL*, *21*(14), 3804–3815.
- Patel, A. A., & Steitz, J. A. (2003). Splicing double: Insights from the second spliceosome. *NATURE REVIEWS MOLECULAR CELL BIOLOGY*, *4*(12), 960–970. <https://doi.org/10.1038/nrm1259>
- Pedrotti, L., Weiste, C., Naegele, T., Wolf, E., Lorenzin, F., Dietrich, K., Mair, A., Weckwerth, W., Teige, M., Baena-Gonzalez, E., & Droege-Laser, W. (2018). Snf1-RELATED KINASE1-Controlled C/S-1-bZIP Signaling Activates Alternative Mitochondrial Metabolic Pathways to Ensure Plant Survival in Extended Darkness. *The Plant Cell*, *30*(2), 495–509. <https://doi.org/10.1105/tpc.17.00414>
- Petrillo, E., Godoy Herz, M. A., Fuchs, A., Reifer, D., Fuller, J., Yanovsky, M. J., Simpson, C., Brown, J. W. S., Barta, A., Kalyna, M., & Kornblihtt, A. R. (2014). A Chloroplast Retrograde Signal Regulates Nuclear Alternative Splicing. *SCIENCE*, *344*(6182), 427–430. <https://doi.org/10.1126/science.1250322>
- Pfeiffer, A., Janocha, D., Dong, Y., Medzihradzsky, A., Schöne, S., Daum, G., Suzaki, T., Forner, J., Langenecker, T., Rempel, E., Schmid, M., Wirtz, M., Hell, R., & Lohmann, J. U. (2016). Integration of light and metabolic signals for stem cell activation at the shoot apical meristem. *ELife*, *5*. <https://doi.org/10.7554/eLife.17023>
- Ramon, M., Dang, T. V. T., Broeckx, T., Hulsmans, S., Crepin, N., Sheen, J., & Rolland, F. (2019). Default Activation and Nuclear Translocation of the Plant Cellular Energy Sensor SnRK1 Regulate Metabolic Stress Responses and



- Development. *The Plant Cell*, 31(7), 1614–1632.  
<https://doi.org/10.1105/tpc.18.00500>
- Rausin, G., Tillemans, V., Stankovic, N., Hanikenne, M., & Motte, P. (2010). Dynamic nucleocytoplasmic shuttling of an Arabidopsis SR splicing factor: Role of the RNA-binding domains. *Plant Physiology*, 153(1), 273–284.  
<https://doi.org/10.1104/pp.110.154740>
- Rebbapragada, I., & Lykke-Andersen, J. (2009). Execution of nonsense-mediated mRNA decay: what defines a substrate? *CURRENT OPINION in CELL BIOLOGY*, 21(3), 394–402. <https://doi.org/10.1016/j.ceb.2009.02.007>
- Reddy, A. S. N. (2004). Plant serine/arginine-rich proteins and their role in pre-mRNA splicing. *Trends in Plant Science*, 9(11), 541–547.  
<https://doi.org/10.1016/j.tplants.2004.09.007>
- Reddy, A. S. N. (2007). Alternative splicing of pre-messenger RNAs in plants in the genomic era. *ANNUAL REVIEW of PLANT BIOLOGY*, 58, 267–294.  
<https://doi.org/10.1146/annurev.arplant.58.032806.103754>
- Reddy, A. S. N., Marquez, Y., Kalyna, M., & Barta, A. (2013). Complexity of the Alternative Splicing Landscape in Plants. *PLANT CELL*, 25(10), 3657–3683.  
<https://doi.org/10.1105/tpc.113.117523>
- Reddy, A. S. N., & Shad Ali, G. (2011). Plant serine/arginine-rich proteins: Roles in precursor messenger RNA splicing, plant development, and stress responses. *Wiley Interdisciplinary Reviews. RNA*, 2(6), 875–889.  
<https://doi.org/10.1002/wrna.98>
- Ren, M., Qiu, S., Venglat, P., Xiang, D., Feng, L., Selvaraj, G., & Datla, R. (2011). Target of rapamycin regulates development and ribosomal RNA expression through kinase domain in Arabidopsis. *Plant Physiology*, 155(3), 1367–1382.  
<https://doi.org/10.1104/pp.110.169045>
- Riegler, S., Servi, L., Scarpin, M. R., Herz, M. A. G., Kubaczka, M. G., Venhuizen, P., Meyer, C., Brunkard, J. O., Kalyna, M., Barta, A., & Petrillo, E. (2021). Light regulates alternative splicing outcomes via the TOR kinase pathway. *CELL REPORTS*, 36(10). <https://doi.org/10.1016/j.celrep.2021.109676>

- Rizzini, L., Favory, J.-J., Cloix, C., Faggionato, D., O'Hara, A., Kaiserli, E., Baumeister, R., Schaefer, E., Nagy, F., Jenkins, G. I., & Ulm, R. (2011). Perception of UV-B by the Arabidopsis UVR8 Protein. *SCIENCE*, 332(6025), 103–106. <https://doi.org/10.1126/science.1200660>
- Rodriguez, M., Parola, R., Andreola, S., Pereyra, C., & Martínez-Noël, G. (2019). Tor and SnRK1 signaling pathways in plant response to abiotic stresses: Do they always act according to the "yin-yang" model? *Plant Science : An International Journal of Experimental Plant Biology*, 288, 110220. <https://doi.org/10.1016/j.plantsci.2019.110220>
- Rosenkranz, R. R. E., Bachiri, S., Vraggalas, S., Keller, M., Simm, S., Schleiff, E., & Fragkostefanakis, S. (2021). Identification and Regulation of Tomato Serine/Arginine-Rich Proteins Under High Temperatures. *Frontiers in Plant Science*, 12, 645689. <https://doi.org/10.3389/fpls.2021.645689>
- Ruehl, C., Stauffer, E., Kahles, A., Wagner, G., Drechsel, G., Raetsch, G., & Wachter, A. (2012). Polypyrimidine Tract Binding Protein Homologs from Arabidopsis Are Key Regulators of Alternative Splicing with Implications in Fundamental Developmental Processes. *PLANT CELL*, 24(11), 4360–4375. <https://doi.org/10.1105/tpc.112.103622>
- Sabatini, D. M., Erdjument-Bromage, H., Lui, M., Tempst, P., & Snyder, S. H. (1994). Raft1: A mammalian protein that binds to FKBP12 in a rapamycin-dependent fashion and is homologous to yeast TORs. *Cell*, 78(1), 35–43. [https://doi.org/10.1016/0092-8674\(94\)90570-3](https://doi.org/10.1016/0092-8674(94)90570-3)
- Schmid, M., Davison, T. S., Henz, S. R., Pape, U. J., Demar, M., Vingron, M., Schölkopf, B., Weigel, D., & Lohmann, J. U. (2005). A gene expression map of Arabidopsis thaliana development. *NATURE GENETICS*, 37(5), 501–506. <https://doi.org/10.1038/ng1543>
- Seluzicki, A., Burko, Y., & Chory, J. (2017). Dancing in the dark: Darkness as a signal in plants. *Plant, Cell & Environment*, 40(11), 2487–2501. <https://doi.org/10.1111/pce.12900>
- Seo, P. J., Park, M.-J., Lim, M.-H., Kim, S.-G., Lee, M., Baldwin, I. T., & Park, C.-M. (2012). A Self-Regulatory Circuit of CIRCADIAN CLOCK-ASSOCIATED1 Underlies the Circadian Clock Regulation of Temperature Responses in

- Arabidopsis. *PLANT CELL*, 24(6), 2427–2442.  
<https://doi.org/10.1105/tpc.112.098723>
- Sheen, J. (2014). Master Regulators in Plant Glucose Signaling Networks. *Journal of Plant Biology = Singmul Hakhoe Chi*, 57(2), 67–79.  
<https://doi.org/10.1007/s12374-014-0902-7>
- Sheerin, D. J., Menon, C., Zur Oven-Krockhaus, S., Enderle, B., Zhu, L., Johnen, P., Schleifenbaum, F., Stierhof, Y.-D., Huq, E., & Hiltbrunner, A. (2015). Light-activated phytochrome A and B interact with members of the SPA family to promote photomorphogenesis in Arabidopsis by reorganizing the COP1/SPA complex. *PLANT CELL*, 27(1), 189–201.  
<https://doi.org/10.1105/tpc.114.134775>
- Shikata, H., Hanada, K., Ushijima, T., Nakashima, M., Suzuki, Y., & Matsushita, T. (2014). Phytochrome controls alternative splicing to mediate light responses in Arabidopsis. *PROCEEDINGS of the NATIONAL ACADEMY of SCIENCES of the UNITED STATES of AMERICA*, 111(52), 18781–18786.  
<https://doi.org/10.1073/pnas.1407147112>
- Shikata, H., Nakashima, M., Matsuoka, K., & Matsushita, T. (2012). Deletion of the RS domain of RRC1 impairs phytochrome B signaling in Arabidopsis. *Plant Signaling & Behavior*, 7(8), 933–936. <https://doi.org/10.4161/psb.20854>
- Shikata, H., Shibata, M., Ushijima, T., Nakashima, M., Kong, S.-G., Matsuoka, K., Lin, C., & Matsushita, T. (2012). The RS domain of Arabidopsis splicing factor RRC1 is required for phytochrome B signal transduction. *The Plant Journal : For Cell and Molecular Biology*, 70(5), 727–738. <https://doi.org/10.1111/j.1365-313X.2012.04937.x>
- Shukla, S., & Oberdoerffer, S. (2012). Co-transcriptional regulation of alternative pre-mRNA splicing. *Biochimica Et Biophysica Acta*, 1819(7), 673–683.  
<https://doi.org/10.1016/j.bbagr.2012.01.014>
- Soledad Tognacca, R., Servi, L., Esteban Hernando, C., Saura-Sanchez, M., Javier Yanovsky, M., Petrillo, E., & Francisco Botto, J. (2019). Alternative Splicing Regulation During Light-Induced Germination of Arabidopsis thaliana Seeds. *Frontiers in Plant Science*, 10. <https://doi.org/10.3389/fpls.2019.01076>

- Staiger, D., & Brown, J. W. S. (2013). Alternative splicing at the intersection of biological timing, development, and stress responses. *PLANT CELL*, 25(10), 3640–3656. <https://doi.org/10.1105/tpc.113.113803>
- Stauffer, E., Westermann, A., Wagner, G., & Wachter, A. (2010). Polypyrimidine tract-binding protein homologues from Arabidopsis underlie regulatory circuits based on alternative splicing and downstream control. *The Plant Journal : For Cell and Molecular Biology*, 64(2), 243–255. <https://doi.org/10.1111/j.1365-313X.2010.04321.x>
- Stein, S. C., Woods, A., Jones, N. A., Davison, M. D., & Carling, D. (2000). The regulation of AMP-activated protein kinase by phosphorylation. *BIOCHEMICAL JOURNAL*, 345, 437–443.
- Sugnet, C. W., Kent, W. J., Ares, M., & Haussler, D. (2004). Transcriptome and genome conservation of alternative splicing events in humans and mice. *Pacific Symposium on Biocomputing. Pacific Symposium on Biocomputing*, 66–77. [https://doi.org/10.1142/9789812704856\\_0007](https://doi.org/10.1142/9789812704856_0007)
- Sun, N., Wang, J., Gao, Z., Dong, J., He, H., Terzaghi, W., Wei, N., Deng, X. W., & Chen, H. (2016). Arabidopsis SAURs are critical for differential light regulation of the development of various organs. *PROCEEDINGS of the NATIONAL ACADEMY of SCIENCES of the UNITED STATES of AMERICA*, 113(21), 6071–6076. <https://doi.org/10.1073/pnas.1604782113>
- Thomas, J., Palusa, S. G., Prasad, K. V. S. K., Ali, G. S., Surabhi, G.-K., Ben-Hur, A., Abdel-Ghany, S. E., & Reddy, A. S. N. (2012). Identification of an intronic splicing regulatory element involved in auto-regulation of alternative splicing of SCL33 pre-mRNA. *The Plant Journal : For Cell and Molecular Biology*, 72(6), 935–946. <https://doi.org/10.1111/tpj.12004>
- Tillemans, V., Dispa, L., Remacle, C., Collinge, M., & Motte, P. (2005). Functional distribution and dynamics of Arabidopsis SR splicing factors in living plant cells. *The Plant Journal : For Cell and Molecular Biology*, 41(4), 567–582. <https://doi.org/10.1111/j.1365-313X.2004.02321.x>
- Tillemans, V., Leponce, I., Rausin, G., Dispa, L., & Motte, P. (2006). Insights into nuclear organization in plants as revealed by the dynamic distribution of

- Arabidopsis SR splicing factors. *The Plant Cell*, 18(11), 3218–3234. <https://doi.org/10.1105/tpc.106.044529>
- van Fuente Bentem, S. de, Anrather, D., Dohnal, I., Roitinger, E., Csaszar, E., Joore, J., Buijnink, J., Carreri, A., Forzani, C., Lorkovic, Z. J., Barta, A., Lecourieux, D., Verhounig, A., Jonak, C., & Hirt, H. (2008). Site-specific phosphorylation profiling of Arabidopsis proteins by mass spectrometry and peptide chip analysis. *Journal of Proteome Research*, 7(6), 2458–2470. <https://doi.org/10.1021/pr8000173>
- van Fuente Bentem, S. de, Anrather, D., Roitinger, E., Djamei, A., Hufnagl, T., Barta, A., Csaszar, E., Dohnal, I., Lecourieux, D., & Hirt, H. (2006). Phosphoproteomics reveals extensive in vivo phosphorylation of Arabidopsis proteins involved in RNA metabolism. *NUCLEIC ACIDS RESEARCH*, 34(11), 3267–3278. <https://doi.org/10.1093/nar/gkl429>
- van Leene, J., Han, C., Gadeyne, A., Eeckhout, D., Matthijs, C., Cannoot, B., Winne, N. de, Persiau, G., van de Slijke, E., van de Cotte, B., Stes, E., van Bel, M., Storme, V., Impens, F., Gevaert, K., Vandepoele, K., Smet, I. de, & Jaeger, G. de (2019). Capturing the phosphorylation and protein interaction landscape of the plant TOR kinase. *NATURE PLANTS*, 5(3), 316–327. <https://doi.org/10.1038/s41477-019-0378-z>
- Wachter, A., Rühl, C., & Stauffer, E. (2012). The Role of Polypyrimidine Tract-Binding Proteins and Other hnRNP Proteins in Plant Splicing Regulation. *Frontiers in Plant Science*, 3, 81. <https://doi.org/10.3389/fpls.2012.00081>
- Wang, P., Xue, L., Batelli, G., Lee, S., Hou, Y.-J., van Oosten, M. J., Zhang, H., Tao, W. A., & Zhu, J.-K. (2013). Quantitative phosphoproteomics identifies SnRK2 protein kinase substrates and reveals the effectors of abscisic acid action. *PROCEEDINGS of the NATIONAL ACADEMY of SCIENCES of the UNITED STATES of AMERICA*, 110(27), 11205–11210. <https://doi.org/10.1073/pnas.1308974110>
- Wang, Z., & Burge, C. B. (2008). Splicing regulation: From a parts list of regulatory elements to an integrated splicing code. *RNA (New York, N. Y.)*, 14(5), 802–813. <https://doi.org/10.1261/rna.876308>

- Wang, Z.-Y., Bai, M.-Y., Oh, E., & Zhu, J.-Y. (2012). Brassinosteroid signaling network and regulation of photomorphogenesis. *Annual Review of Genetics*, *46*, 701–724. <https://doi.org/10.1146/annurev-genet-102209-163450>
- Will, C. L., & Lührmann, R. (2005). Splicing of a rare class of introns by the U12-dependent spliceosome. *Biological Chemistry*, *386*(8), 713–724. <https://doi.org/10.1515/BC.2005.084>
- Will, C. L., & Lührmann, R. (2011). Spliceosome structure and function. *Cold Spring Harbor Perspectives in Biology*, *3*(7). <https://doi.org/10.1101/cshperspect.a003707>
- Wind, J., Smeeckens, S., & Hanson, J. (2010). Sucrose: Metabolite and signaling molecule. *PHYTOCHEMISTRY*, *71*(14-15), 1610–1614. <https://doi.org/10.1016/j.phytochem.2010.07.007>
- Wu, H.-P., Su, Y.-s., Chen, H.-C., Chen, Y.-R., Wu, C.-C., Lin, W.-D., & Tu, S.-L. (2014). Genome-wide analysis of light-regulated alternative splicing mediated by photoreceptors in *Physcomitrella patens*. *Genome Biology*, *15*(1). <https://doi.org/10.1186/gb-2014-15-1-r10>
- Wullschleger, S., Loewith, R., & Hall, M. N. (2006). Tor signaling in growth and metabolism. *Cell*, *124*(3), 471–484. <https://doi.org/10.1016/j.cell.2006.01.016>
- Wurzinger, B., Nukarinen, E., Naegele, T., Weckwerth, W., & Teige, M. (2018). The SnRK1 Kinase as Central Mediator of Energy Signaling between Different Organelles. *Plant Physiology*, *176*(2), 1085–1094. <https://doi.org/10.1104/pp.17.01404>
- Xin, R., Kathare, P. K., & Huq, E. (2019). Coordinated Regulation of Pre-mRNA Splicing by the SFPS-RRC1 Complex to Promote Photomorphogenesis. *PLANT CELL*, *31*(9), 2052–2069. <https://doi.org/10.1105/tpc.18.00786>
- Xin, R., Zhu, L., Salome, P. A., Mancini, E., Marshall, C. M., Harmon, F. G., Yanovsky, M. J., Weigel, D., & Huq, E. (2017). SPF45-related splicing factor for phytochrome signaling promotes photomorphogenesis by regulating pre-mRNA splicing in *Arabidopsis*. *PROCEEDINGS of the NATIONAL ACADEMY of SCIENCES of the UNITED STATES of AMERICA*, *114*(33), E7018-E7027. <https://doi.org/10.1073/pnas.1706379114>

- Xiong, Y., McCormack, M., Li, L., Hall, Q., Xiang, C., & Sheen, J. (2013). Glucose-TOR signalling reprograms the transcriptome and activates meristems. *NATURE*, 496(7444), 181–186. <https://doi.org/10.1038/nature12030>
- Xiong, Y., & Sheen, J. (2012). Rapamycin and glucose-target of rapamycin (TOR) protein signaling in plants. *The Journal of Biological Chemistry*, 287(4), 2836–2842. <https://doi.org/10.1074/jbc.M111.300749>
- Yan, Q., Xia, X., Sun, Z., & Fang, Y. (2017). Depletion of Arabidopsis SC35 and SC35-like serine/arginine-rich proteins affects the transcription and splicing of a subset of genes. *PLoS Genetics*, 13(3), e1006663. <https://doi.org/10.1371/journal.pgen.1006663>
- Yu, H., Tian, C., Yu, Y., & Jiao, Y. (2016). Transcriptome Survey of the Contribution of Alternative Splicing to Proteome Diversity in Arabidopsis thaliana. *MOLECULAR PLANT*, 9(5), 749–752. <https://doi.org/10.1016/j.molp.2015.12.018>
- Zhai, Z., Liu, H., & Shanklin, J. (2017). Phosphorylation of WRINKLED1 by KIN10 Results in Its Proteasomal Degradation, Providing a Link between Energy Homeostasis and Lipid Biosynthesis. *The Plant Cell*, 29(4), 871–889. <https://doi.org/10.1105/tpc.17.00019>
- Zhang, X.-N., & Mount, S. M. (2009). Two alternatively spliced isoforms of the Arabidopsis SR45 protein have distinct roles during normal plant development. *Plant Physiology*, 150(3), 1450–1458. <https://doi.org/10.1104/pp.109.138180>
- Zhou, Z. L., Licklider, L. J., Gygi, S. P., & Reed, R. (2002). Comprehensive proteomic analysis of the human spliceosome. *NATURE*, 419(6903), 182–185. <https://doi.org/10.1038/nature01031>
- Zhou, Z., & Fu, X.-D. (2013). Regulation of splicing by SR proteins and SR protein-specific kinases. *CHROMOSOMA*, 122(3), 191–207. <https://doi.org/10.1007/s00412-013-0407-z>

## Chapter II: Draft manuscript 1





**Breakthrough Report** (planned submission: December 2022)

**SnRK1 and TOR control light-responsive splicing and development in etiolated Arabidopsis seedlings**

Jennifer Saile<sup>1,2,4</sup>, Theresa Wießner-Kroh<sup>2,4</sup>, Katarina Erbstein<sup>1</sup>, Dominik M. Obermüller<sup>2</sup>, Anne Pfeiffer<sup>3</sup>, Denis Janocha<sup>3</sup>, Jan Lohmann<sup>3</sup>, and Andreas Wachter<sup>1,2,\*</sup>

<sup>1</sup>Institute for Molecular Physiology (imP), University of Mainz, Hanns-Dieter-Hüschen-Weg 17, 55128 Mainz, Germany

<sup>2</sup>Center for Plant Molecular Biology (ZMBP), University of Tübingen, Auf der Morgenstelle 32, 72076 Tübingen, Germany

<sup>3</sup>Centre for Organismal Studies, Heidelberg University, Im Neuenheimer Feld 230, 69120 Heidelberg, Germany

<sup>4</sup>These authors contributed equally to the work.

\*Corresponding author: [wachter@uni-mainz.de](mailto:wachter@uni-mainz.de)

Short title: SnRK1/TOR regulate splicing and development

## Contributions

The following manuscript is a shared project with Theresa Wießner-Kroh and myself, who equally contributed to this work. Therefore, parts of this chapter are also included in the dissertation of Theresa Wießner-Kroh (“Functional characterization of SR30 and upstream signaling of light-regulated AS during seedling photomorphogenesis”, University of Tübingen, 2021).

Theresa Wießner-Kroh cloned constitutive and inducible amiR-SnRK1 constructs (Figure 1A) and generated corresponding transgenic Arabidopsis plants, including transformation, selection, and genotyping. The amiR-TOR construct and transgenic line was generated by Anne Pfeiffer and Denis Janocha in the group of Jan Lohmann (University of Heidelberg).

Transcript studies shown in Figure 1B, D, Supplemental Figure 5 and 6A were performed by Theresa Wießner-Kroh. Transcript levels displayed in Figure 3A, Supplemental Figure 9B were done by myself.

Protein extraction and immunoblots shown in Figure 1C and Supplemental Figure 4A were performed by Theresa-Wießner-Kroh. I performed protein analyses displayed in Supplemental Figure 6B, 8B-C and 9C.

Splicing pattern studies displayed in Figure 1E, 3B and Supplemental Figure 4B, 8D were performed by myself. However, Theresa Wießner-Kroh provided the RNA used for Figure 1E and Supplemental Figure 4B. Moreover, Theresa did AS studies that are shown in Supplemental Figure 5C.

Phenotyping experiments of constitutive amiR-SnRK1 lines were performed by Katarina Erbstein under my supervision (Supplemental Figure 2A to D, Supplemental Table 1).

Hypocotyl assays shown in Figure 2A, 3C and Supplemental Figure 3C were done by Theresa Wießner-Kroh. Hypocotyl assay depicted in Supplemental Figure 2E was done by Dominik Obermüller under supervision of Theresa Wießner-Kroh. The hypocotyl assays shown in Supplemental Figure 4C and 8E were done by myself.

Chlorophyll content measurements in amiR-SnRK1 seedlings were performed by myself (Figure 2B, C and Supplemental Figure 7).

Cotyledon opening kinetic assays were all performed by myself (Figure 4A to C, Supplemental Figure 10). For the cotyledon opening assay displayed in Supplemental Figure 9A, Moritz Denecke provided one replicate, the other replicates were done by myself.

The root assay shown in Supplemental Figure 8F was done by Denis Janocha and bending angle measurements were performed by myself (Figure 3D).

Statistical analyses were performed by myself. Moreover, Theresa Wießner-Kroh and myself designed figures and wrote the manuscript together with Andreas Wachter. All authors contributed to data analysis and presentation in the manuscript.

## **Abstract**

The kinases SNF1-related kinase 1 (SnRK1) and target of rapamycin (TOR) are central sensors of the energy status, linking this information via diverse sets of regulatory mechanisms to plant development and stress responses. Despite the well-studied functions of SnRK1 and TOR under conditions of limited or ample energy availability, respectively, only little is known how the two sensor systems specifically act and are integrated in the same molecular process or physiological context. Here, we demonstrate that both SnRK1 and TOR are required for proper skotomorphogenesis in etiolated *Arabidopsis* seedlings, light-induced cotyledon opening, and regular phototropic growth. Furthermore, we identify SnRK1 and TOR as signalling components acting upstream of light- and sugar-regulated alternative splicing events, expanding the known action spectra for these two key players in plant energy signalling. Our findings imply that SnRK1 and TOR activities are present and integrated throughout various phases of plant development, and we propose a model according to which tipping points instead of thresholds in signalling activity modulate developmental programs in response to altered energy availability.

## Introduction

The phototrophic life style of plants requires precise monitoring of the ambient light conditions and its integration with the metabolic status to adjust the plant's physiology on multiple levels, ranging from biochemical to developmental adaptations. The underlying mechanisms of signal perception and transduction have been intensively studied, including multiple classes of photoreceptors for a spectrum of light signals (Galvão and Fankhauser, 2015) and the central energy sensor kinases SNF1-related kinase 1 (SnRK1) and target of rapamycin (TOR) (Li and Sheen, 2016; Sakr et al., 2018; Margalha et al., 2019; Li et al., 2021). However, our understanding at which steps and via which mechanisms light and sugar signals can be integrated is still scarce. A study from Pfeiffer et al. (2016) provided evidence that TOR is required to integrate light and metabolic signals during stem cell activation at the shoot apical meristem in *Arabidopsis thaliana*. TOR has also been demonstrated to contribute to photomorphogenesis of etiolated *A. thaliana* seedlings via translational enhancement, acting downstream of photoreceptors and constitutive photomorphogenesis 1 (COP1), a negative regulator of light-dependent development (Chen et al., 2018).

Several studies have revealed that light-triggered de-etiolation of *A. thaliana* seedlings is accompanied and regulated by changes in alternative precursor mRNA splicing (AS) (Shikata et al., 2014; Hartmann et al., 2016). Importantly, the splicing regulators reduced red-light responses in *cry1cry2* background 1 (RRC1; Shikata et al., 2012; Xin et al., 2019) and splicing factor for phytochrome signalling (SFPS; Xin et al., 2019; Xin et al., 2017) promote photomorphogenesis and interact with the red light receptor phytochrome b (PHYB). However, light-regulated AS events can also be regulated in a photoreceptor-independent manner (Hartmann et al., 2016; Petrillo et al., 2014; Mancini et al., 2016). External sugar supply was found to elicit similar AS changes as illumination in etiolated seedlings (Hartmann et al., 2016), and evidence for an involvement of retrograde signalling from the chloroplast to the nucleus in AS control was provided (Petrillo et al., 2014). In a recent report, inhibition of TOR signalling in light-grown seedlings exposed to an extended dark phase and then treated with light and/or sugars revealed the requirement of TOR for proper AS responses (Riegler et al., 2021), whereas the role of SnRK1 in this context has remained unclear. Illumination of etiolated seedlings is expected to affect both SnRK1 and TOR signalling, but their interplay in the regulation of AS and the skoto-/photomorphogenesis-related developmental processes are unresolved. In this study, we describe that repression of

SnRK1 and TOR signalling can similarly alter light-dependent AS events and developmental processes in etiolated seedlings, providing novel insight into the action spectra and physiological functions of these two central energy sensor kinases in plants.

## Results and Discussion

Similar to their orthologs in yeast and mammals, plant SnRK1 kinases can form heterotrimeric complexes including one catalytic  $\alpha$  subunit (Broeckx et al., 2016; Li and Sheen, 2016; Sakr et al., 2018). Besides this common structure, several plant-specific features of SnRK1 complexes have been reported (Emanuelle et al., 2015; Ramon et al., 2019; Broeckx et al., 2016) that may represent an adaptation of this central energy sensor to the challenges of a phototrophic life style. In *A. thaliana*, the  $\alpha$  subunit is mainly encoded by the homologs *SnRK1.1* (*KIN10*) and *SnRK1.2* (*KIN11*), while the third homolog *SnRK1.3* (*KIN12*) is expressed only at low levels and in specific tissues (Margalha et al., 2019). To elucidate the role of SnRK1 in light-regulated AS and seedling development and to overcome the previously reported lethality of a double *snrk1.1 snrk1.2* knockout (Baena-González et al., 2007), we generated *A. thaliana* lines constitutively expressing artificial microRNAs (amiRs) that can simultaneously target *SnRK1.1* and *SnRK1.2* (Figure 1A; Supplemental Figure 1). Following these mutants' development revealed the frequent occurrence of phenotypical abnormalities, including dwarfism, early bolting, increased mortality rates, and reduced hypocotyl expansion of etiolated seedlings (Supplemental Figure 2). Moreover, ~30% of the transformants that were resistant against the selection agent and therefore must carry the transgene died after the selection step before seed generation (Supplemental Table 1). Analysing three subsequent generations for several independent lines did not result in a non-segregating mutant, suggesting homozygosity causes lethality due to a dose effect. In line with our observations, simultaneous downregulation of *SnRK1.1* and *SnRK1.2* via virus-induced gene silencing in *A. thaliana* also strongly reduced growth and in addition caused anthocyanin accumulation (Mair et al., 2015).

We concluded from these data that our amiRs are likely functional, but need to be expressed in an inducible manner to avoid general growth defects and increased mortality rates. In comparison to the approach from Nukarinen et al. (2016) using an inducible amiR against *SnRK1.2* in a *snrk1.1* T-DNA mutant background, we expected regular activities of both SnRK1 homologs under non-induced conditions. Plant

transformants carrying a transgene for estradiol-inducible amiR expression (*i-amiR-SnRK1*) showed normal development when grown without application of the inducer, suggesting sufficiently tight control of amiR production (Supplemental Figure 3). Comparing hypocotyl lengths in mock- and estradiol-treated etiolated seedlings revealed for both *i-amiR* constructs and several independent lines each reduced hypocotyl lengths upon amiR induction (Supplemental Figure 3). These observations were in agreement with the phenotype seen for our constitutive amiR lines upon seedling growth in darkness. One line from each *i-amiR* construct was propagated in the following generations to obtain homozygous mutants for further characterisation. Exposing etiolated seedlings from such homozygous mutants for three days to estradiol strongly diminished transcript levels of *SnRK1.1* and *SnRK1.2* for both *i-amiR-SnRK1* constructs (Figure 1B). SnRK1 $\alpha$  and related kinases require an activation via the phosphorylation of a conserved threonine (Hawley et al., 1996; Baena-González et al., 2007; Broeckx et al., 2016). Using an antibody directed against phospho-AMPK $\alpha$  (Thr172) confirmed diminished protein levels of the active fractions of SnRK1.1 (upper signal) and SnRK1.2 (lower signal) upon amiR induction (Figure 1C, Supplemental Figure 4). Moreover, reduced transcript levels of *DIN1* (Figure 1D), a transcriptional regulation target of SnRK1 (Baena-González et al., 2007), provided evidence that the inducible *SnRK1* knockdown also reduced SnRK1 activity and signalling.

Based on the previous finding that specific AS events can be regulated by the nutritional status as defined by light and sugar availability (Hartmann et al., 2016), we next examined whether knocking down the energy sensor SnRK1 is sufficient to trigger such AS changes. Indeed, we found AS events in *SR30*, *RRC1*, and *PPD2* to be responsive to SnRK1 repression (Figure 1E), providing evidence that SnRK1 signalling can act upstream of light- and sugar-regulated AS events. The light-regulated AS event in *MYBD* did not significantly change in comparison of the estradiol-treated WT and the two *i-amiR* lines (Supplemental Figure 4), suggesting that in this case other regulators are involved or that a different sensitivity threshold with regard to altered SnRK1 signalling exists. Hypocotyl lengths of WT and *i-amiR-SnRK1* seedlings grown for three days in estradiol did not significantly differ between each other (Supplemental Figure 4), suggesting that longer or earlier onset of amiR expression is required to impair hypocotyl growth. Testing the timing of the responses on mRNA level by treating with estradiol for different durations, we observed that levels of *SnRK1.1* and *SnRK1.2*

transcripts were already strongly reduced after 1 d, while the downstream responses, i.e., the decrease in *DIN1* and the AS ratio of *SR30*, became more pronounced after longer exposure to estradiol for 3 and 6 d (Supplemental Figure 5). We also examined whether exposing etiolated seedlings for 6 h to light and/or sucrose impairs SnRK1 activity given that AS shifts and changes in *DIN* transcript levels can be observed within this time interval (Hartmann et al., 2016). While transcript levels in particular for *SnRK1.1* were slightly reduced, no significant changes in pSnRK1.1 and pSnRK1.2 were detectable (Supplemental Figure 6), suggesting unaltered SnRK1 activity or that the level of phosphorylated SnRK1 proteins detected here via phosphoblots may not fully reflect the SnRK1 signalling status under these conditions. In line with the second interpretation, determining in parallel SnRK1 activity and protein levels of the phosphorylated and non-phosphorylated forms of SnRK1 during bean seed development also did not reveal a direct correlation (Coello and Martínez-Barajas, 2014). We conclude from our observations that plant SnRK1 possesses an expanded action spectrum, which in addition to the previously reported major functions in the regulation of metabolism and transcription via the phosphorylation of enzymes and transcription factors (Sakr et al., 2018; Li and Sheen, 2016; Broeckx et al., 2016; Xiong et al., 2013), respectively, also includes the control of AS decisions. The recent report of SnRK1-mediated phosphorylation of a histone demethylase allowing de-repression of starvation-responsive genes in rice (Wang et al., 2021) further highlights that SnRK1 can control gene expression via a diverse range of mechanisms.

Having established an inducible knockdown system, we examined SnRK1's role in early seedling development at conditions of different energy availability. Simultaneously knocking down *SnRK1.1* and *SnRK1.2* strongly reduced hypocotyl elongation in 6-d-old etiolated seedlings, whereas the single T-DNA insertion mutant *snrk1.1-3* showed WT-like skotomorphogenic development (Figure 2A). Seedling growth at low ( $10 \mu\text{mol m}^{-2} \text{s}^{-1}$ ), medium ( $140 \mu\text{mol m}^{-2} \text{s}^{-1}$ ), and high ( $300 \mu\text{mol m}^{-2} \text{s}^{-1}$ ) light intensity revealed reduced growth and chlorophyll content in the *i-amiR-SnRK1* lines in all three conditions, whereas the single *snrk1.1-3* mutant again was indistinguishable from the WT (Figure 2B, C; Supplemental Figure 7). Interestingly, growth and chlorophyll content of the *i-amiR* mutant lines was most reduced at the low light intensity. In agreement with our findings and using the aforementioned system of an inducible *amiR* against *SnRK1.2* in a *snrk1.1* T-DNA mutant background, Henninger et al. (2021) recently showed the requirement of SnRK1 for the mobilization of seed

storage compounds and proper seedling establishment upon growing *A. thaliana* in light/dark cycles. Taken together, these data underline the critical functions of SnRK1 signalling under conditions of limited energy availability, but also demonstrate the strict requirement of SnRK1 for proper development in both darkness and light.

To expand our analysis how energy signalling can control AS and seedling development, we next wanted to study the role of TOR. In general, TOR is activated when ample levels of nutrients are available, while low energy levels trigger SnRK1 activation that can suppress TOR signalling, as shown for human cells (Gwinn et al., 2008) and as it was also concluded from findings in plants (Nukarinen et al., 2016). The sequestration of SnRK1 in SnRK2-containing complexes was recently described as a novel mechanism to protect TOR from inhibition under growth-promoting conditions (Belda-Palazón et al., 2020). TOR has been implicated in various physiological processes, including glucose-promoted hypocotyl elongation of dark-grown seedlings via phosphorylation of ethylene-insensitive protein 2 (EIN2) that prevents its nuclear localisation and downstream signalling (Fu et al., 2021). TOR can also promote hypocotyl growth via the accumulation of BZR1, a transcription factor in the brassinosteroid pathway (Zhang et al., 2016) and regulate cell expansion in the root via establishing an auxin gradient (Yuan et al., 2020). TOR signalling is also involved in the regulation of the circadian clock in response to glucose, which can be blocked by elevated levels of the metabolite nicotinamide in *A. thaliana* (Zhang et al., 2019). Moreover, a recent study (Riegler et al., 2021) provided first evidence that TOR is required for proper light- and sugar-regulated AS changes in roots. Despite the growing list of functions demonstrated to depend on signalling via SnRK1 or TOR, as well as first evidence for their co-regulation in plants, only little is known about their individual contributions and, even more significantly, their cross-talk in specific developmental processes and stress responses (Margalha et al., 2019).

As previous studies of T-DNA insertion mutants revealed that a complete loss of TOR function in *A. thaliana* is lethal (Menand et al., 2002; Ren et al., 2011), we generated an estradiol-responsive *i-amiR-TOR* line. This genetic tool allowed us to examine the role of TOR signalling under the same conditions as described in the previous sections for SnRK1. In the absence of estradiol, the mutant's phenotype was unaltered compared to the WT (Supplemental Figure 8). Induction of amiR expression at the seedling stage caused strongly reduced *TOR* transcript level (Figure 3A), whereas no significant change was seen on the TOR protein level (Supplemental Figure 8).



However, assessing the level of the phosphorylated form of the known TOR target S6K1 (pS6K1, Xiong and Sheen, 2012) supported the assumption that TOR activity was reduced upon amiR induction (Supplemental Figure 8). We next tested whether impaired TOR signalling also has an effect on the AS outcome in etiolated seedlings. Interestingly, inhibition of TOR signalling similarly changed the patterns of light- and sugar-responsive AS events (Figure 3B, Supplemental Figure 8) as observed upon SnRK1 knockdown. In line with our observations here for etiolated seedlings, TOR kinase was recently reported to be required for proper AS responses in roots of light-grown seedlings after an extended dark period (Riegler et al., 2021). Accordingly, the authors observed that inhibition of TOR signalling using either chemical treatment or an RNAi approach can impair sugar- and light-regulated AS pattern changes in roots and to some extent also in leaves.

TOR repression in etiolated seedlings also strongly reduced hypocotyl growth (Figure 3C, Supplemental Figure 8). In contrast, the root length of the etiolated *i-amiR-TOR* seedlings was increased compared to the WT (Supplemental Figure 8), arguing against a general growth impairment upon TOR suppression. Moreover, induction of amiR expression in the etiolated seedlings caused hypocotyl bending compared to the vertical orientation seen under mock conditions and in the WT (Figure 3D). TOR's function in gravity-dependent growth is also supported by the previous observation of impaired root gravitropism in a *TOR RNAi* line and upon application of the TOR inhibitor Torin-1 in *A. thaliana* seedlings (Schepetilnikov et al., 2013). In line with a reduced skotomorphogenic response, as reflected by reduced and increased lengths of hypocotyls and roots, respectively, a substantial fraction of the 4-d-old *i-amiR-TOR* seedlings had opened cotyledons when grown horizontally on estradiol-containing plates in darkness (Supplemental Figure 9). A smaller fraction displayed closed cotyledons, while the majority of mutant seedlings still had their seed coat attached. Taken together, both TOR and SnRK1 are required in *A. thaliana* seedlings for proper skotomorphogenesis in darkness as well as for regular development in light. Given that these processes require the presence of both kinases and that SnRK1 was previously shown to suppress TOR activity (Nukarinen et al., 2016; Belda-Palazón et al., 2020), we tested for a potential reverse feedback control of SnRK1 activity by TOR. Interestingly, reduced TOR activity resulted in even lower transcript levels of the SnRK1 target *DIN1*, while the phosphorylated forms of SnRK1.1 and SnRK1.2 proteins

were not significantly different in comparison of mock- and estradiol-treated seedlings (Supplemental Figure 9).

We next examined whether impairment of either SnRK1 or TOR signalling also similarly affects the developmental response in the transition phase from darkness to light, based on the measurement of cotyledon opening kinetics for etiolated seedlings upon exposure to white light. Knocking down *SnRK1* and *TOR* both strongly impaired cotyledon opening, as evidenced on the level of opening percentages and average cotyledon angles measured after 6, 12, 24, 48, and 72 h of white light exposure (Figure 4A-C, Supplemental Figure 10). In general, cotyledon opening was even stronger delayed in the *i-amiR-TOR* line compared to the two *i-amiR-SnRK1* lines, which may be explained by the level of inhibition or different contributions of the two pathways. A similar extent of delayed cotyledon opening in response to white light was also seen in a previous study upon knocking down TOR via an inducible RNAi approach (Chen et al., 2018). We conclude from these data that SnRK1 and TOR are required to elicit a full photomorphogenic response upon illumination of etiolated seedlings, whereas in darkness both kinases contribute to suppression of photomorphogenesis.

In conclusion, we have demonstrated that both SnRK1 and TOR can function in the upstream signalling of light- and sugar-regulated AS events, identifying an additional mode of action used by these two central energy sensor kinases to control gene expression and physiological responses. The observation that knocking down SnRK1 in etiolated seedlings triggers similar AS shifts as observed upon light and sugar exposure (Hartmann et al., 2018; Hartmann et al., 2016) is in line with the model that this signalling pathway is mainly active under energy-deprived conditions. Studying in parallel the role of TOR signalling, however, revealed that its suppression comparably alters the AS outcome in dark-grown seedlings as observed upon *SnRK1* knockdown, despite TOR's assumably in general opposing function as regulatory hub at conditions of sufficient energy supply. Moreover, we found that both SnRK1 and TOR are required for proper skoto- and photomorphogenic seedling development. Interestingly, the functions of SnRK1 and TOR changed in response to the environmental input, acting as repressors and activators of photomorphogenesis, respectively, during skotomorphogenesis and upon illumination of etiolated seedlings. Accordingly, both kinases support the developmental program as defined by the environmental condition, i.e., darkness or light in our experimental setup.

Previous transcriptome studies provided evidence for at least partially antagonistic SnRK1- and TOR-specific signatures of gene expression (Margalha et al., 2019). However, only little is known about the direct cross-talk of SnRK1 and TOR signalling and its implications in plants, as most studies of their mechanisms and functions were restricted to only one of these two pathways. The best studied process in this regard is autophagy, for which the analysis of overexpression and partial knockdown mutants for SnRK1 and TOR revealed their role as activator and repressor, respectively (Soto-Burgos et al., 2018). SnRK1 homologs in animals and yeast have been demonstrated to act upstream of TOR as repressors (Margalha et al., 2019), and evidence for the existence of a similar regulatory relationship in plants was provided (Nukarinen et al., 2016). The inducible knockdown lines established here provide suitable tools to study under identical experimental conditions specific and overlapping functions of SnRK1 and TOR. It seems likely that not only seedling development, but also other physiological processes require concurrent activities of SnRK1 and TOR, which are fine-balanced in response to altered energy availability as opposed to a complete switch between the two sensor systems. Such a simple “yin-yang” model with opposing activities of SnRK1 and TOR was also questioned in the context of plant stress responses (Rodriguez et al., 2019). Moreover, Peixoto et al. (2021) proposed oscillation in SnRK1 activity reaching its maximum and minimum at the end of the night and day, respectively. In agreement with our observation that SnRK1 is also needed for regular seedling development under conditions of sufficient energy supply, SnRK1’s requirement in the regulation of metabolism and gene expression in rosettes of *A. thaliana* plants grown under favourable conditions was recently reported (Peixoto et al., 2021).

Based on these observations we propose a model that simultaneous activities of SnRK1 and TOR occur and are required throughout plant development (Figure 4D). Changes in the nutritional status are expected to affect SnRK1 and TOR signalling in an antagonistic manner, e.g., in response to the consumption of storage compounds during skotomorphogenesis. Whereas day/night cycles could trigger oscillating activity patterns for both kinases, as proposed in case of SnRK1 (Peixoto et al., 2021) and in line with the finding that TOR signalling is linked to the circadian clock (Zhang et al., 2019). Key for the activation of SnRK1- and TOR-dependent downstream processes, including an altered AS output as demonstrated here, may be the tipping points in their activity profiles at major transitions, such as upon illumination of etiolated seedlings or

in response to stress exposure. The inducible knockdown of SnRK1 and TOR used in this study could mimic such a state transition involving a change in only one of the components, whereas under natural conditions in general opposite changes for the two energy sensors would be expected. Accordingly, a similar transitional response as part of a general adaptation process may be observed upon the induction of amiRs against *SnRK1* and *TOR*. As a major advantage of such a regulatory system compared to a threshold-dependent triggering mode, plants could more rapidly respond to changes in their nutritional status and easier maintain metabolic homeostasis despite the fluctuating and often highly variable environmental conditions. Future research will need to address these key aspects of SnRK1 and TOR signalling, in particular how their activities are modulated during development and in stress responses, what kind of signals are responsible for the activation of downstream responses, and how signal integration is achieved. Moreover, we also need to obtain a better understanding of the mechanistic links of SnRK1 and TOR signalling to AS regulation, e.g., by testing whether SnRK1 and TOR can directly phosphorylate splicing regulators to induce AS shifts. Interestingly, a phosphoproteome analysis of light-grown *A. thaliana* seedlings treated with Torin2 for the inhibition of TOR signalling revealed the differential phosphorylation of multiple RNA-binding proteins including RNA splicing regulators (Scarpin et al., 2020). Follow-up studies making use of our inducible mutants to suppress SnRK1 and TOR signalling during the response of etiolated seedlings to light and sugar signals will help to address the questions whether splicing regulators are directly phosphorylated by these energy sensor kinases and how this can contribute to the observed AS pattern changes.

## Methods

**Plant material, growth conditions, and phenotyping.** All mutant and WT seeds used in this study were in *Arabidopsis thaliana* Col-0 background. The *i-amiR-TOR* line additionally contained the *WUSCHEL/CLAVATA3* reporter (Pfeiffer et al., 2016). The T-DNA insertion line *snrk1.1-3* (GABI\_579E09) was previously described (Mair et al., 2015). Seeds were surface sterilized in 3.75% NaOCl and 0.01% Triton X-100 and plated on ½ strength Murashige and Skoog (MS) medium (Duchefa, Haarlem, Netherlands), pH 5.7 – 5.8, containing 0.8% plant agar (Duchefa). Depending on the experiment, MS media was lacking or containing 1% or 2% sucrose, as well as 5 µM β-Estradiol (Sigma-Aldrich, St Louis, MO, US) or an equivalent concentration of DMSO (mock).

For segregation analyses of constitutive amiR-SnrRK1 lines, seeds were plated singly on ½ MS plates containing 1% sucrose, 5 mg/L Basta (Bayer, Leverkusen, Germany) and 0.8% plant agar. After stratification (2 days at 4 °C), plates were transferred to regular light (~100 µmol m<sup>-2</sup> s<sup>-1</sup>) and seedlings were grown for 2 weeks at 22 °C, and 60% relative humidity under long day (16-h light/8-h dark) conditions. Plates without sucrose and Basta for WT growth served as controls. After 2 weeks, resistant seedlings were transferred to soil. Transferred plants were grown under a long day regime (16-h light/8-h dark) with a regular light intensity (~100 µmol m<sup>-2</sup> s<sup>-1</sup>) at 22 °C. For phenotypical analysis, plants were rated daily regarding their developmental stage and pictures were taken weekly with a Nikon D3200 camera.

**Hypocotyl assay.** To measure hypocotyl length, seedlings were grown on either 5 µM β-Estradiol-containing or mock solid ½ MS plates without sucrose. Alternatively, seedlings were grown in liquid ½ MS media, and β-Estradiol and mock solution was added after 3 d of growth, respectively. After stratification (2 days at 4 °C), germination was induced by a 2 h light treatment (~100 µmol m<sup>-2</sup> s<sup>-1</sup>) and plates were placed in darkness. 6-d-old seedlings were transferred to ½ MS plates containing 1.5% agar. Plates were scanned and hypocotyl length was measured using ImageJ.

**Cotyledon opening assay.** 4-d-old etiolated seedlings were grown horizontally on ½ MS plates supplemented with 5 µM β-Estradiol and DMSO, respectively. Cotyledon opening percentages were determined in darkness, by analysing three independent experiments. Seedlings with the seed coat still attached to the cotyledons were counted separately.

**Cotyledon opening kinetic assay.** Surfaced sterilized seeds were placed singly on ½ MS plates containing 1.5% plant agar, in the presence or absence of  $\beta$ -Estradiol. After vernalization for 2 days at 4 °C, germination was induced by white light ( $\sim 100 \mu\text{mol m}^{-2} \text{s}^{-1}$ ) for 2 h. Seedlings were grown vertically in darkness for 4 d and then shifted to white light ( $15 \mu\text{mol m}^{-2} \text{s}^{-1}$ ). If seed coat was still present on cotyledons, it was gently removed at the 0 h time point. Cotyledon opening percentages and angles between the cotyledons were analysed at 6, 12, 24, 48 and 72 h. Cotyledons open more than 8° were counted as opened cotyledons. The degree of cotyledon opening was measured with ImageJ.

**Plasmid constructions and generation of transgenic plants.** Two independent amiR sequences for targeting both *SnRK1.1* and *SnRK1.2* (Supplemental Figure 1) were identified and corresponding cloning primers (Supplemental Table 2) designed using the Web MicroRNA Designer (WMD3, <http://wmd3.weigelworld.org>; Schwab et al., 2006; Ossowski et al., 2008). The 35S promoter-driven constructs for constitutive amiR expression (*amiR-SnRK1-I/II*) were generated via Gateway cloning (Invitrogen, Carlsbad, CA, US). Site-directed mutagenesis on pRS300 was performed in three single PCR reactions using Herculase II Fusion DNA Polymerase (Agilent Technologies, Santa Clara, CA, US) and the following primer combinations: For amiR-I, SL11/TW026, TW024/TW025, and SL12/TW023. For amiR-II, SL11/TW030, TW028/TW029, and SL12/TW027. The purified PCR products were mixed with the primer pair SL11/SL12 to perform an overlap PCR for each construct generating the corresponding amiR precursor sequence flanked by *attB* sites. Performing the BP reaction, the DNA insert was introduced into the entry vector pDONR201 (Karimi et al., 2002). Subsequently, the amiR-containing sequences were transferred into the expression vector pB7WG2 via the LR reaction (Karimi et al., 2002).

The constructs for Inducible amiR expression were cloned using the GreenGate system (Lampropoulos et al., 2013). The DNA fragments corresponding to the amiR sequences were generated by overlap PCR, as described before for the constitutive constructs, but using TW080/TW081 as outer primers. The amiR precursor sequences were integrated into the entry vector pGGC000 by restriction with *BsaI* HF (NEB, Ipswich, MA, US) and subsequent ligation using T4 DNA ligase (Thermo Fisher Scientific, Waltham, MA, US), resulting in pGGCTW01 and pGGCTW02 with the *amiR-SnRK1* sequences, and in pAP039 with the *amiR-TOR* sequence. The expression cassettes for XVE and the amiR-containing sequences were assembled and ligated to

intermediate vectors following the procedure described in Lampropoulos et al. (2013). The module pGGC124, containing the cds of chimeric TF XVE, was generated by amplification of the cds from the plasmid pLB12 (PMID: 16896232; Brand et al., 2006) in two PCRs with primers P-878/P-879 and P-880/P-881 to remove the internal *Bsal* site, followed by cloning via flanking *Bsal* sites into pGGC. The combination of modules for generating intermediate vectors pGGMTW01, pGGNTW01, pGGNTW02, pAP039, and pAP043 are listed in Supplemental Table 3. Finally, the expression cassettes were combined using the FH and HA adapter sequences. In case of the *i-amiR-SnRK1* constructs, the XVE-encoding vector pGGMTW01 was mixed with the destination vector pGGZ003 and either pGGNTW01 or pGGNTW02, resulting in the final constructs pGGZTW01 and pGGZTW02, respectively. For the *i-amiR-TOR* construct, the amiR sequence-containing vector pAP039 was mixed with the destination vector pGGZ003 and pAP043, resulting in the final construct pAP044.

For generating the respective *A. thaliana* (Col-0) mutants, the final Gateway and GreenGate constructs were transformed into *Agrobacterium tumefaciens* strain C58C1 or ASE, respectively, followed by the floral dip method (Clough and Bent, 1998). The *i-amiR-TOR* construct was transformed into the *A. thaliana* (Col-0) background of the *WUSCHEL/CLAVATA3* reporter (Pfeiffer et al., 2016).

**Chlorophyll content measurements.** For chlorophyll content analyses, seeds were plated on ½ MS medium supplemented with either 5 µM β-Estradiol or mock and stratified for 2 days at 4 °C. Plates were transferred to low (10 µmol m<sup>-2</sup> s<sup>-1</sup>), regular (140 µmol m<sup>-2</sup> s<sup>-1</sup>) or high (300 µmol m<sup>-2</sup> s<sup>-1</sup>) intensities of white light, followed by plant growth under long day conditions (16-h light/8-h dark). After 14 d, seedlings were photographed, and representative seedlings transferred to ½ MS plates containing 1.5% agar that were then used for scanning. Furthermore, seedlings (22 – 250 mg) were harvested for chlorophyll content measurements, resuspended in 200 µL phosphate buffer [25 mM KH<sub>2</sub>PO<sub>4</sub>, 25 mM K<sub>2</sub>HPO<sub>4</sub> pH 7.0 and 2 mM EDTA (pH 8.0)] and chlorophyll was extracted with 800 µL 100% acetone. Mixtures were incubated for 1 h at room temperature under constant shaking. Subsequently, samples were centrifuged for 2 min at 10.000g and 4°C and supernatants were used for spectrophotometric analysis at 646 nm, 663 nm and 750 nm, respectively. Total chlorophyll was calculated using the previously described formula  $17.76 * OD_{646} + 7.34$

\*  $OD_{663}/1000 \cdot V/FW$ , where  $V$  indicates the volume (mL) and  $FW$  the fresh weight (g) (Porra et al., 1989).

**Light and sucrose treatments.** For light and sucrose treatments, WT seedlings were grown in liquid  $\frac{1}{2}$  MS media in darkness. After 6 d, 1.06% mannitol or 2% sucrose was added to the media. Subsequently, seedlings were either kept in darkness or transferred to white light ( $\sim 100 \mu\text{mol m}^{-2} \text{s}^{-1}$ ) and incubated for 6 h.

**RNA extraction, RT-qPCR, and PCR product analyses.** RNA isolation was performed using the Universal RNA purification kit (Roboklon, EURx, Berlin, Germany). Possible DNA contaminations were eliminated with an on-column DnaseI digest. cDNAs were generated with Superscript II Reverse Transcriptase (Invitrogen, Carlsbad, CA, US) following the manufacturer's instructions. RT-qPCR was performed using the MESA GREEN qPCR Mastermix and a CFX384 real-time PCR cycler (Bio-Rad, Hercules, CA, US). *PP2A* (*AT1G13320*) served as reference transcript for normalisation. A detailed protocol for the RT-qPCR analysis was previously described (Stauffer et al., 2010). For some events, splice variants were co-amplified via RT-PCR and isoform concentrations were determined using the 2100 Bioanalyzer with the DNA1000 kit (Agilent Technologies, Santa Clara, CA, US). The oligonucleotides used for RT-qPCR and RT-PCR are listed in Supplemental Table 4.

**Protein extraction and immunoblot analyses.** If not stated otherwise, immunoblot analyses were carried out as previously described (Hartmann et al., 2016). In brief, 0.2 g of 6-d-old etiolated seedlings were freeze grounded to powder and homogenized in 0.2 mL extraction buffer [50 mM Tris-HCl (pH 7.5), 150 mM NaCl, 0.1% (v/v) Tween 20, 0.1% (v/v)  $\beta$ -mercaptoethanol, 1x protease inhibitor cocktail (Roche) and PhosSTOP™ (Roche)]. Lysates were clarified by centrifugation at 15.000g and 4 °C for 15 min and proteins were denatured by boiling (5 min at 95 °C) in SDS sample buffer. Samples were separated by SDS-PAGE and transferred to a nitrocellulose membrane using semi-dry transfer (transfer buffer: 25 mM Tris, 142 mM glycine, 20% ethanol). Membranes were probed with commercial antibodies: rabbit  $\alpha$ -AKIN10 (AS10919; Agrisera, Vännäs, Sweden), rabbit  $\alpha$ -pAMPK (T172) (2531; Cell Signaling Technology, Danvers, MA, US), rabbit  $\alpha$ -S6K1/2 (AS121855; Agrisera, Vännäs, Sweden), rabbit  $\alpha$ -S6K1 (phospho T449) (ab207399; abcam, Cambridge, UK), and rabbit  $\alpha$ -tubulin (AS10680; Agrisera, Vännäs, Sweden). Anti-rabbit secondary antibody



conjugated with horseradish peroxidase (A6154, Sigma-Aldrich, St Louis, MO, US) was used at 1:10,000 in 5% skim milk in TBST for 1 h.

For immunoblotting TOR and pAMPK in WT and *i-amiR-TOR* seedlings, a modified protocol was used. In brief, etiolated WT and *i-amiR-TOR* seedlings (50 – 200 mg) were grown in liquid ½ MS for 3 d and subjected to 5 µM β-Estradiol- or mock treatment for further 3 d. Seedlings were collected in darkness, flash frozen and ground in liquid nitrogen. Proteins were extracted with 1:1 ratio (mg/µL) 95 °C-pre-heated denaturing buffer [100 mM MOPS (pH 7.6), 100 mM NaCl, 5% SDS, 10% glycerol, 4 mM EDTA, 40 mM β-mercaptoethanol, 2 mM PMSF, 1x protease inhibitor cocktail (Roche)] and boiled at 95 °C for 5 min. Cell debris were removed by two centrifugation steps (10 min, 16.000g, room temperature). Proteins were separated on a 6% (for TOR) and 10% (for pAMPK) SDS gel and transferred to PVDF using wet transfer (standard settings: 1 h, 110 V at 4 °C). For immunoblotting TOR, proteins were transferred in 1 h, 400 V at 4°C using a modified transfer buffer (25 mM Tris, 142 mM glycine, 5% methanol). Membranes were blocked for 1 h and then incubated with rabbit α-pAMPK (T172) (2535; Cell Signaling Technology, Danvers, MA, US) or rabbit α-TOR (AS12 2608, Agrisera, Vännäs, Sweden) at least overnight at 4 °C.

Chemiluminescence was imaged using the Fusion Fx system (Vilber, Collégien, France). The relative band intensities were quantified using the quantification tool of the Evolution-Capt Edge program. Tubulin was detected as a loading control and results were quantified by calculating the volume ratio of AKIN10, pAMPK, or TOR to tubulin.

**Statistical analysis.** All data measurements were taken from distinct samples. Statistical analyses were performed with GraphPad Prism 8.0.2 (GraphPad Software, Inc., CA, US). Statistical details of each experiment including biological replicates (*n*), types of error bars and used test including whether they were one- or two-sided are defined in the results and figure legend sections. The significance level was set to 0.05 in all cases. The following tests and parameter settings were used according to the description in GraphPad Prism. Standard unpaired *t*-test, assuming Gaussian distribution and same standard deviation of both groups. Unequal variance *t*-test (Welch *t*-test) for two groups of data sampled from Gaussian populations, but assuming varying standard deviation. One-sample *t*-test comparing the mean of a data set derived from an assumably Gaussian population to a provided hypothetical mean of 1,

by calculating the  $t$  ratio from dividing the difference between the actual and hypothetical means by the standard error of the mean. One-way ANOVA with posthoc Tukey test, assuming Gaussian distribution and equal standard deviation, and using multiple comparisons of every mean with every other mean. Further details and results of all statistical analysis are provided in Supplemental Data File 1.

Created box plots range from the 25<sup>th</sup> to 75<sup>th</sup> percentiles, and whiskers extend to 1.5x the interquartile range (IQR). Outliers are considered if the value is greater than the sum of the 75<sup>th</sup> percentile plus 1.5 IQR or smaller than the 25<sup>th</sup> percentile minus 1.5 IQR.

### **Accession numbers**

Sequence data from this article can be found in the EMBL/GenBank data libraries under accession numbers: AT3G01090 (SnRK1.1), AT3G29160 (SnRK1.2), AT1G50030 (TOR), AT1G09140 (SR30), AT5G25060 (RRC1), AT1G70000 (MYBD), AT4G14720 (PPD2), AT1G13320 (PP2A).

### **Acknowledgements**

We thank Claudia König for technical assistance and Moritz Denecke for performing an independent replicate analysing cotyledon opening in darkness. This research project was supported by the German Research Foundation (Deutsche Forschungsgemeinschaft – DFG: SFB1101/C03 to A.W. and SFB1101/B07 to J.L.), as well as the European Research Council (ERC grant 282139 “StemCellAdapt” to J. L.).

### **Author contributions**

J.S., T.W.K. and A.W. designed experiments. J.S. and T.W.K. performed experiments and analysed data. Inducible amiR-SnRK1 lines were generated and characterized by T.W.K. J.S. supported T.W.K. in splice pattern analyses and performed chlorophyll assays. J.S. was mainly performing experiments involving the amiR-TOR line, except the hypocotyl assay (6 d dark) that was done by T.W.K and the root assay that was done by D.J. J.S. performed cotyledon opening experiments in different mutant lines. K.E. performed phenotyping experiments of constitutive amiR-SnRK1 lines, which were generated and characterized by T.W.K. with the help of D.M.O. The amiR-TOR line was generated and initially characterized by A.P. and D.J. under supervision of J.L. The manuscript was mainly written by J.S., T.W.K. and A.W. All authors

contributed to data interpretation and approved the manuscript. A.W. conceived the project and supervised the research.

## References

- Baena-González, E., Rolland, F., Thevelein, J.M., and Sheen, J. (2007). A central integrator of transcription networks in plant stress and energy signalling. *Nature* 448 (7156): 938–942.
- Belda-Palazón, B., Adamo, M., Valerio, C., Ferreira, L.J., Confraria, A., Reis-Barata, D., Rodrigues, A., Meyer, C., Rodriguez, P.L., and Baena-González, E. (2020). A dual function of SnRK2 kinases in the regulation of SnRK1 and plant growth. *Nature plants* 6 (11): 1345–1353.
- Brand, L., Hörler, M., Nüesch, E., Vassalli, S., Barrell, P., Yang, W., Jefferson, R.A., Grossniklaus, U., and Curtis, M.D. (2006). A versatile and reliable two-component system for tissue-specific gene induction in *Arabidopsis*. *Plant physiology* 141 (4): 1194–1204.
- Broeckx, T., Hulsmans, S., and Rolland, F. (2016). The plant energy sensor: Evolutionary conservation and divergence of SnRK1 structure, regulation, and function. *Journal of experimental botany* 67 (22): 6215–6252.
- Chen, G.-H., Liu, M.-J., Xiong, Y., Sheen, J., and Wu, S.-H. (2018). TOR and RPS6 transmit light signals to enhance protein translation in deetiolating *Arabidopsis* seedlings. *Proceedings of the National Academy of Sciences of the United States of America* 115 (50): 12823–12828.
- Clough, S.J., and Bent, A.F. (1998). Floral dip: A simplified method for *Agrobacterium*-mediated transformation of *Arabidopsis thaliana*. *The Plant journal for cell and molecular biology* 16 (6): 735–743.
- Coello, P., and Martínez-Barajas, E. (2014). SnRK1 is differentially regulated in the cotyledon and embryo axe of bean (*Phaseolus vulgaris* L) seeds. *Plant physiology and biochemistry PPB* 80: 153–159.
- Emanuelle, S., Hossain, M.I., Moller, I.E., Pedersen, H.L., van de Meene, A.M.L., Doblin, M.S., Koay, A., Oakhill, J.S., Scott, J.W., Willats, W.G.T., Kemp, B.E.,

- Bacic, A., Gooley, P.R., and Stapleton, D.I. (2015). SnRK1 from *Arabidopsis thaliana* is an atypical AMPK. *The Plant journal for cell and molecular biology* 82 (2): 183–192.
- Fu, L., Liu, Y., Qin, G., Wu, P., Zi, H., Xu, Z., Zhao, X., Wang, Y., Li, Y., Yang, S., Peng, C., Wong, C.C.L., Yoo, S.-D., Zuo, Z., Liu, R., Cho, Y.-H., and Xiong, Y. (2021). The TOR-EIN2 axis mediates nuclear signalling to modulate plant growth. *Nature* 591 (7849): 288–292.
- Galvão, V.C., and Fankhauser, C. (2015). Sensing the light environment in plants: Photoreceptors and early signaling steps. *Current opinion in neurobiology* 34: 46–53.
- Gwinn, D.M., Shackelford, D.B., Egan, D.F., Mihaylova, M.M., Mery, A., Vasquez, D.S., Turk, B.E., and Shaw, R.J. (2008). AMPK phosphorylation of raptor mediates a metabolic checkpoint. *Molecular Cell* 30 (2): 214–226.
- Hartmann, L., Drewe-Boß, P., Wießner, T., Wagner, G., Geue, S., Lee, H.-C., Obermüller, D.M., Kahles, A., Behr, J., Sinz, F.H., Rättsch, G., and Wachter, A. (2016). Alternative Splicing Substantially Diversifies the Transcriptome during Early Photomorphogenesis and Correlates with the Energy Availability in *Arabidopsis*. *The Plant cell* 28 (11): 2715–2734.
- Hartmann, L., Wießner, T., and Wachter, A. (2018). Subcellular Compartmentation of Alternatively Spliced Transcripts Defines SERINE/ARGININE-RICH PROTEIN30 Expression. *Plant physiology* 176 (4): 2886–2903.
- Hawley, S.A., Davison, M., Woods, A., Davies, S.P., Beri, R.K., Carling, D., and Hardie, D.G. (1996). Characterization of the AMP-activated protein kinase kinase from rat liver and identification of threonine 172 as the major site at which it phosphorylates AMP-activated protein kinase. *The Journal of biological chemistry* 271 (44): 27879–27887.
- Henninger, M., Pedrotti, L., Krischke, M., Draken, J., Wildenhain, T., Fekete, A., Rolland, F., Müller, M.J., Fröschel, C., Weiste, C., and Dröge-Laser, W. (2021). The evolutionarily conserved kinase SnRK1 orchestrates resource mobilization during *Arabidopsis* seedling establishment. *The Plant cell*.

- Karimi, M., Inzé, D., and Depicker, A. (2002). GATEWAY vectors for Agrobacterium-mediated plant transformation. *Trends in plant science* 7 (5): 193–195.
- Lampropoulos, A., Sutikovic, Z., Wenzl, C., Maegele, I., Lohmann, J.U., and Forner, J. (2013). GreenGate---a novel, versatile, and efficient cloning system for plant transgenesis. *PloS one* 8 (12): e83043.
- Li, L., Liu, K.-H., and Sheen, J. (2021). Dynamic Nutrient Signaling Networks in Plants. *Annual review of cell and developmental biology* 37: 341–367.
- Li, L., and Sheen, J. (2016). Dynamic and diverse sugar signaling. *Current opinion in plant biology* 33: 116–125.
- Mair, A., Pedrotti, L., Wurzinger, B., Anrather, D., Simeunovic, A., Weiste, C., Valerio, C., Dietrich, K., Kirchler, T., Nägele, T., Vicente Carbajosa, J., Hanson, J., Baena-González, E., Chaban, C., Weckwerth, W., Dröge-Laser, W., and Teige, M. (2015). SnRK1-triggered switch of bZIP63 dimerization mediates the low-energy response in plants. *eLife* 4.
- Mancini, E., Sanchez, S.E., Romanowski, A., Schlaen, R.G., Sanchez-Lamas, M., Cerdán, P.D., and Yanovsky, M.J. (2016). Acute Effects of Light on Alternative Splicing in Light-Grown Plants. *Photochemistry and photobiology* 92 (1): 126–133.
- Margalha, L., Confraria, A., and Baena-González, E. (2019). SnRK1 and TOR: Modulating growth-defense trade-offs in plant stress responses. *Journal of experimental botany* 70 (8): 2261–2274.
- Menand, B., Desnos, T., Nussaume, L., Berger, F., Bouchez, D., Meyer, C., and Robaglia, C. (2002). Expression and disruption of the Arabidopsis TOR (target of rapamycin) gene. *Proceedings of the National Academy of Sciences of the United States of America* 99 (9): 6422–6427.
- Nukarinen, E., Nägele, T., Pedrotti, L., Wurzinger, B., Mair, A., Landgraf, R., Börnke, F., Hanson, J., Teige, M., Baena-Gonzalez, E., Dröge-Laser, W., and Weckwerth, W. (2016). Quantitative phosphoproteomics reveals the role of the AMPK plant ortholog SnRK1 as a metabolic master regulator under energy deprivation. *Scientific reports* 6: 31697.

- Ossowski, S., Schwab, R., and Weigel, D. (2008). Gene silencing in plants using artificial microRNAs and other small RNAs. *The Plant journal for cell and molecular biology* 53 (4): 674–690.
- Peixoto, B., Moraes, T.A., Mengin, V., Margalha, L., Vicente, R., Feil, R., Höehne, M., Sousa, A.G., Lilue, J., Stitt, M., Lunn, J.E., and Baena-Gonzalez, E. (2021). Impact of the SnRK1 protein kinase on sucrose homeostasis and the transcriptome during the diel cycle.
- Petrillo, E., Godoy Herz, M.A., Fuchs, A., Reifer, D., Fuller, J., Yanovsky, M.J., Simpson, C., Brown, J.W.S., Barta, A., Kalyna, M., and Kornblihtt, A.R. (2014). A chloroplast retrograde signal regulates nuclear alternative splicing. *Science (New York, N.Y.)* 344 (6182): 427–430.
- Pfeiffer, A., Janocha, D., Dong, Y., Medzihradzky, A., Schöne, S., Daum, G., Suzaki, T., Forner, J., Langenecker, T., Rempel, E., Schmid, M., Wirtz, M., Hell, R., and Lohmann, J.U. (2016). Integration of light and metabolic signals for stem cell activation at the shoot apical meristem. *eLife* 5.
- Porra, R.J., Thompson, W.A., and Kriedemann, P.E. (1989). Determination of accurate extinction coefficients and simultaneous equations for assaying chlorophylls a and b extracted with four different solvents: Verification of the concentration of chlorophyll standards by atomic absorption spectroscopy. *Biochimica et Biophysica Acta (BBA) - Bioenergetics* 975 (3): 384–394.
- Ramon, M., Dang, T.V.T., Broeckx, T., Hulsmans, S., Crepin, N., Sheen, J., and Rolland, F. (2019). Default Activation and Nuclear Translocation of the Plant Cellular Energy Sensor SnRK1 Regulate Metabolic Stress Responses and Development. *The Plant cell* 31 (7): 1614–1632.
- Ren, M., Qiu, S., Venglat, P., Xiang, D., Feng, L., Selvaraj, G., and Datla, R. (2011). Target of rapamycin regulates development and ribosomal RNA expression through kinase domain in Arabidopsis. *Plant physiology* 155 (3): 1367–1382.
- Riegler, S., Servi, L., Scarpin, M.R., Godoy Herz, M.A., Kubaczka, M.G., Venhuizen, P., Meyer, C., Brunkard, J.O., Kalyna, M., Barta, A., and Petrillo, E. (2021). Light regulates alternative splicing outcomes via the TOR kinase pathway. *Cell Reports* 36 (10).

- Rodriguez, M., Parola, R., Andreola, S., Pereyra, C., and Martínez-Noël, G. (2019). TOR and SnRK1 signaling pathways in plant response to abiotic stresses: Do they always act according to the "yin-yang" model? *Plant science an international journal of experimental plant biology* 288: 110220.
- Sakr, S., Wang, M., Dédaldéchamp, F., Perez-Garcia, M.-D., Ogé, L., Hamama, L., and Atanassova, R. (2018). The Sugar-Signaling Hub: Overview of Regulators and Interaction with the Hormonal and Metabolic Network. *International journal of molecular sciences* 19 (9).
- Scarpin, M.R., Leiboff, S., and Brunkard, J.O. (2020). Parallel global profiling of plant TOR dynamics reveals a conserved role for LARP1 in translation. *eLife* 9.
- Schepetilnikov, M., Dimitrova, M., Mancera-Martínez, E., Geldreich, A., Keller, M., and Ryabova, L.A. (2013). TOR and S6K1 promote translation reinitiation of uORF-containing mRNAs via phosphorylation of eIF3h. *The EMBO journal* 32 (8): 1087–1102.
- Schwab, R., Ossowski, S., Riester, M., Warthmann, N., and Weigel, D. (2006). Highly specific gene silencing by artificial microRNAs in Arabidopsis. *The Plant cell* 18 (5): 1121–1133.
- Shikata, H., Hanada, K., Ushijima, T., Nakashima, M., Suzuki, Y., and Matsushita, T. (2014). Phytochrome controls alternative splicing to mediate light responses in Arabidopsis. *Proceedings of the National Academy of Sciences of the United States of America* 111 (52): 18781–18786.
- Shikata, H., Shibata, M., Ushijima, T., Nakashima, M., Kong, S.-G., Matsuoka, K., Lin, C., and Matsushita, T. (2012). The RS domain of Arabidopsis splicing factor RRC1 is required for phytochrome B signal transduction. *The Plant journal for cell and molecular biology* 70 (5): 727–738.
- Soto-Burgos, J., Zhuang, X., Jiang, L., and Bassham, D.C. (2018). Dynamics of Autophagosome Formation. *Plant physiology* 176 (1): 219–229.
- Stauffer, E., Westermann, A., Wagner, G., and Wachter, A. (2010). Polypyrimidine tract-binding protein homologues from Arabidopsis underlie regulatory circuits based on alternative splicing and downstream control. *The Plant journal for cell and molecular biology* 64 (2): 243–255.

- Wang, W., Lu, Y., Li, J., Zhang, X., Hu, F., Zhao, Y., and Zhou, D.-X. (2021). SnRK1 stimulates the histone H3K27me3 demethylase JMJ705 to regulate a transcriptional switch to control energy homeostasis. *The Plant cell* 33 (12): 3721–3742.
- Xin, R., Kathare, P.K., and Huq, E. (2019). Coordinated Regulation of Pre-mRNA Splicing by the SFPS-RRC1 Complex to Promote Photomorphogenesis. *The Plant cell* 31 (9): 2052–2069.
- Xin, R., Zhu, L., Salomé, P.A., Mancini, E., Marshall, C.M., Harmon, F.G., Yanovsky, M.J., Weigel, D., and Huq, E. (2017). SPF45-related splicing factor for phytochrome signaling promotes photomorphogenesis by regulating pre-mRNA splicing in Arabidopsis. *Proceedings of the National Academy of Sciences of the United States of America* 114 (33): E7018-E7027.
- Xiong, Y., McCormack, M., Li, L., Hall, Q., Xiang, C., and Sheen, J. (2013). Glucose-TOR signalling reprograms the transcriptome and activates meristems. *Nature* 496 (7444): 181–186.
- Xiong, Y., and Sheen, J. (2012). Rapamycin and glucose-target of rapamycin (TOR) protein signaling in plants. *The Journal of biological chemistry* 287 (4): 2836–2842.
- Yuan, X., Xu, P., Yu, Y., and Xiong, Y. (2020). Glucose-TOR signaling regulates PIN2 stability to orchestrate auxin gradient and cell expansion in Arabidopsis root. *Proceedings of the National Academy of Sciences of the United States of America* 117 (51): 32223–32225.
- Zhang, N., Meng, Y., Li, X., Zhou, Y., Ma, L., Fu, L., Schwarzländer, M., Liu, H., and Xiong, Y. (2019). Metabolite-mediated TOR signaling regulates the circadian clock in Arabidopsis. *Proceedings of the National Academy of Sciences of the United States of America* 116 (51): 25395–25397.
- Zhang, Z., Zhu, J.-Y., Roh, J., Marchive, C., Kim, S.-K., Meyer, C., Sun, Y., Wang, W., and Wang, Z.-Y. (2016). TOR Signaling Promotes Accumulation of BZR1 to Balance Growth with Carbon Availability in Arabidopsis. *Current biology CB* 26 (14): 1854–1860.



Main figures

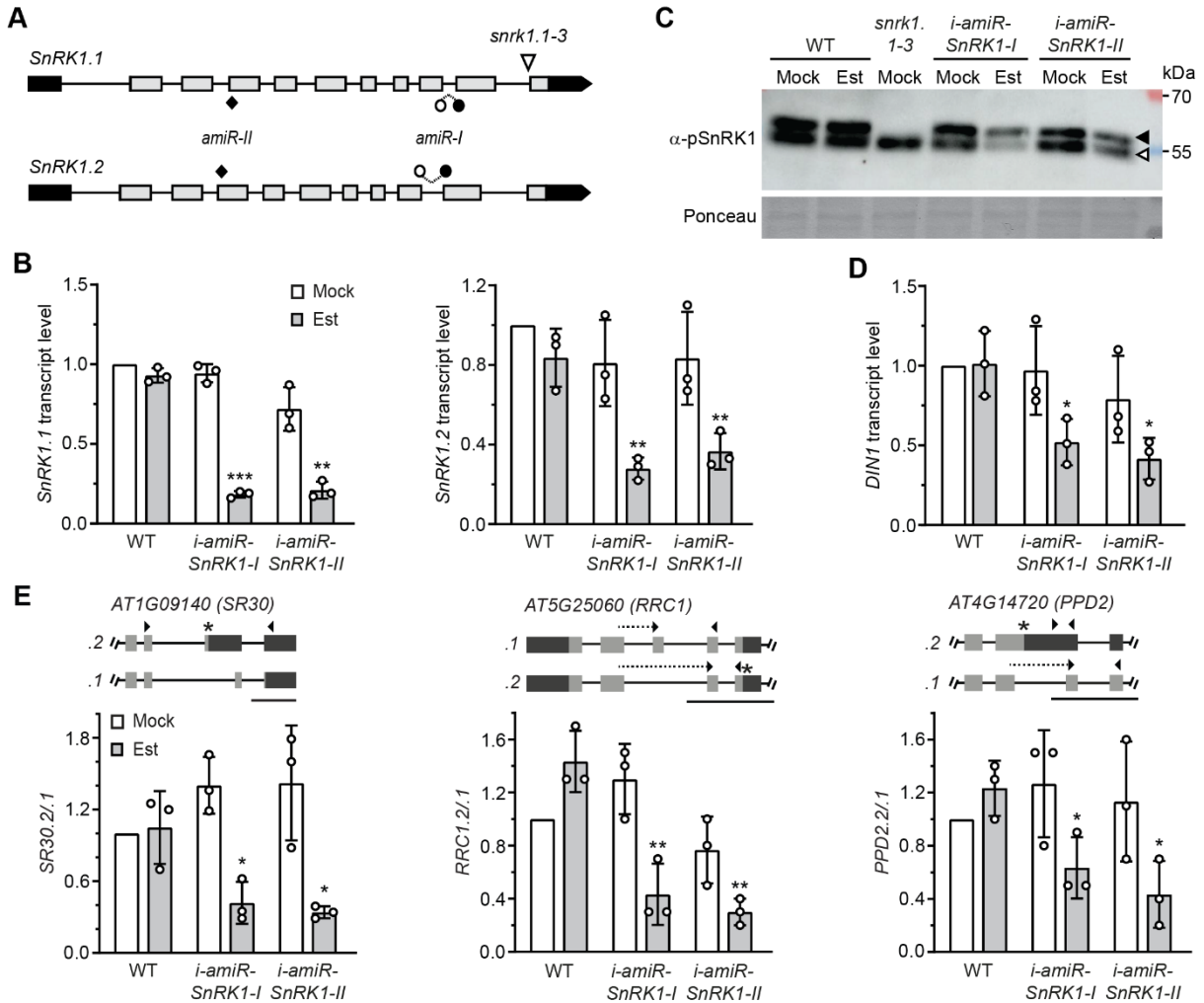


**Figure 1 SnRK1 repression triggers AS changes. (A)** Transcript models of *SnRK1.1* and *SnRK1.2* based on representative gene models and target sites of *amiR-I* (over an exon-exon border) and *amiR-II*. T-DNA insertion site in *snrk1.1-3* is indicated by a triangle. Lines correspond to introns, black and grey shapes depict UTRs and coding exons, respectively. **(B)** Relative transcript levels of *SnRK1.1* and *SnRK1.2* in 6-d-old etiolated WT and mutant seedlings allowing inducible amiR expression (*i-amiR-SnrK1*), treated with either mock or  $\beta$ -Estradiol (Est) for 3 d. Data are mean values (n = 3; individual data points as dots) +SD, normalised to WT mock samples. Statistical comparison to WT mock was performed using a one-sample *t* test (P value: \*\*P < 0.01, \*\*\*P < 0.001). **(C)** Immunoblot detection of phosphorylated SnRK1.1 (black triangle) and SnRK1.2 proteins (white triangle, upper panel) in WT and different *snrk1* mutant seedlings. Ponceau S staining is shown as loading control (lower panel). Black and white triangle indicate pSnRK1.1 and pSnRK1.2 protein, respectively. Other details of plant growth and treatments are as described in (B). **(D)** Relative transcript level of the SnRK1 target *DIN1* in WT and *i-amiR-SnrK1* mutant seedlings. Sample description, data normalisation and statistics as described in (B) (P value: \*P < 0.05). **(E)** Models of splicing variants (details as defined in a; asterisk marks position of premature termination codon, scale bar: 500 bp) and corresponding AS ratios in WT and *i-amiR-*

*SnRK1* seedlings (bottom). Arrowheads depict binding sites of primers used for PCR. Ratios were determined via Bioanalyzer (*SR30*) or RT-qPCR of the single mRNA isoforms (*RRC1*, *PPD2*). Displayed are mean values +SD (n = 3; individual data points as dots) and data was normalised to the WT mock control. An independent *t* test was performed for comparison of Est samples to WT Est, and one-sample *t* test for comparison of mock samples to WT mock (P values: \*P < 0.05, \*\*P < 0.01).

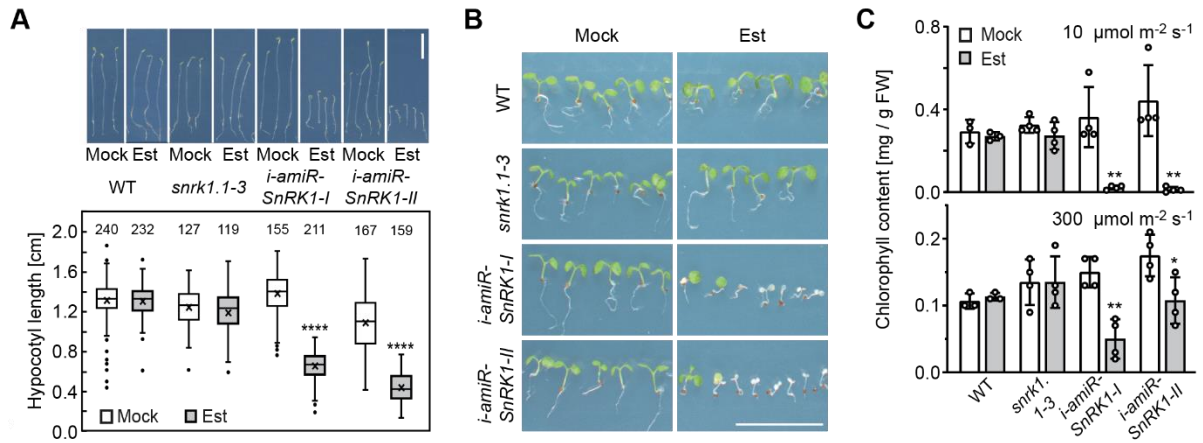


**Figure 2 SnRK1 knockdown particularly impairs seedling development at low energy availability.** **(A)** Representative pictures (upper panel) and quantitation of hypocotyl lengths (lower panel) of 6-d-old wildtype (WT), *snrk1.1-3*, and *i-amiR-SnRK1* seedlings. The seedlings were grown on mock or  $\beta$ -Estradiol (Est)-containing plates. White scale bar indicates 1 cm. The plot depicts interquartile range, maximum as well as minimum of the data set as box and whiskers, respectively. The middle line and the cross represent the median and mean value, respectively. Asterisks indicate significant difference compared to corresponding mock control based on one-way ANOVA with post hoc Tukey test (P value: \*\*\*\*P < 0.0001). n is indicated above each condition. **(B)** Representative photographs of 14-d-old seedlings that were either grown on mock or  $\beta$ -Estradiol-containing plates under low light intensity (10  $\mu\text{mol m}^{-2} \text{s}^{-1}$ ). Scale bar represents 0.5 cm. **(C)** Total chlorophyll content of 14 d-old seedlings grown under low (10  $\mu\text{mol m}^{-2} \text{s}^{-1}$ , top panel) or high (300  $\mu\text{mol m}^{-2} \text{s}^{-1}$ , bottom panel) light. Displayed are mean values +SD (n: 3 – 4; individual data points as dots) and asterisks indicate significant difference compared to corresponding mock control based on independent *t* test (P values: \*P < 0.05, \*\*P < 0.01).

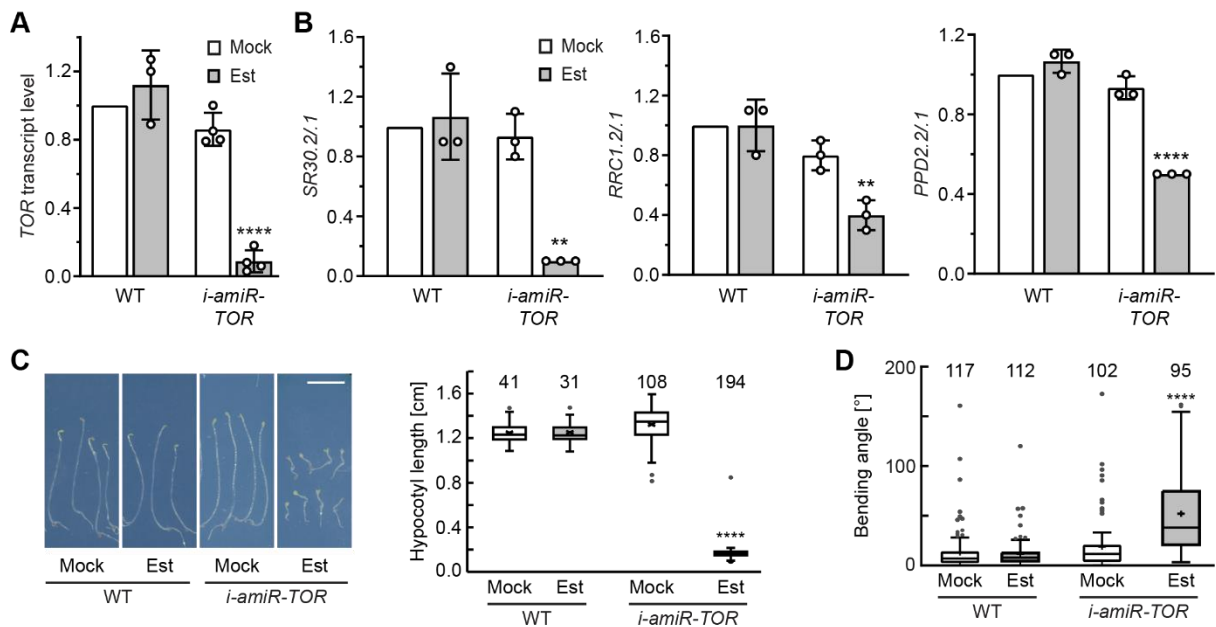


**Figure 3 Inducible TOR repression alters seedling development and AS output. (A)** Relative transcript level of *TOR* in 6-d-old etiolated WT and *i-amiR-TOR* mutant seedlings, treated with either mock or  $\beta$ -Estradiol for 3 d. Data are mean values (WT, n = 3; *i-amiR-TOR*, n = 4; individual data points as dots) + SD, normalised to WT mock samples. Statistical comparison to WT mock was performed using a one-sample *t* test (P value: \*\*\*\*P < 0.0001). **(B)** Splicing ratios were determined in 6-d-old etiolated WT and *i-amiR-TOR* seedlings. Growth conditions and treatments are as described in a. Data were quantified using RT-qPCR of the single mRNA isoforms and normalised to the WT mock control. Displayed are mean values +SD (n = 3 from 2 independent experiments; individual data points as dots). An independent *t* test was performed for comparison of the Est sample to WT Est, and one-sample *t* test for comparison of the mock sample to WT mock (P values: \*\*P < 0.01, \*\*\*P < 0.001, \*\*\*\*P < 0.0001). **(C)** Representative pictures (left) and hypocotyl lengths (right) of 6-d-old wildtype (WT) and *i-amiR-TOR* mutant seedlings. The seedlings were grown on mock or  $\beta$ -Estradiol-containing plates. White scale bar indicates 0.5 cm. The plot depicts interquartile range, maximum as well as minimum of the data set as box and whiskers, respectively. The middle line and the cross represent the median and mean value, respectively, dots show outliers. Asterisks indicate significant difference compared to corresponding mock control based on one-way ANOVA with post hoc Tukey test. n is indicated above each condition (P value: \*\*\*\*P < 0.0001). **(D)** Gravitropic response was analysed in 4-d-old etiolated WT and *i-amiR-TOR* seedlings that were grown vertically in the absence or presence of  $\beta$ -Estradiol. Bending angle in degree relative to vertical hypocotyl orientation was examined from 4 independent experiments; n indicated above each condition. Box limits show the 25<sup>th</sup> and 75<sup>th</sup> percentiles, and whiskers extend to 1.5x the interquartile range (IQR). Statistical analysis was performed using an independent *t* test compared with the corresponding mock control. (P values: \*\*\*\*P < 0.0001).

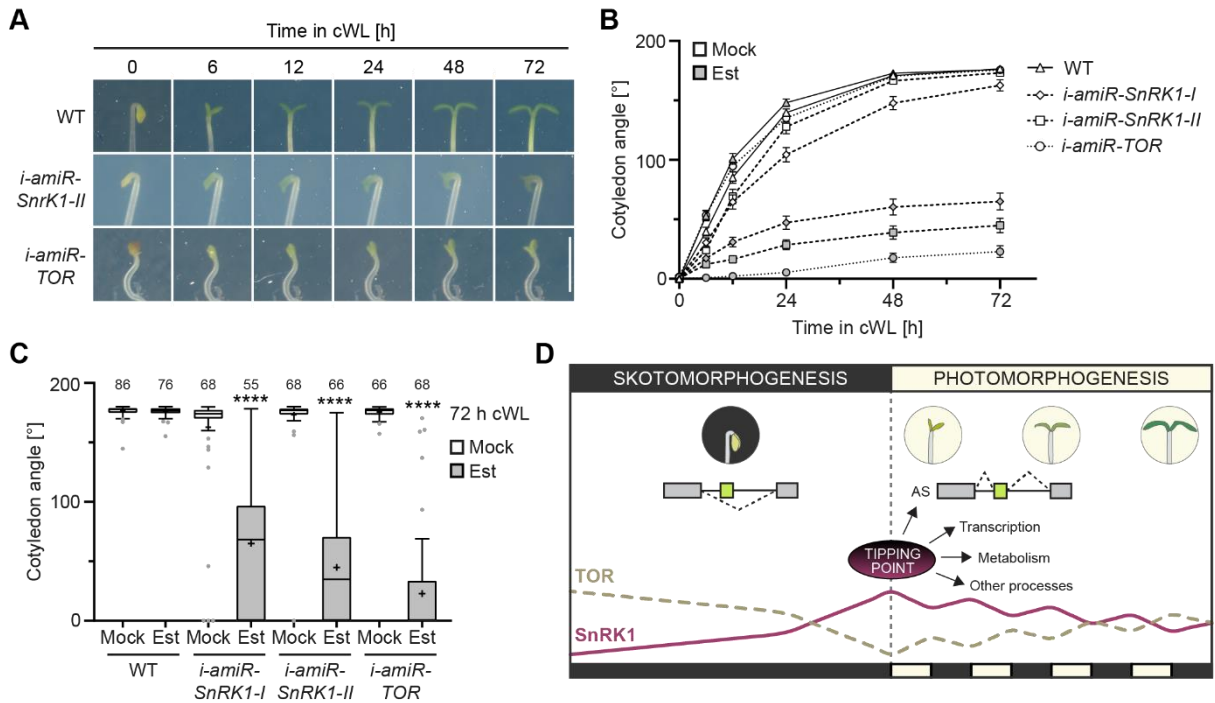


**Figure 4 Both SnRK1 and TOR knockdown delay the photomorphogenic response. (A)** Representative pictures of upper region from WT, *i-amiR-SnrK1-II*, and *i-amiR-TOR* seedlings that were grown for 4 d on  $\beta$ -Estradiol containing plates and then illuminated for the indicated durations with continuous white light ( $15 \mu\text{mol m}^{-2} \text{s}^{-1}$ ). Scale bar = 0.2 cm. **(B)** Cotyledon opening angles of indicated genotypes grown on mock or  $\beta$ -Estradiol containing plates as described in a. Data show mean  $\pm$  SE and is derived from 3 replicates with 14 - 33 samples per replicate. For extended statistical data please see Supplemental Data 1. **(C)** Cotyledon opening angles after 72 h cWL illumination. Data was analysed from three independent experiments. In all box plots, median is represented by the central line, mean by the cross; box limits show the 25<sup>th</sup> and 75<sup>th</sup> percentiles, and whiskers extend to 1.5x the interquartile range (IQR). Statistical significance was determined by two-tailed Student's *t* test against corresponding mock control (*P* value: \*\*\*\**P* < 0.0001). *n* is indicated above each condition. **(D)** Tipping point model of SnRK1/TOR signalling. Hypothetical activity profiles of SnRK1 (dark-red line) and TOR (broken line) during skoto- and photomorphogenesis. Darkness and light intervals indicated by black and light boxes at bottom. Representative AS switch and light-induced cotyledon opening are schematically depicted.

## Supplemental information

### **SnRK1 and TOR control light-responsive splicing and development in etiolated Arabidopsis seedlings**

Jennifer Saile<sup>1,2,4</sup>, Theresa Wießner-Kroh<sup>2,4</sup>, Katarina Erbstein<sup>1</sup>, Dominik M. Obermüller<sup>2</sup>, Anne Pfeiffer<sup>3</sup>, Denis Janocha<sup>3</sup>, Jan Lohmann<sup>3</sup>, and Andreas Wachter<sup>1,2,\*</sup>

<sup>1</sup>Institute for Molecular Physiology (imP), University of Mainz, Johannes von Müller-Weg 6, 55128 Mainz, Germany

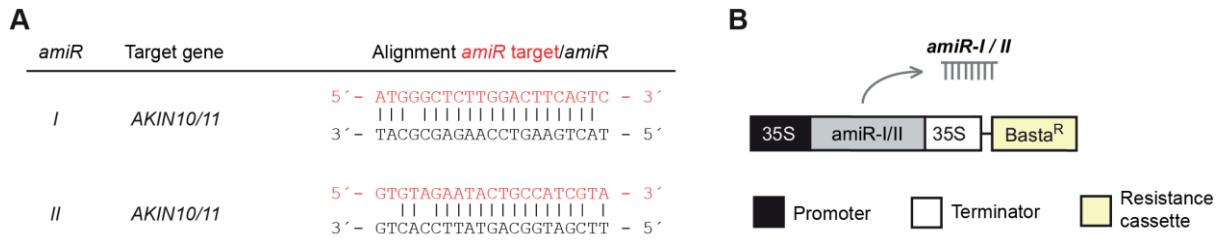
<sup>2</sup>Center for Plant Molecular Biology (ZMBP), University of Tübingen, Auf der Morgenstelle 32, 72076 Tübingen, Germany

<sup>3</sup>Centre for Organismal Studies, Heidelberg University, Im Neuenheimer Feld 230, 69120 Heidelberg, Germany

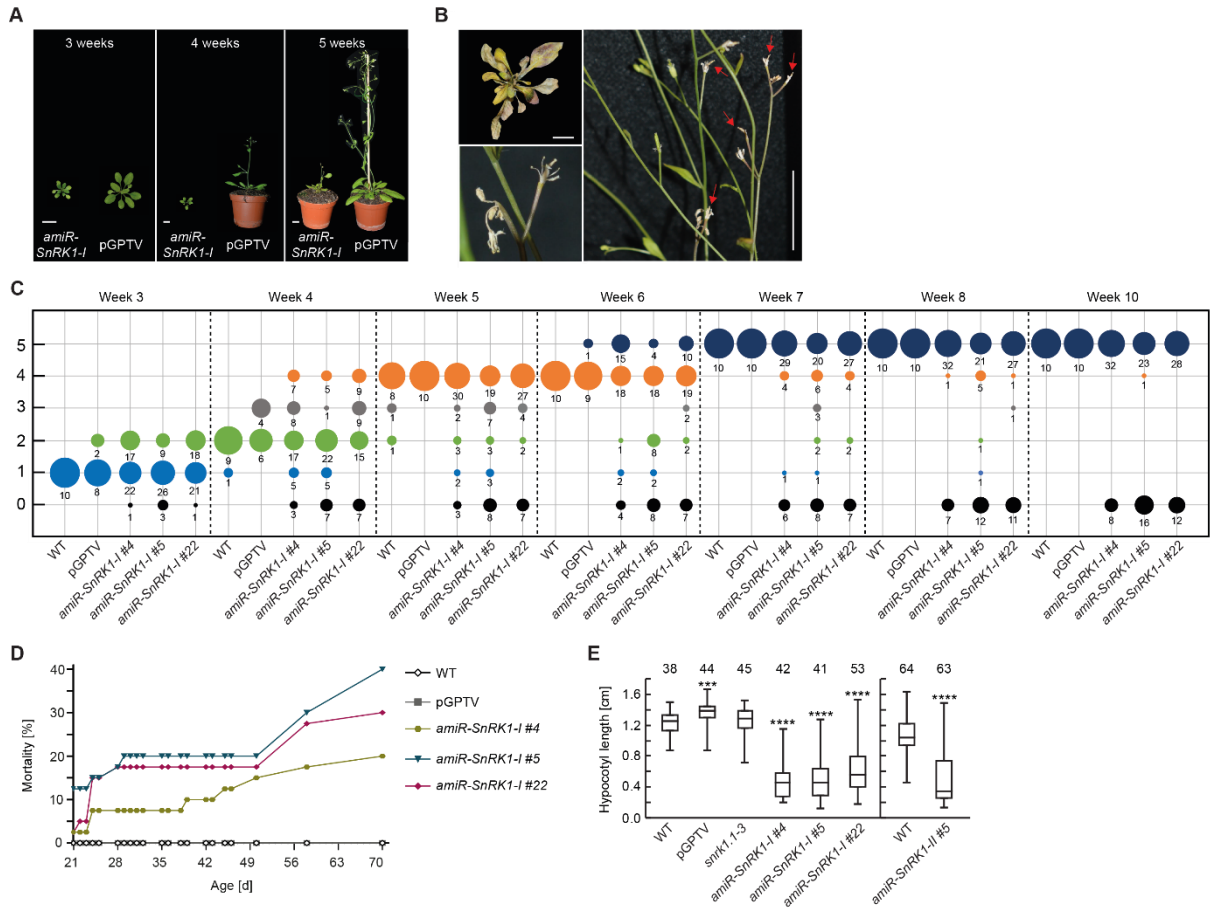
\*Corresponding author: [wachter@uni-mainz.de](mailto:wachter@uni-mainz.de)

<sup>4</sup>These authors contributed equally to the work.

SUPPLEMENTAL FIGURES



**Supplemental Figure 1. Design of *amiR* constructs. (A)** Sequences of *amiRs* (black) aligned to their mRNA target sites (red). **(B)** Cartoon of the constitutive *amiR* (*I*, *II*) constructs under control of the CaMV 35S promoter and terminator, and containing a Basta resistance cassette for plant selection.

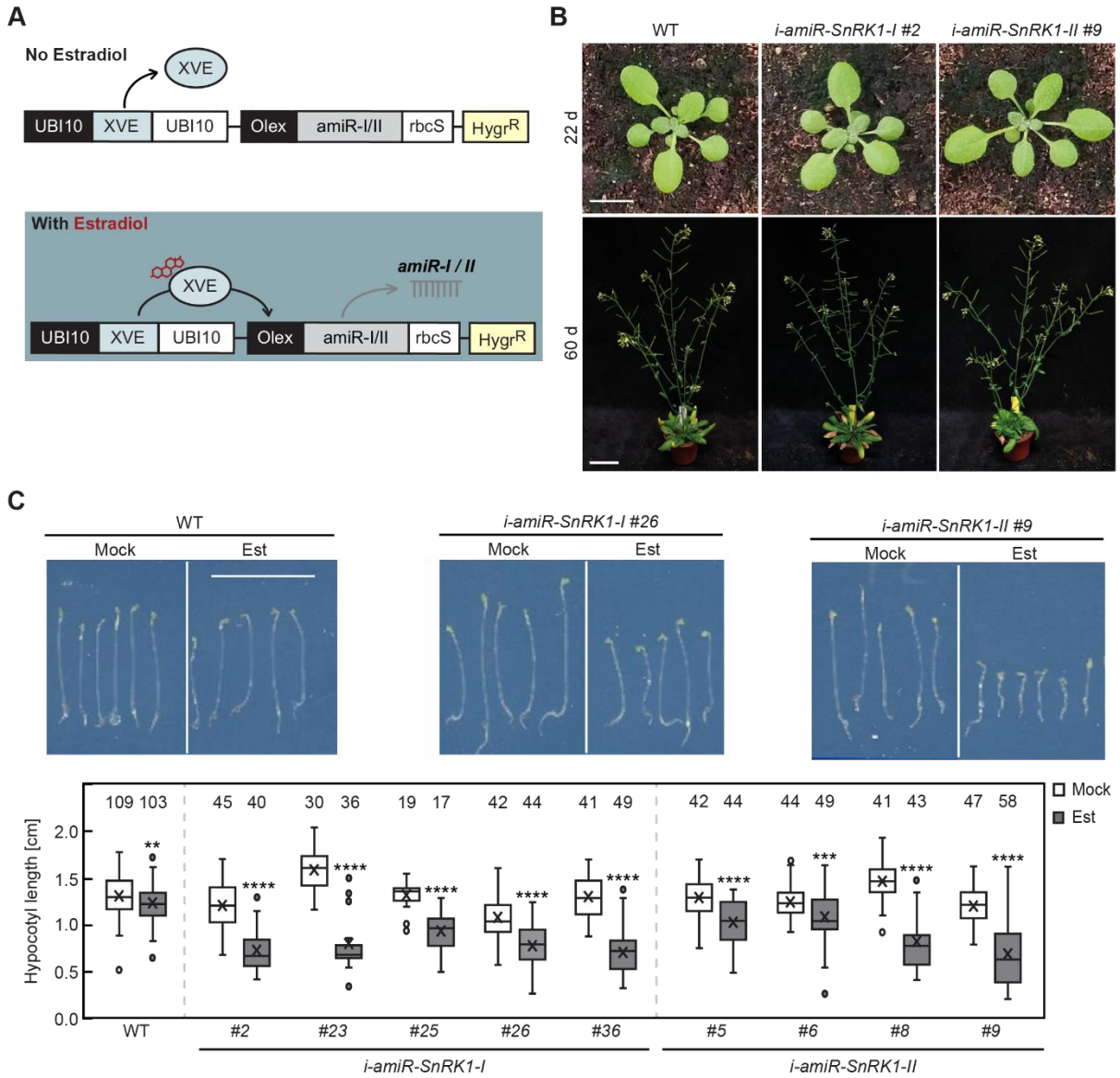


**Supplemental Figure 2. Constitutive *snrk1* knockdown impairs growth and increases premature organ and plant death.**

**(A)** Representative pictures of 3-, 4-, and 5-week-old constitutive *amiR-SnrRK1-1* and pGPTV control plants grown under long day conditions. Scale bar = 1 cm. **(B)** Presumably homozygous *snrk1* mutants are dying at different developmental stages. (Upper left panel) 7-week-old rosette. (Right) Representative picture of a 7-week-old plant displaying aborted flower and siliques, while rosette leaves and main stem were still green. Red arrows indicate aborted siliques. (Lower left panel) Close-up photograph from a 6-week-old plant showing dried flowers and siliques. Scale bar = 1 cm. **(C)** Bubble plot showing developmental stages of *amiR-SnrRK1-1* and controls over time, defined as followed: 0 - dead, 1 - rosette, 2 - bolting, 3 - flowering, 4 – containing siliques, and 5 – siliques ripened. The size of each bubble is proportional to the percentage of analysed plants per genotype at the corresponding developmental stage and the depicted time point. Note that *amiR-SnrRK1-1* and pGPTV plants were transferred from Basta and sugar-containing MS plates to soil, whereas WT plants were grown on MS plates lacking Basta and sucrose. Corresponding n is displayed below each bubble. Total n for WT and pGPTV: 10, total n for each *amiR-SnrRK1-1* line: 40. **(D)** Mortality curve of *amiR-SnrRK1-1* lines and control plants. Plants were grown under long day conditions and mortality (defined as fully dry) was determined in a time period of 3 to 10 weeks. Mortality was scored when plants were fully dried. Before, plants were grown for 14 d on selection or control plates under long day conditions. **(E)** Hypocotyl lengths of *amiR-SnrRK1* lines, WT, pGPTV, and *snrk1.1-3* grown for 6 d under dark conditions. Two sample sets with their corresponding WT controls from two separate hypocotyl assays are displayed. The rectangle spans the interquartile, minimum, and maximum values are shown as whiskers and

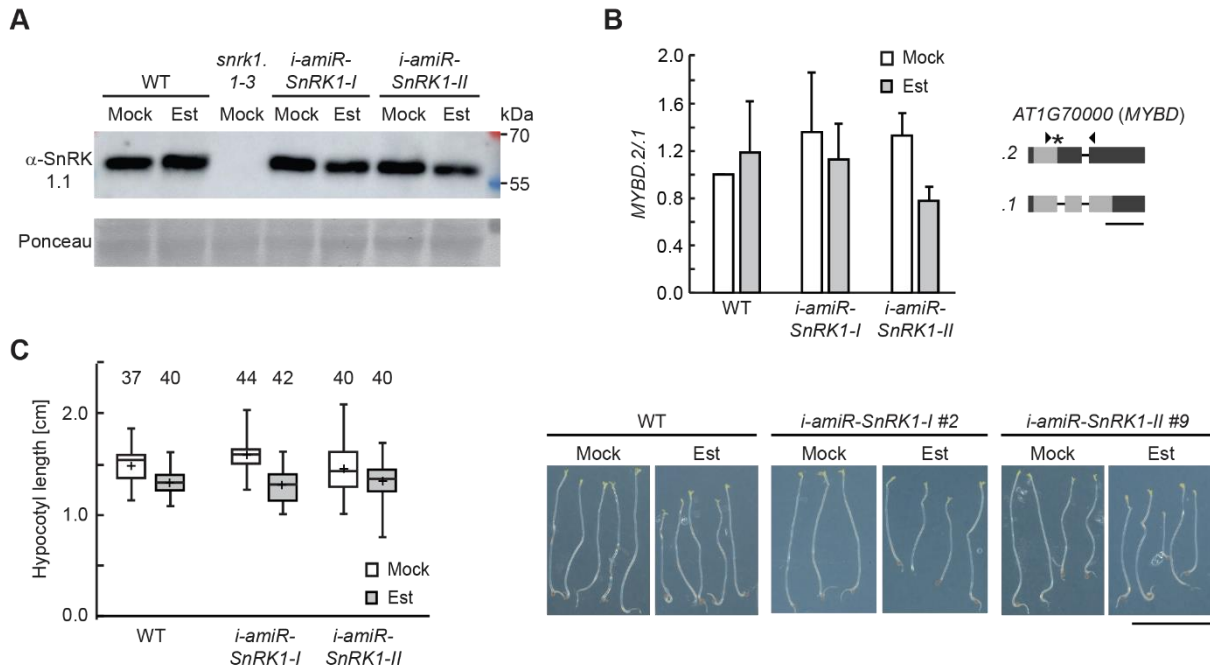


middle line represents the median. Numbers on top indicate seedlings analysed per genotype. Asterisks indicate significant difference of *amiR-SnRK1-I* lines and controls (pGPTV, *snrk1.1-3*) compared to WT based on independent *t* test with unequal variance (Welch *t*-test) and equal variance, respectively. Unequal variance was used for *amiR-SnRK1* seedlings showing segregation. (P values: \*\*\*P < 0.001, \*\*\*\*P < 0.0001). \*\*\*\*P < 0.0001).

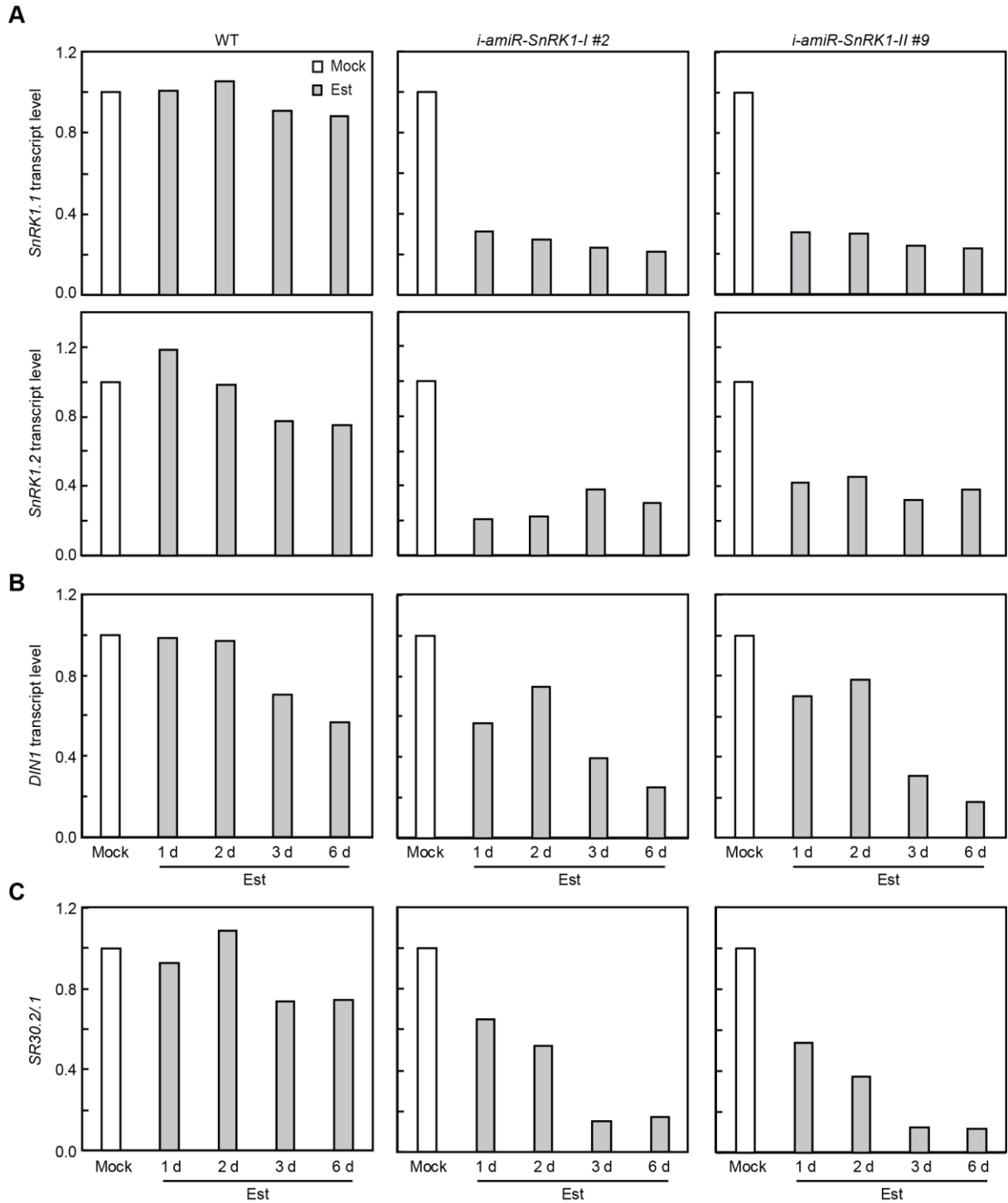


**Supplemental Figure 3. Construct design and phenotypes of *i-amiR-SnRK1* lines. (A)** Cartoon of the inducible *amiR* (*I*, *II*) constructs. Two expression cassettes were modularly fused together. The synthetic transcription factor XVE is under the control of the ubiquitously active UBI10 promoter and the UBI10 terminator. Upon treatment with  $\beta$ -Estradiol, XVE binds to the Olex promoter and activates *amiR* expression. The construct also includes a RuBisCO terminator (*rbcS*) and a Hygromycin resistance cassette. **(B)** Comparable development of WT and *i-amiR-SnRK1* lines under long day conditions and in the absence of  $\beta$ -Estradiol. Representative pictures for each line at the age of 22 days (scale bar = 1 cm) and 60 days (scale bar = 5 cm) after sowing. **(C) (Top)** Representative pictures of etiolated WT and *i-amiR-SnRK1* seedlings upon growth on either mock or  $\beta$ -Estradiol (Est)-containing plates for 6 d. Subsequently, seedlings were transferred to agar plates and scanned. Scale bar = 1 cm. **(Bottom)** Quantitation of hypocotyl lengths for the corresponding lines. Number of measured seedlings per line is indicated above each box plot. Interquartile range, maximum and minimum, median, and mean values are depicted as box, whiskers, middle line and cross, respectively. Dots display outliers. An independent *t* test with unequal variance (Welch *t*-test) was performed for *amiRs*, and an independent *t* test with equal variance for WT (P values: \*\*P < 0.01, \*\*\*P < 0.001, \*\*\*\*P < 0.0001). According to the WT data,

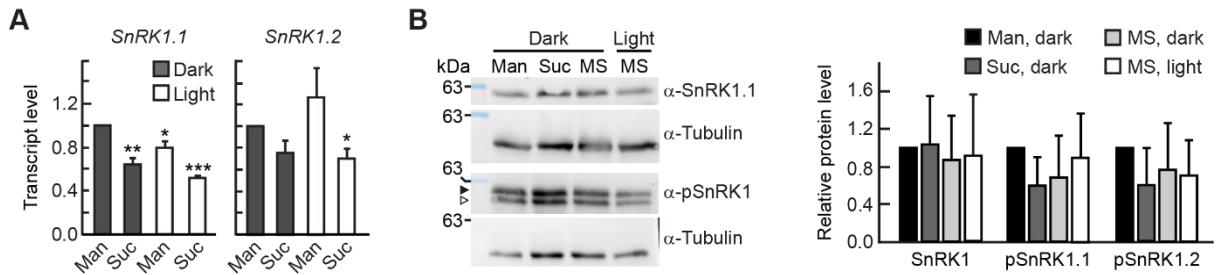
Est treatment can slightly reduce hypocotyl growth in a general manner. Unequal variance was considered for *i-amiR-SnRK1* seedlings since they represent the progenies from heterozygous F1 generations that still show segregation.



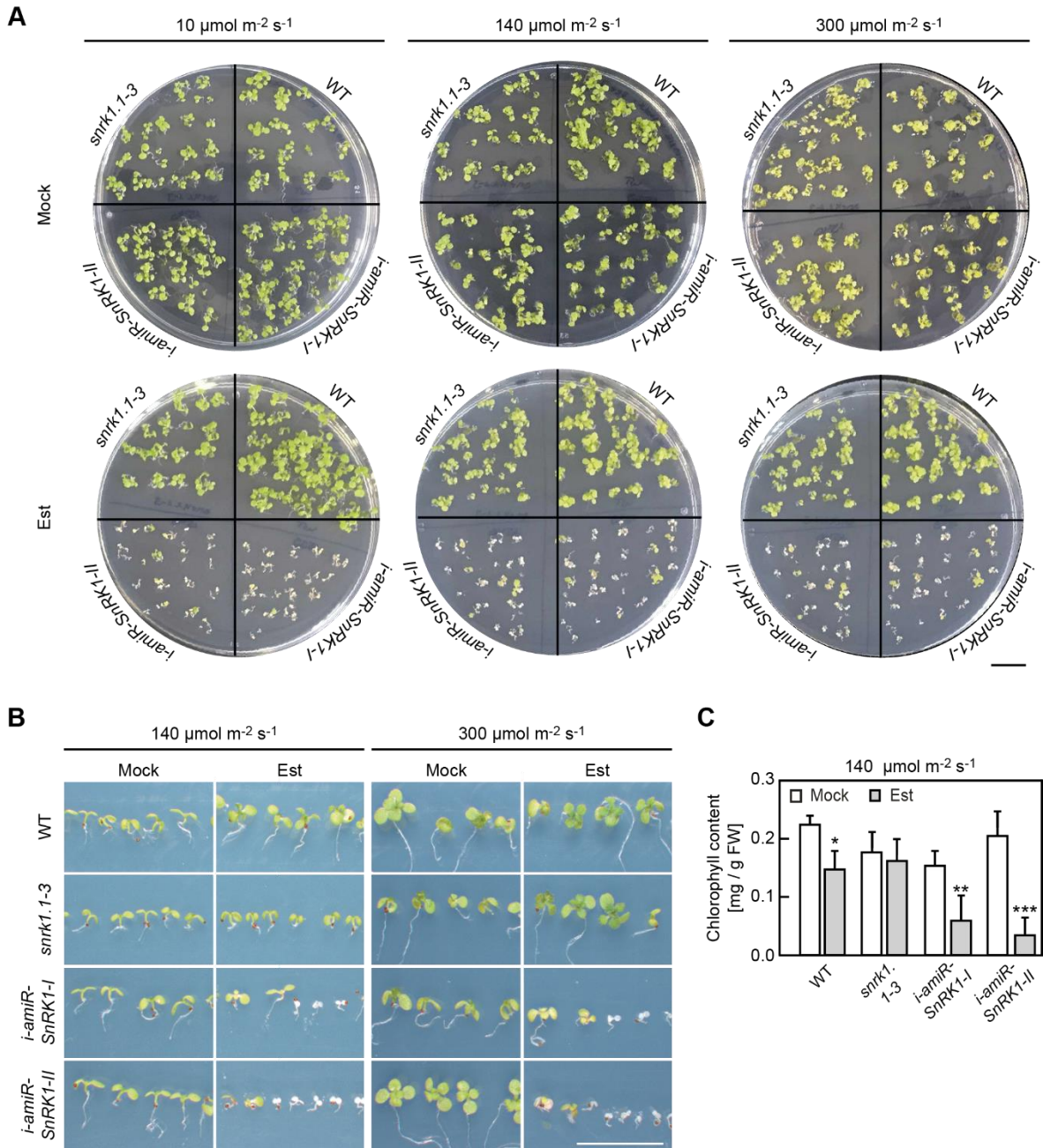
**Supplemental Figure 4. Analysis of *i-amiR-SnRK1* lines in liquid culture assay. (A)** Immunoblot detection of total SnRK1.1 protein (upper panel) in etiolated WT and different *snrk1* mutant seedlings. Ponceau S staining is shown as loading control (lower panel). Other details of plant growth and treatments are as described in Figure 1b. **(B)** Splicing ratio was determined from seedlings samples grown in liquid media for 3 d, followed by a 3-d incubation with either mock or Est solution. Corresponding transcript models are shown on the right; further details see legend to Figure 1e. Splicing variants were co-amplified and quantified on a Bioanalyzer. Displayed are mean values plus SD (n = 3) and data was normalised to the WT mock control. Independent *t* test was performed for comparison of Est samples to WT Est, and one-sample *t* test for comparison of mock samples to WT mock. **(C)** Hypocotyl lengths (left) and representative pictures (right) of etiolated WT and *i-amiR-SnRK1* seedlings derived from a homozygous F2 generation. Details of plant growth and treatments are as described in (B). Scale bar = 1 cm. A statistical analysis via Tukey's multiple comparisons test comparing either the mock or Est samples did not reveal significant differences between the genotypes.



**Supplemental Figure 5. Timing of SnRK1 repression and downstream responses.** 6-d-old dark grown seedlings were treated with mock solution or  $\beta$ -Estradiol for 1, 2, 3 and 6 d before harvest. **(A)** *SnRK1.1*, *SnRK1.2*, and **(B)** *DIN1* transcript levels were measured using RT-qPCR. **(C)** *SR30* splicing ratios were determined via Bioanalyzer-based quantification. All data are normalised to the corresponding mock controls and represent single replicates.

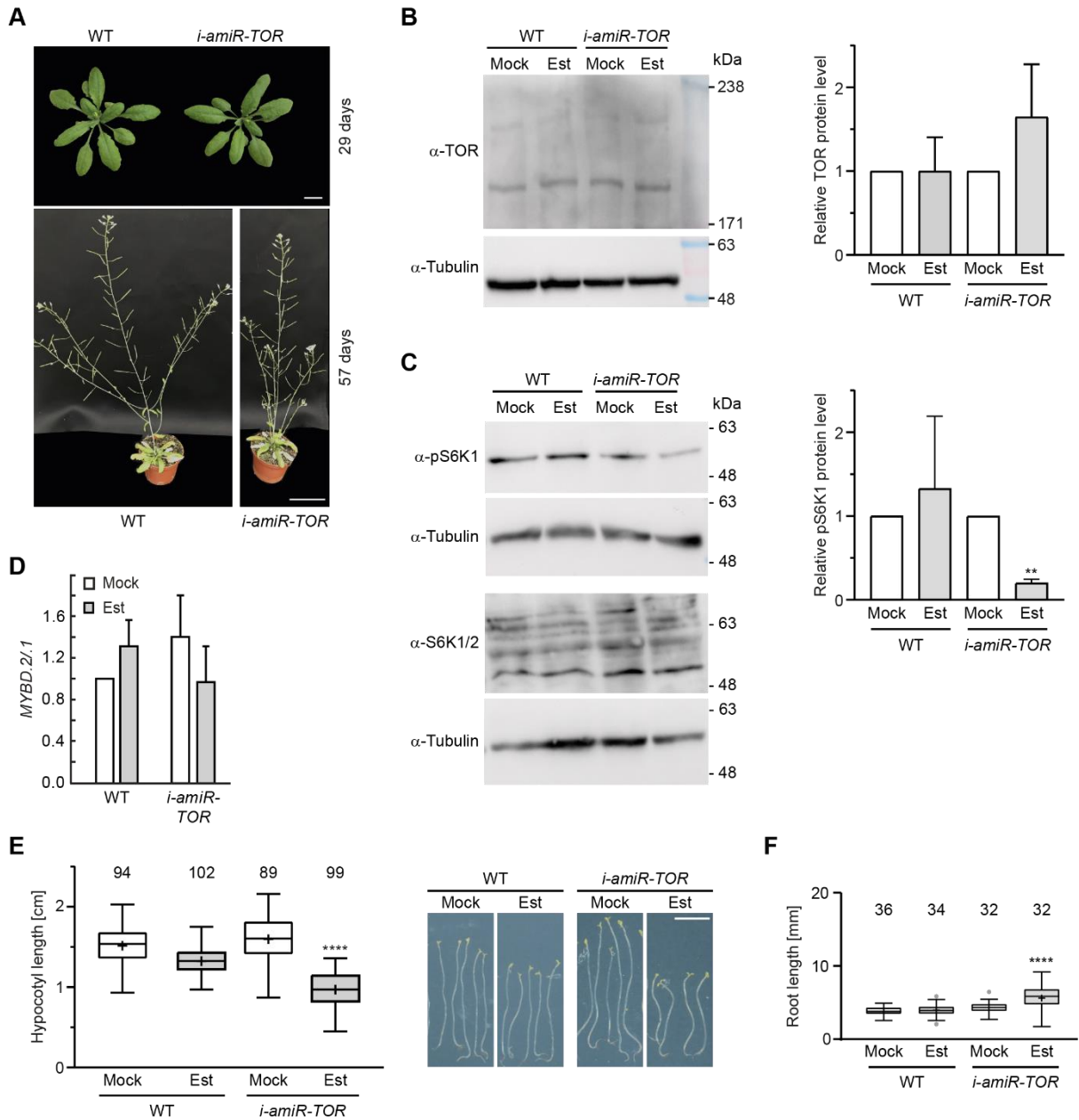


**Supplemental Figure 6. Light and sucrose have a minor effect on SnRK1 expression. (A)** Relative transcript level of *SnRK1.1* and *SnRK1.2* in 6-d-old etiolated WT seedlings exposed for 6 h to light and/or sucrose (Suc) or kept in darkness for 6 h. Mannitol (Man) treatment served as osmotic control. Data was analysed via RT-qPCR from three independent experiments and normalized to the Dark/Man sample. A one-sample *t* test for comparison to Man Dark was performed (P values:) \* $P < 0.05$ , \*\* $P < 0.01$ , \*\*\* $P < 0.001$ . **(B) (Left)** Immunoblot detection of total SnRK1.1 protein, and phosphorylated SnRK1.1 (black triangle) and SnRK1.2 (white triangle). Tubulin served as loading control. Plant growth and treatments are as described in (A). **(Right)** Quantification of relative SnRK1, pSnRK1.1 and pSnRK1.2 protein levels based on mean values + SD from 4 independent experiments. A one-sample *t* test was performed but showed no significant differences in Suc, dark; MS, dark; MS, light samples compared to corresponding Man, dark sample.



**Supplemental Figure 7. Light intensity-dependent effects of SnRK1 knockdown. (A)** Photographs of 14-d-old seedlings that were either grown on mock or  $\beta$ -Estradiol (Est)-containing plates under low (10  $\mu\text{mol m}^{-2} \text{s}^{-1}$ , left), regular (140  $\mu\text{mol m}^{-2} \text{s}^{-1}$ , middle) or high light conditions (300  $\mu\text{mol m}^{-2} \text{s}^{-1}$ , right). Scale bar represents 1 cm. **(B)** Representative pictures of 14-d-old seedlings grown under regular (140  $\mu\text{mol m}^{-2} \text{s}^{-1}$ , left) or high light conditions (300  $\mu\text{mol m}^{-2} \text{s}^{-1}$ , right). Scale bar represents 0.5 cm. **(C)** Total chlorophyll content of 14-d-old seedlings grown under regular light (140  $\mu\text{mol m}^{-2} \text{s}^{-1}$ ) conditions. Displayed are mean values plus SD ( $n = 3 - 4$ ) and asterisks indicate significant difference compared to corresponding mock control based on independent  $t$  test (P values: \* $P < 0.05$ , \*\* $P < 0.01$ , \*\*\* $P < 0.001$ ).

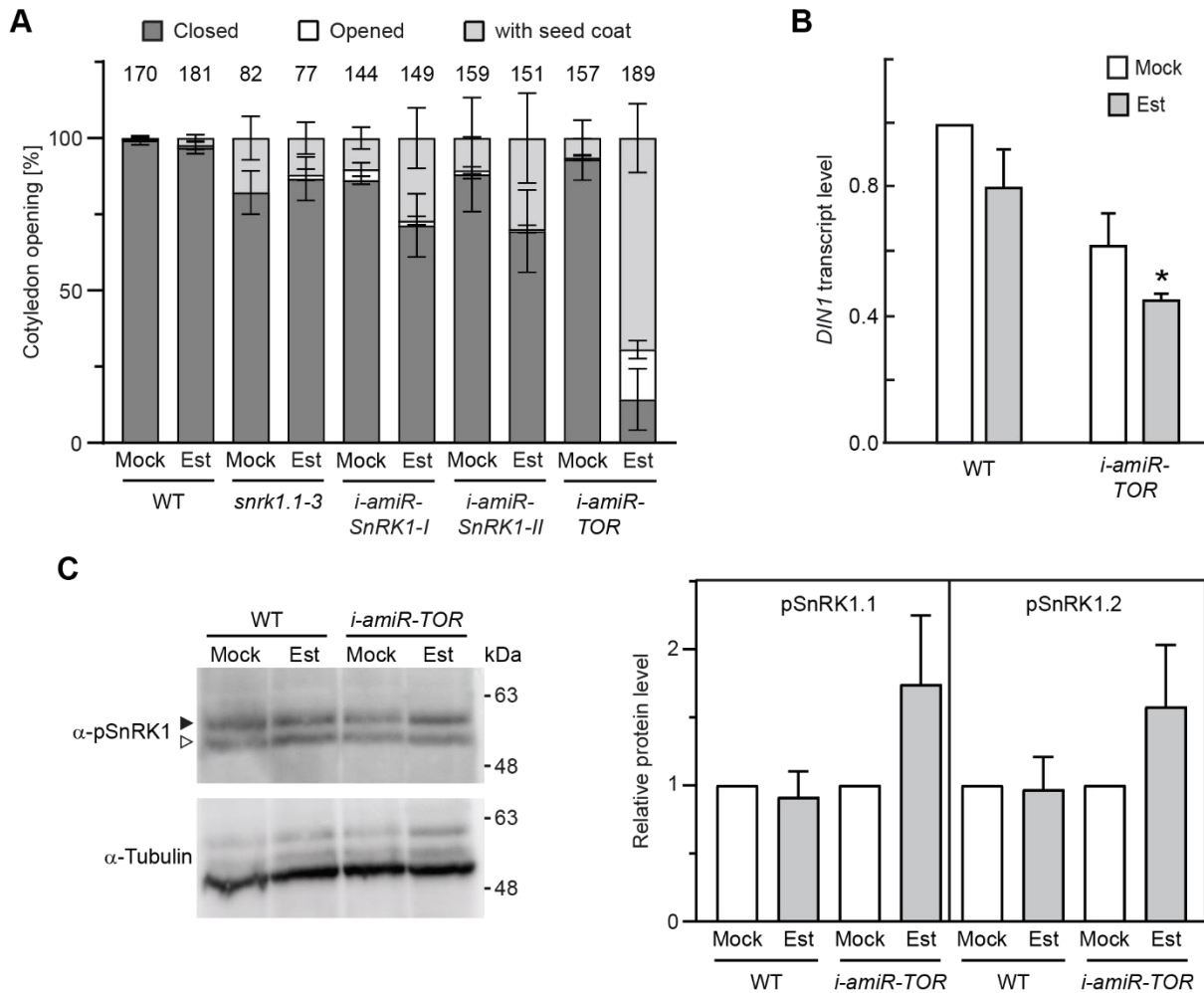




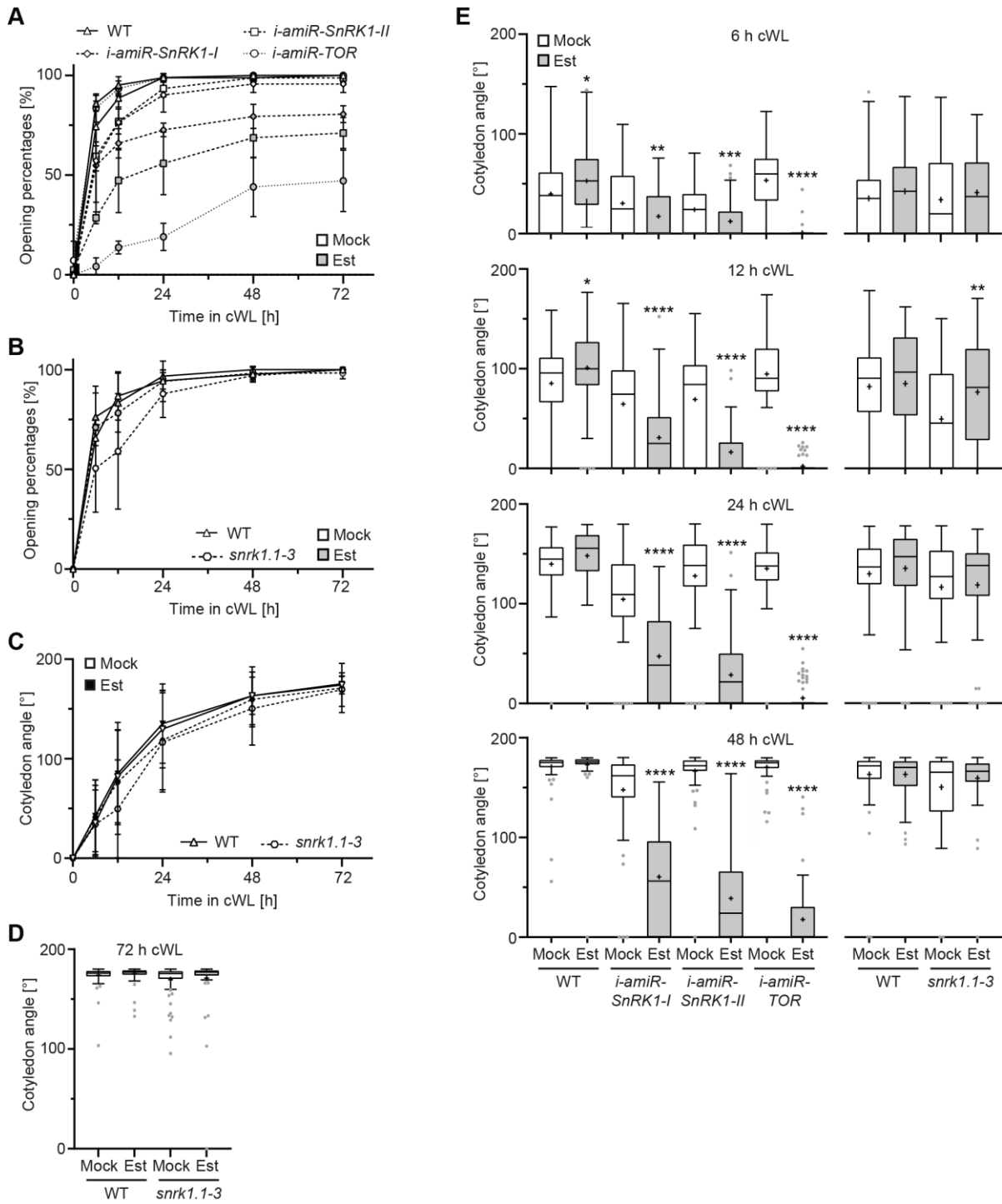
**Supplemental Figure 8. Characterisation of *i-amiR-TOR* line.** (A) Comparable development of WT and *i-amiR-TOR* plants in the absence of  $\beta$ -Estradiol and under long day conditions. Representative pictures are shown at the age of 29 days (scale bar = 1 cm) and 57 days (scale bar = 5 cm) after sowing. (B) (Left) Immunoblot detection of TOR from 6-d-old WT and *i-amiR-TOR* seedlings grown in darkness and treated with mock or  $\beta$ -Estradiol for 3 d. Tubulin was detected on a separate membrane as loading control. (Right) Quantification of relative TOR protein level from 4 independent experiments. A one-sample *t* test was performed and showed no significant differences in Estradiol-treated seedlings compared to the corresponding mock control. (C) (Left) Immunoblot detection of S6K1/2 and pS6K1 from samples as described in (B). Tubulin was detected on a separate (for pS6K1) or on the S6K1/2 membrane and served as loading control. (Right) Quantification of relative pS6K1 protein level from 3 independent experiments. Statistical analysis as described in (B) (P value: \*\*P < 0.01). (D) MYBD splicing ratio was determined from WT and *i-amiR-TOR* seedling samples as described in (B). Data were quantified using RT-qPCR and normalised to the WT mock control. Displayed are mean values



+SD (n = 3 from 2 independent experiments). An independent *t* test was performed for comparison of the Est sample to WT Est, and one-sample *t* test for comparison of the mock sample to WT mock. **(E)** Hypocotyl lengths (left) and representative pictures (right) of etiolated WT and *i-amiR-TOR* seedlings grown in liquid media for 3 d, followed by a 3-d incubation in either mock or  $\beta$ -Estradiol solution. n is indicated above each condition. Scale bar = 0.5 cm. Asterisks indicate significant differences of the comparison of Est samples to WT Est, and mock samples to WT mock based on one-way ANOVA with post hoc Tukey test (P value: \*\*\*\*P < 0.0001). **(F)** Root lengths of 4-d-old etiolated WT and *i-amiR-TOR* seedlings grown on plates. Upon a 6 h light induction, seeds were germinated for 12 h on  $\frac{1}{2}$  MS agar plates without supplements and then transferred to plates containing 10  $\mu$ M  $\beta$ -Estradiol for further growth. Statistical analysis as described in (E) (P value: \*\*\*\*P < 0.0001).



**Supplemental Figure 9. Cotyledon opening in darkness and SnRK1 signalling upon TOR knockdown.** (A) Cotyledon opening percentages was analysed in 4-d-old etiolated WT and kinase mutant seedlings, grown horizontally on  $\beta$ -Estradiol or mock containing plates. Data are shown as mean  $\pm$  SD of three independent experiments (n: 77 – 189). Seedlings with the seed coat still attached were counted separately. (B) Relative transcript level of *DIN1* in 6-d-old etiolated WT and *i-amiR-TOR* mutant seedlings treated with either mock or  $\beta$ -Estradiol for 3 d. Data are mean values (n = 3 from 2 independent experiments) + SD, normalised to WT mock samples. Statistical comparison of the mock and  $\beta$ -Estradiol treated *i-amiR-TOR* mutant was performed using an independent *t* test. In case of the WT, a one-sample *t* test was used (P value: \*P < 0.05). (C) (Left) Immunoblot detection of phosphorylated SnRK1.1 (black triangle) and SnRK1.2 (white triangle) in 6-d-old etiolated WT and *i-amiR-TOR* seedlings. Growth conditions and treatments as described in (B). Tubulin was detected on the same membrane and served as loading control. (Right) Quantification of pSnRK1.1 and pSnRK1.2 signal intensity based on mean values + SD from 4 independent experiments. A one-sample *t* test was performed and showed no significant differences in Estradiol-treated seedlings compared to the corresponding mock control.



**Supplemental Figure 10. Light-induced cotyledon opening in *snrk1* and *tor* mutants.** (A, B) 4-d-old etiolated seedlings were either grown on mock or  $\beta$ -Estradiol containing plates and illuminated with continuous white light ( $15 \mu\text{mol m}^{-2} \text{s}^{-1}$ ) for the indicated time points. Percentages of cotyledon opening at the indicated time points are shown as mean  $\pm$  SD from 3 replicates with 16 – 33 samples per replicate. (C) Cotyledon opening angles over time shown as mean  $\pm$  SE from 3 replicates with 16 - 33 samples per replicate. (D) Cotyledon opening angles after 72 h cWL illumination. Data was analysed from three independent experiments. (E) Cotyledon opening angles at the indicated time points. Details of plant growth and treatments are as described in (A). In all box plots, median is represented by the central line, mean by the cross; box limits show the 25<sup>th</sup> and 75<sup>th</sup> percentiles, and whiskers extend to

1.5x the interquartile range (IQR). Statistical significance was determined by two-tailed Student's *t* test against corresponding mock control (P values: \*P < 0.05, \*\*P < 0.01, \*\*\*P < 0.001, \*\*\*\*P < 0.0001). For extended statistical data please see Supplemental Data 1.

## SUPPLEMENTAL TABLES

**Supplemental Table 1.** Segregation and mortality rates at post-seedling stage of *amiR-SnRK1* mutants.

Lines	Basta <sup>R</sup> [%]	Basta <sup>S</sup> [%]	n <sup>1</sup>	Mortality, weeks n <sup>2</sup>	
				3-10 [%]	
WT	0	100	148	0	10
pGPTV	100	0	138	0	10
<i>amiR-I #4</i>	71	29	133	20	40
<i>amiR-I #5</i>	60	40	90	40	40
<i>amiR-I #22</i>	73	27	121	30	40

<sup>1</sup>Total number of BASTA-selected seedlings<sup>2</sup>Total number of control and BASTA-resistant *amiR* mutant plants assayed for mortality at the post-seedling stage**Supplemental Table 2.** Primers for cloning (*i-*)*amiR-SnRK1* and *i-amiR-TOR* constructs.

Target	Primer	Sequence	Details
<i>amiR-SnRK1-I</i>	TW023	gaTACTGAAGTCCAAGAGCGCA Tctctctttgtattcca	I miR-s <sup>1</sup>
	TW024	agATGCGCTCTTG GACTTCAGTA tcaagagaatcaatga	II miR-a <sup>1</sup>
	TW025	agATACGCTCTTG GAGTT CAGTT cacaggtcgtgatatg	III miR*s <sup>1</sup>
	TW026	gaAACTGAACTCCAAGAGCGTA Tctacatatattccta	IV miR*a <sup>1</sup>
<i>amiR-SnRK1.1-II</i>	TW027	gaTTCGATGGCAGTA TTCCACTGctctctttgtattcca	I miR-s <sup>1</sup>
	TW028	agCAGTGAATACTGCCA TCGAAtcaagagaatcaatga	II miR-a <sup>1</sup>
	TW029	agCAATGGAATACTGGCA TCGA Tcacaggtcgtgatatg	III miR*s <sup>1</sup>
	TW030	gaATCGATGCCAG TA TTCCA TTGctacatatattccta	IV miR*a <sup>1</sup>
<i>amiR-TOR</i>	A04464	gaTTTATAACAACAAGTTGGCG Tctctctttgtattcca	I miR-s <sup>1</sup>
	A04465	agACGCCAACTGTTG TTA TAAAtcaagagaatcaatga	II miR-a <sup>1</sup>
	A04466	agACACCAACTG TTCT TA TAA Tcacaggtcgtgatatg	III miR*s <sup>1</sup>
	A04467	gaATTATAAGAACAAGTTGG TG Tctacatatattccta	IV miR*a <sup>1</sup>
SL11	aaaaagcaggctCTGCAAGGCGATTAAGTTGGGTAAC	Primer A with <i>attB</i> site <sup>1</sup>	
SL12	agaaagctgggtGCGGATAACAATTTACACAGGAAACAG	Primer B with <i>attB</i> site <sup>1</sup>	
TW080	aacaggtctcaggctCTGCAAGGCGATTAAGTTGGGTAAC	Primer A with <i>Bsal</i> site <sup>1</sup>	
TW081	aacaggtctcactgaGCGGATAACAATTTACACAGGAAACAG	Primer B with <i>Bsal</i> site <sup>1</sup>	

<sup>1</sup>primer name in details refers to naming from (Schwab et al., 2006).

P-878 ggtctcaggctatatgaaagcgtaacggccag

---

P-879 ggtctcacgaggccaatcatcaggatctctag

---

P-880 ggtctcactcgtctggcgctccatggagcaccag

---

P-881 ggtctcactgatcagactgtggcagggaaac

---

**Supplemental Table 3.** GreenGate cloning modules and destination constructs.

Name	Type	Reference
<b>Intermediate vectors</b>		
<b>pGGMTW01</b>		
pGGA006	UBQ10 promoter	(Lampropoulos et al., 2013)
pGGB003	B-dummy	(Lampropoulos et al., 2013)
pGGC124	CDS of chimeric TF XVE	Described in this study
pGGD002	D-dummy	(Lampropoulos et al., 2013)
pGGE009	UBQ10 terminator	(Lampropoulos et al., 2013)
pGGG004	FH adapter to combine two expression cassettes in the destination vector	Provided by RG Lohmann
pGGM000	Assembly of expression cassette #1 (intermediate vector)	(Lampropoulos et al., 2013)
<b>pGGNTW01</b>		
pGGG005	250 bp HA adapter	Provided by RG Lohmann
pGGA044	Olex TATA, activated by XVE – EST system	Provided by RG Lohmann
pGGB003	B-dummy	(Lampropoulos et al., 2013)
pGGCTW01	amiR-SnRK1.1/1.2	Generated in this study
pGGD002	D-dummy	(Lampropoulos et al., 2013)
pGGE001	RBCS terminator	(Lampropoulos et al., 2013)
pGGF005	<i>pUBQ10:Hyg<sup>R</sup>:tOCS</i>	(Lampropoulos et al., 2013)
pGGN000	Assembly of expression cassette #2 (intermediate vector)	(Lampropoulos et al., 2013)
<b>pGGNTW02</b>		
pGGG005	250 bp HA adapter	Provided by RG Lohmann
pGGA044	Olex TATA, activated by XVE – EST system	Provided by RG Lohmann
pGGB003	B-dummy	(Lampropoulos et al., 2013)
pGGCTW02	amiR-SnRK1.1/1.2	Generated in this study
pGGD002	D-dummy	(Lampropoulos et al., 2013)
pGGE001	<i>RBCS</i> terminator	(Lampropoulos et al., 2013)
pGGF005	<i>pUBQ10:Hyg<sup>R</sup>:tOCS</i>	(Lampropoulos et al., 2013)
pGGN000	Assembly of expression cassette #2 (intermediate vector)	(Lampropoulos et al., 2013)

**pAP039**

pGGA044	Olex TATA, activated by XVE – EST system	Provided by RG Lohmann
pGGB003	B-dummy	(Lampropoulos et al., 2013)
pGGC/AP39	amiR-TOR	Generated in this study
pGGD002	D-dummy	(Lampropoulos et al., 2013)
pGGE001	RBCS terminator	(Lampropoulos et al., 2013)
pGGG004	FH adapter to combine two expression cassettes in the destination vector	Provided by RG Lohmann
pGGM000	Assembly of expression cassette #1 (intermediate vector)	(Lampropoulos et al., 2013)

**pAP043**

pGGG005	250 bp HA adapter	Provided by RG Lohmann
pGGA006	UBQ10 promoter	(Lampropoulos et al., 2013)
pGGB003	B-dummy	(Lampropoulos et al., 2013)
pGGC124	CDS of chimeric TF XVE	Described in this study
pGGD002	D-dummy	(Lampropoulos et al., 2013)
pGGE009	UBQ10 terminator	(Lampropoulos et al., 2013)
pGGF004	<i>p35S::D-Ala<sup>R</sup>::t35S</i>	(Lampropoulos et al., 2013)
pGGN000	Assembly of expression cassette #2 (intermediate vector)	(Lampropoulos et al., 2013)

**Destination vectors**

<b>pGGZTW01</b>	pGGMTW01	Generated in this study
	pGGNTW01	
	pGGZ003	
<b>pGGZTW02</b>	pGGMTW01	Generated in this study
	pGGNTW02	
	pGGZ003	
<b>pAP44</b>	pAP039	Generated in this study
	pAP043	
	pGGZ003	
<b>pGGZ003</b>	Plant resistance at LB (destination vector)	(Lampropoulos et al., 2013)



**Supplemental Table 4.** Sequences of primers for qPCR and co-amplification PCR.

Primer	Gene ID	Gene	Fwd/Rev	Sequence	Details
TW052	<i>AT3G01090</i>	<i>SnRK1.1</i>	Fwd	TGAGTTTCAAGAGACCATGGAAG	
TW053	<i>AT3G01090</i>	<i>SnRK1.1</i>	Rev	CCAACTCCTTGA TATTCCATCAG	
TW067	<i>AT3G29160</i>	<i>SnRK1.2</i>	Fwd	ACGCAACAGAACACAAAACG	
TW068	<i>AT3G29160</i>	<i>SnRK1.2</i>	Rev	TGTCTCTGAAACTCGGATTCT	
TW013	<i>At4g35770</i>	<i>DIN1</i>	Fwd	GAATGAGCTGCCGGTAGAAG	
TW014	<i>At4g35770</i>	<i>DIN1</i>	Rev	TGATGATTGATACTTGCGTTGAG	
TW170	<i>AT1G50030</i>	<i>TOR</i>	Fwd	GATGGCGAGTG CAGTG GTA	
TW171	<i>AT1G50030</i>	<i>TOR</i>	Rev	CCCCCACGGCAAGTAAAGA	
DNA28	<i>AT1G69960</i>	<i>PP2A</i>	Fwd	GGTAATAACTGCA TCTAAAGACAGAGTTCC	
DNA29	<i>AT1G69960</i>	<i>PP2A</i>	Rev	CCACAACCGCTTGGTCTG	
LH50	<i>AT1G09140</i>	<i>SR30</i>	Fwd	GCAAGAGCAGGAGTGTGTCA	specific for AS variant .1
LH51	<i>AT1G09140</i>	<i>SR30</i>	Rev	TTGATCTTGA TTGGACCTTG	
LH52	<i>AT1G09140</i>	<i>SR30</i>	Fwd	TCACCTGCTAGATCCATTTCC	specific for AS variant .2
LH53	<i>AT1G09140</i>	<i>SR30</i>	Rev	CCCAGCTCGTAGCAGTGAG	
LH302	<i>AT5G25060</i>	<i>RRC1</i>	Fwd	CCTAAGTTGATTCTGAAGGTGA	specific for AS variant .1
LH303	<i>AT5G25060</i>	<i>RRC1</i>	Rev	GTGGTGGTGAAGGAAAGAG	
LH304	<i>AT5G25060</i>	<i>RRC1</i>	Fwd	CCTAAGTTGATTCTGAAGGTATG	specific for AS variant .2
LH305	<i>AT5G25060</i>	<i>RRC1</i>	Rev	CTTTCCTAGGCCTCTCCTC	
JS148	<i>AT1G70000</i>	<i>MYBD</i>	Fwd	CGTGAACGCAAACGAGGAAC	specific for AS variant .1
JS149	<i>AT1G70000</i>	<i>MYBD</i>	Rev	TTCTAGAGATTCTCTCCAATC	
JS150	<i>AT1G70000</i>	<i>MYBD</i>	Fwd	CCAAATCTCATCTCTGTTTTTG	specific for AS variant .2
JS151	<i>AT1G70000</i>	<i>MYBD</i>	Rev	CAGTAAGAAACAATCTATGTTCT	
LH527	<i>AT4G14720</i>	<i>PPD2</i>	Fwd	AGTAAAGAGAAGATGGTGGAGCT	specific for AS variant .1
LH528	<i>AT4G14720</i>	<i>PPD2</i>	Rev	TTTCTGTTGCGCTGACCTC	
LH529	<i>AT4G14720</i>	<i>PPD2</i>	Fwd	TGTCCAATTTTGAAGGAGGCA	specific for AS variant .2
LH530	<i>AT4G14720</i>	<i>PPD2</i>	Rev	CACGAGGCATCTGTAGACACA	

LH4	<i>AT1G09140</i>	<i>SR30</i>	Fwd	GTCACCTGCTAGATCCATTTCC	.1: 200 bp
LH5	<i>AT1G09140</i>	<i>SR30</i>	Rev	AGCCTGAGAAGCTTGAGACG	.2: 550 bp
LH336	<i>AT1G70000</i>	<i>MYBD</i>	Fwd	TCAAACCTCCTGATCCCAACC	.1: 120 bp
LH363	<i>AT1G70000</i>	<i>MYBD</i>	Rev	CTATGTTCTTCCTCTGTCCA	.2: 200 bp

## Chapter III: Draft manuscript 2



## **Splicing regulators of Serine/Arginine-rich (SR) proteins control light-mediated alternative splicing events and integrate light and brassinosteroid signaling to induce cotyledon opening during photomorphogenesis**

Jennifer Saile<sup>1,2</sup>, Moritz Paul Denecke<sup>1</sup>, Sofia Lobato-Gil<sup>3</sup>, Petra Beli<sup>3</sup>, and Andreas Wachter<sup>1,2,\*</sup>

<sup>1</sup>Institute for Molecular Physiology (imP), University of Mainz, Hanns-Dieter-Hüsch-Weg 17, 55128 Mainz, Germany

<sup>2</sup>Center for Plant Molecular Biology (ZMBP), University of Tübingen, Auf der Morgenstelle 32, 72076 Tübingen, Germany

<sup>3</sup>Institute of Molecular Biology (IMB), University of Mainz, Ackermannweg 4, 55128 Mainz, Mainz, Germany.

\*Corresponding author: [wachter@uni-mainz.de](mailto:wachter@uni-mainz.de)

### **Contributions**

The phosphoproteomic study, shown in Figure 1, was performed in collaboration with Sofia Lobato Gil and Petra Beli (IMB Mainz, Germany). Together with Theresa Wießner-Kroh, I grew the plant material and performed light- and sugar treatments. Protein extraction was done by myself, and mass spectrometry and data analysis were performed by Sofia Lobato Gil.

Gabriele Wagner generated 35S::RS-HA<sub>3</sub> and 35S::HA-RS41 constructs and transgenic plants. For segregation analyses (Supplemental Table 3) and transcript studies (Supplemental Figure 6F to I) I was technically supported by Moritz Denecke. Transcript analyses displayed in Supplemental Figure 6B to E, J, K, Supplemental Figure 8E to H were all performed by myself. Transcript analysis shown in Supplemental Figure 23I was done by Moritz Denecke under my supervision. Furthermore, I performed western blot experiments depicted in Supplemental Figure 10.

Higher order T-DNA mutants were generated by myself. This includes crossings and genotyping. For genotyping analyses, I was technically supported by Claudia König.

Furthermore, higher order *rs* CRISPR mutants were generated by myself. This includes guide RNA design, construct cloning, Arabidopsis transformation, selection, genotyping, and sequencing. All phenotyping and pollination experiments shown in Supplemental Figure 2, 3, 4, 5, 7 were done by myself.

Hypocotyl growth assays in *rs* mutants in response to red, blue and far-red light were performed by myself with the help of Laura Schütz and Moritz Denecke (Figure 3, Supplemental Figures 11-20). Corresponding hypocotyl measurements were all done by myself. The hypocotyl growth assay involving RRC1 was also done by myself (Supplemental Figure 21).

Cotyledon opening percentages, angles and hypocotyl growth shown in Supplemental Figure 23 and 24 were all analysed by Moritz Denecke under my supervision.

Cotyledon opening assays in response to light, sucrose and BRZ (shown in Figure 4B to E, Supplemental Figure 25, 26 and 29) were done by myself.

Transcript studies on *COP1*, *PIF3*, *PIF4*, *SAUR-AC1*, *EXPA1* and *BAS1* (Figure 4A, Supplemental Figure 27, 29A) were performed by myself, however, Moritz Denecke provided the RNA for one replicate.

Transgenic lines, expressing the DR5 auxin reporter, were generated by Moritz Denecke under my supervision. Together with Moritz Denecke, I analysed the auxin response by using confocal microscopy (Supplemental Figure 28).

Co-localization studies in *N. benthamiana* (Supplemental Figure 22) were performed by Svenja Saile (University of Tübingen, Germany).

The *RS31* splicing reporter was cloned by Laura Schütz under my supervision. Moritz Denecke performed the splicing assay in *N. benthamiana* (Supplemental Figure 30).

Furthermore, splicing pattern studies in T-DNA and CRISPR mutants were done by myself (Figure 5, Supplemental Figure 30D, Supplemental Figure 31). For the splicing pattern studies in *RS* OE lines, Moritz Denecke provided one replicate, the other two replicates were generated by myself (Supplemental Figure 32).

Statistical analyses and figure design were done by myself. Moreover, I wrote the whole manuscript with contributions from Andreas Wachter.

## Abstract

Light is a crucial environmental factor that controls plant growth and development, including the early seedling stage. Former studies revealed that photomorphogenesis is accompanied by the reprogramming of gene expression via changes in total transcript levels, transcription start sites, translational control, and alternative pre-mRNA splicing (AS). It has already been shown that light-mediated AS involves metabolic and kinase signaling, however, little is known about downstream regulators. In this study we identified RS40 and RS41 splicing regulators of Serine/Arginine-rich (SR) proteins to be specifically phosphorylated in response to light and sugar. A loss of the whole RS subfamily results in almost complete male sterility, hinting towards a major role of RS proteins in reproductive processes. Furthermore, RS proteins play a crucial role in skoto- and photomorphogenic growth, as *RS41* overexpressing lines display enhanced cotyledon opening in darkness as well as in response to light and the brassinosteroid biosynthesis inhibitor brassinazole (BRZ). On the contrary, *rs* triple mutants exhibit reduced cotyledon opening upon illumination. Moreover, we show that *rs* triple mutants are hyposensitive to red light, whereas the overexpression of *RS41* induces red light hypersensitivity, suggesting a possible role of RS proteins in phyB signaling. Using splicing pattern studies, we identified altered responses of light-regulated AS events in dark grown *rs* higher order mutants. Finally, we show that BRZ treatment induces AS changes, mimicking the light response. Therefore, we propose that RS proteins integrate light and brassinosteroid signaling to regulate AS and cotyledon opening during photomorphogenesis.

## Introduction

Plants constantly perceive and respond to environmental changes by adapting their growth and development. Light is a crucial factor that serves as energy source and as signal for developmental reprogramming, including during the early seedling development. After germination in darkness, seedlings grow heterotrophically and aim at rapidly reaching the sunlight to switch from skotomorphogenesis to photomorphogenesis, as a prerequisite of a photoautotrophic lifestyle. Skotomorphogenesis refers to the developmental program in darkness, that is characterized by an elongated hypocotyl, a closed apical hook protecting the shoot apical meristem and closed cotyledons, as well as short roots. After perceiving the first light signals, plants undergo photomorphogenesis. This light-adapted developmental program is accompanied by reduced hypocotyl growth and the opening, greening and expansion of cotyledons, as well as further root development (Gommers & Monte, 2018).

In order to perceive different light qualities, plants have evolved several classes of photoreceptors, including PHYTOCHROMES (phyA-E in Arabidopsis), CRYPTOCHROMES (CRY1, CRY2 and CRY3), PHOTOTROPINS (PHOT1, PHOT2), members of the ZEITLUPE family (ZTL, FKF1, LKP2) and UV RESISTANCE LOCUS 8 (UVR8) (Galvão & Fankhauser, 2015; Paik & Huq, 2019). Multiple transcription factors act downstream of photoreceptors and control light signaling. Typical repressors of photomorphogenesis are the bHLH transcription factors PHYTOCHROME-INTERACTING FACTOR (PIF) proteins, and the E3 ubiquitin ligase complex comprising CONSTITUTIVE PHOTOMORPHOGENIC 1/SUPPRESSOR OF PHYA-105 (COP1/SPA) (Hoecker, 2017; Xu et al., 2015). In darkness, the COP1/SPA complex mediates the degradation of photomorphogenesis-promoting factors, thus facilitating skotomorphogenic growth. The loss of COP1 (*cop1*), SPA1-4 (*spa1 spa2 spa3 spa4*) and PIFs (*pif1 pif3 pif4 pif5*, referred to as *pifq*) all result in a constitutive photomorphogenic phenotype in dark, with opened cotyledons and shortened hypocotyls, mimicking light-grown wildtype (WT) seedlings (Deng & Quail, 1992; Laubinger et al., 2004; Leivar et al., 2008; Leivar et al., 2009). Upon light exposure, activated phytochromes interact with PIFs and COP1/SPA and thus, mediate PIF degradation and COP1/SPA repression (Al-Sady et al., 2006; Ni et al., 2013; Park et al., 2018; Sheerin et al., 2015; Shen et al., 2007). Subsequently, photomorphogenesis

promoting factors, including the transcription factor ELONGATED HYPOCOTYL 5 (HY5) are stabilized and induce light-triggered gene expression to promote de-etiolation (Osterlund et al., 2000).

Light-mediated developmental processes also involve phytohormones, including the steroidal hormones Brassinosteroids (BRs). BRs and light function oppositely in skoto- and photomorphogenesis, as BRs facilitate skotomorphogenic growth by promoting hypocotyl elongation and repression of cotyledon separation in dark (Wang et al., 2012). Nowadays, increasing evidence points to a role for the integration of light and BR signaling pathways to program plant growth and development (Lin et al., 2021). HY5 was found to play a role in BR-mediated cotyledon separation by interacting with the dephosphorylated form of the transcription factor BRASSINAZOLE-RESISTANT1 (BZR1). The interaction results in the sequestration of BZR1 from its target promoters of cotyledon closure genes, thus inducing cotyledon opening (Li & He, 2016). More recently, B-box (BBX) proteins were identified to connect light and BR signaling by controlling cotyledon separation. BBX32 negatively controls photomorphogenesis by interacting with BZR1 and PIF3. BBX32, BZR1 and PIF3 control the expression of common genes to suppress cotyledon opening under dark conditions, thus promoting etiolation (Ravindran et al., 2021).

Light signaling does not only involve transcriptional reprogramming but also pre-mRNA splicing, as revealed by transcriptome wide RNA-seq studies (Hartmann et al., 2016; Mancini et al., 2016; Shikata et al., 2014; Soledad Tognacca et al., 2019; Wu, 2014; Wu et al., 2014). RNA splicing is a co-transcriptional mechanism that is catalysed by a ribonucleoprotein machinery referred to a 'spliceosome' in order to generate a mature mRNA (Chaudhary et al., 2019). Alternative splicing (AS) allows the generation of multiple mRNA isoforms from a single gene by using different splice sites, and plays a major role in adapting to changing environmental conditions by increasing transcriptome and proteome diversity (Staiger & Brown, 2013). Splice site selection is defined by core splicing signals, including 5' and 3' splice site, branch point, polypyrimidine tract and by *cis*- and *trans*-acting elements and factors, respectively. *cis*-acting elements are sequence features within the pre-mRNA that can either positively or negatively affect splice site choice, by acting as splicing enhancer and silencer, respectively. Furthermore, *trans*-acting factors recognize those elements and influence splice site choice (Reddy et al., 2013). *Trans*-acting factors include SR



proteins, that contain one or two N-terminal RNA Recognition Motifs (RRMs) and a C-terminal Arg/Ser-rich (RS) region (Barta et al., 2010). Based on this nomenclature defined by Barta et al., *Arabidopsis thaliana* encodes 18 SR proteins that are grouped into six different subfamilies: SR (ASF/SF2-like, SR34, SR34a, SR34b, and SR30), RSZ (9G8-like, RSZ21, RSZ22, and RSZ22a), SC (ortholog of SC35), SCL (SC35-like, SCL28, SCL30, SCL30a, and SCL33), RS (RS31, RS31a, RS40, and RS41), and RS2Z (RS2Z32, and RS2Z33). The latter three subfamilies are specific for plants (Barta et al., 2010). SR proteins have been linked to developmental processes (Kalyna et al., 2003; Lopato et al., 1999; Reddy & Shad Ali, 2011) and a former study analysed the role of each subfamily, by generating several higher order *sr* mutants (Yan et al., 2017). Yan et al. showed that the *sc35-sc35* like quintuple mutant displays pleiotropic changes in plant morphology and development, accompanied with splicing defects (Yan et al., 2017). To date, however, the role of SR proteins in light signaling has not been addressed. However, there is growing evidence that splicing regulators control light-mediated AS. Recent studies revealed the involvement of SPLICING FACTOR FOR PHYTOCHROME SIGNALLING (SFPS), REDUCED RED-LIGHT RESPONSES IN CRY1 CRY2 BACKGROUND (RRC1), SWAP (SUPPRESSOR-OF-WHITE-APPICOT/SURP RNA BINDING DOMAIN-CONTAINING PROTEIN1) and SWELLMAP 2 (SMP2), in pre-mRNA splicing of light signaling genes in *Arabidopsis* (Kathare et al., 2022; Xin et al., 2017; Xin et al., 2019; Yan et al., 2022). *sfps*, *rrc1* and *swap1* mutants are hyposensitive in response to red light and were identified to interact with phyB (Kathare et al., 2022; Shikata et al., 2012; Xin et al., 2017; Xin et al., 2019). The authors propose that phyB might regulate RRC1, SFPS and SWAP1 activity, thus affecting light-regulated AS.

Using a phosphoproteomic approach we aimed at identifying novel splicing regulators that get specifically phosphorylated in response to light and sugar and hence, control light-mediated AS and photomorphogenic growth by an altered activity. In this work we provide evidence that RS proteins are novel components involved in controlling AS and also skoto- and photomorphogenic growth. We identified RS proteins to get specifically phosphorylated by light and sugar signals, respectively. Simultaneous loss of all four *RS* genes results in a reduced seed yield, caused by pollen malfunctioning. Furthermore, we show that RS proteins control AS in darkness, by acting as a positive regulator of photomorphogenesis. RS proteins function positively in red light signaling and integrate light and BR signaling to regulate cotyledon opening. Overall, our

findings reveal that RS proteins are crucial to regulate light-mediated AS events and further, act as master regulators of skoto- and photomorphogenic growth.

## Results

### Light and sugar specifically induce phosphorylation of RS proteins

Our group has previously provided first evidence that metabolic and kinase signaling contribute to light-regulated AS, thereby controlling plant development during photomorphogenesis (Hartmann et al., 2016). However, the mechanism and *cis*-acting factors that control these AS programs remained elusive. To identify splicing regulators that get specifically phosphorylated by light and sugar signals, and hence, might control light and sugar-regulated AS, we initially performed a MS-based phosphoproteome experiment of 6-d-old etiolated WT seedlings that were exposed to white light or sucrose for 30 min. Among the RNA-binding proteins, we found several phosphopeptides for RS40 and RS41 induced in response to light and sugar exposure, respectively (Figure 1). Consistent with these data, five of the identified six phosphosites in RS41 were also found to be phosphorylated in Arabidopsis roots upon sucrose treatment (Schulze et al., unpublished). RS40 and RS41 belong to the plant specific RS subfamily of SR proteins that share 73.9% amino acid identity. In addition to RS40 and RS41, the RS subfamily comprises another paralogous pair called RS31 and RS31a that are 70.3% identical in their protein sequence. All four RS proteins consist of two RNA recognition motifs (RRMs) at the N-terminus and a C-terminal RS domain with repeated arginine/serine-rich sequences that are targets of phosphorylation (Figure 1C, D, Supplemental Figure 1).

### Generation of *rs* loss-of function mutants

RS40 and RS41 have recently been linked to pre-mRNA splicing and miRNA biogenesis (Chen et al., 2013; Chen et al., 2015). However, their role in photomorphogenesis has not yet been examined. To assess the function of RS proteins during early seedling development, we obtained T-DNA insertion mutants for *RS31*, *RS40*, and *RS41*, referred to as *rs31-1<sub>t</sub>*, *rs31-2<sub>t</sub>*, *rs40-1<sub>t</sub>* and *rs41-1<sub>t</sub>*, as well as a double mutant which was designated as *rs40 rs41<sub>t</sub>* (Supplemental Table 1, Figure 2). In order to circumvent possible functional redundancy among the RS proteins, we generated higher order *rs* mutants. Therefore, we crossed the *rs40 rs41<sub>t</sub>* double mutant with the two obtained *RS31* T-DNA mutants, resulting in *rsT<sub>t</sub> -1* and *rsT<sub>t</sub> -2* triple mutants (Supplemental Table 1). Due to the lack of a suitable *RS31a* T-DNA mutant

line, we additionally used the CRISPR/Cas9 gene editing approach to generate *RS* knockout mutants. We used a system in which *Cas9* expression is driven by an egg cell-specific promoter that has been reported to cause high mutation efficiencies as well as transmissible mutations (Wang et al. 2015). We generated two different CRISPR/Cas9 constructs, each consisting of two single guide RNAs (sgRNAs) to target a paralogous gene pair (i) *RS31* and *RS31a* or (ii) *RS40* and *RS41*. We identified an *rs31<sub>c</sub>* and an *rs31a<sub>c</sub>* single mutant, an *rs31 rs31a<sub>c</sub>* and an *rs40 rs41<sub>c</sub>* double mutant (Supplemental Table 1). Triple and quadruple mutants were then generated by transforming the *Cas9*-free *rs40 rs41<sub>c</sub>* double mutant with the *rs31 rs31a<sub>c</sub>* CRISPR/Cas9 construct. We identified plants with mutations in either *RS31a* or both *RS31* and *RS31a* that we called *rsT<sub>c</sub>* and *rsQ<sub>c</sub>*, respectively.

Sequencing revealed the presence of INDEL mutations in all *RS* genes generated by *Cas9*, resulting in a frameshift that creates a premature termination codon (PTC) downstream of the mutation site (Figure 2). Therefore, it is likely that the corresponding transcripts are unproductive and hence, these plants represent knockout mutants.

### **Loss of all *RS* genes results in reduced fertility**

We next used the generated knockout mutants to examine the role of *RS* proteins in *Arabidopsis* plant growth and development. Upon growth under long day conditions, T-DNA and CRISPR *rs* single, double and triple mutants did not exhibit obvious morphological phenotypes (Supplemental Figure 2). The rosette leaves displayed a slight serrated and curly phenotype (Supplemental Figure 2A to C). Knocking down all *RS* genes resulted in early flowering and severe phenotypical abnormalities during the adult stage (Supplemental Figure 3). *rsQ<sub>c</sub>* mutants displayed a reduced number of anthers (Supplemental Figure 3B) and stunted siliques (Supplemental Figure 3C to E). Interestingly, the loss of *RS40* and *RS41* already significantly reduced the silique length. However, this defect was even more pronounced in *rsQ<sub>c</sub>* (Supplemental Figure 3E). In accordance with the stunted silique growth, *rsQ<sub>c</sub>* mutants were characterized by a drastically reduced seed yield as siliques contained no or only a few seeds. Remarkably, the few produced *rsQ<sub>c</sub>* seeds showed a significantly increased size compared to WT (Supplemental Figure 3F), that could be explained by an increased amount of resources available per seed.

In order to analyse whether the impaired seed production is due to a reduced fertility, we performed pollination experiments. Therefore, *rsQ<sub>c</sub>* stigmas were pollinated with

Col-0 pollen and *vice versa*. Our experiments revealed that *rsQ<sub>c</sub>* mutants are partially male sterile as mutant pollen failed to set seeds in WT plants (Supplemental Figure 4A, C). On the contrary, applying WT pollen to *rsQ<sub>c</sub>* stigmas resulted in the generation of WT-like siliques (Supplemental Figure 4A to C). These data demonstrate that the impaired seed production of the *rsQ<sub>c</sub>* mutant is due to male sterility.

Strikingly, over several generations we observed that some *rsQ<sub>c</sub>* progenies produced WT-like siliques, although identified *rsQ<sub>c</sub>* mutants of the first generation produced almost no seeds. Genotyping revealed heterozygous mutations in at least one *RS* gene, even though plants were previously identified to be transgene-free (Supplemental Figure 5). Very remarkable is the detection of heterozygous mutations in *RS40* and/or *RS41* (Supplemental Table 2), as the *rs40 rs41<sub>c</sub>* double mutant that was used to generate *rsQ<sub>c</sub>*, was formerly identified to be Cas9-free (Supplemental Figure 5).

Taken together, the reduced seed yield in *rsQ<sub>c</sub>* points towards massive defects during pollination. If seeds are generated, a large proportion displays severe abnormalities, including an altered seed size but also a reversion of Cas9-induced mutations. Whether the reversion is based on partial polyploidy or a mechanism similar to revertant mosaicism, remains elusive. However, we selected some of these untypical *rsQ<sub>c</sub>* mutants for seed propagation and preliminary experiments.

### **Generation and characterization of *RS* OE lines**

To further investigate the role of *RS* proteins in *Arabidopsis*, we generated stably transformed *Arabidopsis* plants that constitutively overexpress the cds of individual *RS* genes including the sequence for a C-terminal triple HA-tag (Supplemental Figure 6A). These transgenic plants are designated as *RS* overexpression (OE) lines. Analysing the transcript levels confirmed the overexpression of the *RS* mRNAs in independent sublines within the first generation (Supplemental Figure 6B to E). Lines that showed the highest overexpression were selected and analysed in subsequent generations. Using RT-qPCR we specifically detected the coding isoform of the corresponding *RS* gene. Based on the transcript level, segregation ratio and the amount of available seeds, we then selected specific lines for further experiments. Compared to WT, the selected *RS31* OE #8\_11\_p line showed about 4-fold higher mRNA expression, whereas an 18-fold overexpression was detected in *RS31a* OE #1\_13. Furthermore, the selected *RS40* OE #30\_11 and 30\_14 lines showed about two-fold higher mRNA

expression and an 20-fold overexpression was detected in *RS41* OE #6\_12\_p3 (Supplemental Figure 6F to I). To directly compare the expression levels of the different constructs, we analysed the expression of the *ocs* terminator by detecting its mRNA using *ocs*-specific primers in 10-d-old light grown and 6-d-old etiolated *RS* OE seedlings. RT-qPCR revealed that the *RS41* construct was expressed the most (Supplemental Figure 6J, K). Furthermore, we performed segregation analyses and observed that selected lines displayed almost 100% survival on kanamycin-containing plates (Supplemental Table 3), suggesting that OE lines became homozygous. When we grew these lines under long day conditions, *RS41* OE mutants exhibited a striking phenotype which included dwarfism and downward curled rosette leaves (Supplemental Figure 7A). In addition, *RS31*, *RS40* and *RS41* OE plants were delayed in development, compared to WT, the EGFP control line and *RS31a* OE plants (Supplemental Figure 7B, C), suggesting a role of RS proteins in flowering.

### **Light regulates transcript levels of *RS31* and *RS40***

To determine the general expression of the individual *RS* genes in Arabidopsis, we used a freely available data base called PastDB (<http://pastdb.org.eu/>) that combines gene expression and AS profiles of a variety of Arabidopsis samples that differ in developmental stages, tissues, or stress responses (Martín et al., 2021). We were particularly interested in the *RS* mRNA levels in etiolated Arabidopsis seedlings as well as upon illumination. Interestingly, we noted that *RS31*, *RS40* and *RS41* showed a similar expression level, whereas *RS31a* was significantly less abundant (Supplemental Figure 8A to D). Remarkably, the expression of *RS31* and *RS40* was negatively regulated by light (Supplemental Figure 8A, C). These results were confirmed by RT-qPCR (Supplemental Figure 8E to H). Consequently, we wondered whether the light-dependent repression on transcript level is caused by light-regulated AS of *RS31* and *RS40*. To test this hypothesis, we used the RNA-seq data set from (Hartmann et al., 2016) and observed that *RS31* undergoes AS in a light-dependent manner (Supplemental Figure 9A). Light-regulated AS of *RS31* was further analysed via co-amplification PCR, followed by agarose gel electrophoresis and revealed light-induced skipping of the cassette exon, thus generating the protein-coding isoform (Supplemental Figure 9B). Light-induced switching from an 'unproductive' variant mainly produced under dark conditions to a productive isoform upon illumination is a common phenomenon observed during photomorphogenesis (Hartmann et al., 2016). Several splicing regulators, including RRC1, show a light-dependent switching form an

unproductive variant that is degraded via nonsense mediated mRNA decay (NMD) to a protein-coding isoform upon illumination (Hartmann et al., 2016). As productive isoforms are typically more stable than NMD targets, it is rather unlikely that the AS pattern change in *RS31* triggers the change on transcript level. However, the altered transcript level might be due to reduced transcription or increased turnover.

### **RS41 and RS31 protein abundance is regulated by light**

Since we observed light-induced changes on *RS* transcript levels, we became interested if *RS* protein levels are also light responsive. As the 35S promoter activity is not significantly altered in darkness vs. light (Zhai et al., 2019), we studied *RS* protein levels in 6-d-old dark grown *RS41* OE seedlings that were transferred to white light for different periods. For comparison, we included *RS31* OE seedlings and observed that *RS31* tagged protein levels decreased in response to light signals (Supplemental Figure 10A). Interestingly, *RS41* tagged protein levels increased upon white light illumination (Supplemental Figure 10A).

To analyse whether the increase in *RS41* protein abundance is white light specific, we exposed etiolated *Arabidopsis* seedlings to red light for different time points. After 24 h of illumination, seedlings were shifted back to darkness. We observed that also red light triggered an increase of *RS41* tagged protein level. This increase was reversible as *RS41* tagged protein abundance decreased after transfer back to darkness (Supplemental Figure 10B, C). Remarkably, the transgenic *RS41* protein showed an upward shifted band that accumulated upon illumination. This band, however, was less diminished after transfer back to darkness.

Taken together, our results suggest that the stability of *RS31* and *RS41* tagged proteins is light-regulated. Transgenic *RS31* protein shows a light-induced destabilization and the *RS41* tagged protein a light-mediated stabilization. Moreover, we observed an upward shifted *RS41* band that might correspond to conformers of *RS41*. However, future studies are required to determine the identity of the upward shifted band and should also focus on the endogenous *RS* protein levels that might behave differently compared to the *RS* protein levels from the OE lines.

### RS proteins act as positive regulators in red light signaling

To investigate a potential role of RS proteins in skoto- and photomorphogenesis, we studied the hypocotyl growth as a readout for the light response in different *rs* mutants and *RS* OE lines. Hypocotyl lengths in *rs40<sub>t</sub>* and *rs41<sub>t</sub>* single and the double mutants *rs31 rs31<sub>a<sub>c</sub></sub>*, *rs40 rs41<sub>c</sub>* and *rs40 rs41<sub>t</sub>* were unaffected in response to different light qualities (Supplemental Figure 11, Supplemental Figure 12, Supplemental Figure 13). Only the *rs40 rs41* mutants displayed shortened hypocotyls under dark conditions (Supplemental Figure 12A, Supplemental Figure 13A to B), suggesting that RS40 and RS41 may act redundantly in controlling hypocotyl elongation in darkness. The unaffected hypocotyl lengths in response to red, blue and far-red light, could either suggest that RS proteins do not play a role in light-induced hypocotyl growth or that the remaining RS proteins execute the response. To pursue both hypotheses, we next investigated hypocotyl elongation in *rs* triple mutants. Since we generated several *rs* triple mutants by either crossing the *rs40 rs41<sub>t</sub>* double mutant with different *rs31<sub>t</sub>* alleles or by the CRISPR/Cas9 approach which resulted in a *rs31<sub>a</sub> rs40 rs41<sub>c</sub>* mutant, we first screened the available *rsT* mutants for differences in hypocotyl length in darkness (Supplemental Figure 14). Notably, *rsT<sub>t</sub>-1* displayed significantly elongated hypocotyl lengths upon growth for 4 or 6 d under constant darkness, whereas *rsT<sub>t</sub>-2* and *rsT<sub>c</sub>* showed similar lengths as WT (Supplemental Figure 14A). Overall, these findings point towards a major role of RS31 in controlling hypocotyl growth under dark conditions. The unaffected hypocotyl length in *rsT<sub>t</sub>-2* could be explained by the intronic position of the T-DNA that might be spliced out during mRNA processing (Figure 2A) and the unchanged hypocotyl growth in *rsT<sub>c</sub>* further supports the hypothesis that the remaining RS31 functions in dark-induced hypocotyl elongation. Based on these results, we selected *rsT<sub>t</sub>-1* and *rsT<sub>c</sub>* and in addition, included the *RS41* OE line for the following light response experiments. *RS41* OE lines were of particular interest, as those plants displayed conspicuous dwarfism under long day conditions (Supplemental Figure 7A) and altered phenotypes during skotomorphogenesis (data not shown). Upon 4 d of growth in continuous red light, we found *rs* triple mutants to be hyposensitive, as those mutants displayed elongated hypocotyls in response to red light (Figure 3B). On the contrary, *RS41* OE seedlings showed significantly reduced hypocotyl lengths in darkness or continuous red light (Figure 3A, B), suggesting that *RS41* overexpression impairs skotomorphogenesis in dark and induces a hypersensitivity towards red light. To exclude the light-independent growth effect, we additionally normalized the average

hypocotyl lengths of all tested seedlings in red light to the corresponding average length in darkness (Supplemental Figure 15). Still, longer and shorter hypocotyls, respectively, of the *rs* triple mutants and the *RS41* OE line compared to the WT were observed (Supplemental Figure 15). To investigate whether the observed phenotypes are red light specific, we examined the hypocotyl growth of *rsT<sub>c</sub>* in response to various light qualities, including continuous red, blue and far-red light. In accordance with our previous findings, we observed that *rsT<sub>c</sub>* had elongated hypocotyls compared to the WT under dark and red light conditions (Supplemental Figure 16A to C) and slightly longer hypocotyls in response to far-red light (Supplemental Figure 16G). However, *rsT<sub>c</sub>* hypocotyl growth did not differ from WT in response to blue light (Supplemental Figure 16D, E). These results hint towards a major role of RS proteins in red light signaling.

Although our findings clearly indicate a major role of RS proteins in red light signaling, we could not rule out the possibility that the remaining RS activity in the *rs* triple mutant is required for the light-induced hypocotyl growth under blue light. Therefore, we determined hypocotyl lengths in the available *rsQ<sub>c</sub>* mutants, which produced an uncharacteristically increased amount of seeds, and included *rsT<sub>c</sub>* mutants as control. Due to a limited amount of atypical *rsQ<sub>c</sub>* seeds (Supplemental Figure 3F), we were only able to analyse hypocotyl growth under constant darkness and in response to continuous red and blue light. We found that the loss of all *RS* genes resulted in a striking phenotype with significantly elongated hypocotyls under all tested light conditions (Supplemental Figure 17). Furthermore, *rsQ<sub>c</sub>* mutants displayed strongly expanded cotyledons and an increased root length compared to *rsT<sub>c</sub>* and WT seedlings (Supplemental Figure 17B, C, Supplemental Figure 18). We propose that this magnified phenotype might be either caused by an enhanced resource allocation in the available atypical *rsQ<sub>c</sub>* seeds that we previously identified to be significantly larger compared to WT (Supplemental Figure 3F) or by a partial polyploidy. Hence, those atypical *rsQ<sub>c</sub>* mutant seedlings are not suitable for the analysis of light-mediated growth responses.

Lastly, we examined whether the overexpression of certain *RS* genes affects light responses. Therefore, we compared the hypocotyl growth in 4-d-old *RS* OE and WT seedlings that were either grown in constant darkness (Supplemental Figure 19A, Supplemental Figure 20A) or under different fluence rates of continuous red



(Supplemental Figure 19B, C, Supplemental Figure 20B, C), blue (Supplemental Figure 19D, E, Supplemental Figure 20D, E) and far-red light (Supplemental Figure 19F, G, Supplemental Figure 20F, G), respectively. In contrast to our previous observations (Figure 3A), *RS41* OE lines did not show a significantly shortened hypocotyl in the dark and hypocotyl lengths of other dark grown *RS* OE seedlings were also not drastically altered compared to WT (Supplemental Figure 19A, Supplemental Figure 20A). Also, in response to light, we did not observe any significant differences in hypocotyl elongation of seedlings overexpressing *RS31*, *RS31a*, *RS40* (Supplemental Figure 19B to G, Supplemental Figure 20B to G). *RS41* OE seedlings, however, displayed reduced hypocotyl lengths upon growth under red and far-red light conditions (Supplemental Figure 19B, C, F, G), whereas hypocotyls were not affected in response to blue light (Supplemental Figure 19D, E). These findings demonstrate the hypersensitivity of *RS41* OE to red and far-red light.

Taken together, we observed altered red and far-red light phenotypes in *rs* mutants and *RS41* OE lines, demonstrating that RS proteins positively function in red light signaling. The lack of significant hypocotyl phenotypes in the *RS31*, *RS31a* and *RS40* OE lines, might be either due to a specific role of *RS41* in hypocotyl growth in response to light or caused by different expression levels of *RS* genes (Supplemental Figure 6).

### **Loss of *RRC1* enhances red light hyposensitivity in *rs* mutants**

To get a better understanding of the mechanism underlying RL-controlled hypocotyl growth, we analysed the relationship between RS proteins and another SR-like splicing regulator, *RRC1*. Therefore, we crossed the *rsT<sub>t</sub>-1* triple mutant with mutants carrying the *rrc1-2* and *rrc1-3* T-DNA alleles, respectively (Supplemental Figure 21A). *rrc1-2* and *rrc1-3* were previously described as knockdown alleles, that display elongated hypocotyls in response to red light (Hartmann et al., 2016; Shikata et al., 2012; Xin et al., 2019). Hence, *RRC1* is an SR-like splicing factor with a major role in phyB signaling. To test the relationship between RS proteins and *RRC1*, we compared the hypocotyl length of the *rsT<sub>t</sub> rrc1* quadruple mutants with *rsT<sub>t</sub>-1* triple and *rrc1* single mutants as well as WT. Under dark conditions, *rsT<sub>t</sub> rrc1* quadruple mutants displayed similar hypocotyl lengths as the *rsT<sub>t</sub>-1* triple mutant (Supplemental Figure 21B). Interestingly, all mutants showed markedly elongated hypocotyls under red light conditions, with the *rsT<sub>t</sub> rrc1* quadruple mutant exhibiting the strongest phenotype (Supplemental Figure 21C). Normalization to the corresponding average dark length

did not change this observation (Supplemental Figure 21D). Remarkably, *rrc1* single mutants had longer hypocotyls than the *rsT<sub>i</sub>-1* triple mutant under red light. In response to blue and far-red light, relative hypocotyl lengths of, *rsT<sub>i</sub> rrc1* and *rrc1* did not differ significantly from WT, except *rrc1-2* and *rsT<sub>i</sub>-1* which displayed significantly elongated hypocotyls under blue (Supplemental Figure 21E to H) and far-red light conditions (Supplemental Figure 21G), respectively. A previous study reported elongated hypocotyls in *rrc1-3* under red, far red and blue light conditions (Xin et al., 2019). These controversial findings might be attributed to light intensity differences.

Together, our findings revealed that the combined loss of *RRC1* and *RS31*, *RS40* and *RS41* triggers a strong red light hyposensitivity, suggesting that the proteins might act in independent complexes.

### **RS41 does not co-localize with phyB in *N. benthamiana***

The observed red light hyposensitivity phenotype of *rs* mutants prompted us to test whether RS proteins interact with the red-light photoreceptor phyB. RS41 was recently identified to localize in the nucleus of light-kept Arabidopsis protoplasts, where it was distributed in the nucleoplasm but also concentrated in nuclear speckles (Chen et al. 2015). On the contrary, phyB was found to re-localize in response to light from the cytosol into the nucleus where it associates with photobodies (Kircher et al., 1999; Klose et al., 2015). To test a potential interaction between RS proteins and phyB, we examined whether RS41 co-localizes with phyB *in vivo*. Therefore, a double construct of RS41 caused by a cloning artifact, referred to as RS41-RS41-EGFP, was transiently co-expressed with phyB-tRFP in *N. benthamiana*. After infiltration, plants were either kept in white light or transferred to darkness. Confocal imaging confirmed the nuclear localization of RS41 fusion proteins. Under dark conditions, RS41-RS41-EGFP was localized in nuclear speckles and the nucleoplasm (Supplemental Figure 22, upper panels). In contrast, however, upon growth in light, RS41 was mainly localized in the nucleoplasm and phyB-tRFP was found in photobodies (Supplemental Figure 22, lower panels). Thus, we did not observe a co-localization of RS41 and phyB in the nucleus of light-grown *N. benthamiana* plants. These unexpected results might be due to the highly artificial RS41 double construct or the artificial *N. benthamiana* system that does not reflect the actual *in planta* situation.

***RS41* overexpression induces cotyledon opening in darkness**

When analysing the hypocotyl growth of *rs* mis-expression lines, we noted that *RS* OE seedlings displayed opened cotyledons in darkness, whereas most cotyledons of WT and higher order *rs* mutants remained closed. Interestingly, seedlings overexpressing *RS41* showed the most relative number of open cotyledons that were also associated with significantly enhanced opening angles (Supplemental Table 4). Together, both the opened cotyledons and the shortened hypocotyls of *RS41*-HA<sub>3</sub> OE seedlings in darkness (Figure 3A) are reminiscent of a de-etiolation phenotype.

To further investigate a potential role of *RS41* in photomorphogenesis, we analysed typical characteristics of a de-etiolation phenotype, including cotyledon opening and hypocotyl lengths in several *RS41*-HA<sub>3</sub> OE sublines that were grown for 4 and 6 d in darkness, respectively. Upon growth in darkness, all *RS41*-HA<sub>3</sub> OE sublines displayed opened cotyledons that were associated with significantly increased opening angles, compared to WT (Supplemental Figure 23A to C, E to G). Additionally, three of four *RS41*-HA<sub>3</sub> OE sublines exhibited a significantly shorter hypocotyl compared to WT (Supplemental Figure 23D, H). These findings demonstrate a positive role of *RS41* in photomorphogenesis.

In order to determine whether cotyledon opening correlates with the *RS41* expression level, we studied *RS41* total transcript level in 6-d-old dark grown *RS41* OE sublines. RT-qPCR analyses revealed that *RS41* OE #6\_1 showed a 40-fold overexpression of *RS41* compared to WT (Supplemental Figure 23I). Hence *RS41* OE #6\_1 is the subline with the highest overexpression. Consistent with the high *RS41* transcript level, *RS41* OE #6\_1 displayed the most prominent cotyledon phenotype with most cotyledons being open and having the largest cotyledon opening angles compared to the other sublines (Supplemental Figure 23B, C, F, G). The relative number of cotyledons and opening angles of *RS41* OE #7\_1, displaying only 10-fold overexpression compared to WT (Supplemental Figure 23I), were smaller than in #6\_1 (Supplemental Figure 23A to C, E to G). These findings suggest that there is a positive correlation between cotyledon opening and the expression level of *RS41*. To make a clear conclusion, further replicates are needed to reveal whether the expression level of *RS41* correlates with the degree of de-etiolation.

To verify that *RS41* overexpression induces de-etiolation, we analysed an independent *RS41* OE line, referred to as HA-*RS41* OE. In contrast to the *RS41*-HA<sub>3</sub> OE line used

before (C-terminal fusion with triple HA), HA-*RS41* contains the tag sequence, encoding a single HA tag, at the N-terminus (Supplemental Figure 24). When we screened multiple HA-*RS41* sublines for an open cotyledon phenotype in darkness, we observed a reduced number of seedlings exhibiting opened cotyledons compared to *RS41*-HA<sub>3</sub> OE sublines (Supplemental Figure 24B, C, F, G). Additionally, cotyledon opening angles of HA-*RS41* OE sublines were smaller compared to *RS41*-HA<sub>3</sub> OE and did not significantly differ from WT (Supplemental Figure 24D, H). In contrast, however, hypocotyl length was significantly reduced in almost all tested HA-*RS41* OE sublines compared to WT (Supplemental Figure 24E, I). Taken together, cotyledon opening results are less pronounced compared to *RS41*-HA<sub>3</sub> OE findings, which might be explained by variations in *RS41* expression level. Nevertheless, these findings further support a positive role of *RS41* during photomorphogenesis.

### **RS proteins play a positive role in light-induced cotyledon opening**

Since *RS41* upregulation results in cotyledon opening in darkness (Supplemental Figure 23), we wondered whether RS proteins play a role in light-induced cotyledon opening. Therefore, we examined cotyledon opening as a response during the transition from dark to light in *rsT<sub>t</sub>-1*, *RS41* OE and WT seedlings (Supplemental Figure 25A to G). After transferring the seedlings to continuous white light, we observed that a 6 h light treatment was sufficient to induce cotyledon opening in all WT and *RS41* OE seedlings, whereas only 50% of the cotyledons in the *rsT<sub>t</sub>-1* were open (Supplemental Figure 25A). Remarkably, a 24 h white light treatment was required to induce complete cotyledon opening in *rsT<sub>t</sub>-1* (Supplemental Figure 25A). When we determined the cotyledon opening angles, we observed that in particular at the early time points *rsT<sub>t</sub>-1* mutants displayed significantly smaller opening angles compared to WT (Supplemental Figure 25B to D). On the contrary, *RS41* OE lines showed constantly increased cotyledon opening angles compared to WT, however, the difference was not significant (Supplemental Figure 25B to G). After 72 h of illumination, all lines showed fully opened cotyledons with angles greater than 150 degrees (Supplemental Figure 25G).

Based on the altered red light phenotypes we have observed before in *rsT* and *RS41* OE lines (Figure 3), we next studied cotyledon opening in response to red light (Supplemental Figure 25H to N). 6 h after transfer to red light, all *RS41* OE lines displayed fully open cotyledons (Supplemental Figure 25H). At that time point, 85% of

WT and 67% of *rsT<sub>t</sub>-1* showed separated cotyledons (Supplemental Figure 25H). After 72 h of red light illumination, all WT seedlings exhibited opened cotyledons, whereas cotyledon opening in *rsT<sub>t</sub>-1* seedlings was still retarded, with 20% of the cotyledons still being closed (Supplemental Figure 25H). Angle measurements revealed that *RS41* OE constantly displayed greater opening angles compared to WT, whereas *rsT<sub>t</sub>-1* displayed much smaller angles (Supplemental Figure 25I to N).

In summary, we observed faster cotyledon opening kinetics in *RS41* OE seedlings, whereas *rsT<sub>t</sub>-1* mutants showed slower kinetic with reduced opening angles in response to white and red light, respectively (Supplemental Figure 25). These findings suggest that RS proteins play a positive role in light-induced cotyledon opening and point towards a major role of RS proteins during photomorphogenesis.

### **Sucrose does not induce cotyledon opening in darkness**

As light triggers cotyledon opening, we wondered whether sucrose, as major product of photosynthesis, may be sufficient to induce cotyledon opening in darkness. To test this idea, we grew WT and *RS* OE seedlings in the absence or presence of 2% sucrose and kept the plates in darkness for 6 d. In the absence of sucrose, 70% of *RS41* OE seedlings displayed separated cotyledons with significantly increased opening angles (Supplemental Figure 26A, B, E). On the contrary, cotyledon opening in *RS31* and *RS40* OE seedlings did not significantly differ from WT (Supplemental Figure 26A, B, E). When seedlings were grown in the presence of sucrose, cotyledon opening was neither affected in WT, nor in *RS31* and *RS40* OE seedlings (Supplemental Figure 26C to E). Surprisingly, *RS41* OE seedlings were no longer able to open their cotyledons and hence, remained mainly closed (Supplemental Figure 26C to E). These findings clearly suggest that sucrose cannot take over the role of light in inducing cotyledon opening. However, sucrose seems to have a major impact on the function of *RS41* and thus, inhibits *RS41*-induced cotyledon opening.

## **COP, PIFs and auxin are not the major players controlling RS-induced cotyledon opening**

In this study we identified the RS proteins as essential factors for cotyledon opening and hypocotyl elongation and thus, observed a de-etiolation phenotype with shortened hypocotyls and opened cotyledons upon *RS41* overexpression. This phenotype resembles the constitutive photomorphogenic (cop) phenotype observed in mutants defective in negative regulators of photomorphogenesis, including *cop1* (Deng & Quail, 1992) and *pifQ* (Leivar et al., 2008; Leivar et al., 2009). We speculated that *COP1* and/or *PIF* levels might be decreased in *RS41* OE lines. To test this hypothesis, we performed RT-qPCR using 6-d-old dark grown *RS* OE seedlings. RT-qPCR analyses revealed that transcript levels of *COP1* and *PIF4* were not significantly changed by *RS* overexpression (Supplemental Figure 27A, C). However, *PIF4* transcript level showed high variation, likely caused by different harvesting time points, as *PIF4* expression was found to exhibit a diurnal rhythm (Nusinow et al., 2011). Thus, further replicates are needed to clarify whether *PIF4* transcript level might be altered by *RS* mis-expression. Surprisingly, we observed a significantly increase of the *PIF3* transcript level in *RS41* OE seedlings (Supplemental Figure 27B). Currently, we do not understand the mechanism that leads to increased *PIF3* levels upon *RS41* overexpression. However, former studies observed altered *PIF3* levels in the splicing regulator mutants *sfps* and *rrc1*, caused by alternative splicing of *PIF3* (Xin et al., 2017; Xin et al., 2019). Whether a similar link exists for *RS41* requires further studies. Nevertheless, based on the role of PIFs in repressing photomorphogenesis, we assume that altered/increased *PIF* transcript levels are not the reason for the cop-like phenotype observed in *RS41* OE seedlings.

A recent report revealed a function of the phytohormone auxin in controlling cotyledon closure and opening during transition from dark to light, involving light inducing *SMALL AUXIN UP RNA (lirSAUR)* genes (Dong et al., 2019). During de-etiolation, *lirSAURs* are expressed in cotyledons which is accompanied by an accumulation of auxin but their expression is repressed in hypocotyls (Sun et al., 2016). To examine whether *RS41*-induced cotyledon opening depends on altered auxin levels, we transformed the auxin double reporter DR5v2-ntdTomato-DR5-n3GFP (Liao et al., 2015) in *RS41* OE and WT plants (Supplemental Figure 28A). The reporter contains auxin-responsive elements in the DR5 and DR5v2 promoter, respectively, that are bound by auxin response factors (ARFs). The auxin-responsive element in DR5v2 possesses a higher

ARF binding affinity than the element in DR5 and hence, auxin sensitivity is increased in DR5v2 compared to DR5 (Liao et al., 2015). Using confocal imaging we studied the auxin response in cotyledons of 4-d-old etiolated seedlings. We detected a strong auxin accumulation at the inner side of the apical hook and hypocotyl and a strong DR5 activity in cotyledons (Supplemental Figure 28B). However, we did not observe obvious differences in auxin distribution between transgenic *RS41* OE and WT seedlings (Supplemental Figure 28B). Together, these findings suggest that changes in auxin distribution cannot explain *RS41*-induced cotyledon opening.

### **RS-induced cotyledon opening involves BR signaling**

BRs play a crucial role during photomorphogenesis, by acting as negative regulators (Wang et al., 2012). Previously, it has been reported that BR biosynthesis mutants, including *det1-2*, exhibit a cop-like phenotype, with shortened hypocotyls and opened cotyledons (Chory et al., 1991; Li et al., 1996). To investigate whether RS-induced cotyledon opening involves BR signaling, we first analysed the expression of BR-responsive genes, including *SAUR-AC1*, *EXPA1* and *BAS1* in 6-d-old dark grown *RS* OE seedlings. *SAUR-AC1* was formerly used as marker of the endogenous BR response (Hamasaki et al., 2020). In our study we identified significantly reduced *SAUR-AC1* levels in *RS31* and *RS41* OE seedlings, as well as significantly decreased *EXPA1* transcript levels upon *RS41* overexpression (Figure 4A). On the contrary, RT-qPCR analyses revealed high variations in the transcript levels of *SAUR-AC1*, *EXPA1* and *BAS1* in *RS31a* and *RS40* *RS* OE lines, probably caused by developmental differences (Figure 4A, Supplemental Figure 29A).

Since the *RS41* OE seedlings show the most prominent de-etiolation phenotype when grown in dark and clearly affected expression of BR-responsive genes, we further studied the potential link between *RS*-induced cotyledon opening and BR signaling. Therefore, we grew *RS* OE and *rsT<sub>c</sub>* in the presence of the BR biosynthetic inhibitor brassinazole (BRZ) in darkness. BRZ was previously identified to induce cotyledon opening in dark grown WT seedlings (Asami et al., 2000). In case *RS*-induced cotyledon separation involves BR signaling, *RS* OE lines would be hypersensitive towards BRZ and hence, would display larger opening angles compared to WT. In contrast, *rsT<sub>c</sub>* mutants are expected to be BRZ hyposensitive and thus, opening angles are expected to be smaller compared to WT. Under mock conditions, *RS* OE seedlings displayed increased opening percentages with enhanced opening angles compared to

WT and *rsT<sub>c</sub>*, with the most pronounced phenotype caused by *RS41* overexpression (Figure 4B to D). When seedlings were grown in the presence of BRZ, cotyledon separation was induced (Figure 4B). The relative number of open cotyledons as well as the cotyledon opening angles positively correlated with the BRZ concentration (Figure 4B to D). In the presence of 0.25  $\mu$ M BRZ, all *RS* OE lines showed significantly increased cotyledon opening angles compared to WT, whereas *rsT<sub>c</sub>* mutants exhibited a reduced number of seedlings with opened cotyledons that displayed smaller angles (Figure 4D). However, the decreased opening angle in *rsT<sub>c</sub>* did not significantly differ from WT seedlings.

With increasing BRZ concentrations, cotyledon opening became saturated and hence, no significant changes between *rs* mis-expression lines and WT were observed (Figure 4D, Supplemental Figure 29B). Furthermore, we noted that BRZ treatment results in the inhibition of hypocotyl growth (Figure 4E). However, hypocotyl lengths did not significantly differ in *RS41* OE, *rsT<sub>c</sub>* and WT in response to BRZ.

Taken together, our results revealed that *RS* OE lines, in particular *RS41* and *RS31*, are hypersensitive in response to BRZ-induced cotyledon opening, whereas BRZ-triggered hypocotyl inhibition is unaffected. Thus, our findings point towards the involvement of BR-signaling in *RS*-induced cotyledon opening.

### **Inhibition of BR-signaling induces AS changes**

Previously, it has been reported that light and BRs control photomorphogenesis in an opposite manner (Wang et al., 2012). Since light exposure induces AS changes (Hartmann et al., 2016; Mancini et al., 2016; Shikata et al., 2014), we wondered whether BRs might also act as regulator of AS during photomorphogenesis. To this end, we analysed *SR30* splicing patterns in WT, *RS41* OE and *rsT<sub>c</sub>* seedlings that were grown for 3 d on mock and BRZ-containing media, respectively. In addition, some of the plates were supplemented with 1.5% sucrose, serving as a control for light-induced AS changes. Interestingly, we found significant AS changes of *SR30* in response to BRZ treated WT seedlings (Figure 4F). BRZ treatment induced a splicing shift towards the productive *SR30.1* variant, resembling the splicing changes observed by light or sugar treatment. Remarkably, this splicing shift was further enhanced in the presence of sucrose, compared to the sucrose mock control (Figure 4F). Next to WT seedlings, we also observed a BRZ-induced splicing shift in *RS41* OE and *rsT<sub>c</sub>* seedlings, although AS starting ratios differed (Figure 4F).



Taken together, our data illustrate that the inhibition of BR signaling as well as the mis-expression of *RS* genes affects the AS decision. Thus, we propose that BRs are involved in controlling AS changes and hence, plant development during photomorphogenesis.

### **RS proteins control alternative splicing in darkness**

Based on the findings showing that the mis-expression of *RS* genes alters the AS decision (Figure 4F) and the fact that RS40 and RS41 are specifically phosphorylated in response to light and sugar (Figure 1), we further investigated the potential role of the *RS* subfamily in controlling light- and sugar-mediated AS during photomorphogenesis. To this end, we first generated an *RS31* splicing reporter based on the light-regulated AS events in *RS31* (Supplemental Figure 30A). Transient co-expression with individual *RS* proteins or the control protein luciferase (LUC) in *N. benthamiana* allowed a direct comparison of *RS* contributions to *RS31* pre-mRNA splicing. Co-expressing LUC with the *RS31* reporter had no impact on *RS31* splicing. Hence, the productive *RS31.1* isoform was most abundant, followed by the unproductive variants *RS31.2* and *RS31.3* (Supplemental Figure 30B). Interestingly, *RS31a* had a positive impact on *RS31* splicing, as *RS31a* induced an AS shift towards the protein coding isoform *RS31.1* (Supplemental Figure 30B, C). On the contrary, *RS41* negatively controlled *RS31* splicing, by changing the *RS31* AS ratio towards the unproductive *RS31.2* and *RS31.3* variants (Supplemental Figure 30B, C). Remarkably, *RS31* and *RS40* had no major impact on the AS pattern of *RS31* (Supplemental Figure 30B, C).

As an independent proof that *RS40/RS41* are involved in *RS31* splicing, we studied the splicing pattern in the *Arabidopsis rs40 rs41<sub>c</sub>* mutant. Co-amplification PCR, followed by gel electrophoresis revealed a splicing shift towards the productive variant of *RS31.1* (Supplemental Figure 30D). These findings indicate that *RS* proteins can control light-mediated AS events and additionally cross-regulate their expression via AS.

To further confirm the role of *RS* proteins in light-mediated AS, we next compared splicing patterns in etiolated *rs* CRISPR double, triple (*rs31a rs40 rs41<sub>c</sub>*) and quadruple mutants and the *rs* T-DNA triple (*rs31 rs40 rs41<sub>t</sub>*) mutant. WT seedlings were included as control.

First, we analysed the splicing patterns of different light-regulated AS events in the double mutant *rs31 rs31a<sub>c</sub>*. Under dark conditions, *rs31 rs31a<sub>c</sub>* showed a significant change in the splicing ratio of *SR30*, *RRC1* and *PPD2* towards the productive isoforms (Figure 5A to C). Furthermore, we observed weaker AS changes towards the protein coding variants of *MYBD* and *PPL1* (Figure 5D, E). Together, these findings suggest that RS31 and RS31a can regulated light-mediated AS events in dark. To analyse whether RS40 and RS41 similarly contribute to the regulation of light-mediated AS events, we next examined selected AS events in dark grown *rs40 rs41<sub>c</sub>* mutants. Unlike as observed in *rs31 rs31a<sub>c</sub>*, the loss of RS40 and RS41 did not result in any splicing change in *SR30* (Figure 5A). However, *rs40 rs41<sub>c</sub>* mutants showed a significant change in the splicing ratio of *RRC1* towards the productive *RRC1.1* variant, and weak splicing changes of *PPD2* and *MYBD*, similar to the *rs31 rs31a<sub>c</sub>* mutant (Figure 5B to D). In contrast to *rs31 rs31a<sub>c</sub>*, the loss of RS40 and RS41 did not affect *PPL1* splicing (Figure 5E), suggesting an important role of RS31 and RS31a in controlling this AS event.

Finally, we examined the splicing change in RS31/RS31a and RS40/RS41 combined mutants, such as *rsT<sub>c</sub>* and the available *rsQ<sub>c</sub>* mutants, that untypically generated more seeds. Interestingly, the previously observed splicing shift of *SR30* in *rs31 rs31a<sub>c</sub>* was lost and antagonized in *rsT<sub>c</sub>* and *rsQ<sub>c</sub>*, respectively (Figure 5A), whereas the other AS events showed similar changes in the AS ratio towards the productive isoforms (Figure 5B to E), as already observed in *rs31 rs31a<sub>c</sub>*.

Overall, our findings reveal that RS proteins can control light-regulated AS events in dark by altering the splicing pattern towards the unproductive isoforms. One exception is the *SR30* AS event, that is oppositely controlled in the *rsQ<sub>c</sub>* mutant, compared to the *rs31 rs31a<sub>c</sub>* mutant, although *rs40 rs41<sub>c</sub>* mutants showed a WT-like *SR30* splicing pattern. As *SR30* encodes a SR splicing regulator, these contradictory findings might be due to complex networks between splicing regulators that undergo AS themselves.

Lastly, we compared the splicing patterns of light-regulated AS events in the T-DNA triple mutant (*rs31 rs40 rs41<sub>t</sub>*) with the findings obtained for the *rs* CRISPR mutants. Similar to the *rsQ<sub>c</sub>* mutant, we observed a change in the splicing ratio of *SR30* towards the unproductive isoform (Figure 5F). In contrast, the other AS events (including *RRC1*, *PPD2* and *MYBD*) showed all an opposite splicing change towards the productive variants (Figure 5G to I), similar to the *rs* CRISPR triple mutant. These results further

highlight a differential regulation of *SR30* by RS proteins compared to other light-controlled AS events.

To determine whether RS proteins are required for light- and sugar-regulated AS, we further analysed the splicing response in *rsT<sub>t</sub>-1* and WT seedlings that were exposed to sugar and light for 6 h. As previously reported, light and sugar trigger splicing pattern changes in WT, resulting in the relative enrichment of the protein-coding variant of several light-regulated AS events, including *SR30*, *RRC1*, *PPD2*, and *MYBD* (Hartmann et al., 2016). Interestingly, we noted that *rsT<sub>t</sub>-1* mutants were still able to respond to light and sugar signals (Supplemental Figure 31A to D). To analyse the relative change, we calculated the AS responsiveness by normalizing the light/sugar response to the corresponding dark control. Although the *rsT<sub>t</sub>* mutant showed in most AS events different steady state levels in darkness compared to WT (Figure 5F to I), the relative AS changes in response to light and sugar were highly comparable to those in WT (Supplemental Figure 31E to H). These results point to the involvement of additional factors (probably also including the remaining RS31a) that trigger the light- and sugar response.

#### **Overexpression of *RS41* affects *SR30* and *PPD2* splicing in darkness**

Based on our findings that the loss of RS proteins triggers splicing changes of light-controlled AS events, we next investigated the splicing patterns in response to RS overexpression (Supplemental Figure 32, 33). As the loss of RS31 and RS31a induced changes in the splicing ratio of several light-regulated AS events in dark (Figure 5A to E), we first analysed the splicing ratio in dark grown *RS31* OE lines, followed by *RS31a* OE seedlings. The overexpression of *RS31* slightly changed the AS ratio towards the unproductive *SR30.2* variant and the productive *PPD2.1* isoform (Supplemental Figure 32A, B), however, splicing changes were not significantly altered compared to WT. Moreover, *RS31* OE seedlings showed WT-like splicing patterns of *RRC1*, *MYBD* and *PPL1* (Supplemental Figure 32C to E), suggesting that the overexpression of *RS31* does not significantly contribute to the regulation of these AS events in dark. These findings were also observed by the overexpression of *RS31a*, as changes in the AS ratio of light-regulated AS events were not significantly altered in *RS31a* OE lines, compared to WT (Supplemental Figure 32). We only detected a weak change in the splicing ratio of *PPD2* towards the unproductive variant (Supplemental Figure 32B), as well as a weak response in the splicing ratio of *MYBD* towards the productive isoform

(Supplemental Figure 32D), suggesting that the overexpression of *RS31a* weakly affects *PPD2* and *MYBD* splicing. Together, our findings indicate that the overexpression of *RS31* and *RS31a* does not significantly contribute to the regulation of light-mediated AS events in dark. To analyse whether this is also true for overexpressed *RS40* and *RS41* proteins, we next studied the splicing pattern in etiolated *RS40* and *RS41* OE lines. The overexpression of *RS40* did also not significantly alter the splicing pattern of all selected AS events (Supplemental Figure 32). However, changes in the *PPD2* and *MYBD* splicing ratio were slightly altered by *RS40* expression (Supplemental Figure 32B, D), similar as observed in *RS31a* OE lines. In contrast, the overexpression of *RS41* induced opposite changes in *PPD2* and *MYBD* towards the productive and unproductive isoform, respectively (Supplemental Figure 32B, D). Furthermore, a significant splicing shift towards *SR30.1* was observed by the overexpression of *RS41* (Supplemental Figure 32A), that was not detected in any other *RS* OE lines. In contrast, *RRC1* and *PPL1* splicing patterns were WT-like in *RS41* OE seedlings (Supplemental Figure 32C, E). Taken together, our findings suggest that the overexpression of *RS31*, *RS31a* and *RS40* does not significantly contribute to the regulation of light-mediated AS events in darkness. However, overexpressed *RS41* proteins might play a specific role in controlling *SR30* and *PPD2* splicing in dark.

Finally, we tested whether the overexpression of *RS* genes affects the light- and sugar-mediated AS response. Therefore, etiolated *RS* OE and WT seedlings were treated with sucrose or exposed to white light for 6 h. Light and sucrose treatment changed the splicing ratio towards the protein coding isoform in WT seedlings (Supplemental Figure 32). We also observed a comparable light and sugar response upon *RS* mis-expression and calculated the responsiveness. Our analysis revealed that the relative AS changes in response to light and sugar were comparable to those in WT seedlings (Supplemental Figure 33). These findings further hint towards a specific role of *RS* proteins in AS regulation under dark conditions or might be due to the altered *RS* activity in response to light and sugar.

## Discussion

### RS proteins are novel regulators of AS during the early seedling stage

Genome wide analyses have previously revealed that light induces massive AS changes in plants, which provides powerful means to regulate gene expression and hence, to adapt to changing environmental conditions (Godoy Herz et al., 2019; Hartmann et al., 2016; Shikata et al., 2014; Xin et al., 2017). However, little is known about upstream regulators that affect light-mediated AS. Former studies identified splicing regulators, including SFPS, RRC1 and SWAP1, as essential components controlling pre-mRNA splicing of light-related genes in order to promote photomorphogenesis (Kathare et al., 2022; Shikata et al., 2012; Xin et al., 2017; Xin et al., 2019). More recently, SMP2 was uncovered as negative regulator of photomorphogenesis, by affecting light-mediated AS of the clock regulator gene *RVE8* (Yan et al., 2022).

In this study we provide evidence that RS proteins are novel regulators of light-mediated AS events that play important roles during plant development, in particular during the early seedling stage and in response to red light. We show that higher order *rs* mutants display elongated hypocotyls under continuous red-light conditions. Previously, phyB was uncovered to be a major regulator controlling hypocotyl elongation in response to red light (Li et al., 2011), suggesting that RS proteins might play a role in phyB-mediated signaling. However, RS41 does not co-localize with phyB after transient expression in *N. benthamiana*. SR speckle formation and appearance in *N. tabacum* and Arabidopsis cells was reported to differ greatly (Lorković et al., 2004) and is consistent with our observations (data unpublished). Accordingly, it seems possible that RS proteins might co-localize and interact with phyB in illuminated Arabidopsis seedlings. In support of this idea, the splicing regulators SFPS, RRC1, SWAP1, NOT9B and SMP2 were linked to phytochrome signaling in Arabidopsis, as they can interact with either phyA or phyB *in vivo*. Moreover, corresponding mutants display altered phenotypes in response to red light (Kathare et al., 2022; Schwenk et al., 2021; Shikata et al., 2012; Xin et al., 2017; Xin et al., 2019; Yan et al., 2022). Kathare et al. revealed that SFPS, RRC1 and SWAP1 form a tetrameric complex and cooperatively regulate pre-mRNA splicing of light-related genes under dark and light conditions, promoting photomorphogenesis (Kathare et al., 2022). In addition, all three splicing regulators control specific mRNA targets, suggesting distinct functions

(Kathare et al., 2022). Here we show that RS proteins act as positive regulators of photomorphogenesis that control AS of selected light-regulated AS events in dark. Remarkably, RS40 and RS41 function oppositely to RS31 and RS31a in *SR30*, *PPD2* and *PPL1* AS control, suggesting different functions of small vs. large RS protein pairs in AS regulation. However, RS proteins similarly regulate AS of *RRC1* and MYBD, which may suggest that RS proteins act in the same complex to regulate these AS events. To investigate whether RS proteins actually form a complex, co-immunoprecipitation experiments, followed by MS could provide further insights into the RS interactome.

Our complex splicing pattern findings might be explained by specific splicing networks of splicing regulators. In line with our hypothesis are previous studies showing that splicing regulator mutants display extensive splicing changes in genes that encode for splicing regulators (Kathare et al., 2022; Shikata et al., 2012; Xin et al., 2017). In addition, complexity of AS regulation is also confirmed by studies using *SR* overexpression lines. Several studies demonstrated that *SR* overexpression induces AS changes of a variety of *SR* mRNAs, that (co)-regulate target genes which affects plant development (Ali et al., 2007; Kalyna et al., 2003; Lopato et al., 1999). Therefore, we propose that AS of splicing regulators themselves, contribute to complex splicing networks, that help to adjust gene regulation and plant development. However, the mechanism by which splicing regulators differentially control light-regulated AS events remains elusive. We speculate that AS regulation might depend on different motifs present in the target pre-mRNAs that can be either bound in a cooperative manner or by outcompeting the other regulators (Fu & Ares, 2014). Previously, it has been reported that the splicing regulator SCL30 binds specifically to AGAAGA sequences in a cooperative manner with SR45 (Yan et al., 2017). Hence, identifying target binding sites of RS proteins are required to better understand the function of splicing regulators in controlling pre-mRNA splicing.

Interestingly, our results revealed that RS proteins show WT-like splicing patterns of light-regulated AS events in response to white light and sugar. These findings suggest that either RS31a in *rsT<sub>i</sub>* can compensate for the loss of the other RS proteins or alternatively, that other splicing regulators contribute to light-dependent AS changes. In the latter case, SFPS, RRC1 and SWAP1 might be potential candidates, as all three

regulators have been linked previously to light-mediated AS in Arabidopsis (Kathare et al., 2022; Xin et al., 2017; Xin et al., 2019).

However, we cannot rule out other regulatory mechanisms that affect light-mediated AS. Apart from splicing regulators (Kathare et al., 2022; Xin et al., 2017; Xin et al., 2019; Yan et al., 2022), the phyB photoreceptor was found to participate in AS regulation in response to red light (Dong, J. et al., 2020; Shikata et al., 2014; Wu, 2014). Recently, photoactivated phyB was directly linked to AS control by regulating intron retention of *PIF3*, thus resulting in reduced PIF3 protein levels and hence, promotion of photomorphogenesis (Dong, J. et al., 2020). Apart from phytochrome and phytochrome-interacting splicing regulators, retrograde signaling from the chloroplast to the nucleus (Petrillo et al., 2014) as well as the RNA polymerase II transcriptional elongation rate (Godoy Herz et al., 2019), were found to control light-mediated AS. These findings provide evidence for the complexity of light-regulated AS and further suggest that several pathways might co-exist.

Our group has previously shown that metabolic and kinase signaling play a major role upstream of AS responses, as sugar and the inhibition of kinase signaling induced similar AS changes as observed by light (Hartmann et al., 2016). In line with our findings, Riegler et al. revealed that the TOR kinase affects AS in response to light and exogenous sugar treatment in Arabidopsis roots (Riegler et al., 2021). However, the mechanism by which TOR controls AS is elusive. A recent phosphoproteomic study identified an altered phosphorylation pattern of several RNA-binding proteins, including RS40 and RS41, upon TOR inhibition (Scarpin et al., 2020). Therefore, it might be possible that post-translational modifications of RS proteins affect their activity and/or subcellular localization, which alters target binding and hence, the AS response. However, further studies are required to uncover the mechanism by which RS proteins control light-regulated AS and photomorphogenic growth.

**Light affects *RS31* and *RS40* transcript abundance**

Our study revealed that *RS31* and *RS40* transcript levels are altered in response to light. Light-induced transcriptional reprogramming was previously detected during the transition from dark to light, which is accompanied by phenotypical changes (Jiao et al., 2005; Jiao et al., 2007). Since AS affects gene expression, we wondered whether *RS31* and *RS40* might be alternatively spliced upon illumination. Former studies demonstrated that *SR* genes are targets of AS themselves, that can be drastically affected in response to abiotic stress (Palusa et al., 2007; Yoon et al., 2018). Here, we used an available RNA-seq data set and observed that *RS31* is alternatively spliced in response to different light qualities (Hartmann et al., 2016). These observations are consistent with previous findings, demonstrating that *RS31* and *RS40* undergo AS upon exposure to light (Godoy Herz et al., 2019; Shikata et al., 2012; Shikata et al., 2014). AS of *SR* genes is often coupled to NMD, thus providing effective means to quantitatively control transcript levels and hence, regulate gene expression (Palusa & Reddy, 2010). However, our analyses revealed that light-induced AS of *RS31* results in the production of the protein-coding isoforms. These findings are consistent with previous data showing that light promotes the generation of a productive variant at the expense of an unproductive transcript that contains NMD-inducing characteristics (Hartmann et al. 2016). This phenomenon was observed in more than 60% of all light-regulated AS events in etiolated *Arabidopsis* seedlings, suggesting that it is a common mechanism to activate gene expression during photomorphogenesis (Hartmann et al., 2016). Remarkably, light-induced generation of the productive *RS31* variant is untypical for the repression on transcript level, as productive isoforms are typically more stable than NMD targets. Therefore, reduced transcription or increased transcript turnover is the most likely explanation for the changes on transcript level. In favour of an increased turnover rate are the findings on the protein level, showing a rapid *RS31* protein turnover in response to light. Hence, *RS31* transcripts might also show altered turnover rates, as already observed for the splicing regulator *SR30* (Hartmann et al. 2018). The protein-coding isoform *SR30.1* was found to be clearly less stable than the unproductive *SR30.2* variant, that is retained in the nucleus (Hartmann et al. 2018). As *RS31* encodes a protein-coding isoform (*RS31.1*) and two unproductive variants that are targeted by NMD (*RS31.2*) and kept in the nucleus (*RS31.3*), respectively, it might be possible that the *RS31.1* isoform is less stable than the nuclear retained *RS31.3* variant. If this would be true, the light-induced AS shift towards the protein-coding



*RS31.1* variant could lead to a decrease on transcript level. However, it remains to be determined whether *RS31* mRNA isoforms show altered turnover rates. Furthermore, light induced repression on transcript level might be also controlled by chromatin modifications (Fisher & Franklin, 2011). Light-induced chromatin changes were observed for example for *phyA*. *phyA* is marked with activating and repressive Histone H3 modifications in dark and light, respectively, allowing rapid switching between activation and repression of *phyA* gene expression (Jang et al., 2011). Whether a similar mechanism exists for the regulation of *RS31* and *RS40* gene expression requires, however, further studies.

### **Light affects RS31 and RS41 protein stability that might involve post-translational modifications**

Here, we show that overexpressed RS31 and RS41 tagged proteins are regulated in a light-dependent manner, as the transgenic RS31 protein is destabilized and RS41 tagged protein stabilized in response to light. These findings might be either due to altered protein synthesis, degradation rates or a changed extractability of RS proteins upon illumination.

Previously, it was shown that positive regulators of photomorphogenesis, including HY5, interact with the E3 ubiquitin ligase complex COP1/SPA, and consequently trigger HY5 ubiquitination and degradation in darkness (Osterlund et al., 2000). Upon illumination, COP1/SPA complex is repressed by photoreceptors, resulting in the stabilization of HY5. Since HY5 and RS41 are both positive regulators of photomorphogenesis, we wondered whether RS41 protein abundance might be also regulated by COP1/SPA in darkness. Former studies reported that COP1-interacting proteins share a common VP (valine, proline) motif that might act as COP1-binding site (Holm et al., 2001; Lau et al., 2019). However, we did not identify any VP motif in RS41. Therefore, we propose that RS41 protein stability might be regulated independently of COP1.

Apart from protein degradation by COP1/SPA, decreased/increased protein levels might also be caused by an altered protein synthesis or protein stability. On the one hand, it has been reported that light promotes protein translation by the TOR-RPS6 pathway which is crucial for plant development during photomorphogenesis (Chen et al., 2018). On the other hand, it has also been demonstrated that light-induced phosphorylation of PIF proteins by phytochromes induces a rapid PIF turnover (Al-

Sady et al., 2006; Shen et al., 2008). Our current results show that RS31 does not undergo a light-dependent phosphorylation. However, it might be possible that RS31 undergoes other post-translational modifications (PTMs) in response to light, that affect its protein stability. In support with this idea, SUMOplot analyses predicted several SUMOylation motifs in RS31. SUMO is a small ubiquitin-related modifier that is covalently attached to lysine residues and can either promote or repress the target protein degradation (Geoffroy & Hay, 2009). Recently, SUMOylation was found to negatively affect FAR-RED ELONGAETD HYPOCOTYL 1 (FHY1) degradation in response to far-red light (Qu et al., 2020). Whether a similar regulatory mechanism exists for RS31 needs, however, to be determined. Therefore, IP-MS experiments are of utmost importance to identify RS31 PTM sites *in vivo* that are altered in a light-dependent manner.

Apart from light-induced protein destabilization, a recent study in *Phycomitrella patens* showed that protein levels of the splicing regulator PphnRNP-F1 increased in response to red light, involving the red light photoreceptor PpPHY4, either by stabilizing or enhancing PphnRNP-F1 translation (Lin et al., 2020). Based on our results, showing that RS41 gets specifically phosphorylated in response to light, we propose that the phosphorylation state might affect RS41 protein stability, possibly also involving its subcellular localization. Subcellular localization of SR proteins is highly dynamic and regulated by their phosphorylation state of the RS domain (Ali et al., 2003; Docquier et al., 2004; Misteli, 2000; Tillemans et al., 2006). Preliminary results show that RS41 undergoes a light-dependent nuclear re-localization from the nucleoplasm into nuclear speckles (see Chapter IV). The altered localization might affect RS41 protein stability and extractability, as speckles may be inaccessible for the degradation machinery and may show an altered extractability compared to nucleoplasm localized RS41 proteins, respectively. Whether the phosphorylation state indeed affects RS41 localization and stability, requires further studies. Therefore, future work should focus on the generation of phosphomutants to uncover the mechanism of RS41 'turnover' in response to light. These studies will further help to increase our insights into the biological relevance of RS phosphorylation sites.

**RS41 positively controls cotyledon opening that involves BR signaling**

Light and BRs are major signals required for developmental and physiological processes. Recent reports demonstrated that light signaling components interact with BR signaling modulators in order to integrate light and BR signals (Lin et al., 2021). While light promotes photomorphogenesis, BRs act oppositely and facilitate skotomorphogenesis (Wang et al., 2012). To date, BZR1 and BES1 (BRASSINAZOLE-RESISTANT 2) transcription factors are thought to act as integration points of light and BR signaling pathways. Recent progress revealed that BZR1 and/or BES1 interact with photoreceptors, including phyB, CRY1/2 and UVR8 to repress BZR1/BES1 transcriptional activity and hence, DNA-binding ability (Dong, H. et al., 2020; He et al., 2019; Liang et al., 2018; Wang et al., 2018; Wu et al., 2019). In addition, BRZ1 interacts with light signaling components, including COP1, PIF4 and HY5 (Kim et al., 2014; Li & He, 2016; Oh et al., 2012). The BZR1/COP1 interaction results in the degradation of the phosphorylated (inactive) form of BZR1, thus increasing the relative proportion of the dephosphorylated (active) form of BZR1 to promote hypocotyl growth (Kim et al., 2014). Hypocotyl elongation is also regulated by the interaction of BZR1 and PIF4, that co-regulate specific target genes involved in cell elongation (Oh et al., 2012). Recent progress suggested a major role of BRs in regulating cotyledon opening dynamics. HY5 was found to interact with dephosphorylated BZR1, thus reducing its DNA binding ability of cotyledon closure genes, inducing cotyledon opening (Li & He, 2016). More recently, BBX32 was identified as interaction partner of BZR1 and PIF3, co-regulating common target genes to mediate cotyledon closure (Ravindran et al., 2021).

In our study we provide evidence that RS proteins act as novel molecular hub integrating light and BR signaling. We showed that the overexpression of *RS* genes induces cotyledon opening in dark, with the most prominent cotyledon phenotype in *RS41* OE lines. Overexpression of *RS41* represses BR-responsive gene expression, suggesting that *RS41* negatively controls BR signaling. This is consistent with previous reports, demonstrating that positive regulators of photomorphogenesis (e.g. HY5) repress BR responses (Li & He, 2016), whereas negative regulators (e.g. COP1, PIFs) promote BR signaling (Kim et al., 2014; Oh et al., 2012). We further revealed that *RS* OE seedlings are hypersensitive to BRZ-induced cotyledon opening, that was repressed in the *rs* triple mutant. Remarkably, BRZ-induced hypocotyl growth repression was similar in *rs* mis-expression lines and WT, suggesting a specific role of RS proteins in BR-controlled cotyledon opening. These data support previous findings

from Li et al. who revealed a specific function of HY5 in BR-regulated cotyledon opening but not in BR-controlled hypocotyl growth (Li & He, 2016). Apparently, our results point towards a correlation between RS41-induced cotyledon opening and BR signaling. Since the transcription factor BZR1 is the major integrator of light and BR signaling pathways, we propose that RS proteins can either interact with BZR1 or affect splicing of *BZR1* or other BR-responsive target genes to induce photomorphogenic growth. In support with the first idea, it was shown that dephosphorylated BZR1 localizes to the nucleus (Wang et al., 2021), the subcellular compartment, where also RS proteins are localized. Therefore, it would be possible that the RS/BZR1 interaction induces the sequestration of dephosphorylated BZR1. Accordingly, the DNA binding ability of BZR1 might be reduced, similar as proposed for HY5. As BZR1 protein stability and phosphorylation status are affected by light, the interaction between RS proteins and BZR1 might be highly dynamic (Li et al., 2017).

Another link between RS proteins and BR-controlled cotyledon opening might be drawn by the observed unopened cotyledons of sucrose-treated *RS41* OE seedlings. A former study reported that sucrose increases BZR1 protein levels in dark and light, suggesting an upregulation of BR-responsive genes and hence, skotomorphogenic growth (Li et al., 2017). Therefore, it might be possible that closed cotyledons in sucrose-treated *RS41* OE seedlings are caused by elevated BZR1 protein levels. Therefore, western blot studies of BZR1 in sucrose/mock-treated *RS41* OE seedlings will help to prove this hypothesis.

Moreover, we showed that repression of BR signaling affects light-regulated AS of *SR30*. To our knowledge, this is the first report linking BR signaling to AS. Since other hormones, including auxin, abscisic acid and cytokine were found to affect AS of *SR* genes (*SR34*, *SR34b* and *SCL33*), it might be possible that BRs only affect AS of *SR* genes that play a role in BR-mediated processes (Palusa et al., 2007). To analyse whether BR is either a novel regulator mediating light-induced AS to control plant development during photomorphogenesis, or a regulator of *SR* genes, further splice pattern studies of additional light-regulated AS events are required.

Taken together, we identified RS proteins to be a molecular hub integrating light and BR signaling to drive cotyledon opening by repressing BR-responsive gene expression. Future studies should focus on the possible interaction between RS proteins and BR modulators, including BZR1. Furthermore, it will be interesting to

analyse whether a complete loss of the RS subfamily fully represses BRZ-induced cotyledon opening and whether the application of brassinolide, the most active form of BRs, can induce cotyledon closure in *RS* OE seedlings. Preliminary experiments using brassinolide have shown that cotyledons of *RS41* OE and *rsT<sub>c</sub>* seedlings remained opened and closed, respectively. Strikingly, dark grown WT seedlings also displayed opened cotyledons in the presence of brassinolide, suggesting that the brassinolide concentration needs to be adjusted in future experiments.

Based on our findings, we propose a model in which RS proteins control photomorphogenic growth by regulating BR signaling (Figure 6). Under dark conditions, RS proteins are evenly distributed within the nucleoplasm, and the COP1/SPA complex mediates the proteasomal degradation of transcription factors, including HY5. Furthermore, PIF proteins and dephosphorylated BZR1 bind to target promoters, thereby regulating gene expression to promote skotomorphogenic growth. Skotomorphogenic growth includes cell elongation as well as cotyledon closure.

In the presence of light, activated phytochromes move into the nucleus and interact with PIFs and COP1/SPA, resulting in PIF degradation and COP1/SPA repression. Subsequently, stabilized HY5 sequesters dephosphorylated BZR1, and binds to target promoters, in order to induce gene expression that promotes photomorphogenesis. Photomorphogenesis is further induced by RS proteins, that get specifically phosphorylated in response to light and accumulate within nuclear speckles. Light-induced phosphorylation of RS proteins might be mediated by TOR, a master regulator of energy signaling. We propose that RS proteins might interact with the photoactivated phyB, thus affecting RS phosphorylation and/or stabilization.

### **RS proteins are involved in reproductive development**

Our study revealed that RS proteins play a major role in skoto- and photomorphogenesis, including hypocotyl growth and cotyledon opening, but are also involved in reproductive development, such as flowering and seed yield. The most prominent abnormalities were observed in the *rsQ<sub>c</sub>* mutant. Almost all lines that were identified as *rsQ<sub>c</sub>* mutant in the first generation produced no seeds. However, we found a few *rsQ<sub>c</sub>* lines that generated some seeds. These untypical *rsQ<sub>c</sub>* lines were then selected for seed propagation and corresponding progenies used for splicing pattern studies and hypocotyl growth measurements. Although those mutants were previously identified to be transgene-free, we observed that progenies segregated and hence,

were no longer homozygously mutated in all four *RS* alleles. Currently, the reason for this reversion is unclear, but we propose that it might involve either polyploidy or revertant mosaicism in the whole plant. Polyploidy can drastically alter the physiology and morphology of plants and hence their capability in adjusting to changing environmental conditions (Leitch & Leitch, 2008). As the untypical *rsQ<sub>c</sub>* lines display enlarged seeds and an increased morphology, it might be possible that those mutants are polyploid. On the other hand, the reversion of the mutation might also involve revertant mosaicism. Revertant mosaicism is a mechanism by which disease-causing mutations are spontaneously corrected and is often associated with genetic skin disorders (Meyer-Mueller et al., 2022). Different kinds of revert mosaicism have been observed, including nucleotide substitution (van den Akker et al., 2012). Whether the back mutations in *rsQ<sub>c</sub>* involves revertant mosaicism or is due to polyploidy remains elusive. What can be stated in any case is that *rsQ<sub>c</sub>* mutants display massive pollen malfunctioning, as revealed by pollination experiments. These observations are contradictory to the findings reported by Yan et al., as the T-DNA *rs* quadruple mutant generated by them did not show any morphological phenotype (Yan et al., 2017). However, the overall lack of expression data in their study makes their reported knockout lines questionable. Therefore, our results indicate functional redundancy of *RS* proteins and imply an essential role of *RS* proteins during pollination. Remarkably, *RS31*, *RS40* and *RS41* were identified to be expressed at low levels in pollen (Palusa et al., 2007), however, they appear to have a great impact on pollen production and functionality. Previously, only *SR45*, which is an atypical *SR* protein, was linked to reproduction as the *sr45-1* mutant displays stunted siliques (Zhang et al., 2017). Furthermore, it was revealed that *SR45* associates with reproduction-regulating transcripts in inflorescences (Zhang et al., 2017). If *RS* proteins associate with those transcripts, including the mRNA of *FPA*, an RNA-binding protein that promotes flowering, and/or affect splicing of genes involved in reproduction, needs to be addressed in future.

## Materials and Methods

### Plant material and growth conditions

Arabidopsis mutants used in this study include *rs40-1<sub>t</sub>* (WiscDsLox382G12.0; Chen et al., 2013), *rs41-1<sub>t</sub>* (SAIL-64-C03; Chen et al., 2013), *rs31-1<sub>t</sub>* (WiscDsLox481-484D23.1), *rs31-2<sub>t</sub>* (SAIL\_632\_A04.0), *rrc1-2* (SALK\_121526) (Shikata et al., 2012), *rrc1-3* (SALK\_011832) (Shikata et al., 2012) *rs40 rs41<sub>t</sub>*, *rsT<sub>t</sub>-1*, *rsT<sub>t</sub>-2*, *rsT<sub>t</sub>-1 rrc1-2*, *rsT<sub>t</sub>-1 rrc1-3*, *rs31<sub>c</sub>*, *rs31a<sub>c</sub>*, *rs31 rs31a<sub>c</sub>*, *rs40 rs41<sub>c</sub>*, *rsT<sub>c</sub>* and *rsQ<sub>c</sub>* (Supplemental Table 1). All mutants are in the Col-0 background, except *rs41-1<sub>t</sub>* which is in Col-3. The *rsT<sub>t</sub>* triple mutants were generated by crossing *rs40 rs41<sub>t</sub>* with either *rs31-1<sub>t</sub>* or *rs31-2<sub>t</sub>*. The *rsT<sub>t</sub> rrc1* quadruple mutants were generated by crossing *rsT<sub>t</sub>-1* with either *rrc1-2* or *rrc1-3*. CRISPR triple *rsT<sub>c</sub>* and quadruple *rsQ<sub>c</sub>* mutants were generated by transforming the *rs31 rs31a<sub>c</sub>* construct in Cas9-free *rs40 rs41<sub>c</sub>* mutants (Supplemental Table 1).

Arabidopsis seeds were surface sterilized using 3.75% sodium hypochlorite solution and 0.01% Triton X-100. Seeds were plated on ½ Murashige and Skoog (MS) medium (Duchefa, Haarlem, Netherlands; pH 5.7 – 5.8; without sucrose) and 0.8% plant agar. After 2 d of stratification, germination was induced by exposing to white light (~100 μmol m<sup>-2</sup> s<sup>-1</sup>) for 2 h. Depending on the experiment, plates were either shifted to different monochromatic light conditions or darkness.

For BRZ experiments, sterilized seeds were plated singly onto ½ MS plates containing different concentrations of BRZ (SML1406 Sigma-Aldrich, St. Louis, MO, US), in the presence or absence of 1.5% sucrose. Mock plates containing DMSO served as control. Seedlings were then grown horizontally for 3 or 6 d in darkness.

For segregation analyses of *RS* OE lines, sterilized seeds were plated on ½ MS media supplemented with 2% sucrose and 25 μg/ml kanamycin. Plates lacking kanamycin served as control. After stratification (2 d), plates were transferred to regular light (~100 μmol m<sup>-2</sup> s<sup>-1</sup>) and seedlings were grown under long day conditions (16 h light, 8h dark, 22 °C) for 10 d.

### Generation and characterization of *RS* overexpression lines

Coding sequences (cds) of *RS31*, *RS31a*, *RS40* and *RS41* genes were cloned into the vector pBinAR-HA3 containing the constitutive CaMV promoter. All cds were amplified from plasmids, with ES232/233 (*RS31*), AWTU374/375 (*RS31a*), AWTU376/377 (*RS40*) and ES248/249 (*RS41*). Generated inserts were cloned into pBinAR-HA3 via *KpnI/BamHI*.

For HA-*RS41*, cds and partial HA-tag was amplified with ES206/ES207. PCR product was used as template for a second PCR with ES208/ES207, adding a *BamHI* and *SaII* overhangs, respectively, and complete HA-sequence. Generated insert was finally cloned into pBinAR via *BamHI/SaII* (HOFGEN & WILLMITZER, 1992). All nucleotides used to generate *RS* OE constructs are listed in Supplemental Table 5.

### Generation and characterization of CRISPR mutants

For the assembly of two sgRNA expression cassettes, sgRNA inserts were amplified from pCBC-DT1T2 (Xing et al., 2014) using Phusion® High-Fidelity DNA Polymerase (NEB, MA, US) and two inner and two outer primers that were partially overlapping and contained the sgRNA target sites. pHEE401E vector (Wang et al., 2015) and sgRNA expression cassettes (T1T2-PCR) were purified, diluted to a final concentration of 200 ng/μl and used for *BsaI* cut ligation. The reaction was incubated in a thermocycler at 37 °C for 5 h, followed by 50 °C for 5 min and 80 °C for 10 min. 1 μl of each reaction was transformed into *Escherichia coli* XL1-blue and positive clones were confirmed by sequencing as well as digestion. Final pHEE401E\_T1T2\_RS-sgRNA constructs were transformed into *Agrobacterium tumefaciens* strain C58C1 and used for transforming *A. thaliana* Col-0 wild-type plants via floral dipping (Clough & Bent, 1998). Seeds from T0 plants were surface sterilized using 80% ethanol and 0.05% Triton X-100 and plated on ½ MS (pH 5.7 – 5.8) containing 20 μg/ml hygromycin. Resistant seedlings (T1) were transferred to soil and genomic DNA was extracted to analyse mutations in corresponding *RS* genes. Therefore, fragments surrounding the target sites were amplified, purified, and sequenced. Transgene free plants, still containing the corresponding mutations, were identified in the subsequent generations.

Triple and quadruple *rs<sub>c</sub>* mutants were generated by transforming transgene free *rs40* *rs41<sub>c</sub>* mutant plants with *A. tumefaciens* containing the *rs31 rs31a<sub>c</sub>* construct.



Detailed information about oligonucleotides that were used for cloning and genotyping can be found Supplemental Table 6 and 8, respectively.

### **Genotyping**

Genomic DNA was isolated using Edwards buffer [200 mM Tris-HCl pH 7.5, 250 mM NaCl, 25 mM EDTA, 0.5% SDS] as described by (Edwards et al., 1991). In brief, plant material was ground in liquid nitrogen, resuspended in Edwards extraction buffer and cleared by centrifugation. 300  $\mu$ l of the supernatant was mixed with 300  $\mu$ l isopropanol, incubated at room temperature for 5 min, followed by centrifugation. DNA pellet was once washed with 70% ethanol, dried and finally resuspended in  $\frac{1}{2}$  TE buffer.

For information about oligonucleotides used for genotyping, please see Supplemental Table 7 to 9.

### **Generation of *RS31* splicing reporter and splicing assay in *N. benthamiana***

Cloning of a splicing reporter based on pBinAR-EGFP was previously described in (Wachter et al., 2007). Partial sequence of *RS31* including the region of the AS event was amplified from genomic WT DNA with JS186/JS208. *RS31* insert was digested with *NheI* and *KpnI* and cloned into *XbaI*/*KpnI* restricted pBinAR-EGFP.

Agrobacteria-mediated leaf infiltration was performed according to (Wachter et al., 2007). In brief, *Agrobacterium tumefaciens* containing different constructs were grown overnight at 28 °C. The next day, Agrobacteria cultures were centrifuged, cells resuspended in water and OD<sub>600</sub> adjusted to 0.8. Infiltration mixtures were prepared, by mixing equal amounts of different constructs. All mixtures contained the *RS31* reporter, mOrange2 and P19, for fluorescence normalization and silencing suppression, respectively. Furthermore, Luciferase (LUC) as unrelated control protein or individual RS protein constructs were added. Subsequently, Agrobacteria mixtures were infiltrated in leaves of 3- to 4-week-old *N. benthamiana* plants. For direct comparison, leaves were 'divided' into 2 halves and one side was infiltrated with the control mixture (LUC) and the other side with the RS-containing mixture. After infiltration, plants were kept in shade for 1 d. 2 days post infiltration, plant material was harvested that was further used for RNA extraction.

**Hypocotyl assay**

To measure hypocotyl length, seedlings were grown horizontally for 4 or 6 d in darkness or under different monochromatic light conditions. Seedlings were then transferred to ½ MS plates containing 1.5% plant agar and scanned. Hypocotyl lengths were measured using the ImageJ software. Absolute as well as relative hypocotyl lengths are depicted. Relative hypocotyl length was normalized to corresponding mean hypocotyl length in darkness.

**Cotyledon opening assay**

To measure cotyledon opening percentages and angles, seedlings were grown horizontally for 4 or 6 d in darkness. Seedlings were carefully transferred under green light to ½ MS plates supplemented with 1.5% plant agar and plates were scanned. Images were then used to measure cotyledon opening angle using ImageJ. Cotyledons were counted as opened when angles were greater than 6 degrees.

**Cotyledon opening kinetic assay**

Seedlings were grown vertically on ½ MS plates containing 1.5% plant agar. After growth for 4 d in darkness, plates were shifted to either cWL ( $10.6 \mu\text{mol m}^{-2} \text{s}^{-1}$ ) or cRL ( $8.4 \mu\text{mol m}^{-2} \text{s}^{-1}$ ) and scanned at different time points. Angle measurement was performed in ImageJ.

**Light and sucrose treatment**

Etiolated seedlings were grown for 6 d in liquid ½ MS media lacking sucrose. At day 6, MS media was exchanged by ½ MS supplemented with either 1.06% mannitol or 2% sucrose. Subsequently, seedlings were either kept in darkness or shifted to white light ( $\sim 100 \mu\text{mol m}^{-2} \text{s}^{-1}$ ) for 6 h.

**RNA extraction, RT-qPCR, and PCR product analyses**

Total RNA was isolated from Arabidopsis seedlings using the Universal RNA purification kit (Roboklon, EURx, Berlin, Germany), including an on-column DNaseI treatment. cDNA syntheses were carried out using either Superscript II Reverse Transcriptase (Invitrogen, Carlsbad, CA, US) or AMV Reverse Transcriptase Native (Roboklon, EURx, Berlin, Germany), following the manufacturer's instructions. RT-qPCR was performed using MESA GREEN qPCR Mastermix on a CFX384 real-time PCR cycler (Bio-Rad, Hercules, CA, US). Data was analysed as reported before

(Stauffer et al., 2010). Co-amplification PCRs were performed with homemade Taq Polymerase, visualized using Agarose gel electrophoresis and quantified on a Bioanalyzer using the DNA1000 kit (Agilent Technologies, Santa Clara, CA, US). All oligonucleotides are provided in Supplemental Table 10 and 11.

### **Protein extraction and immunoblot analyses**

Seedlings were grown for 6 d either on ½ MS plates (Supplemental Figure 10A) or in liquid ½ MS media (Supplemental Figure 10B, C).

150 µl of *extraction buffer I* [50 mM Tris-HCl pH 7.9, 120 mM NaCl, 2 mM MgCl<sub>2</sub>, 0.1% Triton X-100, 10 % glycerol, 1 mM β-mercaptoethanol, 2 mM PMSF, 1x protease inhibitor cocktail and 1x Phos-stop] was added to 100 mg etiolated seedlings. Plant material was homogenized by vortexing, and cell debris collected by centrifugation at 10.000 *g* for 5 min, 4 °C. Protein extracts were heated up to 95 °C for 5 min and 10 µg protein was loaded onto 12% SDS-PAGE. After gel running, proteins were transferred using semi-dry transfer (12 V, 400 mA, 50 min) onto a PVDF membrane.

*Extraction buffer II* [100 mM NaH<sub>2</sub>PO<sub>4</sub> pH 7.8, 130 mM NaCl, 0.1% NP-40, 10% glycerol, 1x protease inhibitor cocktail] was added in a 1:1 ratio to frozen plant material. Samples were spun down at 13.000 *g* for 10 min, 4 °C and supernatant was boiled at 70 °C for 10 min. 15 µg protein was loaded onto 10% SDS-PAGE and proteins were transferred using wet transfer (110 V, 400 mA, 1 h).

Membranes were blocked in 5% skim milk for 1 h, followed by the first antibody incubation using anti-HA (11867423001, Roche, Basel, Switzerland) at 4 °C overnight. Secondary antibody incubation was performed using anti-rat (31470, Thermo Fisher Scientific, Waltham, MA, US) for 1 h at room temperature and chemiluminescence was imaged using the Fusion Fx system (Vilber, Collégien, France). Tubulin (AS10 680, Agrisera, Vännäs, Sweden) was used as loading control.

### **Phosphoproteomics**

#### Plant material and protein extraction

Arabidopsis WT seedlings were grown in liquid ½ MS lacking sucrose for 6 d. Subsequently, etiolated seedlings were either treated with (i) 2% sucrose in dark or (ii) 1.06% mannitol and transferred to white light (~100 µmol m<sup>-2</sup> s<sup>-1</sup>) for 30 min. (iii) A 0 h dark sample served as control. 6 to 10 g plant material was ground in liquid nitrogen

and suspended in extraction buffer [8 M urea, 40 mM NaCl, 50 mM Tris pH 7.5, 2 mM MgCl<sub>2</sub>, PhosSTOP (Roche, Basel, Switzerland), phosphatase inhibitor mix I (Serva, Heidelberg, Germany), Complete Protease Inhibitor Mixture (Roche)] in a 1:1.5 ratio. Cell debris were collected by centrifugation (30 min, 4000 rpm, 4 °C) and supernatant was filtered through Miracloth. Both steps were repeated once, and filtrated protein extracts were further processed by MS.

#### In solution digest

Dithiothreitol was added to a final concentration of 1 mM to the precipitated plant proteins and incubated at room temperature (RT) for 45 min at 300 rpm. The alkylation reagent Chloroacetamide was added to a final concentration of 5.5 mM and incubated at RT for 1 hour in the dark with gentle shaking. Proteins were predigested by adding 1 µg Lysyl Endopeptidase (FUJIFILM Wako Pure Chemical Corporation, Osaka, Japan) per 150 µg protein at RT for 4 hours and after dilution with 4 volumes water digested with 1 µg Trypsin (Sigma, St. Louis, MO, US) per 150 µg protein overnight at RT. The digestion was stopped by pipetting trifluoroacetic acid (TFA, final 0.5 %) to the samples and incubating at 4 °C at least 30 minutes. Peptides were centrifuged at 4 °C and 4000 rpm for 10 minutes, the supernatant was filtered with a 0.45 µm PES-filter and transferred into a new tube. Sep-Pak C18 Classic Cartridges (Waters) assembled to a 10 ml syringe were used for purification of the peptides. Columns were activated with 5 ml 100 % acetonitrile (ACN) and washed three times with 5 ml 0.1 % TFA. The clarified peptide mixture was loaded on the column and the column washed again three times with 10 ml 0.1 % TFA. Peptides were eluted with 4.5 ml 50 % ACN and the concentration measured with a NanoDrop spectrometer (A280 value).

#### Phosphopeptide enrichment

The peptide solution in 50 % ACN with a final concentration of 6 % TFA was incubated with Titansphere TiO<sub>2</sub> (GL Science, Tokyo, Japan; mass 1.5 fold more TiO<sub>2</sub> spheres than peptides) two times for one hour on a rotation wheel. The peptide-bound spheres from the two incubations were washed two times with 50 % ACN, 6 % TFA and again two times with 50 % ACN, 0.1 % TFA with a 1000 x g centrifugation step in between the washes. Beads were transferred to C8 47 mm extraction disk (3M Empore C8 Extraction Disk, assembled in a 200 µl pipette tip) and centrifuged at 600 x g. Enriched phosphopeptides were eluted in the next step in two steps first with 5 % ammonia and

second with 10 % ammonia, 25 % ACN at 400 x g in a 2 ml tube. The eluate was vacuum-concentrated at 45 °C for 15 min and acidified with TFA to pH 2.

#### C18 stage tipping

For desalting and peptide concentration C18 tips were prepared by cutting out two C18 47 mm extraction disks (3M Empore C18 Extraction Disk) and putting them into a 200 µl pipette tip. The C18 tips were washed several times and centrifuged at 400-600 x g (1 x 25 µl methanol, 1 x 25 µl buffer B, 2 x 25 µl buffer A'). The acidified eluate was passed through the C18 tip by centrifuging at 400-600 x g and washed once with 50 µl buffer A''. Peptides were eluted in a 24-well Thermo-Fast PCR-plate (Thermo Fisher, Waltham, MA, US) with 50 µl elution buffer and vacuum-concentrated at 45 °C to a volume of 4-5 µl. For the further Mass spectrometry analysis the sample was diluted with buffer A\* to 6-7µl.

Buffer B (80% acetonitrile, 0.1% formic acid)

Buffer A' (3% acetonitrile, 1% trifluoroacetic acid)

Buffer A'' (8% acetonitrile, 0.1% formic acid)

Elution buffer (50% acetonitrile, 0.1% formic acid)

Buffer A\* (5% acetonitrile, 0.1% trifluoroacetic acid)

#### Mass spectrometry analysis

MS raw data was analyzed using MaxQuant software 1.5.2.8. Proteins were searched against the *A. thaliana* database Araport 11 (download 2019). For more details please see (Borisova et al., 2017).

#### **Statistical analysis**

Statistical analysis as well as graph plotting was performed using GraphPad Prism 8.0.2 (GraphPad Software, Inc., CA, US). Statistical details of each experiment including biological replicates (*n*), types of error bars and used test are defined in the figure legends.

### **Conflict of interests**

The authors declare that they have no conflict of interest.

### **Author contributions**

J.S. and A.W. designed the research. J.S. performed and analysed experiments with the help of M.P.D. Phosphoproteome experiment was performed and analysed by S.L.G. and P.B.; J.S. wrote the manuscript with contributions from A.W.

### **Acknowledgements**

We thank Claudia König and Laura Schütz for technical support and Svenja Saile for performing co-localization studies. We are grateful to Liming Xiong for sharing *rs40-1*, *rs41-1* and *rs40-1 rs40-1* seeds with us. This work was supported by the German Research Foundation (Deutsche Forschungsgemeinschaft – DFG: SFB1101/C03).

### **References**

- Ali, G. S., Golovkin, M., & Reddy, A. S. N. (2003). Nuclear localization and in vivo dynamics of a plant-specific serine/arginine-rich protein. *The Plant Journal : For Cell and Molecular Biology*, 36(6), 883–893. <https://doi.org/10.1046/j.1365-313x.2003.01932.x>
- Ali, G. S., Palusa, S. G., Golovkin, M., Prasad, J., Manley, J. L., & Reddy, A. S. N. (2007). Regulation of Plant Developmental Processes by a Novel Splicing Factor. *PLOS ONE*, 2(5). <https://doi.org/10.1371/journal.pone.0000471>
- Al-Sady, B., Ni, W., Kircher, S., Schäfer, E., & Quail, P. H. (2006). Photoactivated phytochrome induces rapid PIF3 phosphorylation prior to proteasome-mediated degradation. *Molecular Cell*, 23(3), 439–446. <https://doi.org/10.1016/j.molcel.2006.06.011>
- Asami, T., Min, Y. K., Nagata, N., Yamagishi, K., Takatsuto, S., Fujioka, S., Murofushi, N., Yamaguchi, I., & Yoshida, S. (2000). Characterization of brassinazole, a triazole-type brassinosteroid biosynthesis inhibitor. *PLANT PHYSIOLOGY*, 123(1), 93–99.

- Barta, A., Kalyna, M., & Reddy, A. S. N. (2010). Implementing a rational and consistent nomenclature for serine/arginine-rich protein splicing factors (SR proteins) in plants. *The Plant Cell*, 22(9), 2926–2929. <https://doi.org/10.1105/tpc.110.078352>
- Borisova, M. E., Wagner, S. A., & Beli, P. (2017). Mass Spectrometry-Based Proteomics for Quantifying DNA Damage-Induced Phosphorylation. *Methods in Molecular Biology (Clifton, N.J.)*, 1599, 215–227. [https://doi.org/10.1007/978-1-4939-6955-5\\_16](https://doi.org/10.1007/978-1-4939-6955-5_16)
- Chaudhary, S., Khokhar, W., Jabre, I., Reddy, A. S. N., Byrne, L. J., Wilson, C. M., & Syed, N. H. (2019). Alternative Splicing and Protein Diversity: Plants Versus Animals. *FRONTIERS in PLANT SCIENCE*, 10, 708. <https://doi.org/10.3389/fpls.2019.00708>
- Chen, G.-H., Liu, M.-J., Xiong, Y., Sheen, J., & Wu, S.-H. (2018). Tor and RPS6 transmit light signals to enhance protein translation in deetioliating Arabidopsis seedlings. *Proceedings of the National Academy of Sciences of the United States of America*, 115(50), 12823–12828. <https://doi.org/10.1073/pnas.1809526115>
- Chen, T., Cui, P., Chen, H., Ali, S., Zhang, S., & Xiong, L. (2013). A KH-Domain RNA-Binding Protein Interacts with FIERY2/CTD Phosphatase-Like 1 and Splicing Factors and Is Important for Pre-mRNA Splicing in Arabidopsis. *PLoS Genetics*, 9(10), e1003875. <https://doi.org/10.1371/journal.pgen.1003875>
- Chen, T., Cui, P., & Xiong, L. (2015). The RNA-binding protein HOS5 and serine/arginine-rich proteins RS40 and RS41 participate in miRNA biogenesis in Arabidopsis. *Nucleic Acids Research*, 43(17), 8283–8298. <https://doi.org/10.1093/nar/gkv751>
- Chory, J., Nagpal, P., & Peto, C. A. (1991). Phenotypic and Genetic Analysis of det2, a New Mutant That Affects Light-Regulated Seedling Development in Arabidopsis. *PLANT CELL*, 3(5), 445–459. <https://doi.org/10.1105/tpc.3.5.445>
- Clough, S. J., & Bent, A. F. (1998). Floral dip: A simplified method for Agrobacterium-mediated transformation of Arabidopsis thaliana. *The Plant Journal : For Cell and Molecular Biology*, 16(6), 735–743. <https://doi.org/10.1046/j.1365-313x.1998.00343.x>

- Deng, X.-W., & Quail, P. H. (1992). Genetic and phenotypic characterization of cop1 mutants of *Arabidopsis thaliana*. *The Plant Journal : For Cell and Molecular Biology*, 2(1), 83–95. <https://doi.org/10.1111/j.1365-313X.1992.00083.x>
- Docquier, S., Tillemans, V., Deltour, R., & Motte, P. (2004). Nuclear bodies and compartmentalization of pre-mRNA splicing factors in higher plants. *Chromosoma*, 112(5), 255–266. <https://doi.org/10.1007/s00412-003-0271-3>
- Dong, H., Liu, J., He, G., Liu, P., & Sun, J. (2020). Photoexcited phytochrome B interacts with brassinazole-resistant 1 to repress brassinosteroid signaling in *Arabidopsis*. *JOURNAL of INTEGRATIVE PLANT BIOLOGY*, 62(5), 652–667. <https://doi.org/10.1111/jipb.12822>
- Dong, J., Chen, H., Deng, X. W., Irish, V. F., & Wei, N. (2020). Phytochrome B Induces Intron Retention and Translational Inhibition of PHYTOCHROME-INTERACTING FACTOR3. *PLANT PHYSIOLOGY*, 182(1), 159–166. <https://doi.org/10.1104/pp.19.00835>
- Dong, J., Sun, N., Yang, J., Deng, Z., Lan, J., Qin, G., He, H., Deng, X. W., Irish, V. F., Chen, H., & Wei, N. (2019). The Transcription Factors TCP4 and PIF3 Antagonistically Regulate Organ-Specific Light Induction of SAUR Genes to Modulate Cotyledon Opening during De-Etiolation in *Arabidopsis*. *The Plant Cell*, 31(5), 1155–1170. <https://doi.org/10.1105/tpc.18.00803>
- Edwards, K., Johnstone, C., & Thompson, C. (1991). A simple and rapid method for the preparation of plant genomic DNA for PCR analysis. *Nucleic Acids Research*, 19(6), 1349. <https://doi.org/10.1093/nar/19.6.1349>
- Fisher, A. J., & Franklin, K. A. (2011). Chromatin remodelling in plant light signalling. *PHYSIOLOGIA PLANTARUM*, 142(4), 305–313. <https://doi.org/10.1111/j.1399-3054.2011.01476.x>
- Fu, X.-D., & Ares, M., JR. (2014). Context-dependent control of alternative splicing by RNA-binding proteins. *NATURE REVIEWS GENETICS*, 15(10), 689–701. <https://doi.org/10.1038/nrg3778>
- Galvão, V. C., & Fankhauser, C. (2015). Sensing the light environment in plants: Photoreceptors and early signaling steps. *Current Opinion in Neurobiology*, 34, 46–53. <https://doi.org/10.1016/j.conb.2015.01.013>



- Geoffroy, M.-C., & Hay, R. T. (2009). An additional role for SUMO in ubiquitin-mediated proteolysis. *NATURE REVIEWS MOLECULAR CELL BIOLOGY*, *10*(8), 564–568. <https://doi.org/10.1038/nrm2707>
- Godoy Herz, M. A., Guillermina Kubaczka, M., Brzyzek, G., Servi, L., Krzyszton, M., Simpson, C., Brown, J., Swiezewski, S., Petrillo, E., & Kornblihtt, A. R. (2019). Light Regulates Plant Alternative Splicing through the Control of Transcriptional Elongation. *Molecular Cell*, *73*(5), 1066–+. <https://doi.org/10.1016/j.molcel.2018.12.005>
- Gommers, C. M. M., & Monte, E. (2018). Seedling Establishment: A Dimmer Switch-Regulated Process between Dark and Light Signaling. *PLANT PHYSIOLOGY*, *176*(2), 1061–1074. <https://doi.org/10.1104/pp.17.01460>
- Hamasaki, H., Ayano, M., Nakamura, A., Fujioka, S., Asami, T., Takatsuto, S., Yoshida, S., Oka, Y., Matsui, M., & Shimada, Y. (2020). Light Activates Brassinosteroid Biosynthesis to Promote Hook Opening and Petiole Development in *Arabidopsis thaliana*. *Plant & Cell Physiology*, *61*(7), 1239–1251. <https://doi.org/10.1093/pcp/pcaa053>
- Hartmann, L., Drewe-Boß, P., Wießner, T., Wagner, G., Geue, S., Lee, H.-C., Obermüller, D. M., Kahles, A., Behr, J., Sinz, F. H., Rättsch, G., & Wachter, A. (2016). Alternative Splicing Substantially Diversifies the Transcriptome during Early Photomorphogenesis and Correlates with the Energy Availability in *Arabidopsis*. *The Plant Cell*, *28*(11), 2715–2734. <https://doi.org/10.1105/tpc.16.00508>
- He, G., Liu, J., Dong, H., & Sun, J. (2019). The Blue-Light Receptor CRY1 Interacts with BZR1 and BIN2 to Modulate the Phosphorylation and Nuclear Function of BZR1 in Repressing BR Signaling in *Arabidopsis*. *Molecular Plant*, *12*(5), 689–703. <https://doi.org/10.1016/j.molp.2019.02.001>
- Hoecker, U. (2017). The activities of the E3 ubiquitin ligase COP1/SPA, a key repressor in light signaling. *Current Opinion in Plant Biology*, *37*, 63–69. <https://doi.org/10.1016/j.pbi.2017.03.015>
- HOFGEN, R., & WILLMITZER, L. (1992). TRANSGENIC POTATO PLANTS DEPLETED FOR THE MAJOR TUBER PROTEIN PATATIN VIA EXPRESSION OF ANTISENSE RNA. *PLANT SCIENCE*, *87*(1), 45–54.

- Holm, M., Hardtke, C. S., Gaudet, R., & Deng, X. W. (2001). Identification of a structural motif that confers specific interaction with the WD40 repeat domain of Arabidopsis COP1. *EMBO JOURNAL*, 20(1-2), 118–127.
- Jang, I.-C., Chung, P. J., Hemmes, H., Jung, C., & Chua, N.-H. (2011). Rapid and Reversible Light-Mediated Chromatin Modifications of Arabidopsis Phytochrome A Locus. *PLANT CELL*, 23(2), 459–470. <https://doi.org/10.1105/tpc.110.080481>
- Jiao, Y. L., Ma, L. G., Strickland, E., & Deng, X. W. (2005). Conservation and divergence of light-regulated genome expression patterns during seedling development in rice and Arabidopsis. *PLANT CELL*, 17(12), 3239–3256. <https://doi.org/10.1105/tpc.105.035840>
- Jiao, Y., Lau, O. S., & Deng, X. W. (2007). Light-regulated transcriptional networks in higher plants. *NATURE REVIEWS GENETICS*, 8(3), 217–230. <https://doi.org/10.1038/nrg2049>
- Kalyna, M., Lopato, S., & Barta, A. (2003). Ectopic expression of atRSZ33 reveals its function in splicing and causes pleiotropic changes in development. *Molecular Biology of the Cell*, 14(9), 3565–3577. <https://doi.org/10.1091/mbc.e03-02-0109>
- Kathare, P. K., Xin, R., Ganesan, A. S., June, V. M., Reddy, A. S. N., & Huq, E. (2022). SWAP1-SFPS-RRC1 splicing factor complex modulates pre-mRNA splicing to promote photomorphogenesis in Arabidopsis. *BioRxiv*, 2022.04.26.489584. <https://doi.org/10.1101/2022.04.26.489584>
- Kim, B., Jeong, Y. J., Corvalán, C., Fujioka, S., Cho, S., Park, T., & Choe, S. (2014). Darkness and gulliver2/phyB mutation decrease the abundance of phosphorylated BZR1 to activate brassinosteroid signaling in Arabidopsis. *The Plant Journal : For Cell and Molecular Biology*, 77(5), 737–747. <https://doi.org/10.1111/tpj.12423>
- Kircher, S., Kozma-Bognar, L., Kim, L., Adam, E., Harter, K., Schafer, E., & Nagy, F. (1999). Light quality-dependent nuclear import of the plant photoreceptors phytochrome A and B. *PLANT CELL*, 11(8), 1445–1456.
- Klose, C., Viczián, A., Kircher, S., Schäfer, E., & Nagy, F. (2015). Molecular mechanisms for mediating light-dependent nucleo/cytoplasmic partitioning of

- phytochrome photoreceptors. *The New Phytologist*, 206(3), 965–971. <https://doi.org/10.1111/nph.13207>
- Lau, K., Podolec, R., Chappuis, R., Ulm, R., & Hothorn, M. (2019). Plant photoreceptors and their signaling components compete for COP1 binding via VP peptide motifs. *EMBO JOURNAL*, 38(18). <https://doi.org/10.15252/emj.2019102140>
- Laubinger, S., Fittinghoff, K., & Hoecker, U. (2004). The SPA quartet: A family of WD-repeat proteins with a central role in suppression of photomorphogenesis in arabidopsis. *PLANT CELL*, 16(9), 2293–2306. <https://doi.org/10.1105/tpc.104.024216>
- Leitch, A. R., & Leitch, I. J. (2008). Perspective - Genomic plasticity and the diversity of polyploid plants. *SCIENCE*, 320(5875), 481–483. <https://doi.org/10.1126/science.1153585>
- Leivar, P., Monte, E., Oka, Y., Liu, T., Carle, C., Castillon, A., Huq, E., & Quail, P. H. (2008). Multiple phytochrome-interacting bHLH transcription factors repress premature seedling photomorphogenesis in darkness. *Current Biology : CB*, 18(23), 1815–1823. <https://doi.org/10.1016/j.cub.2008.10.058>
- Leivar, P., Tepperman, J. M., Monte, E., Calderon, R. H., Liu, T. L., & Quail, P. H. (2009). Definition of early transcriptional circuitry involved in light-induced reversal of PIF-imposed repression of photomorphogenesis in young Arabidopsis seedlings. *PLANT CELL*, 21(11), 3535–3553. <https://doi.org/10.1105/tpc.109.070672>
- Li, J. M., Nagpal, P., Vitart, V., McMorris, T. C., & Chory, J. (1996). A role for brassinosteroids in light-dependent development of Arabidopsis. *SCIENCE*, 272(5260), 398–401.
- Li, J., Li, G., Wang, H., & Wang Deng, X. (2011). Phytochrome signaling mechanisms. *The Arabidopsis Book*, 9, e0148. <https://doi.org/10.1199/tab.0148>
- Li, Q.-F., & He, J.-X. (2016). Bzr1 Interacts with HY5 to Mediate Brassinosteroid- and Light-Regulated Cotyledon Opening in Arabidopsis in Darkness. *Molecular Plant*, 9(1), 113–125. <https://doi.org/10.1016/j.molp.2015.08.014>

- Li, Q.-F., Huang, L.-C., Wei, K., Yu, J.-W., Zhang, C.-Q., & Liu, Q.-Q. (2017). Light involved regulation of BZR1 stability and phosphorylation status to coordinate plant growth in Arabidopsis. *Bioscience Reports*, 37(2). <https://doi.org/10.1042/BSR20170069>
- Liang, T., Mei, S., Shi, C., Yang, Y., Peng, Y., Ma, L., Wang, F., Li, X., Huang, X., Yin, Y., & Liu, H. (2018). Uvr8 Interacts with BES1 and BIM1 to Regulate Transcription and Photomorphogenesis in Arabidopsis. *Developmental Cell*, 44(4), 512-523.e5. <https://doi.org/10.1016/j.devcel.2017.12.028>
- Liao, C.-Y., Smet, W., Brunoud, G., Yoshida, S., Vernoux, T., & Weijers, D. (2015). Reporters for sensitive and quantitative measurement of auxin response. *NATURE METHODS*, 12(3), 207-+. <https://doi.org/10.1038/NMETH.3279>
- Lin, B.-Y., Shih, C.-J., Hsieh, H.-Y., Chen, H.-C., & Tu, S.-L. (2020). Phytochrome Coordinates with a hnRNP to Regulate Alternative Splicing via an Exonic Splicing Silencer. *PLANT PHYSIOLOGY*, 182(1), 243–254. <https://doi.org/10.1104/pp.19.00289>
- Lin, F., Cao, J., Yuan, J., Liang, Y., & Li, J. (2021). Integration of Light and Brassinosteroid Signaling during Seedling Establishment. *INTERNATIONAL JOURNAL of MOLECULAR SCIENCES*, 22(23). <https://doi.org/10.3390/ijms222312971>
- Lopato, S., Kalyna, M., Dorner, S., Kobayashi, R., Krainer, A. R., & Barta, A. (1999). Atsrp30, one of two SF2/ASF-like proteins from Arabidopsis thaliana, regulates splicing of specific plant genes. *Genes & Development*, 13(8), 987–1001. <https://doi.org/10.1101/gad.13.8.987>
- Lorković, Z. J., Hilscher, J., & Barta, A. (2004). Use of Fluorescent Protein Tags to Study Nuclear Organization of the Spliceosomal Machinery in Transiently Transformed Living Plant Cells. *Molecular Biology of the Cell*, 15(7), 3233–3243. <https://doi.org/10.1091/mbc.E04-01-0055>
- Mancini, E., Sanchez, S. E., Romanowski, A., Schlaen, R. G., Sanchez-Lamas, M., Cerdán, P. D., & Yanovsky, M. J. (2016). Acute Effects of Light on Alternative Splicing in Light-Grown Plants. *Photochemistry and Photobiology*, 92(1), 126–133. <https://doi.org/10.1111/php.12550>

- Martín, G., Márquez, Y., Mantica, F., Duque, P., & Irimia, M. (2021). Alternative splicing landscapes in *Arabidopsis thaliana* across tissues and stress conditions highlight major functional differences with animals. *Genome Biology*, *22*(1), 35. <https://doi.org/10.1186/s13059-020-02258-y>
- Meyer-Mueller, C., Osborn, M. J., Tolar, J., Boull, C., & Ebens, C. L. (2022). Revertant Mosaicism in Epidermolysis Bullosa. *Biomedicines*, *10*(1). <https://doi.org/10.3390/biomedicines10010114>
- Misteli, T. (2000). Cell biology of transcription and pre-mRNA splicing: nuclear architecture meets nuclear function. *JOURNAL of CELL SCIENCE*, *113*(11), 1841–1849.
- Ni, W., Xu, S.-L., Chalkley, R. J., Pham, T. N. D., Guan, S., Maltby, D. A., Burlingame, A. L., Wang, Z.-Y., & Quail, P. H. (2013). Multisite light-induced phosphorylation of the transcription factor PIF3 is necessary for both its rapid degradation and concomitant negative feedback modulation of photoreceptor phyB levels in *Arabidopsis*. *PLANT CELL*, *25*(7), 2679–2698. <https://doi.org/10.1105/tpc.113.112342>
- Nusinow, D. A., Helfer, A., Hamilton, E. E., King, J. J., Imaizumi, T., Schultz, T. F., Farre, E. M., & Kay, S. A. (2011). The ELF4-ELF3-LUX complex links the circadian clock to diurnal control of hypocotyl growth. *Nature*, *475*(7356), 398–U161. <https://doi.org/10.1038/nature10182>
- Oh, E., Zhu, J.-Y., & Wang, Z.-Y. (2012). Interaction between BZR1 and PIF4 integrates brassinosteroid and environmental responses. *Nature Cell Biology*, *14*(8), 802–809. <https://doi.org/10.1038/ncb2545>
- Osterlund, M. T., Hardtke, C. S., Wei, N., & Deng, X. W. (2000). Targeted destabilization of HY5 during light-regulated development of *Arabidopsis*. *Nature*, *405*(6785), 462–466. <https://doi.org/10.1038/35013076>
- Paik, I., & Huq, E. (2019). Plant photoreceptors: Multi-functional sensory proteins and their signaling networks. *SEMINARS in CELL & DEVELOPMENTAL BIOLOGY*, *92*, 114–121. <https://doi.org/10.1016/j.semcdb.2019.03.007>
- Palusa, S. G., & Reddy, A. S. N. (2010). Extensive coupling of alternative splicing of pre-mRNAs of serine/arginine (SR) genes with nonsense-mediated decay.

- NEW PHYTOLOGIST*, 185(1), 83–89. <https://doi.org/10.1111/j.1469-8137.2009.03065.x>
- Palusa, S. G., Ali, G. S., & Reddy, A. S. N. (2007). Alternative splicing of pre-mRNAs of Arabidopsis serine/arginine-rich proteins: Regulation by hormones and stresses. *The Plant Journal : For Cell and Molecular Biology*, 1091–1107. <https://doi.org/10.1111/j.1365-313X.2006.03020.x>
- Park, E., Kim, Y., & Choi, G. (2018). Phytochrome B Requires PIF Degradation and Sequestration to Induce Light Responses across a Wide Range of Light Conditions. *PLANT CELL*, 30(6), 1277–1292. <https://doi.org/10.1105/tpc.17.00913>
- Petrillo, E., Godoy Herz, M. A., Fuchs, A., Reifer, D., Fuller, J., Yanovsky, M. J., Simpson, C., Brown, J. W. S., Barta, A., Kalyna, M., & Kornblihtt, A. R. (2014). A Chloroplast Retrograde Signal Regulates Nuclear Alternative Splicing. *SCIENCE*, 344(6182), 427–430. <https://doi.org/10.1126/science.1250322>
- Qu, G.-P., Li, H., Lin, X.-L., Kong, X., Hu, Z.-L., Jin, Y. H., Liu, Y., Song, H.-L., Kim, D. H., Lin, R., Li, J., & Jin, J. B. (2020). Reversible SUMOylation of FHY1 Regulates Phytochrome A Signaling in Arabidopsis. *Molecular Plant*, 13(6), 879–893. <https://doi.org/10.1016/j.molp.2020.04.002>
- Ravindran, N., Ramachandran, H., Job, N., Yadav, A., Vaishak, K. P., & Datta, S. (2021). B-box protein BBX32 integrates light and brassinosteroid signals to inhibit cotyledon opening. *PLANT PHYSIOLOGY*, 187(1), 446–461. <https://doi.org/10.1093/plphys/kiab304>
- Reddy, A. S. N., Marquez, Y., Kalyna, M., & Barta, A. (2013). Complexity of the Alternative Splicing Landscape in Plants. *PLANT CELL*, 25(10), 3657–3683. <https://doi.org/10.1105/tpc.113.117523>
- Reddy, A. S. N., & Shad Ali, G. (2011). Plant serine/arginine-rich proteins: Roles in precursor messenger RNA splicing, plant development, and stress responses. *Wiley Interdisciplinary Reviews. RNA*, 2(6), 875–889. <https://doi.org/10.1002/wrna.98>
- Riegler, S., Servi, L., Scarpin, M. R., Herz, M. A. G., Kubaczka, M. G., Venhuizen, P., Meyer, C., Brunkard, J. O., Kalyna, M., Barta, A., & Petrillo, E. (2021). Light

- regulates alternative splicing outcomes via the TOR kinase pathway. *CELL REPORTS*, 36(10). <https://doi.org/10.1016/j.celrep.2021.109676>
- Scarpin, M. R., Leiboff, S., & Brunkard, J. O. (2020). Parallel global profiling of plant TOR dynamics reveals a conserved role for LARP1 in translation. *ELife*, 9. <https://doi.org/10.7554/eLife.58795>
- Schwenk, P., Sheerin, D. J., Ponnu, J., Staudt, A.-M., Lesch, K. L., Lichtenberg, E., Medzihradzky, K. F., Hoecker, U., Klement, E., Viczián, A., & Hiltbrunner, A. (2021). Uncovering a novel function of the CCR4-NOT complex in phytochrome A-mediated light signalling in plants. *ELife*, 10. <https://doi.org/10.7554/eLife.63697>
- Sheerin, D. J., Menon, C., Zur Oven-Krockhaus, S., Enderle, B., Zhu, L., Johnen, P., Schleifenbaum, F., Stierhof, Y.-D., Huq, E., & Hiltbrunner, A. (2015). Light-activated phytochrome A and B interact with members of the SPA family to promote photomorphogenesis in Arabidopsis by reorganizing the COP1/SPA complex. *PLANT CELL*, 27(1), 189–201. <https://doi.org/10.1105/tpc.114.134775>
- Shen, H., Zhu, L., Castillon, A., Majee, M., Downie, B., & Huq, E. (2008). Light-induced phosphorylation and degradation of the negative regulator PHYTOCHROME-INTERACTING FACTOR1 from Arabidopsis depend upon its direct physical interactions with photoactivated phytochromes. *PLANT CELL*, 20(6), 1586–1602. <https://doi.org/10.1105/tpc.108.060020>
- Shen, Y., Khanna, R., Carle, C. M., & Quail, P. H. (2007). Phytochrome induces rapid PIF5 phosphorylation and degradation in response to red-light activation. *PLANT PHYSIOLOGY*, 145(3), 1043–1051. <https://doi.org/10.1104/pp.107.105601>
- Shikata, H., Hanada, K., Ushijima, T., Nakashima, M., Suzuki, Y., & Matsushita, T. (2014). Phytochrome controls alternative splicing to mediate light responses in Arabidopsis. *Proceedings of the National Academy of Sciences of the United States of America*, 111(52), 18781–18786. <https://doi.org/10.1073/pnas.1407147112>
- Shikata, H., Shibata, M., Ushijima, T., Nakashima, M., Kong, S.-G., Matsuoka, K., Lin, C., & Matsushita, T. (2012). The RS domain of Arabidopsis splicing factor RRC1

- is required for phytochrome B signal transduction. *The Plant Journal : For Cell and Molecular Biology*, 70(5), 727–738. <https://doi.org/10.1111/j.1365-313X.2012.04937.x>
- Soledad Tognacca, R., Servi, L., Esteban Hernando, C., Saura-Sanchez, M., Javier Yanovsky, M., Petrillo, E., & Francisco Botto, J. (2019). Alternative Splicing Regulation During Light-Induced Germination of *Arabidopsis thaliana* Seeds. *FRONTIERS in PLANT SCIENCE*, 10. <https://doi.org/10.3389/fpls.2019.01076>
- Staiger, D., & Brown, J. W. S. (2013). Alternative splicing at the intersection of biological timing, development, and stress responses. *PLANT CELL*, 25(10), 3640–3656. <https://doi.org/10.1105/tpc.113.113803>
- Stauffer, E., Westermann, A., Wagner, G., & Wachter, A. (2010). Polypyrimidine tract-binding protein homologues from *Arabidopsis* underlie regulatory circuits based on alternative splicing and downstream control. *The Plant Journal : For Cell and Molecular Biology*, 64(2), 243–255. <https://doi.org/10.1111/j.1365-313X.2010.04321.x>
- Sun, N., Wang, J., Gao, Z., Dong, J., He, H., Terzaghi, W., Wei, N., Deng, X. W., & Chen, H. (2016). *Arabidopsis* SAURs are critical for differential light regulation of the development of various organs. *Proceedings of the National Academy of Sciences of the United States of America*, 6071–6076. <https://doi.org/10.1073/pnas.1604782113>
- Tillemans, V., Leponce, I., Rausin, G., Dispa, L., & Motte, P. (2006). Insights into nuclear organization in plants as revealed by the dynamic distribution of *Arabidopsis* SR splicing factors. *The Plant Cell*, 18(11), 3218–3234. <https://doi.org/10.1105/tpc.106.044529>
- van den Akker, P. C., Nijenhuis, M., Meijer, G., Hofstra, R. M. W., Jonkman, M. F., & Pasmooij, A. M. G. (2012). Natural gene therapy in dystrophic epidermolysis bullosa. *Archives of Dermatology*, 148(2), 213–216. <https://doi.org/10.1001/archdermatol.2011.298>
- Wachter, A., Tunc-Ozdemir, M., Grove, B. C., Green, P. J., Shintani, D. K., & Breaker, R. R. (2007). Riboswitch control of gene expression in plants by splicing and alternative 3' end processing of mRNAs. *PLANT CELL*, 19(11), 3437–3450. <https://doi.org/10.1105/tpc.107.053645>



- Wang, R., Wang, R., Liu, M., Yuan, W., Zhao, Z., Liu, X., Peng, Y., Yang, X., Sun, Y., & Tang, W. (2021). Nucleocytoplasmic trafficking and turnover mechanisms of BRASSINAZOLE RESISTANT1 in *Arabidopsis thaliana*. *Proceedings of the National Academy of Sciences of the United States of America*, *118*(33). <https://doi.org/10.1073/pnas.2101838118>
- Wang, W., Lu, X., Li, L., Lian, H., Mao, Z., Xu, P., Guo, T., Xu, F., Du, S., Cao, X., Wang, S., Shen, H., & Yang, H.-Q. (2018). Photoexcited CRYPTOCHROME1 Interacts with Dephosphorylated BES1 to Regulate Brassinosteroid Signaling and Photomorphogenesis in *Arabidopsis*. *PLANT CELL*, *30*(9), 1989–2005. <https://doi.org/10.1105/tpc.17.00994>
- Wang, Z.-P., Xing, H.-L., Dong, L., Zhang, H.-Y., Han, C.-Y., Wang, X.-C., & Chen, Q.-J. (2015). Egg cell-specific promoter-controlled CRISPR/Cas9 efficiently generates homozygous mutants for multiple target genes in *Arabidopsis* in a single generation. *Genome Biology*, *16*, 144. <https://doi.org/10.1186/s13059-015-0715-0>
- Wang, Z.-Y., Bai, M.-Y., Oh, E., & Zhu, J.-Y. (2012). Brassinosteroid signaling network and regulation of photomorphogenesis. *Annual Review of Genetics*, *46*, 701–724. <https://doi.org/10.1146/annurev-genet-102209-163450>
- Wu, H.-P., Su, Y.-S., Chen, H.-C., Chen, Y.-R., Wu, C.-C., Lin, W.-D., & Tu, S.-L. (2014). Genome-wide analysis of light-regulated alternative splicing mediated by photoreceptors in *Physcomitrella patens*. *Genome Biology*, *15*(1), R10. <https://doi.org/10.1186/gb-2014-15-1-r10>
- Wu, J., Wang, W., Xu, P., Pan, J., Zhang, T., Li, Y., Li, G., Yang, H., & Lian, H. (2019). Phyb Interacts with BES1 to Regulate Brassinosteroid Signaling in *Arabidopsis*. *Plant & Cell Physiology*, *60*(2), 353–366. <https://doi.org/10.1093/pcp/pcy212>
- Wu, S.-H. (2014). Gene expression regulation in photomorphogenesis from the perspective of the central dogma. *Annual Review of Plant Biology*, *65*, 311–333. <https://doi.org/10.1146/annurev-arplant-050213-040337>
- Xin, R., Kathare, P. K., & Huq, E. (2019). Coordinated Regulation of Pre-mRNA Splicing by the SFPS-RRC1 Complex to Promote Photomorphogenesis. *The Plant Cell*, *31*(9), 2052–2069. <https://doi.org/10.1105/tpc.18.00786>

- Xin, R., Zhu, L., Salomé, P. A., Mancini, E., Marshall, C. M., Harmon, F. G., Yanovsky, M. J., Weigel, D., & Huq, E. (2017). Spf45-related splicing factor for phytochrome signaling promotes photomorphogenesis by regulating pre-mRNA splicing in Arabidopsis. *Proceedings of the National Academy of Sciences of the United States of America*, *114*(33), E7018-E7027. <https://doi.org/10.1073/pnas.1706379114>
- Xing, H.-L., Dong, L., Wang, Z.-P., Zhang, H.-Y., Han, C.-Y., Liu, B., Wang, X.-C., & Chen, Q.-J. (2014). A CRISPR/Cas9 toolkit for multiplex genome editing in plants. *BMC PLANT BIOLOGY*, *14*. <https://doi.org/10.1186/s12870-014-0327-y>
- Xu, X., Paik, I., Zhu, L., & Huq, E. (2015). Illuminating Progress in Phytochrome-Mediated Light Signaling Pathways. *Trends in Plant Science*, *20*(10), 641–650. <https://doi.org/10.1016/j.tplants.2015.06.010>
- Yan, Q., Xia, X., Sun, Z., & Fang, Y. (2017). Depletion of Arabidopsis SC35 and SC35-like serine/arginine-rich proteins affects the transcription and splicing of a subset of genes. *PLoS Genetics*, *13*(3), e1006663. <https://doi.org/10.1371/journal.pgen.1006663>
- Yan, T., Heng, Y., Wang, W., Li, J., & Deng, X. W. (2022). SWELLMAP 2, a phyB-Interacting Splicing Factor, Negatively Regulates Seedling Photomorphogenesis in Arabidopsis. *FRONTIERS in PLANT SCIENCE*, *13*. <https://doi.org/10.3389/fpls.2022.836519>
- Yoon, E. K., Krishnamurthy, P., Kim, J. A., Jeong, M.-J., & Lee, S. I. (2018). Genome-wide Characterization of Brassica rapa Genes Encoding Serine/arginine-rich Proteins: Expression and Alternative Splicing Events by Abiotic Stresses. *JOURNAL of PLANT BIOLOGY*, *61*(4), 198–209. <https://doi.org/10.1007/s12374-017-0391-6>
- Zhai, Y., Peng, H., Neff, M. M., & Pappu, H. R. (2019). Putative Auxin and Light Responsive Promoter Elements From the Tomato spotted wilt tospovirus Genome, When Expressed as cDNA, Are Functional in Arabidopsis. *FRONTIERS in PLANT SCIENCE*, *10*. <https://doi.org/10.3389/fpls.2019.00804>
- Zhang, X.-N., Shi, Y., Powers, J. J., Gowda, N. B., Zhang, C., Ibrahim, H. M. M., Ball, H. B., Chen, S. L., Lu, H., & Mount, S. M. (2017). Transcriptome analyses reveal SR45 to be a neutral splicing regulator and a suppressor of innate immunity in

Arabidopsis thaliana. *BMC Genomics*, 18(1), 772.  
<https://doi.org/10.1186/s12864-017-4183-7>

### **Theses**

Saile, Jennifer (2017): Role of RS proteins in light- and sugar-regulated alternative splicing. Master thesis.

Denecke, Moritz Paul (2019): Photomorphogenesis response in RS splicing regulator mutants. Bachelor thesis.

## Main figures

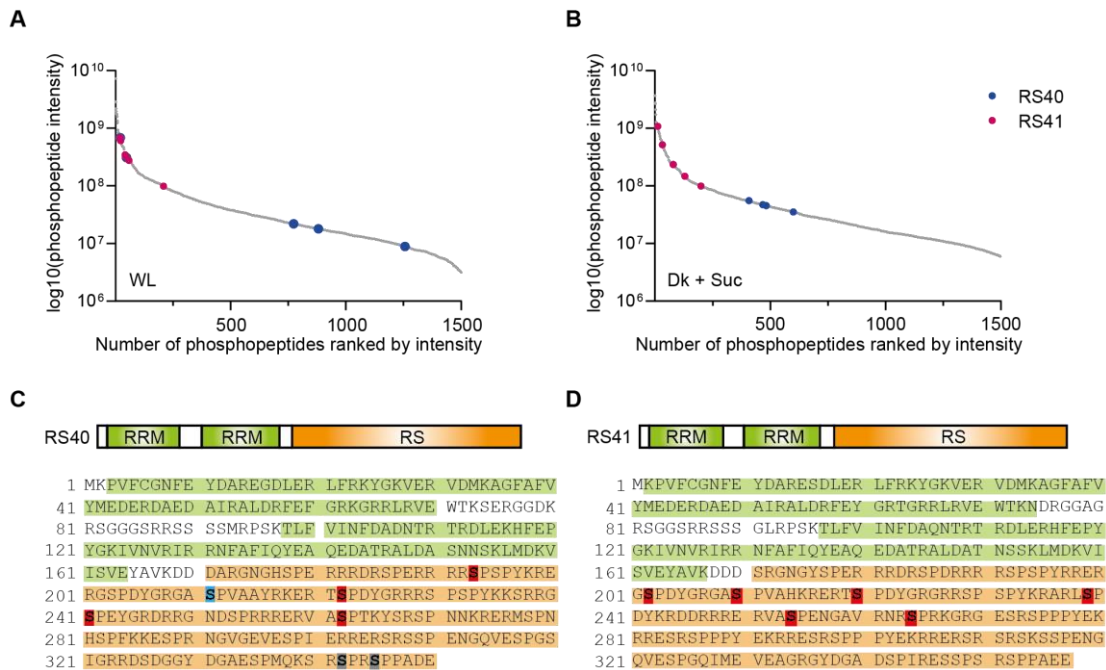


**Figure 1: Light and sugar induce rapid and specific phosphorylation of RS40 and RS41.** (A, B) 6-d-old etiolated WT seedlings were either exposed to white light (WL) (A) or treated with 2% sucrose (B) for 30 min. Phosphopeptides were identified by MS and the most abundant phosphopeptides, in this case 1500, are depicted. RS40 and RS41 peptides that were differentially phosphorylated in response to light or sucrose are highlighted as blue and purple dots, respectively. (C, D) RS40 and RS41 domain models and protein sequences. RS proteins consist of two RNA-recognition motifs (RRMs, highlighted in green) at the N-terminus and a C-terminal Arginine/Serine-rich (RS) domain (marked in orange). Serine residues marked in red are differentially phosphorylated in response to light and sugar. Blue and grey mark residues that are differentially phosphorylated in response to sucrose and light, respectively.

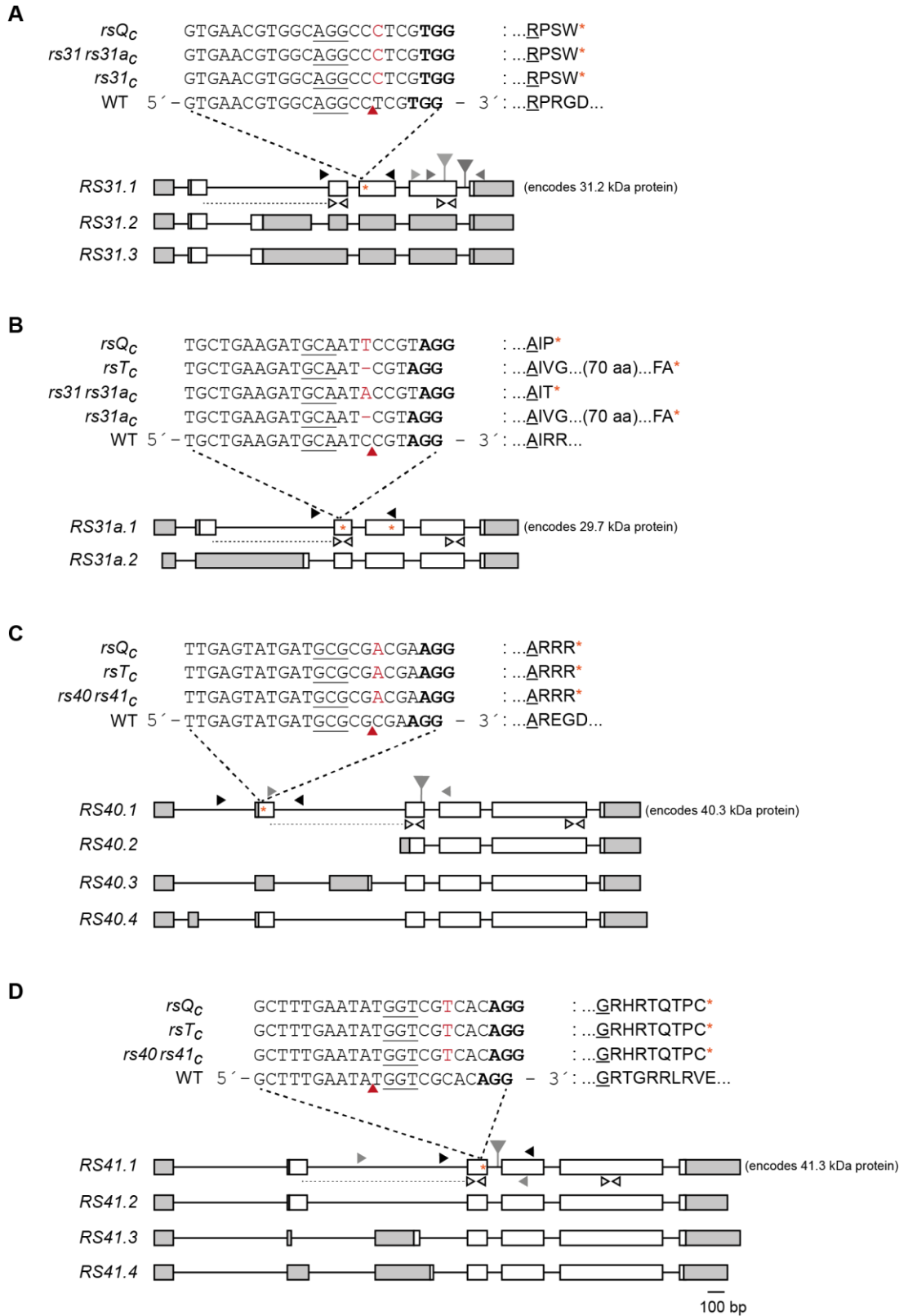


**Figure 2: RS transcript models.** Transcript models of major splicing variants from *RS31* (A), *RS31a* (B), *RS40* (C), and *RS41* (D). Introns are shown as lines, exons as white boxes. UTRs are coloured in grey. The T-DNA insertion site is depicted as triangle, and the sgRNA target site indicated by dashed lines above transcript models. sgRNA target sequence is shown above the corresponding model, with the bold sequence showing the PAM motif. Cas9 cleavage site is indicated by the red arrowhead and

corresponding mutations (insertion or deletion) are marked in red, followed by the resulting amino acid (aa) sequence (right). The aa sequence starts with the triplet prior the cleavage site (underlined). A premature termination codon is generated by the mutation-induced frameshift and marked as asterisk (orange). Positions of primers used for genotyping (black and grey) as well as RT-qPCR (white) are shown as arrowheads. Primers for genotyping are shown above the first variant, whereas primer pairs used for RT-qPCR are displayed below. Primer with dotted line indicates primer binding site at a spliced junction and corresponding primer pair was used to detect specifically the coding isoform of the corresponding *RS* gene by RT-qPCR, whereas the second RT-qPCR primer pair was used to analyse all isoforms. Drawn to scale.

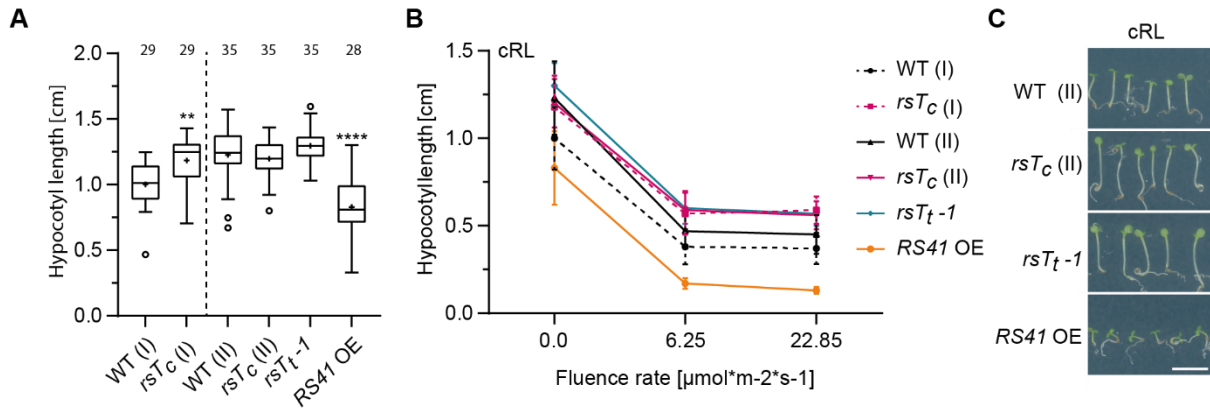


**Figure 3: Altered red light response in *rs* mutants and *RS41* OE seedlings. (A)** Hypocotyl lengths of 4-d-old dark grown seedlings. I or II refers to different generations. Interquartile range, maximum and minimum, median, and mean values are depicted as box, whiskers, middle line and plus, respectively. Dots display outliers. Asterisks indicate significant difference compared to corresponding WT control based on one-way ANOVA with post hoc Tukey test (P values: \*P < 0.05; \*\*P < 0.01, \*\*\*P < 0.001, \*\*\*\*P < 0.0001). **(B)** Absolute hypocotyl length of 4-d-old seedlings that were either grown in darkness (fluence rate = 0) or continuous red light (cRL). Dark samples represent seedlings described in (A). Mean values  $\pm$ SD are depicted ( $n = 27$  to 39). Corresponding relative lengths are depicted in Supplemental Figure 15. **(C)** Representative pictures of seedlings described in (B) that were grown under cRL at 22.85  $\mu\text{mol m}^{-2}\text{s}^{-1}$ . Scale bar: 5 mm.

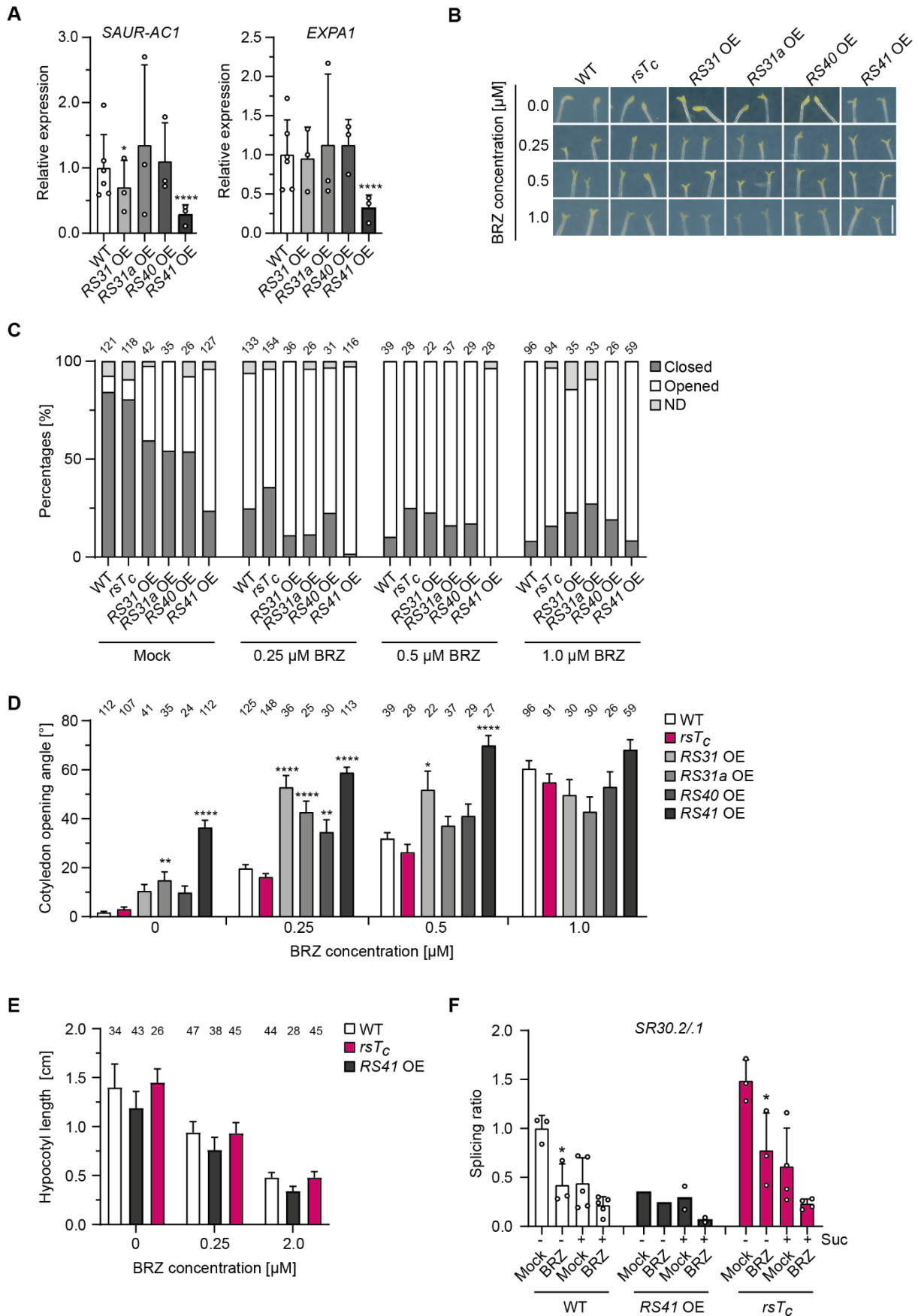


**Figure 4: BRZ treatment affects cotyledon opening in RS-dependent manner and changes AS outcome. (A)** Relative expression of brassinosteroid (BR) induced genes in 6-d-old dark grown WT and



*RS* OE seedlings. Displayed are mean values ( $n$ : 3 to 6; individual data points are shown as dots) +SD, normalized to average level of WT ( $n$ : 6). Statistical test was performed using an unpaired  $t$  test by comparing *OE* lines with WT (P values: \*P < 0.05; \*\*P < 0.01, \*\*\*P < 0.001, \*\*\*\*P < 0.0001). **(B)** Pictures of randomly selected 6-d-old etiolated seedlings that were grown on  $\frac{1}{2}$  MS plates containing different concentrations of BRZ. Scale bar: 2 mm. **(C)** Percentages of closed and opened cotyledons in WT, *rsT<sub>c</sub>* and *RS* OE seedlings described in (B). ND was assigned when cotyledons were not clearly visible. **(D)** Quantification of cotyledon opening angle of seedlings shown in (B). Bars represent mean values +SEM.  $n$  (24 to 148) is indicated above each bar. Asterisks indicate significant difference compared to WT, based on one-way ANOVA with post hoc Tukey test (P values: \*P < 0.05; \*\*P < 0.01, \*\*\*P < 0.001, \*\*\*\*P < 0.0001). **(E)** Quantification of hypocotyl length in 6-d-old etiolated seedlings that were grown on  $\frac{1}{2}$  MS plates containing different concentrations of BRZ in the absence of sucrose. Displayed are mean values +SD ( $n$ : 28 to 47). **(F)** *SR30* splicing ratio in WT, *RS41* OE and the *rsT<sub>c</sub>*. Seedlings were grown for 3 d on  $\frac{1}{2}$  MS plates supplemented or lacking 1.5% sucrose in the presence or absence of 1  $\mu$ M BRZ. Plates without BRZ served as mock control. Splicing ratio was quantified via Bioanalyzer and normalised to average level of WT mock lacking sucrose ( $n$ : 3). Bars represent mean values +SD ( $n$ : 1 to 5). An unpaired  $t$  test was performed to compare the BRZ response to the corresponding mock sample (P: \*P < 0.05).

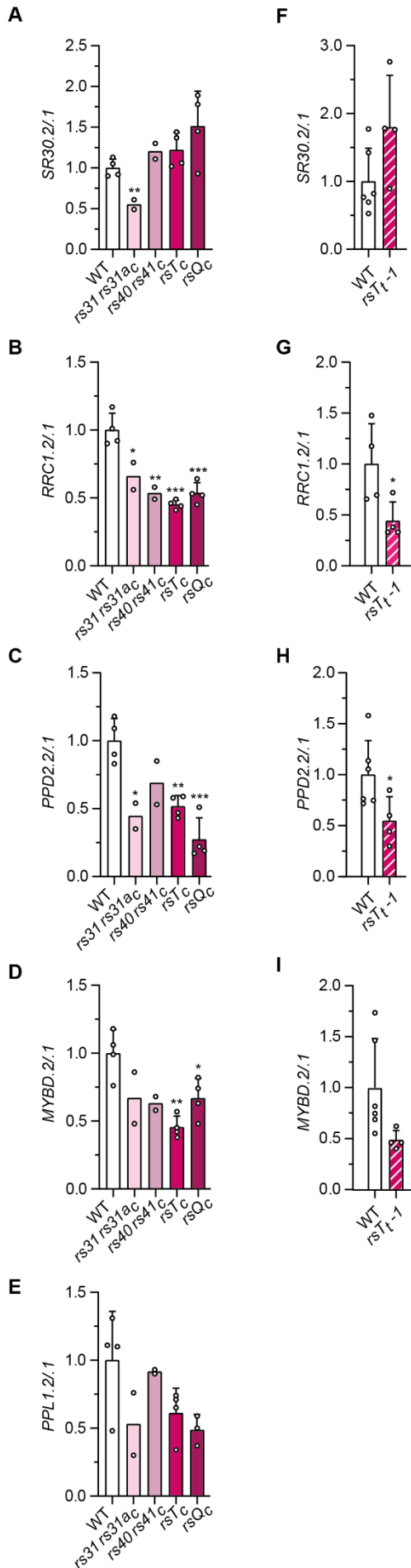


**Figure 5: RS proteins control alternative pre-mRNA splicing in darkness. (A to E)**

Quantification of splicing variants of known light-regulated AS events in *rs* CRISPR mutants. Seedlings were grown for 6 d in liquid ½ MS media and kept in darkness. Splicing variants were detected via RT-qPCR (**A, E**) or co-amplified via PCR and quantified using a Bioanalyzer (**B to D**). All AS ratios were normalized to average ratio of WT samples from two independent experiments. Displayed are mean values +SD with dots showing individual data points (*n*: 2 to 4). Statistical analysis was performed using an independent *t* test and compared with WT (P values: \*P < 0.05, \*\*P < 0.01, \*\*\*P < 0.001). (**F to I**) Quantification of splicing isoforms via RT-qPCR of 6-d-old WT and *rsT<sub>i</sub>* seedlings that were grown in liquid ½ MS media in darkness. Splicing ratios were normalized to the average ratio of WT samples (*n*: 4 to 6). Displayed are mean values +SD, single dots represent individual data points (*n*: 3 to 6 from 3 independent experiments). Normalized ratios of *rsT<sub>i</sub>* Dark Man were compared with WT Dark Man using an independent *t* test (P values: \*P < 0.05). Corresponding (relative) AS changes in response to light and sugar are displayed in Supplemental Figure 31.

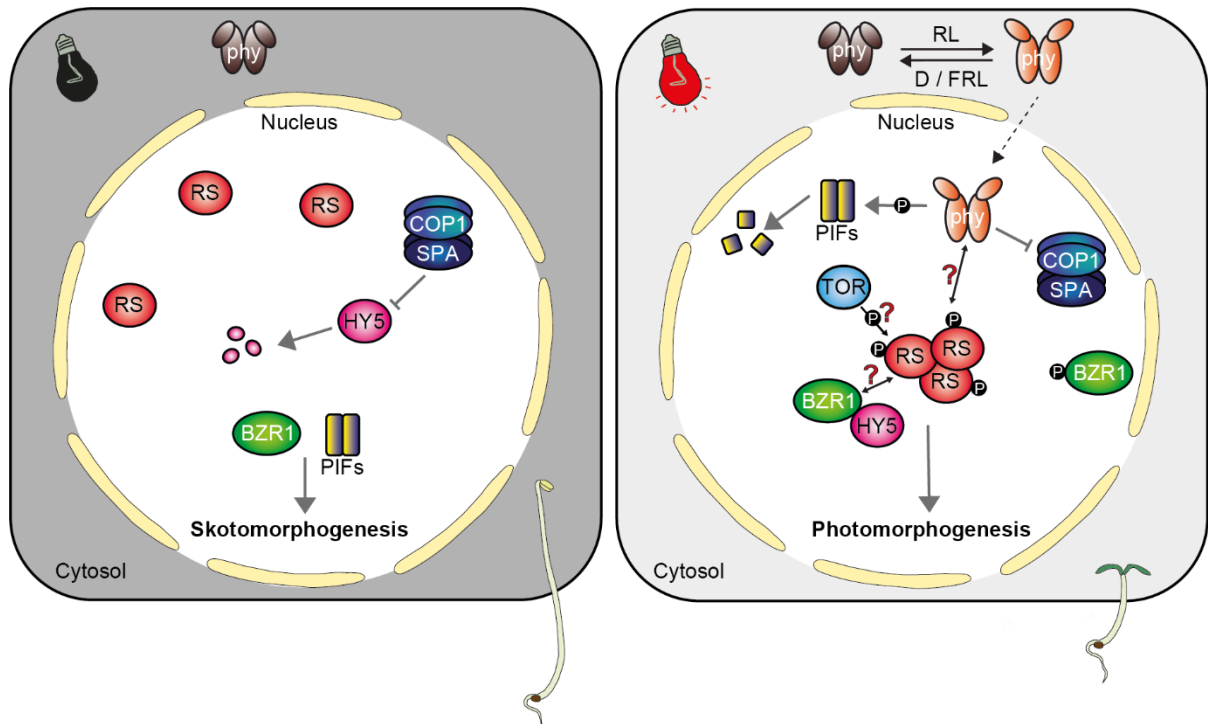


**Figure 6: Role of RS proteins in skoto- and photomorphogenic growth. (Left)** Under dark conditions, RS proteins are distributed within the nucleoplasm and HY5 transcription factors are targeted for proteasomal degradation by the COP1/SPA complex. Positive regulators of skotomorphogenesis, including dephosphorylated BZR1 (active state) and PIFs, induce the expression of genes involved in cell elongation and cotyledon closure that promotes skotomorphogenic growth. **(Right)** In response to light, RS proteins get phosphorylated, which triggers their nuclear re-localization into nuclear speckles. Light-mediated phosphorylation of RS proteins might be caused by TOR. Furthermore, illumination also induces BZR1 phosphorylation (inactive state) and the translocation of photoactivated phyB into the nucleus. Photoactivated phyB triggers the phosphorylation-dependent degradation of PIF proteins as well as the repression of the COP1/SPA complex that results in the stabilization of HY5. Moreover, we propose that photoactivated phyB might also interact with RS proteins, affecting RS phosphorylation and/or stabilization. Stabilized HY5 sequesters available dephosphorylated BZR1, and together with RS proteins, promote photomorphogenic growth, that results in the repression of cell elongation and induction of cotyledon opening.

## Supplemental information

### **Splicing regulators of Serine/Arginine-rich (SR) proteins control light-mediated alternative splicing events and integrate light and brassinosteroid signaling to induce cotyledon opening during photomorphogenesis**

Jennifer Saile<sup>1,2</sup>, Moritz Paul Denecke<sup>1</sup>, Sofia Lobato-Gil<sup>3</sup>, Petra Beli<sup>3</sup>, and Andreas Wachter<sup>1,2,\*</sup>

<sup>1</sup>Institute for Molecular Physiology (imP), University of Mainz, Hanns-Dieter-Hüschen-Weg 17, 55128 Mainz, Germany


<sup>2</sup>Center for Plant Molecular Biology (ZMBP), University of Tübingen, Auf der Morgenstelle 32, 72076 Tübingen, Germany

<sup>3</sup>Institute of Molecular Biology (IMB), University of Mainz, Ackermannweg 4, 55128 Mainz, Mainz, Germany.

\*Corresponding author: [wachter@uni-mainz.de](mailto:wachter@uni-mainz.de)


## SUPPLEMENTAL FIGURES

A

RS31 

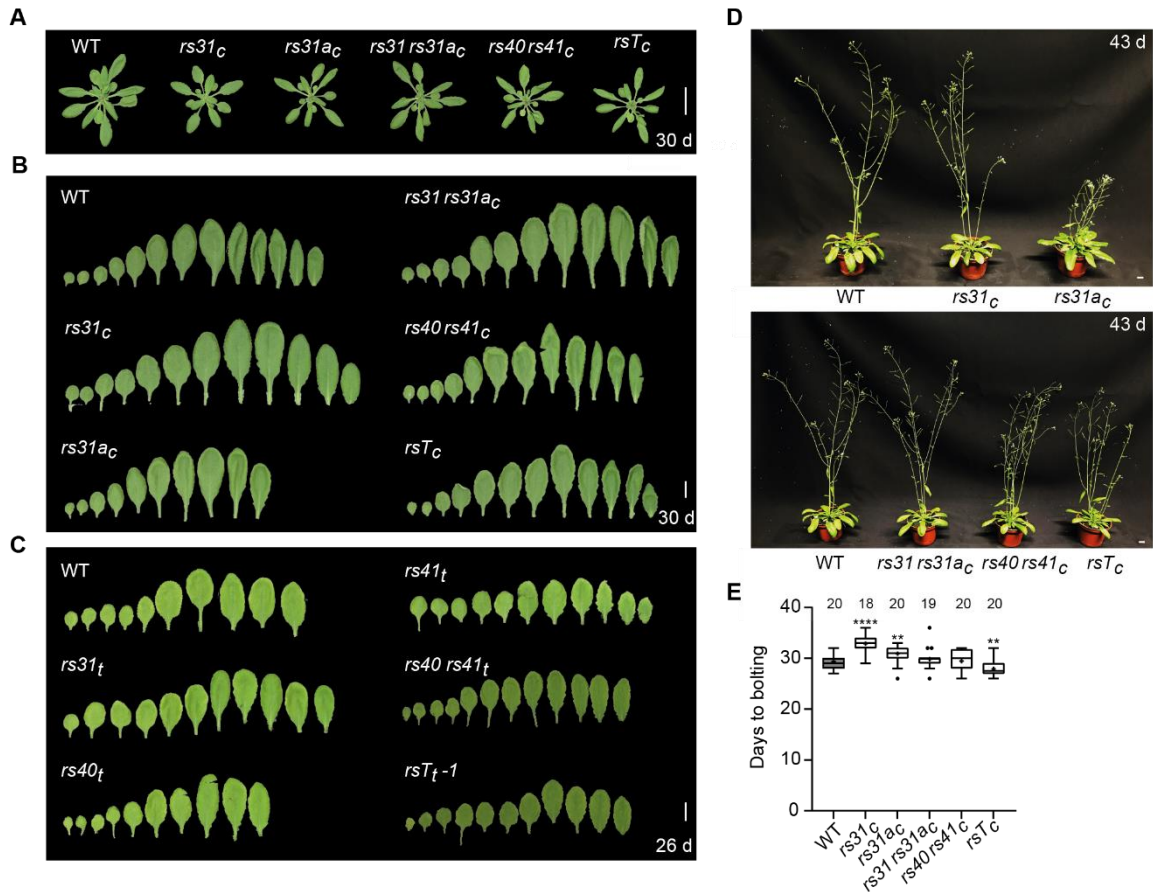
1 MRPVEVGNFE YETRQSDLER LFDKYGRVDR VDMKSGYAFV  
 41 YFEDERDAED AIRKLDNFPF GYEKRRLSVE WAKGERGRPR  
 81 GDAKAPSNLK PTKTLEVINP DPIRTKEHDI EKHFEFPGKV  
 121 TNVRIIRNFS FVQFETQEDA TKALEATQRS KILDRVVSVE  
 161 YALKDDDERD DRNGGRSPRR SLSPVYRRRP SPDYGRRPSR  
 201 GQGRRPSPDY GRARSPEYDR YKGPAAAYERR RSPDYGRSS  
 241 DYGRQRSPGY DRYRSRSPVP RGRP

B

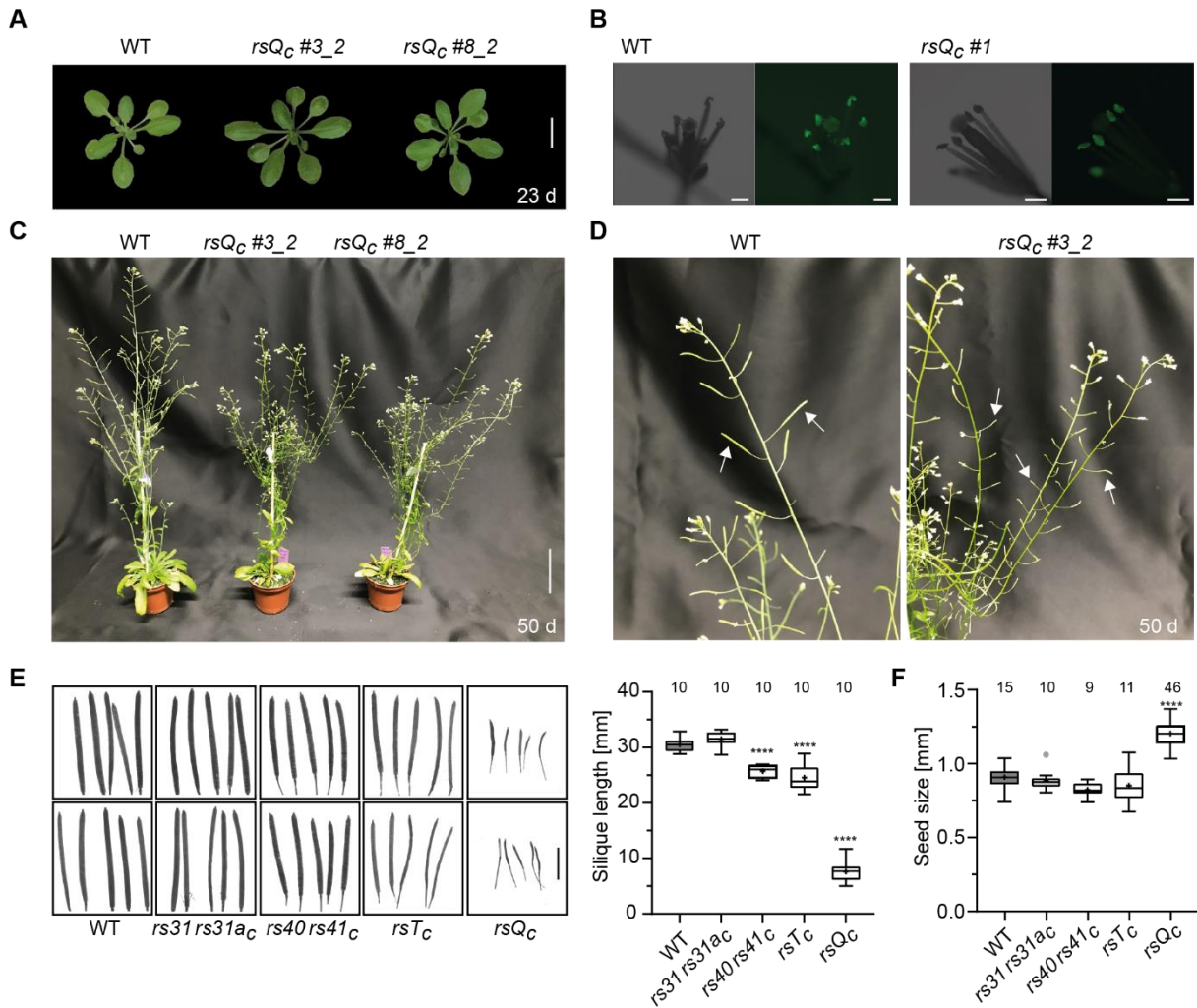
RS31a 

1 MRHVYVGNED YDTRHSDLER LFSKFGRVGR VDMKSGYAFV  
 41 YFEDERDAED AIRRTDNTTF GYGRRLSVE WAKDFQGERG  
 81 KPRDGKAVSN QRPTKTLFVI NFDPIRTREMERHFEPYG  
 121 KVLNVRMRRN FAFVQFATQE DATKALDSTH NSKLLDKVVS  
 161 VEYALREAGE REDRYAGSRR RRSPPSPVYRR RSPDYTRRR  
 201 SPEYDRYKGP APYERRKSPD YGRSSDYGR ARARSPGYDR  
 241 SRSPIQRARG

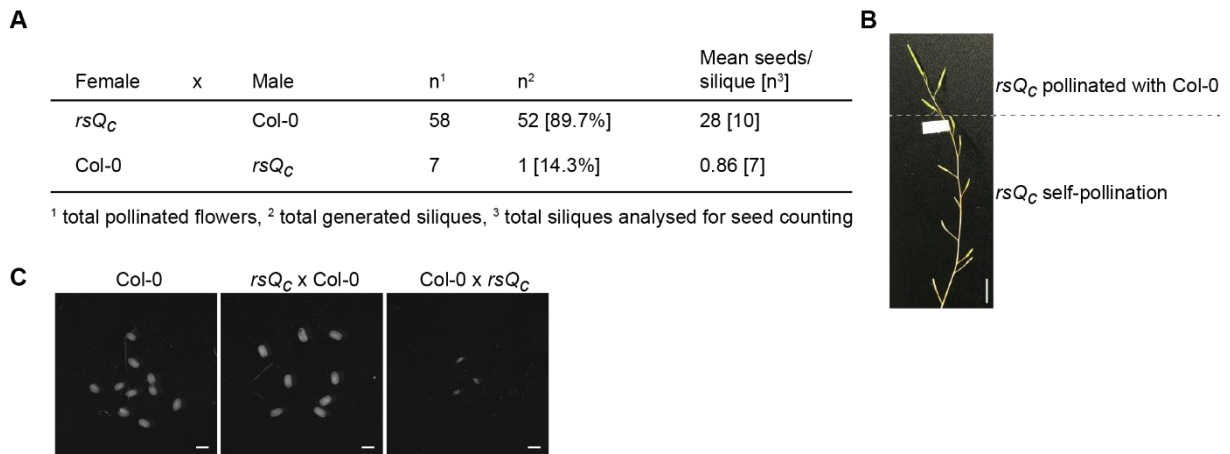
**Supplemental Figure 1: Domain structure and protein sequence of RS31 and RS31a.** RS proteins consist of two RNA-recognition motifs (RRMs, highlighted in green) at the N-terminus and contain a C-terminal Arginine/Serine-rich (RS) domain (marked in orange).



**Supplemental Figure 2: Phenotypes of *rs* CRISPRs and T-DNA mutants.** **(A)** Rosette phenotypes of Col-0 and different *rs* CRISPR (*rs<sub>c</sub>*) mutants that were grown for 30 d under long day (LD) conditions (16 h light, 8 h dark). Scale bar: 5 cm. **(B, C)** Rosette leaves of 30 d-old *rs<sub>c</sub>* **(B)** and 26-d-old T-DNA (*rs<sub>t</sub>*) mutants **(C)** with corresponding WT. *rs<sub>c</sub>* mutants were grown on soil whereas *rs<sub>t</sub>* lines were first grown vertically on ½ MS plates for 9 d and then transferred to soil. Rosette leaves of another plant are displayed and therefore, might explain phenotypical differences compared to the rosette shown in (A). Scale bar: 1 cm. **(D)** Photographs of randomly chosen 43 d-old *rs31<sub>c</sub>* and *rs31a<sub>c</sub>* single (upper panel) and *rs31a rs31<sub>c</sub>*, *rs40 41<sub>c</sub>* and *rsT<sub>c</sub>* CRISPR mutants (lower panel) grown under LD conditions. Scale bar: 1 cm. **(E)** Days to bolting (defined as  $\geq 1$  cm of inflorescence stem) of Col-0 and *rs<sub>c</sub>* mutants. Interquartile range, maximum and minimum, median, and mean values are depicted as box, whiskers, middle line and plus, respectively. Dots display outliers (*n*: 18 to 20). An unpaired *t*-test with equal variance was performed (P values: \*\*P < 0.01, \*\*\*P < 0.001, \*\*\*\*P < 0.0001).

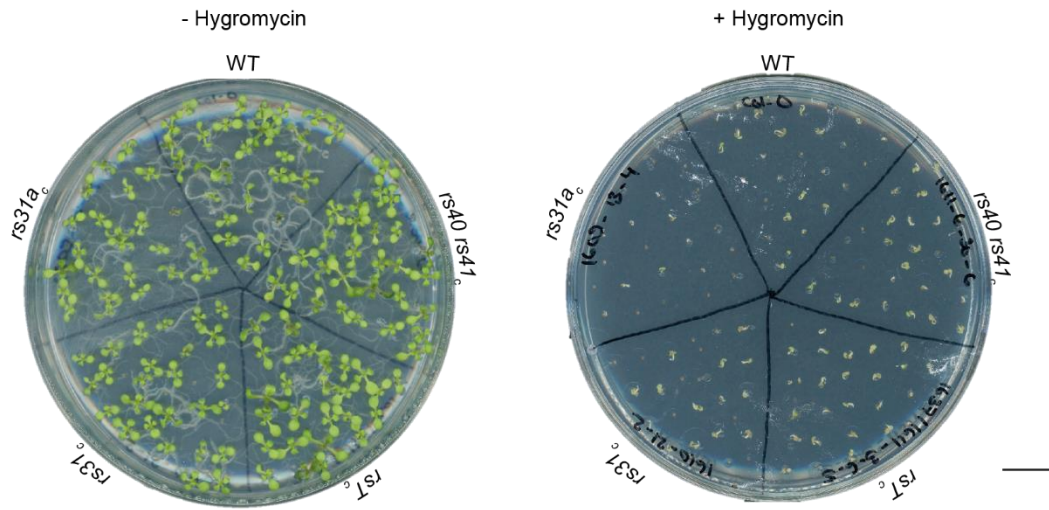


**Supplemental Figure 3: *rsQ<sub>C</sub>* mutants show severe phenotypes in reproductive phase.** (A) Rosette of Col-0 and *rsQ<sub>C</sub>* mutants grown under long day conditions for 23 d. Scale bar: 1 cm. (B) WT and *rsQ<sub>C</sub>* stamen and pistil phenotypes at anthesis. Channels showing transmission (left) and fluorescence (right) are displayed, and pollen grains display autofluorescence upon blue light excitation. Scale bar: 0.5 mm. (C) Phenotypes of selected lines described in (A) at the age of 50 d. Scale bar: 5 cm. (D) Closeup picture of 50 d-old WT and mutant stem. Arrows point at representative siliques that differ in their size in WT and *rsQ<sub>C</sub>* mutants. (E, left) Comparison of WT and different *rs<sub>C</sub>* mutant siliques. Scale bar: 10 mm. (Right) Quantification of silique length. (F) Quantification of seed size. *n* is indicated above each genotype. Middle line of the box plot shows median, the plus indicates the mean. Interquartile range and maximum and minimum are displayed as the bounds of the box and whiskers, respectively. The grey dot represents an outlier. Asterisks indicate significant differences of WT and *rs<sub>C</sub>* mutants based on one-way ANOVA with post hoc Tukey test (P value: \*\*\*\*P < 0.0001).

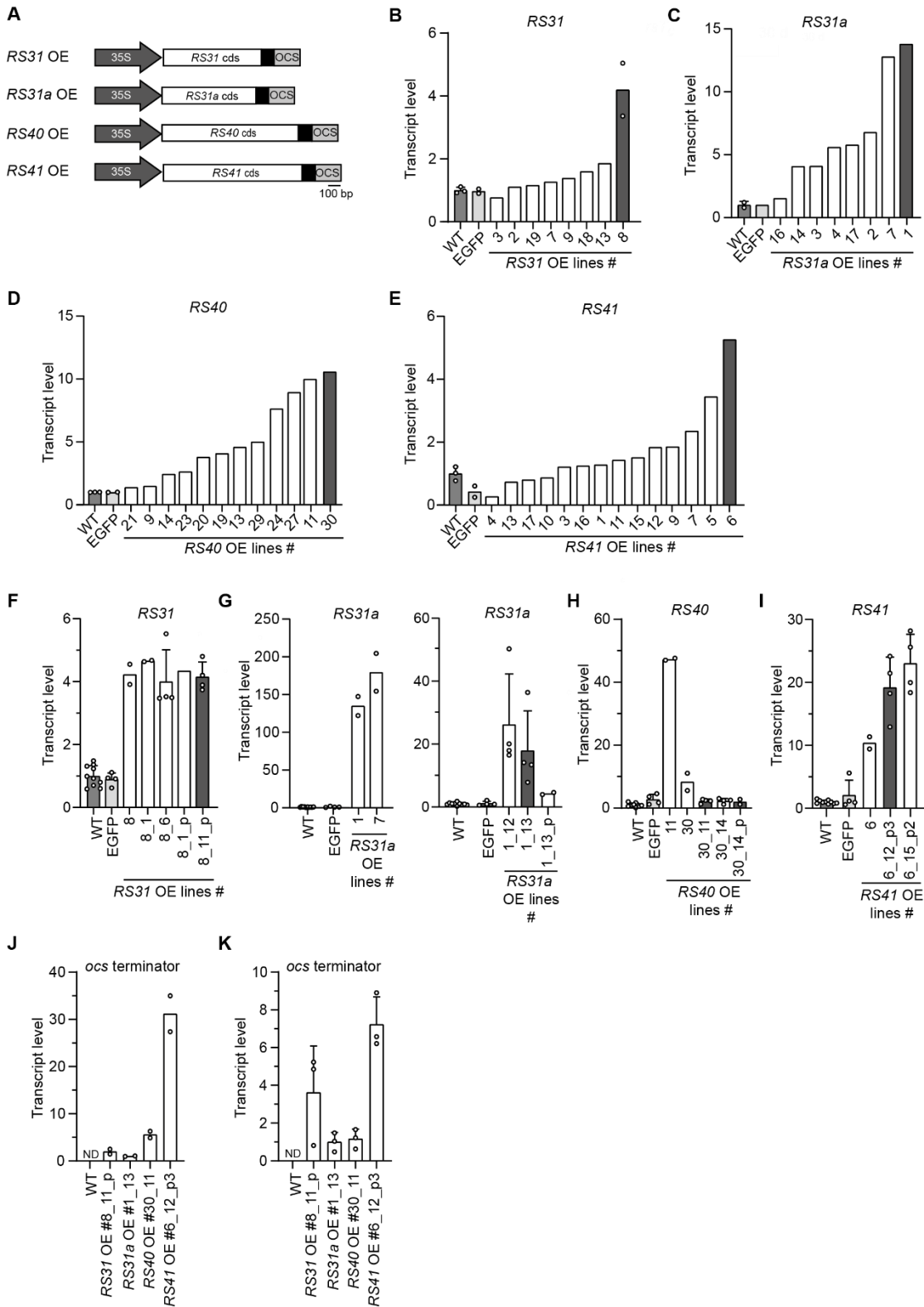


**Supplemental Figure 4: *rsQ<sub>c</sub>* mutant plants are almost completely male sterile. (A)** For pollination experiments *rsQ<sub>c</sub>* mutant plants were pollinated with wildtype Col-0 pollen or vice versa. **(B)** Stem with siliques of a *rsQ<sub>c</sub>* mutant plant that was pollinated with Col-0 pollen (above the line) or self-pollinated (below the line). Scale bar: 1 cm. **(C)** Representative seeds derived from pollination experiment. Col-0 seeds derived from self-pollination served as control. Scale bar: 1 mm.



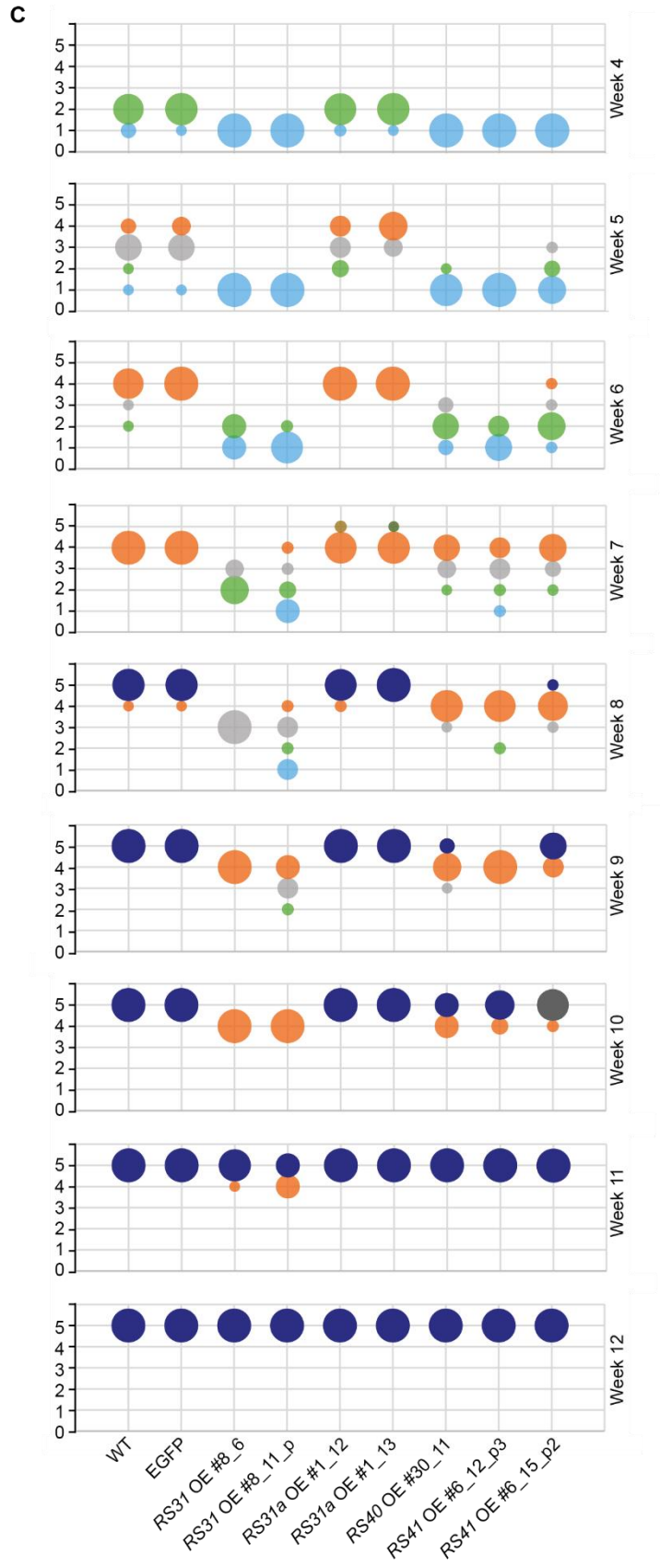
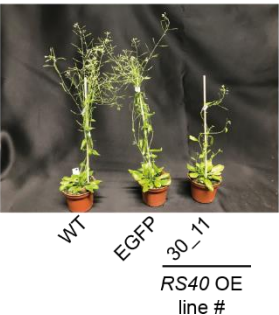
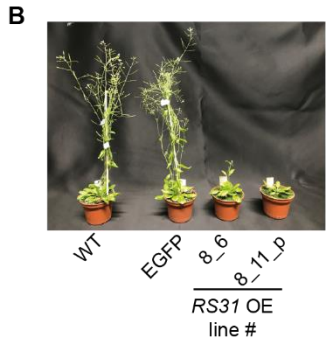
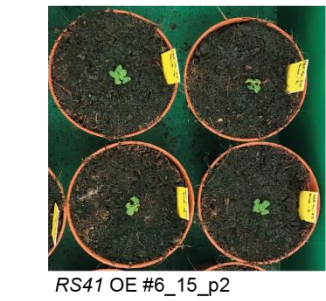


**Supplemental Figure 5: *rs* CRISPR mutants are Cas9-free.** *rs* CRISPR mutants were grown for 9 d on  $\frac{1}{2}$  MS plates (+ 2% sucrose) in the absence (left) or presence (right) of 20  $\mu$ g/ml hygromycin. Col-0 WT served as control. Scale bar: 1 cm.

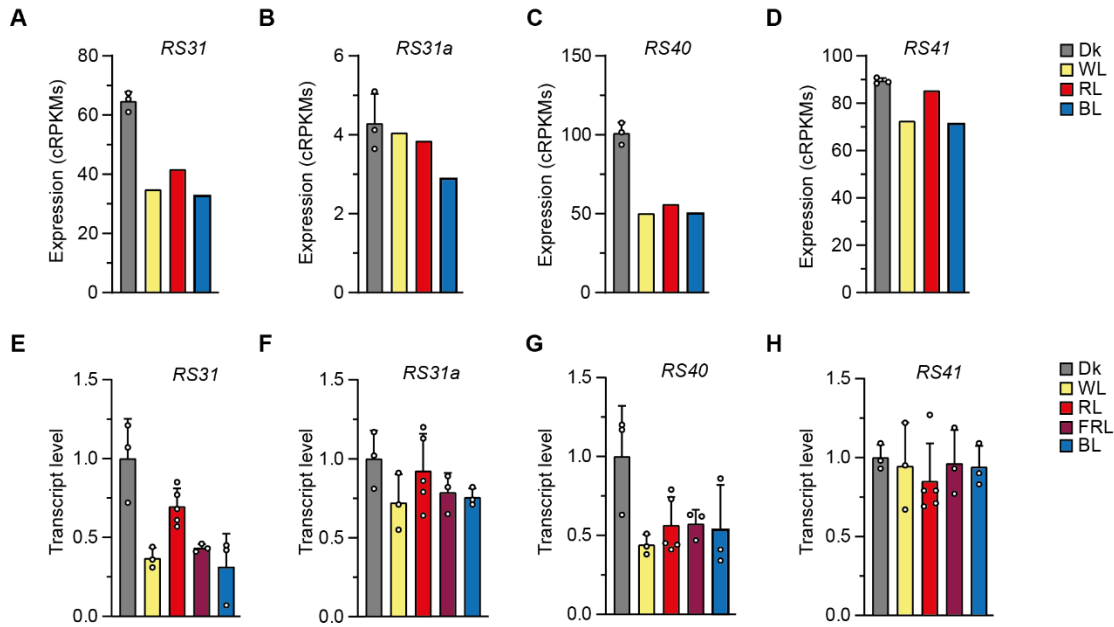


**Supplemental Figure 6: RS transcript level in several Arabidopsis RS OE lines. (A)** Schematic model of RS overexpression (OE) constructs. The coding sequence (cds) of the corresponding RS gene is under the control of the Cauliflower Mosaic Virus 35S promoter and the octopine synthase (OCS) terminator. Black box represents the triple HA-tag. Drawn to scale. **(B to E)** Relative transcript levels of *RS31* **(B)**, *RS31a* **(C)**, *RS40* **(D)**, and *RS41* **(E)** in independent Arabidopsis OE lines (T1) that were grown under long day conditions. Transgenic seedlings were grown for 10 d on ½ MS plates

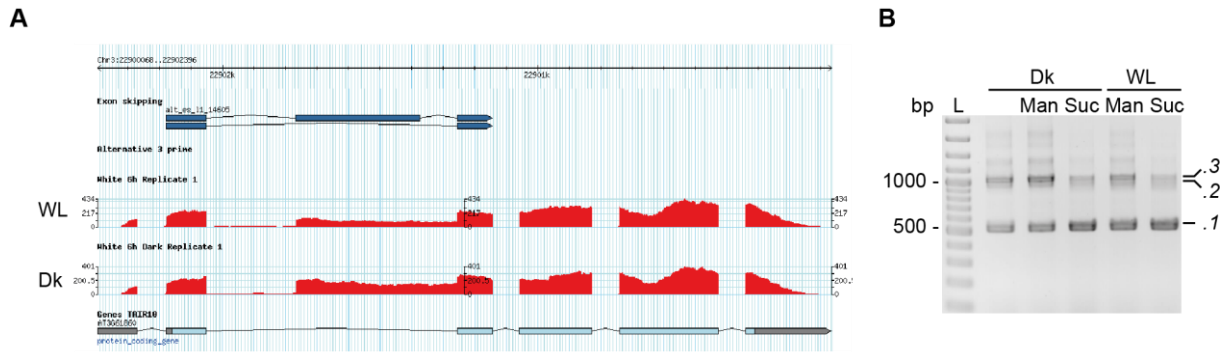
supplemented with kanamycin. WT Col-0 and a vector control EGFP (pBinAR-EGFP) were included as control (marked in grey). Data are mean values +SD in case of WT, normalized to the averaged WT level.  $N = 1$  to 3, with individual data points shown as dots. Data are from master thesis (Saile J., Role of RS proteins in light- and sugar-regulated alternative splicing, 2017). Primer binding sites are indicated in Figure 2 and were used to detect all *RS* splicing isoforms. **(F to I)** Relative expression level of the coding isoform of *RS31* **(F)**, *RS31a* **(G)**, *RS40* **(H)**, and *RS41* **(I)** in lines that were previously identified to have the highest OE level. Therefore, expression level was analysed in different generations (T 1, T2 and T3) in selected lines. Transgenic seedlings were grown for 10 d in the presence of kanamycin and 2% sucrose. WT and EGFP served as control. Data are mean values ( $n = 2$  to 10; individual data points are shown as dots) +SD, normalized to the averaged WT level. Transgenic lines that were used for further experiments are highlighted in dark grey, and controls are shown in light grey. For details about primer binding sites please see Figure 2. **(J, K)** Transgene expression based on primer binding to the *ocs* terminator region in 10 d-old OE seedlings **(J)** as described in (F to I) ( $n: 2$ ), and 6-d-old etiolated OE seedlings **(K)** that were treated with 1.06 % mannitol for 6 h ( $n: 3$ ). Data was normalized to mean *ocs* transcript level in *RS31a* OE #1\_13 and values represent means +SD (in K). Individual data points are shown as dots.



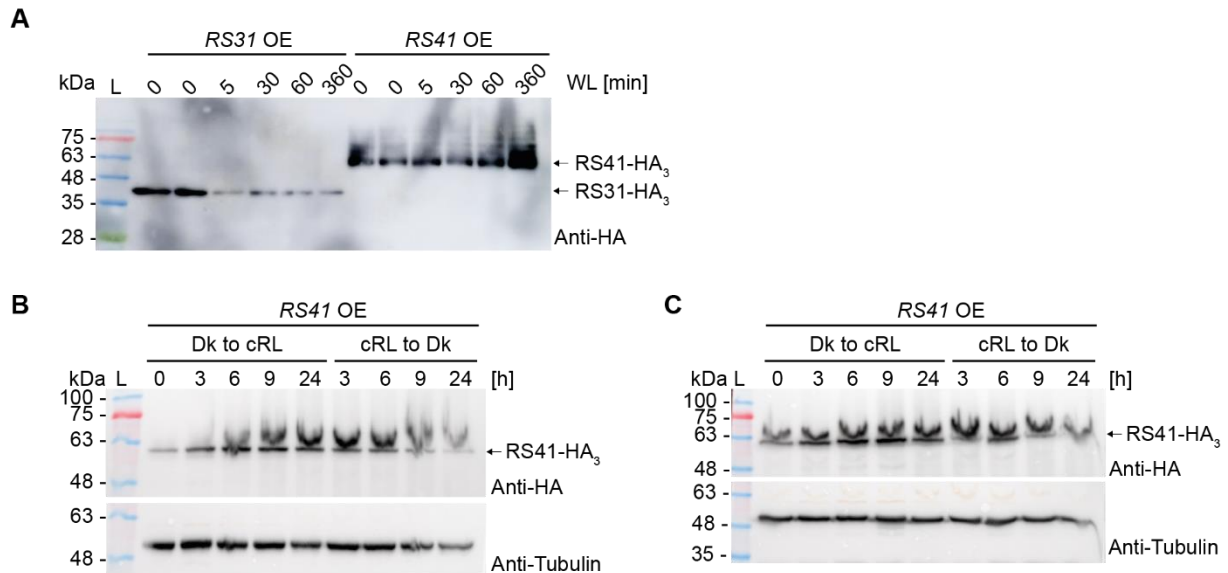
**Supplemental Figure 7: *RS31*, *RS40* and *RS41* OE plants are delayed in development.** Transgenic *RS* OE and EGFP plants, as well as WT, were grown under long day conditions over several weeks. **(A)** Close up picture of 28 d-old WT and *RS41* OE plants. Scale bar: 1 cm. **(B)** Representative photographs of 50 d-old *RS*OE plants that were used for phenotyping experiment. Scale bar: 5 cm. **(C)** Developmental stages were rated once per week and are defined as followed: 1: Rosette; 2: Bolting; 3: First opened flower; 4: No new buds; 5: (First) siliques. The size of each bubble is proportional to the percentage of analysed plants per genotype at the corresponding developmental stage and the depicted time point. *N*: 8 to 10 plants/*OE* line and *n*: 10/control line.



**Supplemental Figure 8: Light regulates transcript levels of *RS31* and *RS40*.** (A to D) Expression levels (cRPKMs) of *RS31* (A), *RS31a* (B), *RS40* (C), and *RS41* (D) in 6-d-old etiolated *Arabidopsis* WT seedlings that were illuminated with white light (WL;  $130 \mu\text{mol m}^{-2}\text{s}^{-1}$ ), red light (RL;  $14 \mu\text{mol m}^{-2}\text{s}^{-1}$ ) and blue light (BL;  $6 \mu\text{mol m}^{-2}\text{s}^{-1}$ ) for 6 h or kept in darkness (Dk), respectively. RNA-seq datasets derived from Hartmann et al. 2016 were analysed by the software *vast-tools* and accessed from *PastDB* (<http://pastdb.crg.eu>; Martín et al. 2020). Dark samples represent means +SD ( $n$ : 3). (E to H) Total transcript level of *RS31* (E), *RS31a* (F), *RS40* (G) and *RS41* (H) in 6-d-old etiolated WT seedlings that were either kept in darkness or exposed to WL ( $\sim 10 \mu\text{mol m}^{-2}\text{s}^{-1}$ ), RL ( $\sim 8 \mu\text{mol m}^{-2}\text{s}^{-1}$ ), far-red (FRL;  $\sim 6 \mu\text{mol m}^{-2}\text{s}^{-1}$ ) or BL ( $\sim 8 \mu\text{mol m}^{-2}\text{s}^{-1}$ ) for 6 h. Values are means ( $n$ : 3 to 5; individual data points are shown as dots) +SD, normalized to average WT level in dark.

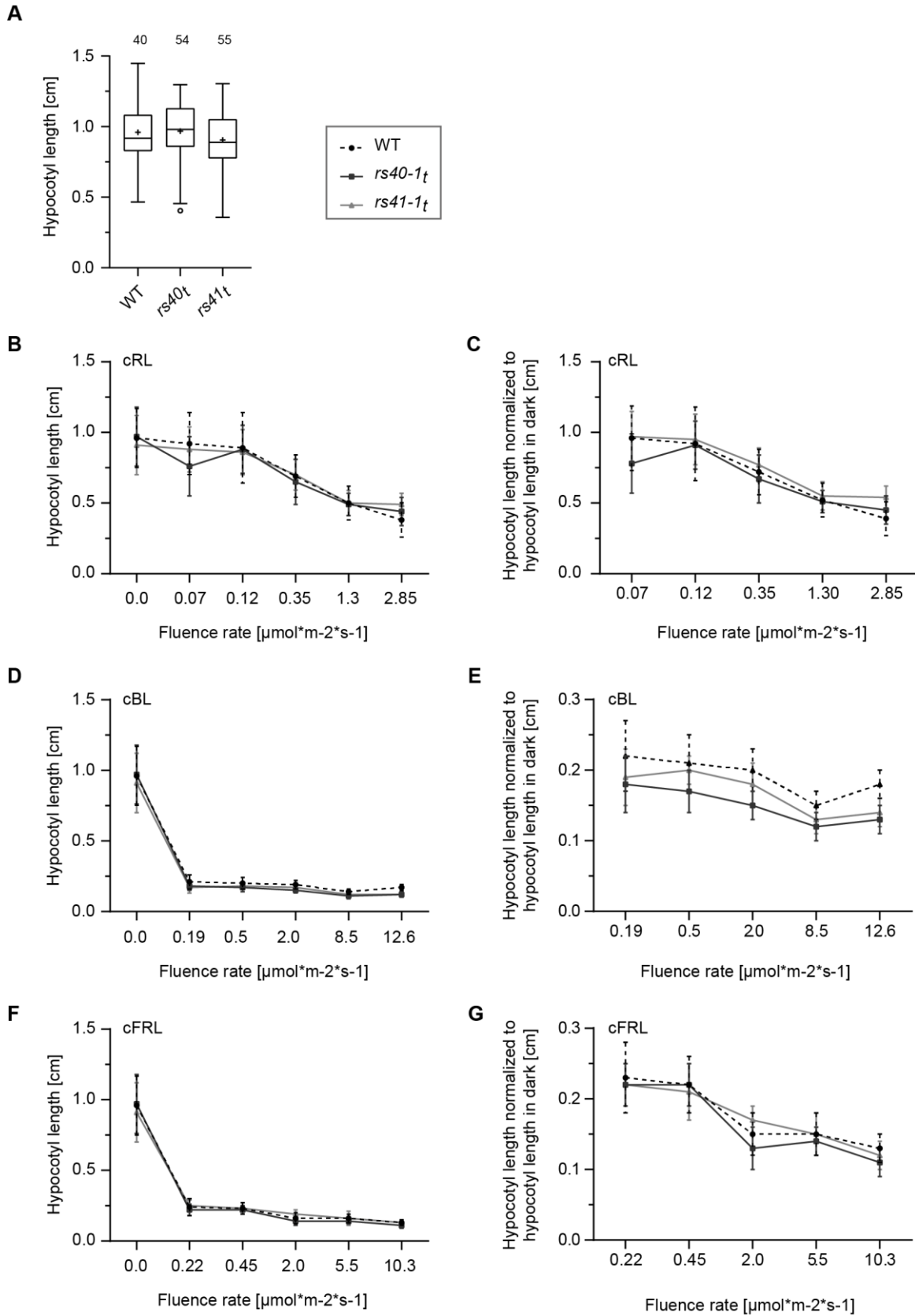


**Supplemental Figure 9: Light induces skipping of exon 2 in *RS31* pre-mRNA. (A)** *RS31* coverage plot from samples of 6-d-old etiolated WT seedlings, that were either kept in darkness (Dk) or transferred to white light (WL) for 6 h. RNA-seq data set derived from Hartmann et al. 2016. **(B)** Co-amplification PCR of endogenous *RS31* in 6-d-old etiolated WT seedlings that were kept in darkness (Dk) or treated with white light (WL), and exposed to 1.06% mannitol (Man) or 2% sucrose (Suc) for 6 h.



**Supplemental Figure 10: Light regulates RS31 and RS41 protein stability. (A)** Proteins were extracted using extraction buffer I from 6-d-old etiolated *RS31* and *RS41* OE seedlings that were transferred to white light ( $\sim 100 \mu\text{mol m}^{-2} \text{s}^{-1}$ ) for indicated time points. Same amount of protein was loaded, and 0 h time point samples represent replicates. Transgene-derived proteins were detected via HA antibody. L marks pre-stained protein ladder. **(B, C)** 6-d-old etiolated *RS41* OE seedlings were transferred to continuous red light (cRL;  $\sim 0.4$  (B) and  $8 \mu\text{mol m}^{-2} \text{s}^{-1}$  (C)). After 24 h of RL illumination, seedlings were moved back to darkness for the indicated time points. Proteins were extracted using extraction buffer II and RS41 tagged proteins were detected via anti-HA antibody. Tubulin served as loading control.



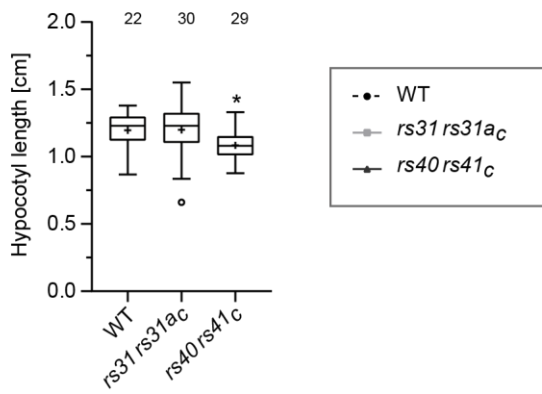


**Supplemental Figure 11: *rs40-1t* and *rs41-1t* single mutants are unaffected in hypocotyl growth.**

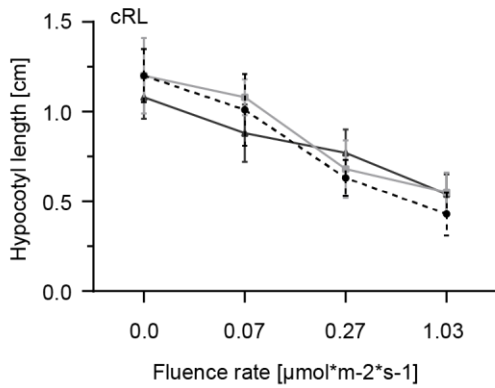
**(A)** Hypocotyl elongation in 4-d-old dark grown WT and *rs40* and *rs41* T-DNA single mutants. Interquartile range, maximum and minimum, median, and mean values are depicted as box, whiskers, middle line and plus, respectively. *n* is indicated above each genotype. **(B-G)** Hypocotyl growth in

response to different fluence rates of cRL (**B, C**) with  $n$ : 19 to 32, cBL (**D, E**) with  $n$ : 15 to 40, and cFRL (**F, G**) with  $n$ : 25 to 38 of 4-d-old seedlings. (**B, D, F**) show absolute hypocotyl lengths and (**C, E, G**) relative lengths that were normalized to the corresponding average length in darkness. Displayed are mean values  $\pm$ SD.

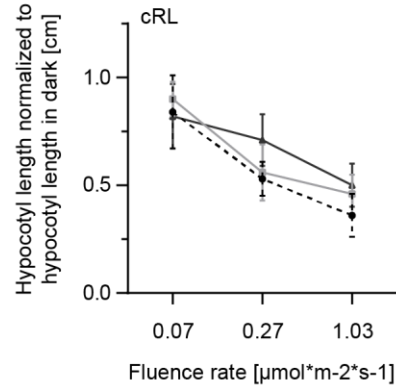
A



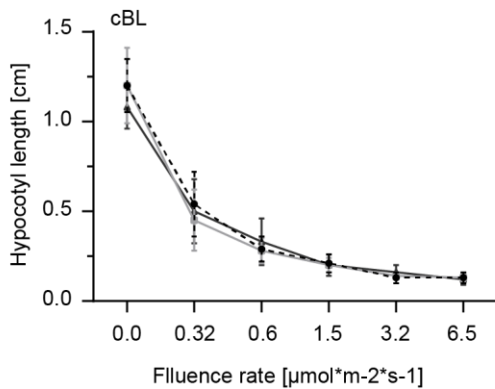
B



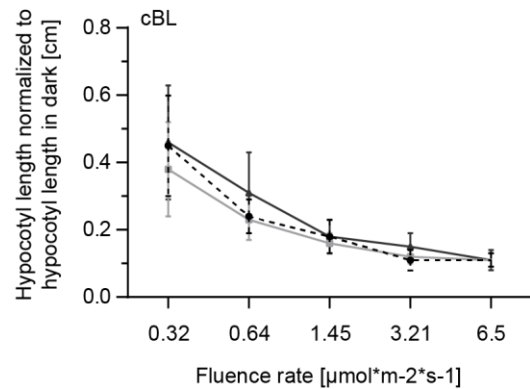
C



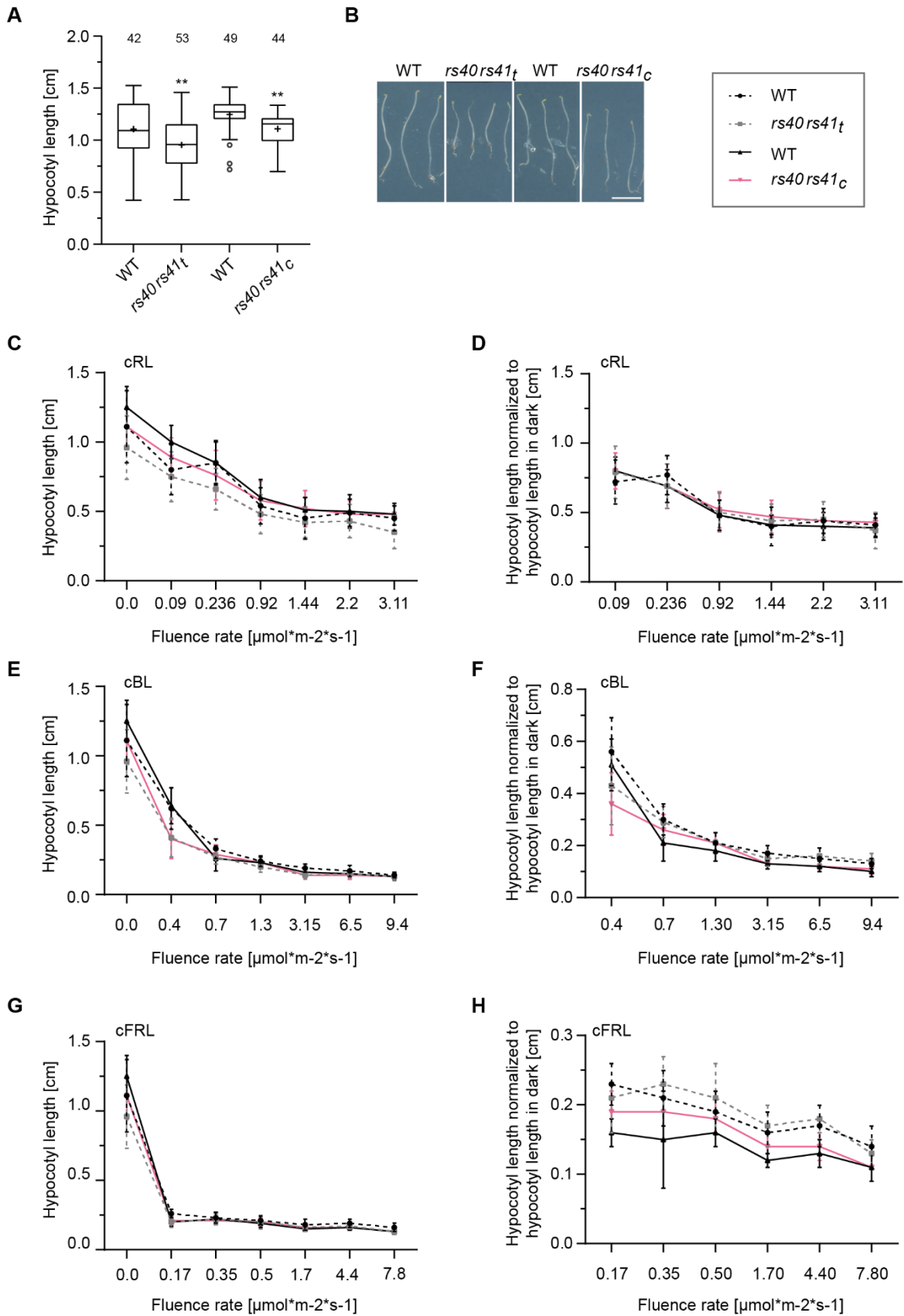
D



E

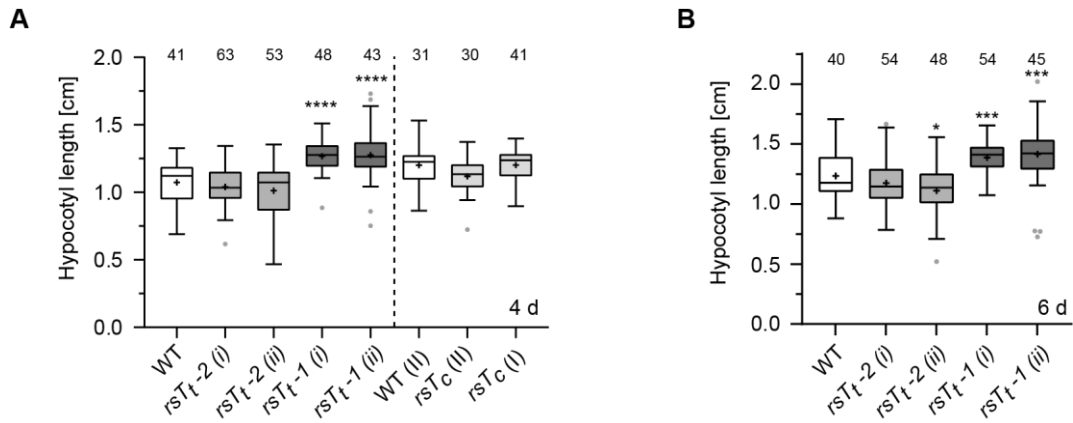


**Supplemental Figure 12: Hypocotyl elongation in CRISPR double mutants is unaffected in response to light.** (A) Hypocotyl elongation in 4-d-old etiolated WT and CRISPR double mutants. Interquartile range, maximum and minimum, median, and mean values are depicted as box, whiskers, middle line and plus, respectively.  $n$  is indicated above each genotype. (B-E) Hypocotyl growth in response to different fluence rates of cRL (B, C) ( $n$ : 23 to 34), cBL (D, E) ( $n$ : 26 to 41) of 4-d-old seedlings. (B, D, F) show absolute hypocotyl lengths and (C, E, G) relative lengths that were normalized to the corresponding average length in darkness. Displayed are mean values  $\pm$ SD.



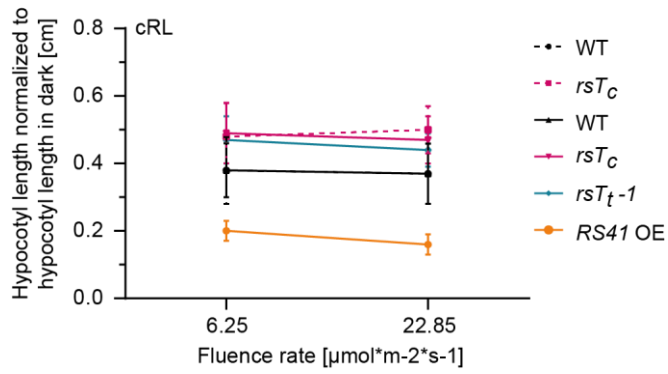
**Supplemental Figure 13: *rs40 rs41* double mutants display an unaffected hypocotyl elongation in response to light.** (A) Hypocotyl lengths of 4-d-old etiolated seedlings. Interquartile range, maximum and minimum, median, and mean values are depicted as box, whiskers, middle line and plus,

respectively. *n* is indicated above each genotype. Asterisks indicate significant difference compared to corresponding WT control based on one-way ANOVA with post hoc Tukey test (P values: \*P < 0.05; \*\*P < 0.01). **(B)** Representative photographs of seedlings described in (A). Scale bar: 5 mm. **(C-H)** Hypocotyl length in response to different fluence rates of cRL **(C, D)** (*n*: 15 to 38), cBL **(E to F)** (*n*: 18 to 37) and cFRL **(G to H)** (*n*: 16 to 37) in 4-d-old seedlings. **(C, E, G)** show absolute hypocotyl length, whereas **(D, F, H)** display relative lengths that were normalized to corresponding mean length in darkness. Depicted are mean values  $\pm$ SD. Genotypes with a dashed lines are part of one set (T-DNA set) and genotypes with solid lines are part of another set (CRISPR set).

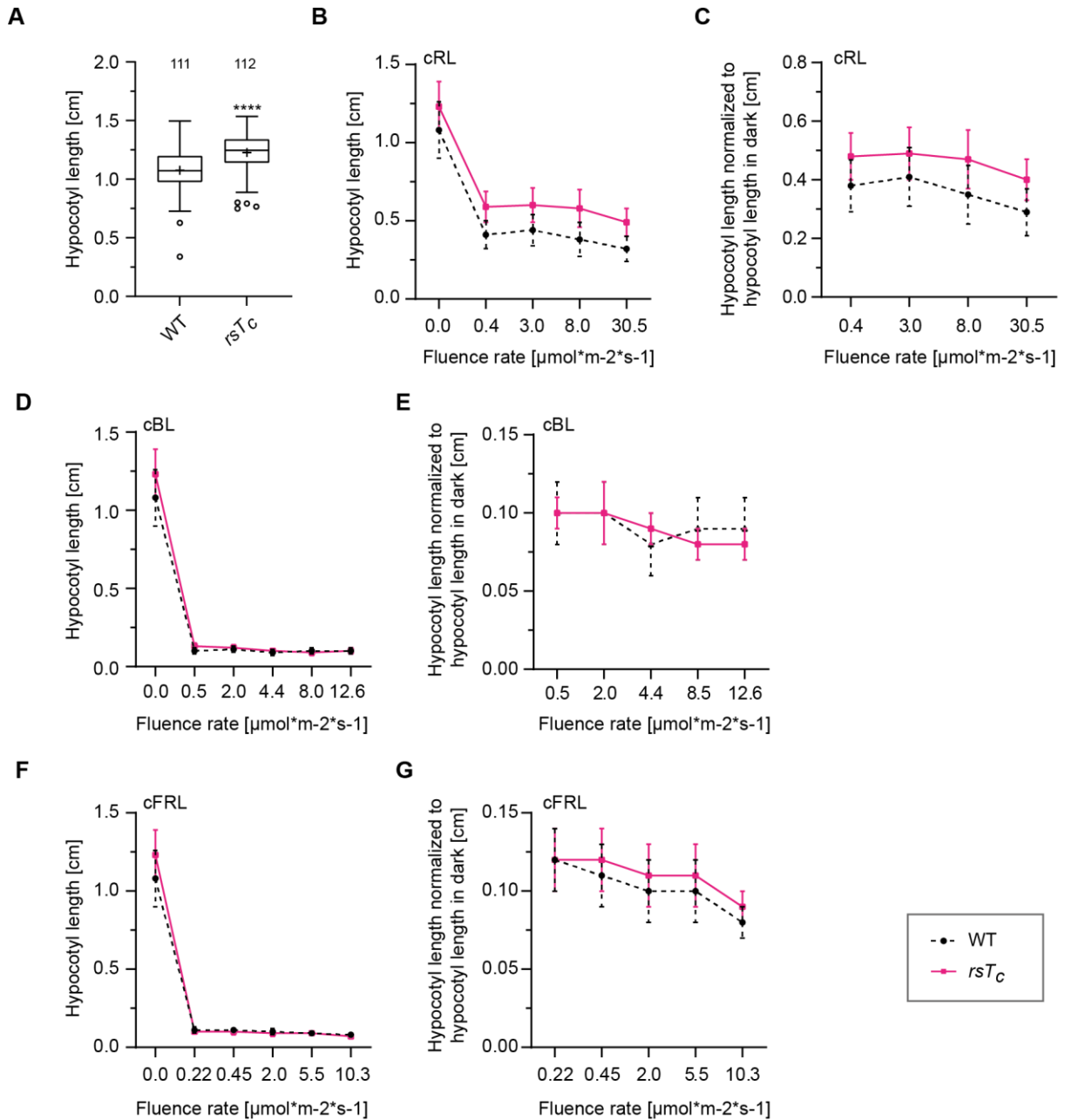


**Supplemental Figure 14: T-DNA triple mutant exhibits elongated hypocotyl in darkness.**

Hypocotyl length in WT and different *rsT<sub>t</sub>* and *rsT<sub>c</sub>* mutants. (i) and (ii) represent the progenies from independent crossings, whereas (I) and (II) refer to different generations. Seedlings were grown for 4 d **(A)** and 6 d **(B)** in darkness. Corresponding *n* is indicated above each line. Data from *rsT<sub>c</sub>* is also described and depicted in Supplemental Figure 17. Middle line of the box plot shows median, the plus indicates the mean. Interquartile range and maximum and minimum are displayed as the bounds of the box and whiskers, respectively. Outliers are shown as grey dots. A one-way ANOVA with Dunnett's multiple comparison test was performed (P values: \*P < 0.05, \*\*P < 0.01, \*\*\*P < 0.001, \*\*\*\*P < 0.0001).

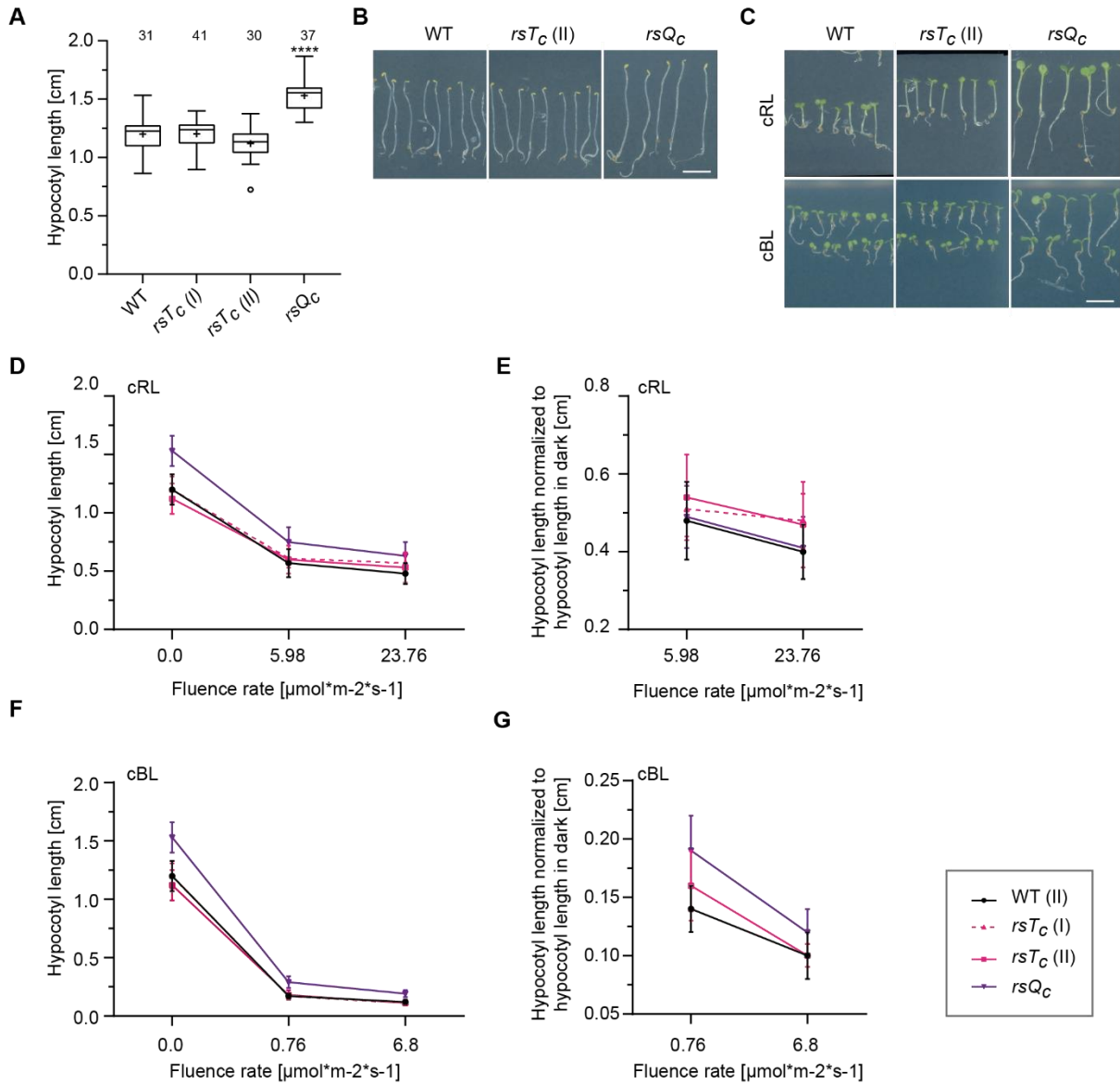


**Supplemental Figure 15: *rs* triple mutants are hyposensitive to red light.** Relative hypocotyl length of seedlings described and depicted in Figure 3B, C. Hypocotyl length was normalized to hypocotyl length in darkness. Displayed are mean values  $\pm$ SD ( $n$ : 27 to 39). The dashed WT overlaps with the other WT and is therefore not visible.

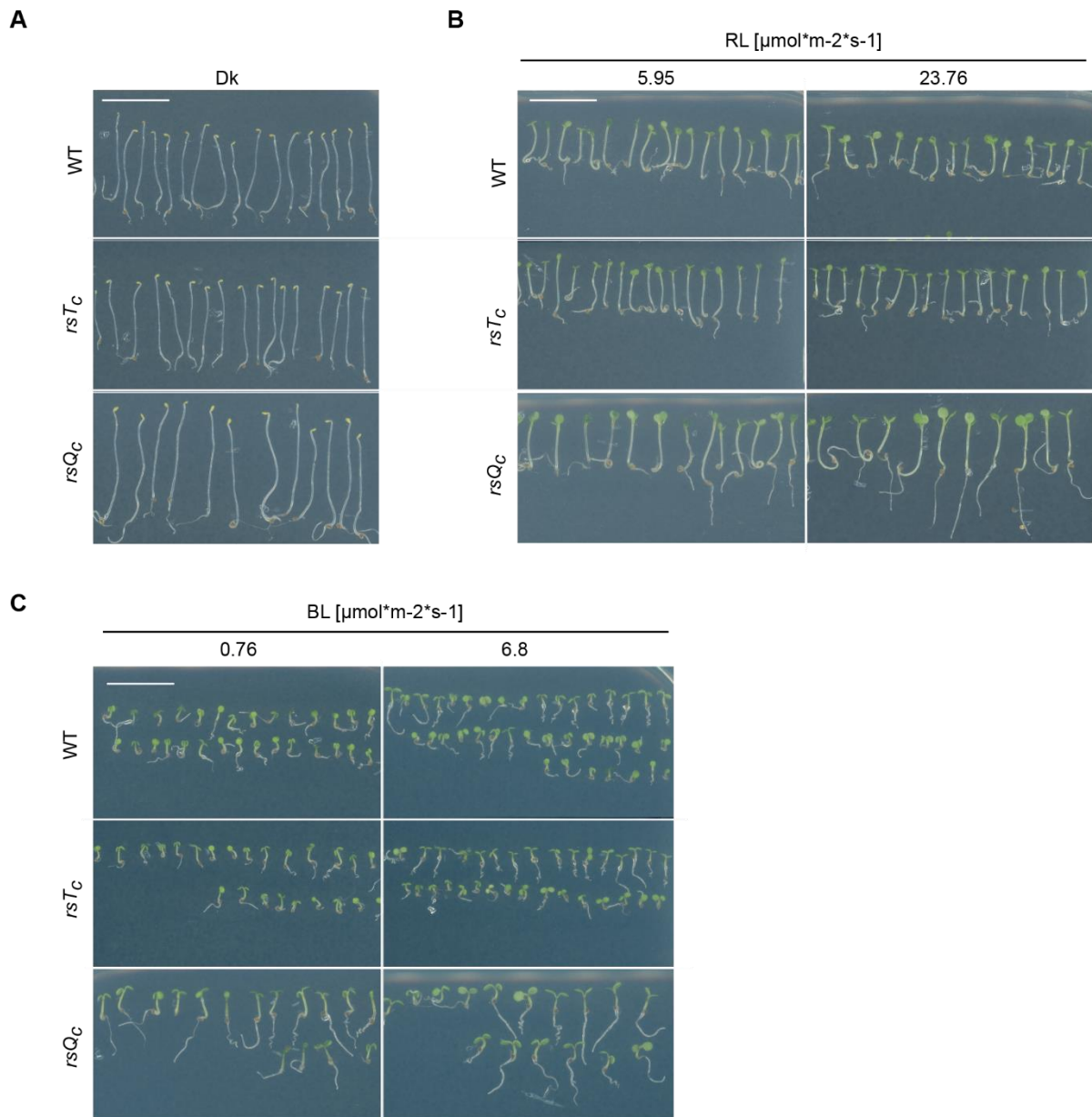


**Supplemental Figure 16: *rsT<sub>c</sub>* mutant shows a reduced red and far-red light sensitivity. (A)** Hypocotyl elongation in 4-d-old dark grown WT and *rsT<sub>c</sub>*. Middle line of the box plot shows median, the plus indicates the mean. Interquartile range and maximum and minimum are displayed as the bounds of the box and whiskers, respectively. Outliers are shown as dots. Asterisks indicate significant difference compared to WT control based on one-way ANOVA with post hoc Tukey test (P values: \*P < 0.05; \*\*P < 0.01, \*\*\*P < 0.001, \*\*\*\*P < 0.0001). *n* is indicated above each genotype. **(B to G)** Hypocotyl growth in response to different fluence rates of cRL **(B, C)** (*n*: 51-119), cBL **(D, E)** (*n*: 51 to 106) and cFRL **(F, G)** (*n*: 41 to 61) of 4-d-old seedlings. **(B, D, F)** show absolute hypocotyl lengths and **(C, E, G)** relative lengths that were normalized to the corresponding average length in darkness. Displayed are mean values  $\pm$ SD.

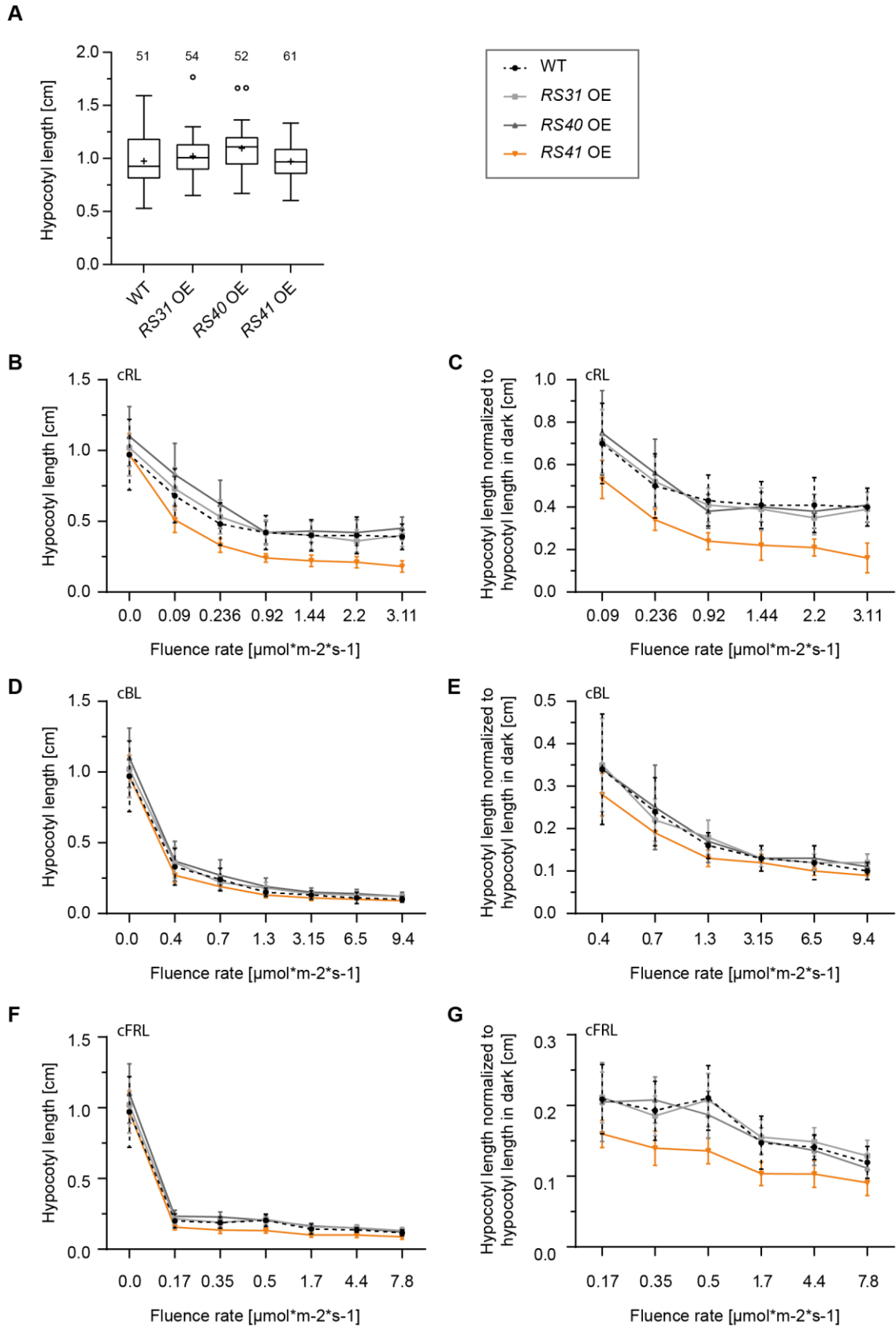




**Supplemental Figure 17: *rsQ<sub>C</sub>* mutants exhibit increased growth in darkness, red and blue light.** **(A)** Hypocotyl length of 4-d-old etiolated seedlings. I or II refers to different generations that were included as control. Middle line of the box plot shows median, the plus indicates the mean. Interquartile range and maximum and minimum are displayed as the bounds of the box and whiskers, respectively. Asterisks indicate significant difference compared to corresponding WT control based on one-way ANOVA with post hoc Tukey test (P values: \*P < 0.05; \*\*P < 0.01, \*\*\*P < 0.001, \*\*\*\*P < 0.0001). n: 30 to 41. **(B)** Representative pictures of etiolated seedlings described in (A). Scale bar: 5 mm. **(C)** Representative photographs of 4-d-old seedlings grown under continuous red light (cRL; 23.76  $\mu\text{mol m}^{-2} \text{s}^{-1}$ ) and continuous blue light (BL; 6.8  $\mu\text{mol m}^{-2} \text{s}^{-1}$ ), respectively. Scale bar: 5 mm. **(D-G)** Hypocotyl length in response to different fluence rates of cRL **(D, E)** (n: 23 to 37), cBL **(F to G)** (n: 26 to 43) 4-d-old seedlings. **(D, F)** show absolute hypocotyl length, **(E, G)** display relative lengths that were normalized to corresponding mean length in darkness. Depicted are mean values  $\pm$ SD.



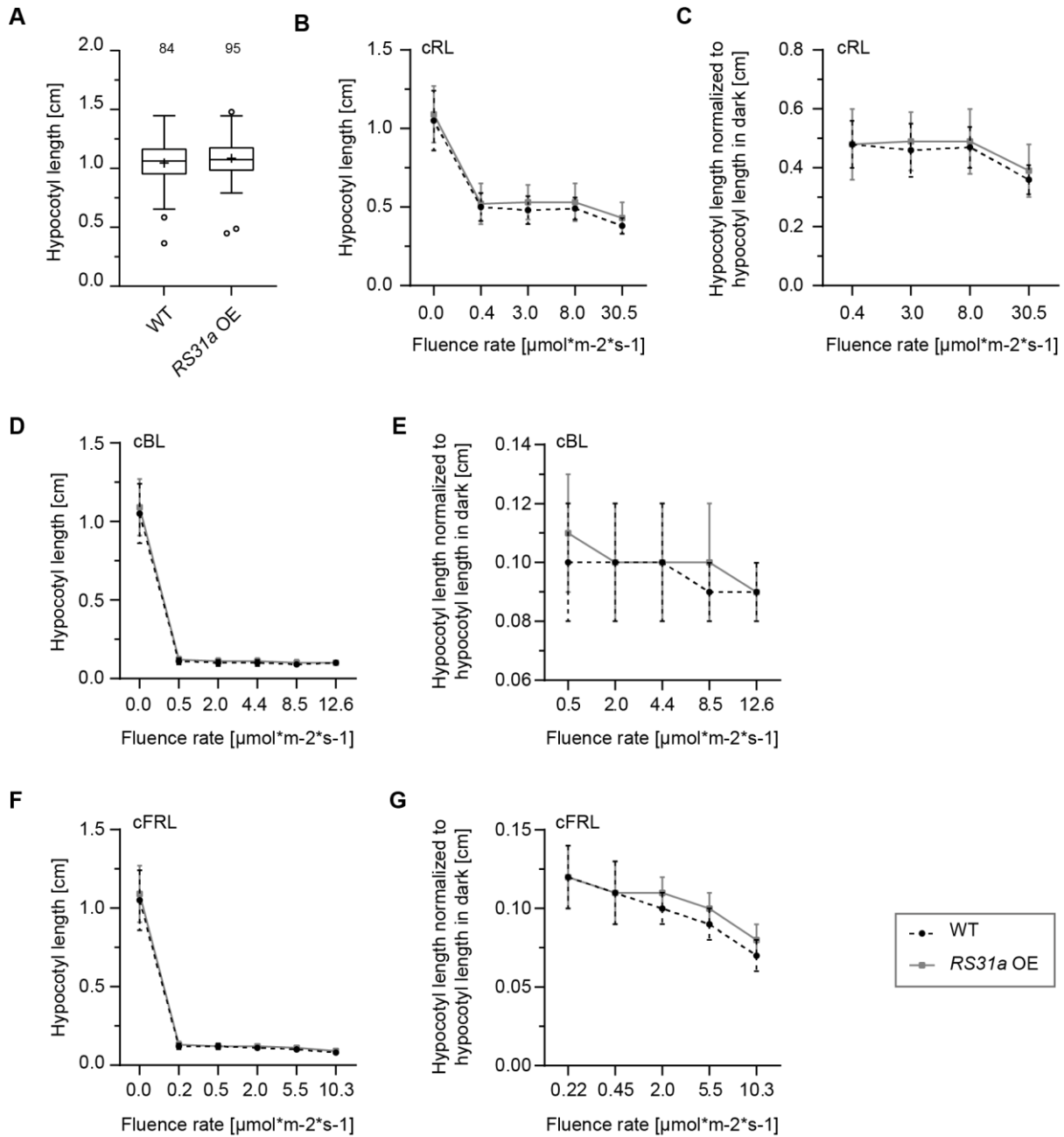
**Supplemental Figure 18: Phenotypes of *rsT<sub>c</sub>* and *rsQ<sub>c</sub>* seedlings.** WT and CRISPR mutants were grown for 4 d in darkness (**A**), continuous red light (**B**) and continuous blue light (**C**), respectively. Scale bar: 1 cm. For details about corresponding hypocotyl lengths, please see Supplemental Figure 17.



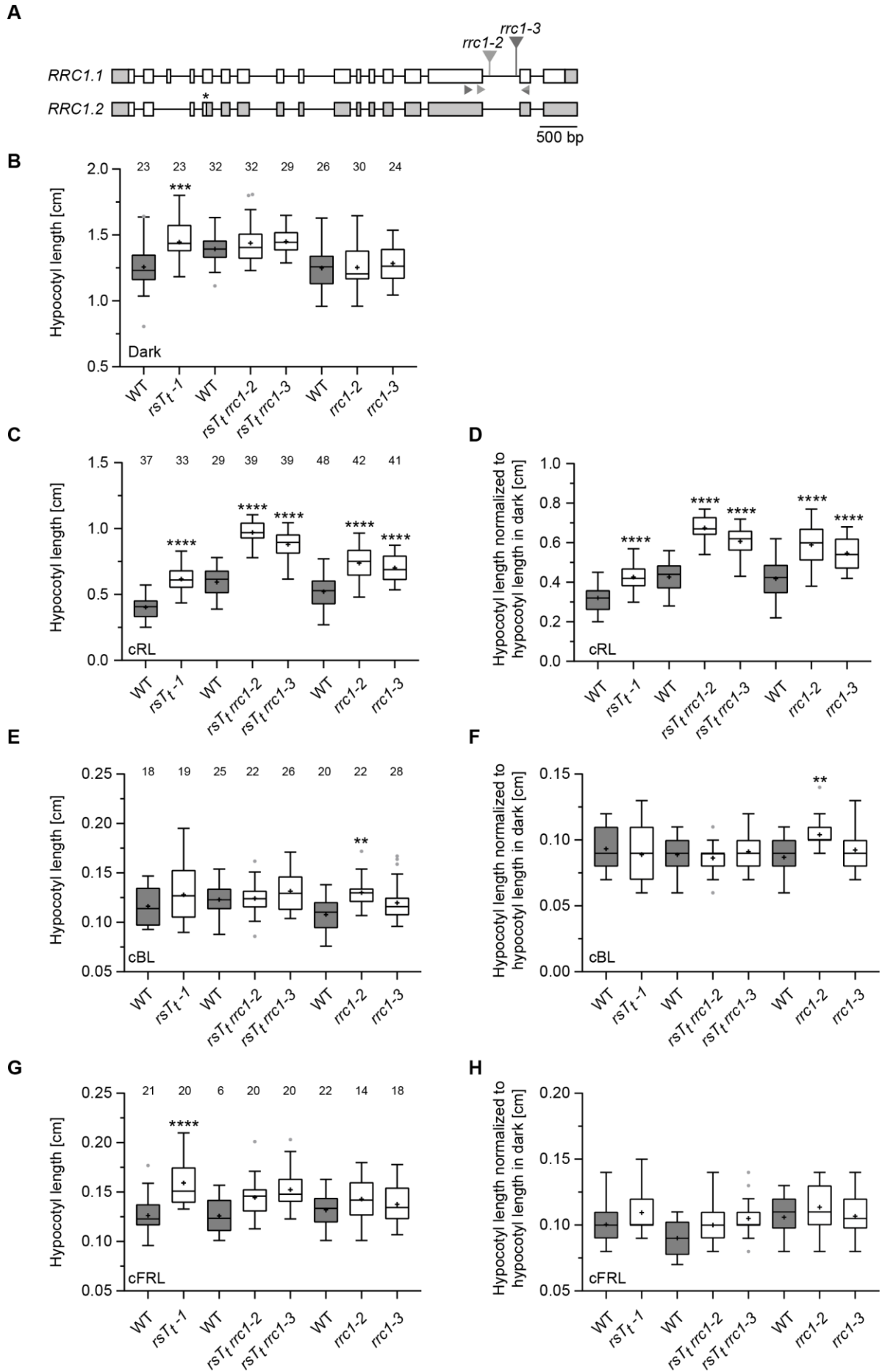
**Supplemental Figure 19: Hypocotyl growth response in *RS31*, *RS40* and *RS41* OE seedlings. (A)**

Hypocotyl elongation in 4-d-old dark grown WT and RS OE seedlings. Middle line of the box plot shows median, the plus indicates the mean. Interquartile range and maximum and minimum are displayed as the bounds of the box and whiskers, respectively. Outliers are shown as dots. *N* is indicated above each

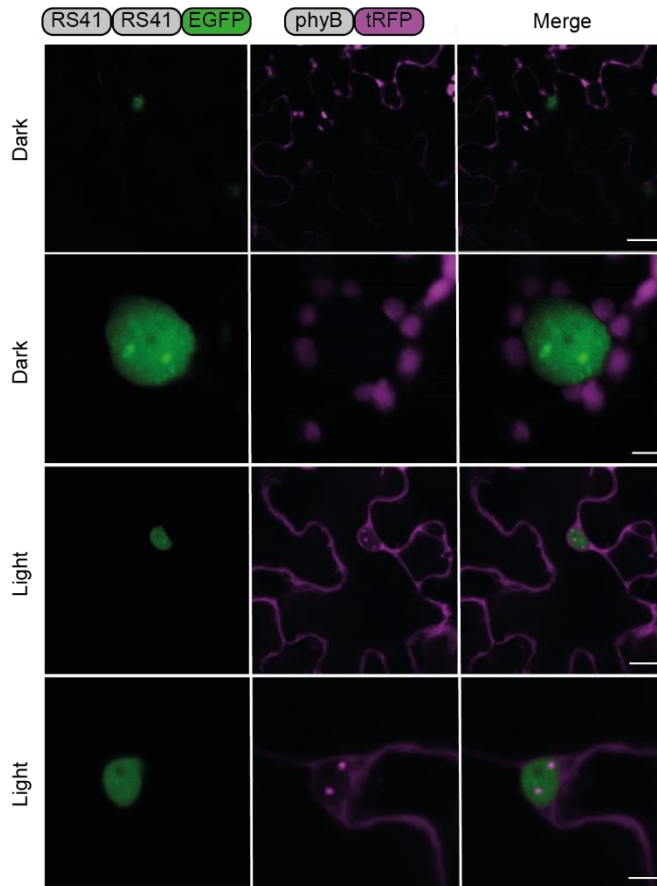
genotype. **(B-G)** Hypocotyl growth in response to different intensities of cRL **(B, C)** (*n*: 23 to 36), cBL **(D, E)** (*n*: 26 to 40) and cFRL **(F, G)** (*n*: 23 to 36) of 4-d-old seedlings. **(B, D, F)** show absolute hypocotyl lengths and **(C, E, G)** relative lengths that were normalized to the corresponding average length in darkness. Displayed are mean values  $\pm$ SD.



**Supplemental Figure 20: Hypocotyl growth response in *RS31a* OE seedlings:** **(A)** Hypocotyl elongation in 4-d-old dark grown WT and *RS31a* OE seedlings. Middle line of the box plot shows median, the plus indicates the mean. Interquartile range and maximum and minimum are displayed as the bounds of the box and whiskers, respectively. Outliers are shown as dots. *N* is indicated above each genotype. **(B-G)** Hypocotyl growth in response to different intensities of cRL **(B, C)** (*n*: 42 to 95), cBL **(D, E)** (*n*: 38 to 114) and cFRL **(F, G)** (*n*: 22 to 50) of 4-d-old seedlings. **(B, D, F)** show absolute hypocotyl lengths and **(C, E, G)** relative lengths that were normalized to the corresponding average length in darkness.

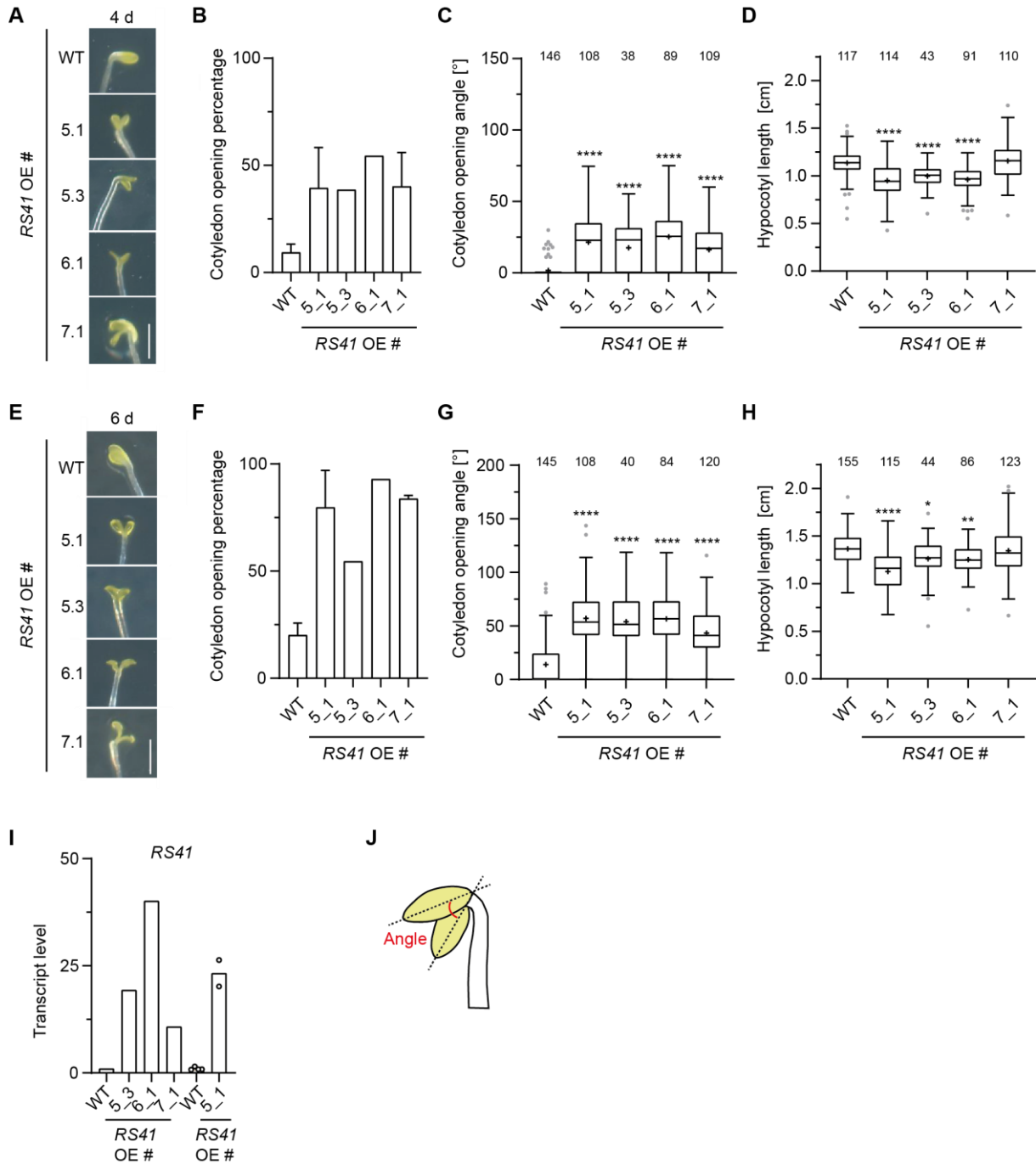


**Supplemental Figure 21: *rs* and *rrc1* mutants exhibit reduced red light sensitivity.** **(A)** Transcript models of major *RRC1* splicing variants. Boxes represent exons, lines introns. UTRs are marked in grey. Triangles indicate T-DNA insertion sites and arrowheads show primer binding sites that were used for genotyping. The asterisk displays a premature termination codon (PTC). Drawn to scale. **(B to H)** Quantification of hypocotyl length of 4-d-old seedlings, that were grown in darkness **(B)**, continuous red light (cRL) at  $11.88 \mu\text{mol m}^{-2} \text{s}^{-1}$  **(C, D)**, continuous blue light (cBL) at  $13.2 \mu\text{mol m}^{-2} \text{s}^{-1}$  **(E, F)** or continuous far red light (cFRL) at  $8.69 \mu\text{mol m}^{-2} \text{s}^{-1}$  **(G, H)**. **(C, E, G)** show absolute hypocotyl lengths and **(D, F, H)** relative lengths that were normalized to the corresponding average length in darkness. Interquartile range, maximum and minimum, median, and mean values are depicted as box, whiskers, middle line and plus, respectively. *n* is indicated above each genotype. Asterisks indicate significant difference compared to corresponding WT control based on one-way ANOVA with post hoc Tukey test (P values: \*P < 0.05, \*\*P < 0.01, \*\*\*P < 0.001, \*\*\*\*P < 0.0001).



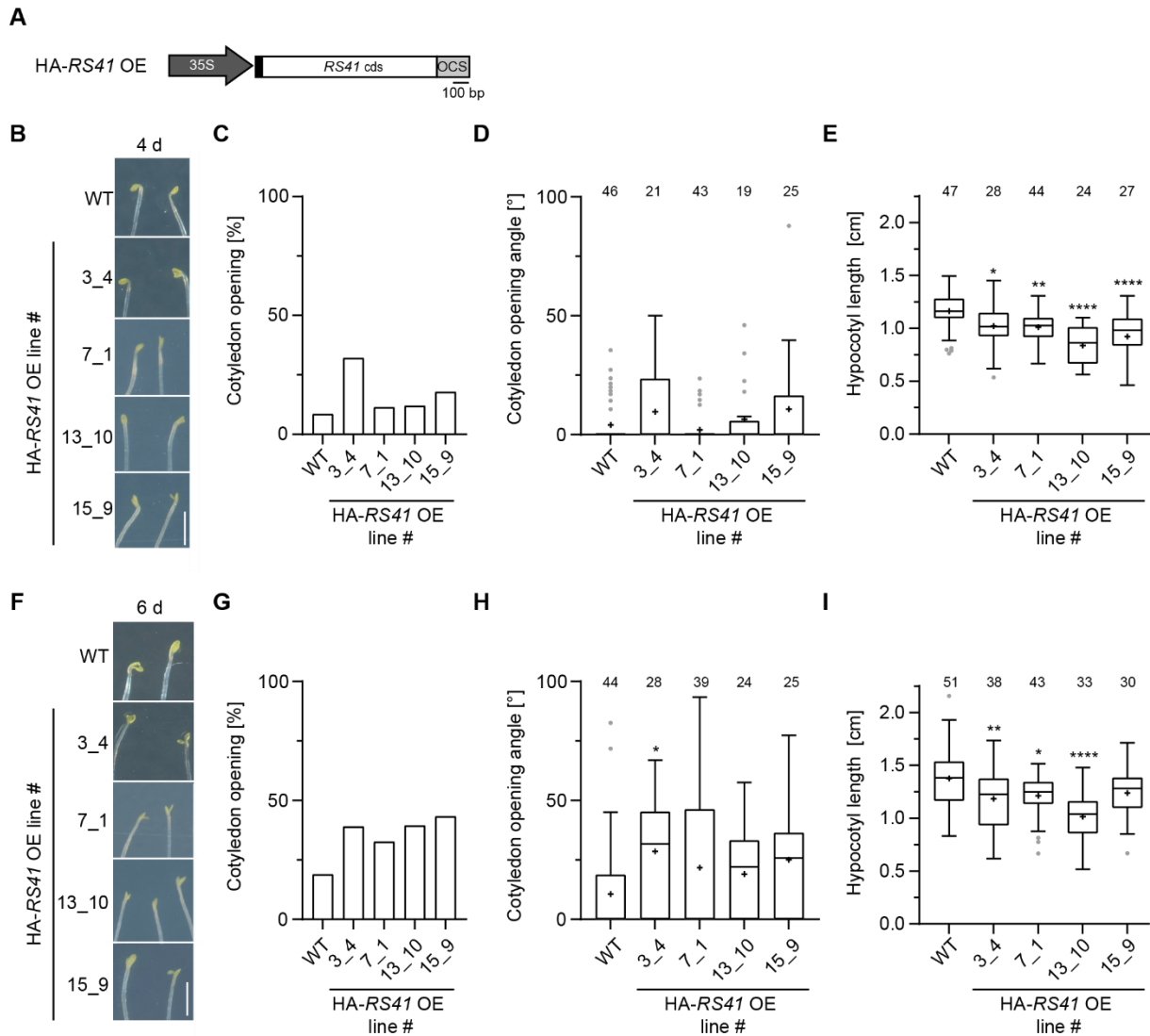
**Supplemental Figure 22: RS41 does not co-localize with phyB in *N. benthamiana*.** RS41-RS41-EGFP was co-expressed with phyB-tRFP in *N. benthamiana*. After infiltration, plants were either transferred to darkness (upper panels) or kept in white light (lower panels). Subcellular localization was analysed at 3 dpi using confocal microscopy. Autofluorescence of chloroplasts is visible in phyB-tRFP channel under dark conditions. Scale bar in first and third row picture shows 20 μm, and in second and fourth row picture it represents 10 μm.



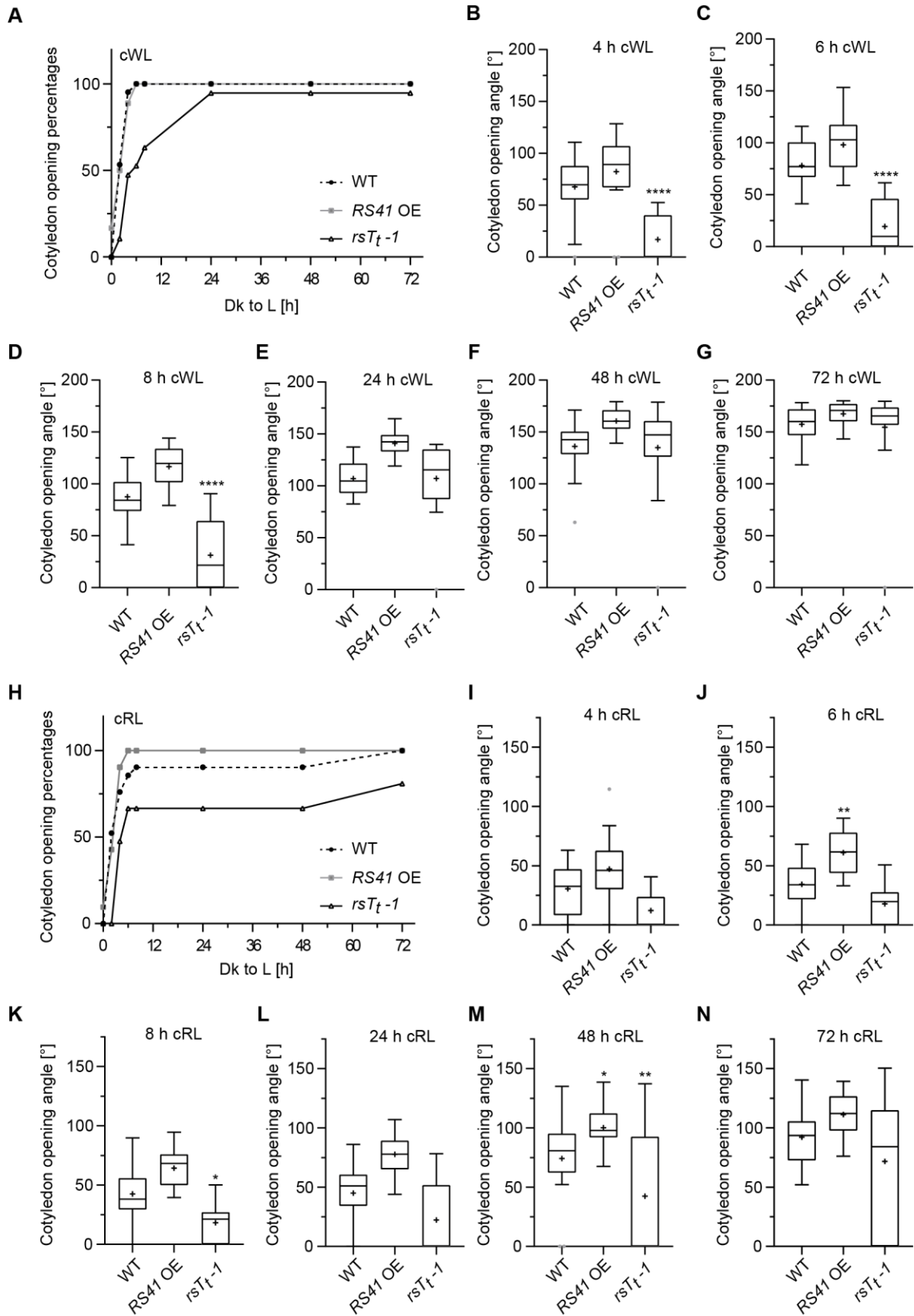


**Supplemental Figure 23: *RS41-HA<sub>3</sub>* overexpression promotes cotyledon opening in darkness.**

Phenotypes and growth characteristics including cotyledon opening percentage, cotyledon opening angle and hypocotyl length of **(A to D)** 4 d, **(E to H)** 6-d-old dark grown WT and *RS41-HA<sub>3</sub>* OE seedlings. Asterisks show significant differences to WT based a one-way ANOVA with post hoc Tukey test (P values: \*P < 0.05, \*\*P < 0.01, \*\*\*P < 0.001, \*\*\*\*P < 0.0001). **(A, E)** Representative photographs show cotyledons of dark grown WT and *RS41* OE seedlings. Scale bar: 1 mm. **(B, F)** Cotyledon opening percentages display mean values +SD, from 1 to 3 independent experiments ((B) *n*: 33 to 89 per experiment; (F) *n*: 33 to 87 per experiment). **(I)** *RS41* transcript level in 6-d-old dark grown *RS41-HA<sub>3</sub>* OE sublines. Displayed are mean values, dots show individual data points (*n*: 1 to 4). Transcript level was normalized to corresponding WT. **(J)** Schematic visualization of cotyledon opening angle measurement in an etiolated *Arabidopsis* seedling.

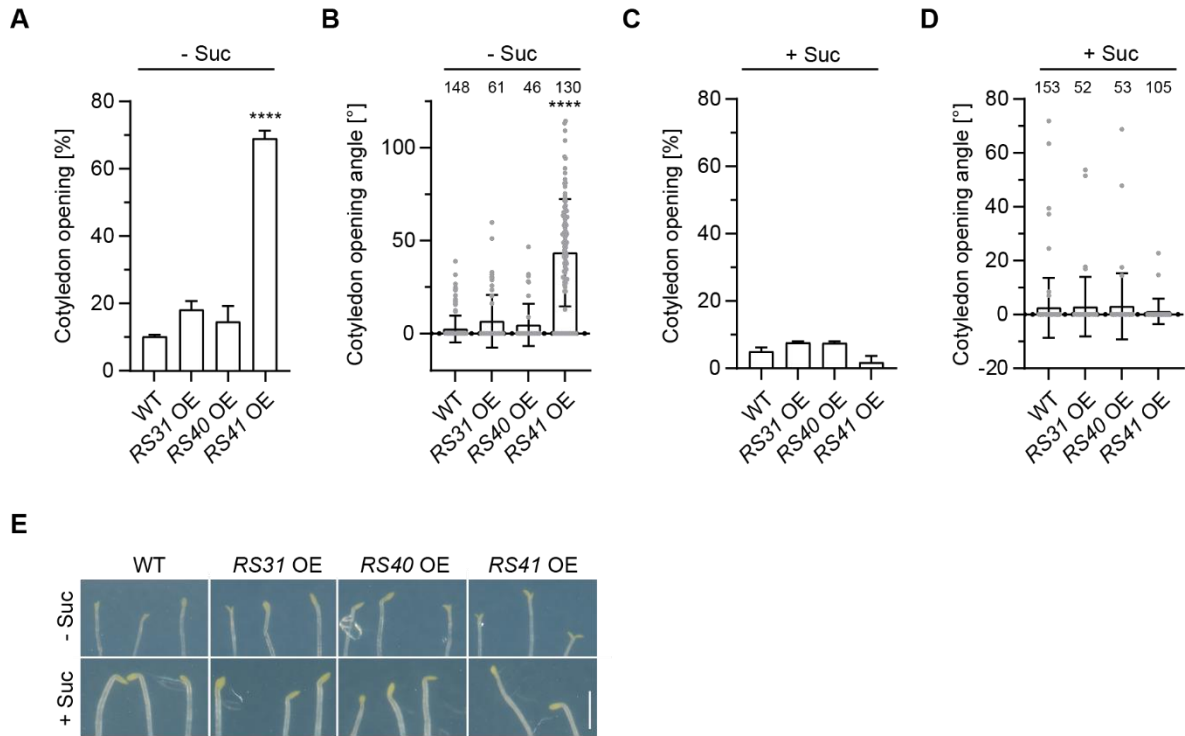


**Supplemental Figure 24: HA-RS41 OE seedlings do not display a distinct cotyledon opening phenotype in darkness. (A)** Schematic overview of HA-RS41 construct. The coding sequence (cds) of *RS41* is under control of the 35S promoter and the octopine synthase (OCS). Black box represents the sequence for the single HA-tag. Drawn to scale. Phenotypes and growth characteristics including cotyledon opening percentages, angle, and hypocotyl length of 4 d (**B to E**), 6 d (**F to I**) old dark grown WT and HA-RS41 OE seedlings. Middle line of the box plot shows median, the plus indicates the mean. Interquartile range and maximum and minimum are displayed as the bounds of the box and whiskers, respectively. Outliers are shown as grey dots. Asterisks show significant differences to WT based on one-way ANOVA with post hoc Tukey test (P values: \* $P < 0.05$ , \*\* $P < 0.01$ , \*\*\* $P < 0.001$ , \*\*\*\* $P < 0.0001$ ).  $n$  is indicated above each genotype ( $n$ : 19 to 51). (**B, F**) Representative photographs show cotyledons of etiolated WT and HA-RS41 OE seedlings. Scale bar: 2 mm.



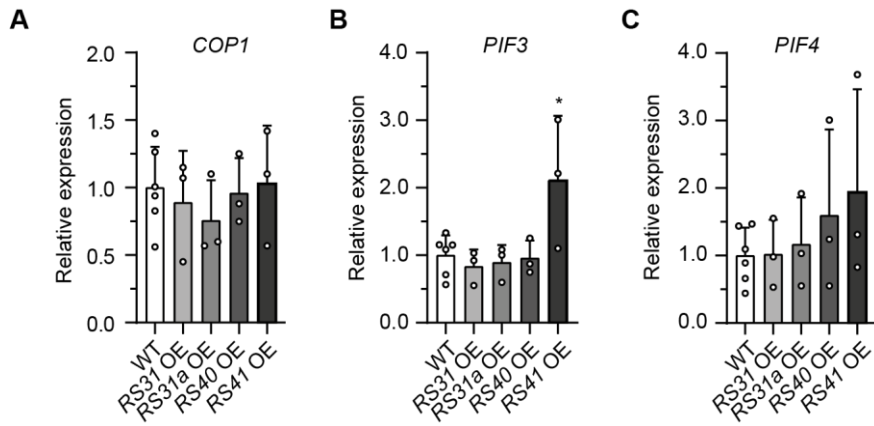
**Supplemental Figure 25: RS proteins contribute to light-induced cotyledon opening.** Seedlings were grown for 4 d in darkness and subsequently transferred to continuous white light (cWL at  $10.6 \mu\text{mol m}^{-2} \text{s}^{-1}$ ) (**A to G**) and red light (cRL at  $8.4 \mu\text{mol m}^{-2} \text{s}^{-1}$ ) (**H to N**) for different time points. For each

time point, cotyledon opening percentages were analysed in 18 to 22 seedlings per line (**A, H**), and cotyledon opening angle measurements was performed with 15 to 21 seedlings per line (**B to G, I to N**). Middle line of the box plot shows median, the plus indicates the mean. Interquartile range and maximum and minimum are displayed as the bounds of the box and whiskers, respectively. Asterisks show significant difference compared to the WT control, based on one-way ANOVA with post hoc Tukey test (P values: \*P < 0.05, \*\*P < 0.01, \*\*\*P < 0.001, \*\*\*\*P < 0.0001).



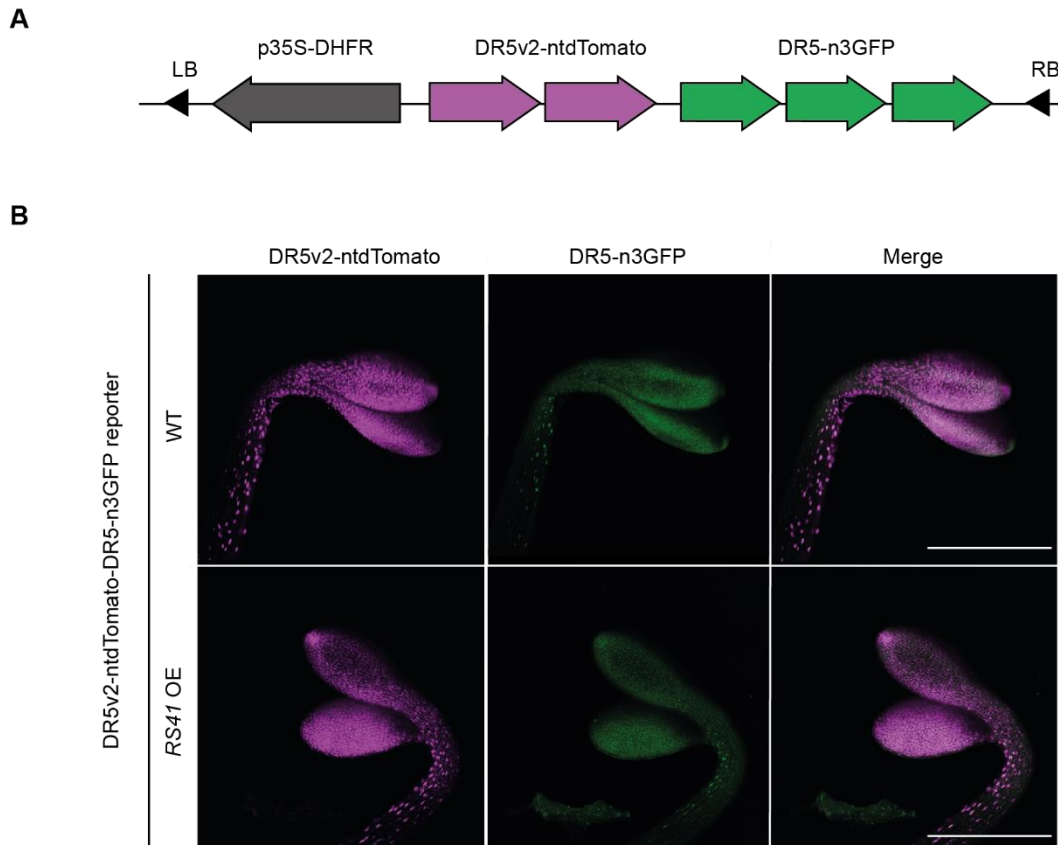
**Supplemental Figure 26: Sucrose does not induce cotyledon opening in dark grown seedlings.**

Percentage of opened cotyledons and corresponding cotyledon angles in 6-d-old etiolated seedlings. Seedlings were grown horizontally in the absence (**A, B**) or presence (**C, D**) of 2% sucrose. (**A, C**) Cotyledon opening percentages display mean values  $\pm$ SEM from 2 to 4 experiments ( $n$ : 20 to 48 seedlings per experiment). (**B, D**) Scatter plots show mean value  $\pm$ SD, and dots display individual data points. (**E**) Representative photographs of etiolated seedlings described in (A to D). Scale bar: 2 mm. Asterisks indicate significant differences compared to WT based on one-way ANOVA with post hoc Tukey test (P value: \*\*\*\* $P < 0.0001$ ).

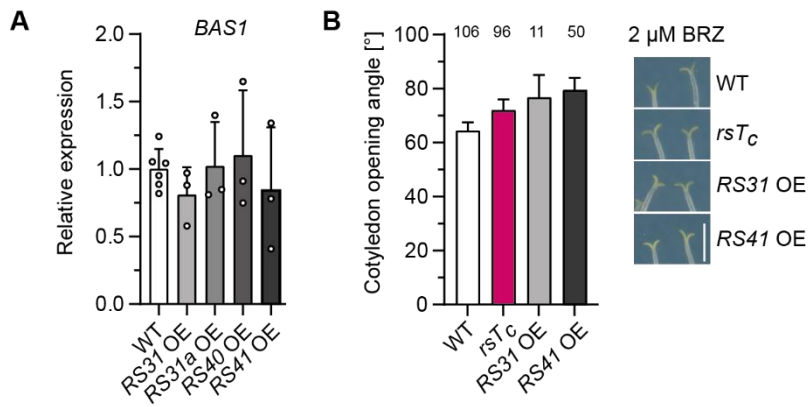


**Supplemental Figure 27: *COP1*, and *PIF4* transcript levels are unaffected in *RS* OE seedlings:**

Relative expression level of *COP1* (A), *PIF3* (B) and *PIF4* (C) in 6-d-old etiolated WT and *RS* OE seedlings. Displayed are mean values +SD, single dots show individual data points ( $n$ : 3 to 6). Data were normalized to average WT level ( $n$ : 6). Statistical comparison of *RS* OE with WT was performed using an unpaired  $t$  test (P: \*P < 0.05).

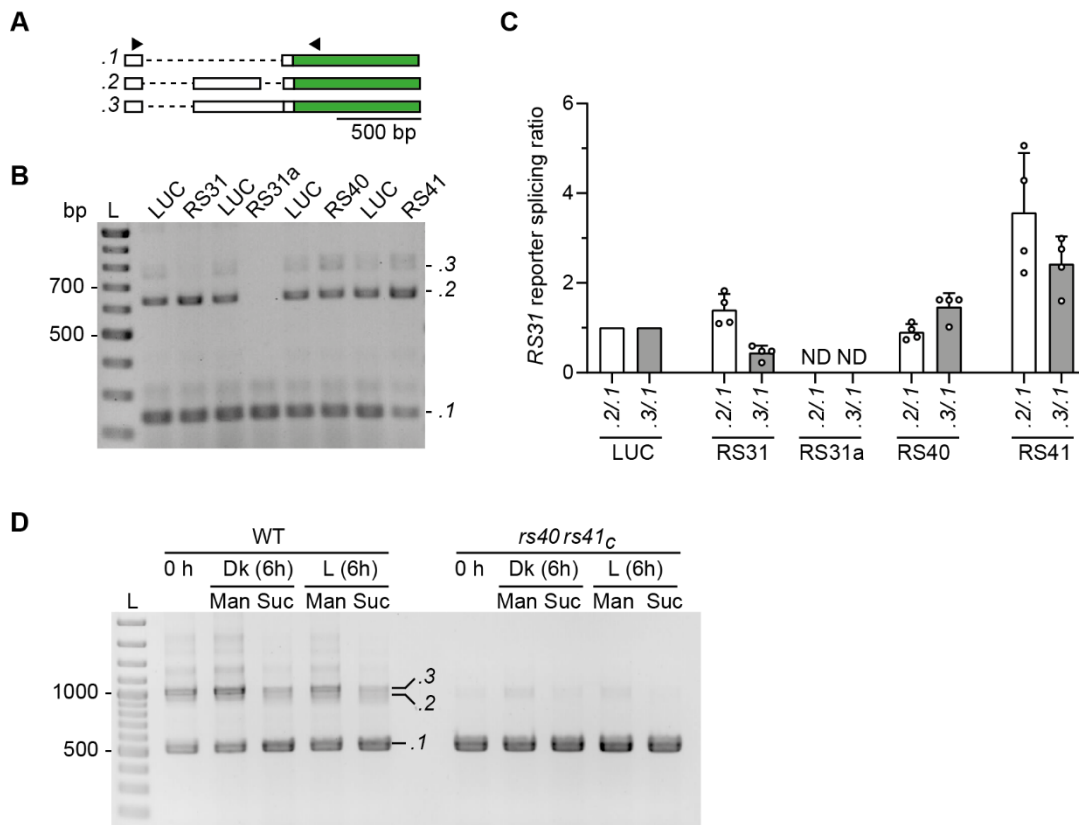


**Supplemental Figure 28: Auxin distribution seems to be unaffected in cotyledons of etiolated *RS41* OE seedlings. (A)** Schematic overview of the auxin double reporter DR5v2-ntdTomato-DR5-n3GFP. DR5 binding sequences are upstream of either nuclear tandem Tomato (ntdTomato) or nuclear 3xEGFP (n3GFP). The construct carries a methotrexate resistance gene (DHFR) that is under the control of the 35S promoter. Furthermore, the construct is flanked by a left and right border (LB, RB). The model was modified from Liao et al. 2015. **(B)** Auxin signalling was monitored in cotyledons of 4-d-old etiolated *Arabidopsis* seedlings expressing the double reporter in either the WT or *RS41* OE background. Depicted are images from z stacks (21 images) with 1  $\mu$ m intervals. Brightness and contrast of GFP channel pictures were adjusted using photoshop. Scale bar: 500  $\mu$ m.

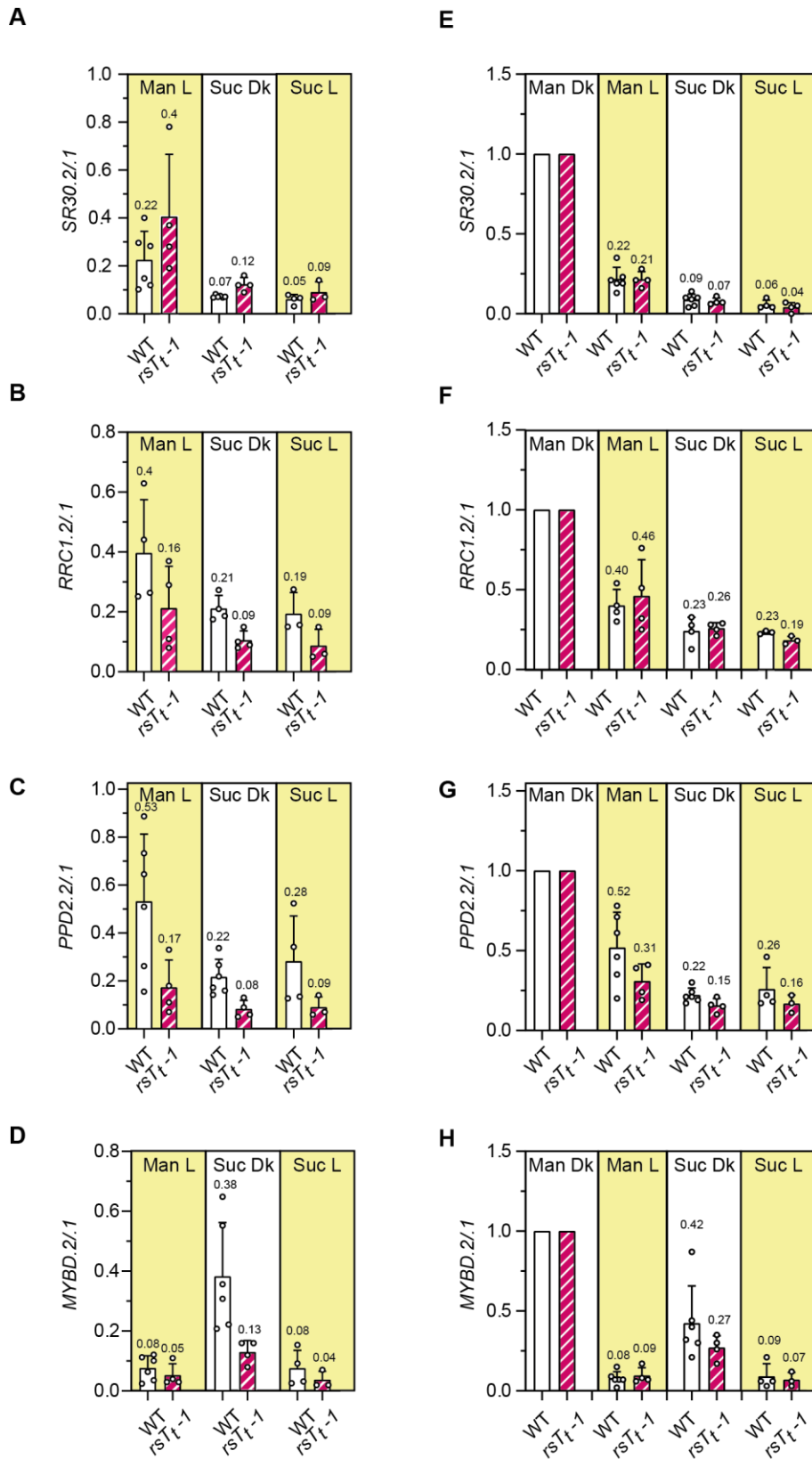


**Supplemental Figure 29: BRZ induces cotyledon opening in darkness: (A)** Relative expression of the BR induced gene *BAS1*. Expression was analysed in 6-d-old dark grown seedlings. Bars represent means +SD, normalized to WT ( $n$ : 3 to 6). **(B, left)** Cotyledon opening angle in 6-d-old etiolated WT, *rsT<sub>c</sub>* and RS31 and RS41 OE seedlings. Seedlings were grown horizontally on  $\frac{1}{2}$  MS plates containing 2 μM BRZ. Values are means +SEM ( $n$ : 11 to 106). **(Right)** Representative images of cotyledon opening angles. Scale bar: 2 mm.



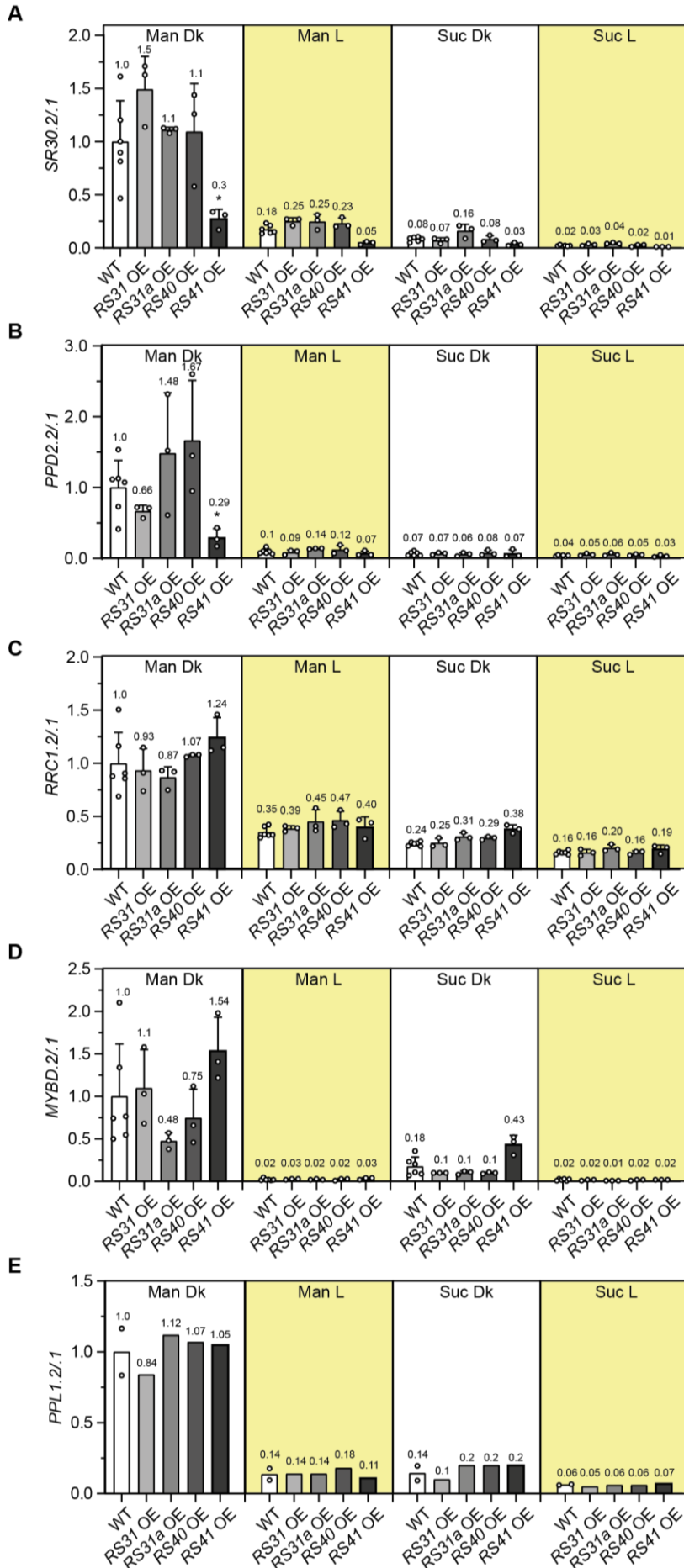


**Supplemental Figure 30: RS proteins control *RS31* splicing.** **(A)** The *RS31*-based splicing reporter can generate three splicing variants that include the sequence for a C-terminal EGFP-tag. Arrowheads indicate primer binding sites used for co-amplification PCR. Drawn to scale. **(B)** Indicated RS proteins or Luciferase (LUC) as unrelated control were transiently co-expressed with the splicing reporter in *N. benthamiana*. Co-amplification PCR on the reporter was performed, and PCR products were separated via agarose gel electrophoresis. **(C)** Splicing variants shown in (B) were quantified using a Bioanalyzer. **(D)** Splicing pattern of endogenous *RS31* in etiolated Arabidopsis WT and *rs40 rs41c* mutants that were either kept in darkness (Dk) or transferred to white light (L) and treated with either mannitol (Man) or sucrose (Suc) for 6 h. Endogenous *RS31* was co-amplified via PCR and PCR products were separated via agarose gel electrophoresis.

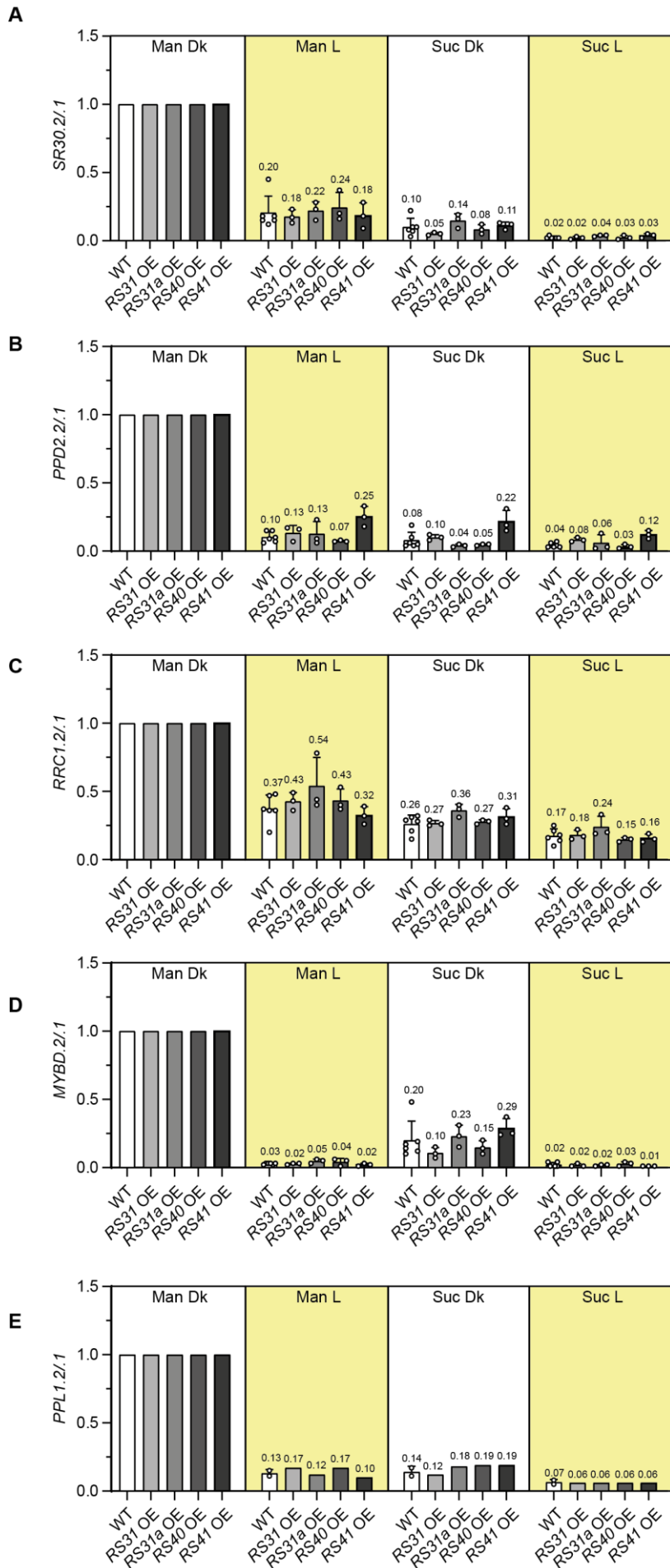


**Supplemental Figure 31: WT and *rs* mutants respond similarly to light and sugar signals on the splicing level. (A to D)** Quantification of splicing isoforms via RT-qPCR of 6-d-old etiolated WT and *rsTi* seedlings that were treated with 2% sucrose (Suc) or 1.06% mannitol (Man) and either kept in darkness (Dk) or transferred to white light (L) (~100  $\mu\text{mol m}^{-2}\text{s}^{-1}$ ) for 6 h. Splicing ratios were normalized to the average ratio of WT samples ( $n$ : 4 to 6). Displayed are mean values +SD, single dots represent

individual data points ( $n$ : 3 to 6 from 3 independent experiments). Corresponding Man dark samples are depicted in Figure 5 F to I. **(E to H)** Corresponding relative AS changes in WT and  $rs_t - 1$  mutant in response to light and sugar signals. Splicing changes were normalized to the corresponding Man dark sample. Numbers above the bars represent mean values.



**Supplemental Figure 32: Splicing changes in etiolated *RS OE* lines that were exposed to light and sugar. (A-E)** Quantification of splicing ratios for known light-regulated AS events in *RS OE* seedlings compared to WT. Etiolated seedlings were grown for 6 d in liquid ½ MS media. At day 6, etiolated seedlings were either treated with 2% sucrose (Suc) or 1.06% mannitol (Man), serving as an osmotic control. Plates were either kept in darkness (Dk) or shifted to white light (L) (~100  $\mu\text{mol m}^{-2}\text{s}^{-1}$ ) and plant material was collected after a 6 h treatment. Co-amplification PCR of selected AS events was performed, and splicing variants were quantified using a Bioanalyzer. Data represent mean values +SD that were normalized to the mean value of WT Man Dk samples. Numbers above the bars represent mean values. Another normalization to the corresponding Man dark sample is depicted in Supplemental Figure 33. Individual data points are shown as dots ( $n = 3$  to 6, except for PPL1, which has been analysed in single replicate for the mutants and two replicates for WT). Data from 3 independent experiments, except for *PPL1* which represents only one experiment). Normalized ratios of *RS OE* Dark Man were compared with WT Dark Man using an independent *t* test (P values: \*P < 0.05).



**Supplemental Figure 33: Relative splicing changes in *RS* OE seedlings in response to light and sugar.** AS responses were already depicted in Supplemental Figure 32, however, this figure used a different normalization. AS changes were normalized to the corresponding Man dark sample. Numbers above the bars represent mean values. For details about growth conditions please see Supplemental Figure 32.

## SUPPLEMENTAL TABLES

**Supplemental Table 1:** Description of *Arabidopsis thaliana* T-DNA and CRISPR mutants used in this study. All mutants are in the Col-0 background except *rs41-1* which is in Col-3. T-DNA higher order mutants were generated by crossing *rs40 rs41<sub>t</sub>* with different *rs31<sub>t</sub>* single mutants, CRISPR triple and quadruple mutants by transforming the *rs31 rs31<sub>a<sub>c</sub></sub>* construct in Cas9-free *rs40 rs41<sub>c</sub>* double mutants via *Agrobacterium tumefaciens*. All mutants were confirmed by genotyping.

Mutant	Mutant ID	RS31	RS31 <sub>a</sub>	RS40	RS41	RRC1	Reference
T-DNA	<i>rrc1-2</i>	WT	WT	WT	WT	SALK_1 21526	Shikata et al. 2012
	<i>rrc1-3</i>	WT	WT	WT	WT	SALK_0 11832	Shikata et al. 2012
	<i>rs31-1<sub>t</sub></i>	WiscDsLox4 81-484D23.1	WT	WT	WT	WT	
	<i>rs31-2<sub>t</sub></i>	SAIL_632_A 04.0	WT	WT	WT	WT	
	<i>rs40-1<sub>t</sub></i>	WT	WT	WiscDsLox 382G12.0	WT	WT	Chen et al. 2013
	<i>rs41-1<sub>t</sub></i>	WT	WT	WT	SAIL_64_ C03	WT	Chen et al. 2013
	<i>rs40 rs41<sub>t</sub></i>	WT	WT	<i>rs40-1</i>	<i>rs41-1</i>	WT	Provided by Liming Xiong
	<i>rsT<sub>t</sub>-1</i>	<i>rs31<sub>w</sub></i>	WT	<i>rs40-1</i>	<i>rs41-1</i>	WT	Generated in this study
	<i>rsT<sub>t</sub>-2</i>	<i>rs31<sub>s</sub></i>	WT	<i>rs40-1</i>	<i>rs41-1</i>	WT	Generated in this study
	<i>rsT<sub>t</sub> rrc1-2</i>	<i>rs31<sub>w</sub></i>	WT	<i>rs40-1</i>	<i>rs41-1</i>	<i>rrc1-2</i>	Generated in this study
<i>rsT<sub>t</sub> rrc1-3</i>	<i>rs31<sub>w</sub></i>	WT	<i>rs40-1</i>	<i>rs41-1</i>	<i>rrc1-3</i>	Generated in this study	
CRISPR	<i>rs31<sub>c</sub></i>	+1 bp (C)	WT	WT	WT	WT	Generated in this study
	<i>rs31<sub>a<sub>c</sub></sub></i>	WT	-1bp (C)	WT	WT	WT	Generated in this study



<i>rs31</i> <i>rs31a<sub>c</sub></i>	+1 bp (C)	+1bp (A)	WT	WT	WT	Generated in this study
<i>rs40</i> <i>rs41<sub>c</sub></i>	WT	WT	+1bp (A)	+1 bp (T)	WT	Generated in this study
<i>rsT<sub>c</sub></i>	WT	-1bp (C)	+1bp (A)	+1 bp (T)	WT	Generated in this study
<i>rsQ<sub>c</sub></i>	+1 bp (C)	+1bp (T)	+1bp (A)	+1 bp (T)	WT	Generated in this study

**Supplemental Table 2:** Genotyping revealed that selected *rsQ* plants (T6) with normal siliques were heterozygous in *RS40* and/or *RS41*. Strikingly, *RS40* and *RS41* were previously confirmed to be homozygous in the Cas9-free *rs40 rs41<sub>c</sub>* double mutant, which was used to generate *rsQ*, as well as in previous generations of *rsQ*. Sequencing results for two plants from independent lines are depicted as example. Red arrowhead marks Cas9 cleavage site and corresponding mutations are shown in red.

Line	<i>RS31</i>	<i>RS31a</i>	<i>RS40</i>	<i>RS41</i>	Comment
WT	GTGAACGTGGCAGGCC <sup>▲</sup> TCG	TGCTGAAGATGCAATCCGT	TTGAGTATGATGCGCG <sup>▲</sup> CGA	GCTTTGAATATGGT <sup>▲</sup> CGCAC	
<i>rsQ<sub>c</sub></i> 2_19 _4	GTGAACGTGGCAGGCC <sup>C</sup> TCG	TGCTGAAGATGCAAT <sup>C</sup> TCGT	TTGAGTATGATGCGCGCGA TTGAGTATGATGCGCG <sup>A</sup> CGA	GCTTTGAATATGGT <sup>C</sup> TCAC	Heterozygous in <i>RS40</i>  Normal siliques
<i>rsQ<sub>c</sub></i> 6_3_ 1	GTGAACGTGGCAGGCC <sup>C</sup> TCG	TGCTGAAGATGCAAT <sup>C</sup> /ACGT	TTGAGTATGATGCGCGCGA TTGAGTATGATGCGCG <sup>A</sup> CGA	GCTTTGAATATGGT <sup>C</sup> CGCAC GCTTTGAATATGGT <sup>C</sup> TCAC	Heterozygous in <i>RS40</i> and <i>RS41</i>  Normal siliques

**Supplemental Table 3:** Segregation analysis of selected *RS* overexpression (OE) lines. Seedlings were grown on ½ MS plates supplemented with 2% sucrose and 25 µg/ml kanamycin under long day conditions. Col-0 WT and EGFP seedlings served as control. The corresponding RT-qPCR expression analyses can be found in Supplemental Figure 6F to I.

Line	Subline #	Generation	Number of plants	% resistant [n <sup>1</sup> ]
<i>RS31</i> OE	8	T1	37	84 [31]
	8_1	T2	16	81 [94]
	8_1_p	T3	41	71 [29]
	8_6	T2	108	100 [108]
	<b>8_11_p*</b>	<b>T3</b>	<b>102</b>	<b>100 [102]</b>
<i>RS31a</i> OE	1	T1	37	89 [31]
	1_12	T2	82	98 [80]
	<b>1_13</b>	<b>T2</b>	<b>193</b>	<b>99 [191]</b>
	1_13_p	T3	35	100 [35]
	7	T1	35	83 [29]
<i>RS40</i> OE	11	T1	47	83 [39]
	30	T1	79	87 [69]
	<b>30_11</b>	<b>T2</b>	<b>97</b>	<b>99 [96]</b>
	30_11_p	T3	39	95 [37]
<i>RS41</i> OE	30_14	T2	134	88 [118]
	6	T1	26	81 [21]
	<b>6_12_p</b>	<b>T3</b>	<b>69</b>	<b>97 [67]</b>
WT	6_15_p	T3	68	97 [66]
		T1	14	0 [0]
		T2	89	0 [0]
EGFP		T3	133	0 [0]
		T3	164	79 [129]

<sup>1</sup> total number of kanamycin resistant seedlings

\*p represents pool. If 100% of the corresponding subline survived on kanamycin supplemented plates, seeds were pooled, as the transgenic line became homozygous. This was the case for all T3 lines that are described here.

**Supplemental Table 4:** Cotyledon opening percentages and opening angle in *RS* overexpression (OE) and *rsT<sub>c</sub>* seedlings. Seedlings were grown in darkness for 6 d on ½ MS plates lacking sucrose.

Line	Number of plants	% Opened cotyledons [n <sup>1</sup> ]	Opening angle [°]
WT	112	8.3 [10]	1.6
<i>RS31</i> OE #8_11_p	41	38.1 [16]	10.5
<i>RS31a</i> OE #1_13	35	45.7 [16]	14.8
<i>RS40</i> OE #30_14_p	24	38.5 [10]	9.8
<i>RS41</i> OE # 6_12_p	122	72.4 [92]	36.4
<i>rsT<sub>c</sub></i>	107	10.2 [12]	3.0

<sup>1</sup> total seedlings showing opened cotyledons

**Supplemental Table 5:** Oligonucleotides used to generate *RS* OE constructs. For further details please see corresponding material and method part.

Gene	Primer ID	F / R	Sequence	Details
<i>RS31-HA<sub>3</sub></i>	ES232	F	ATGCGGTACCATGAGGCCAGTGTTCGTCG	<u>KpnI</u>
	ES233	R	ATGCGGATCCAGGTCTTCCTCTTGGA	<u>BamHI</u>
<i>RS31a-HA<sub>3</sub></i>	AWTU374	F	ATGCGGTACCATGAGACATGTGTACGTTGGG	<u>KpnI</u>
	AWTU375	R	ATGCGGATCCACCTCTTGCTCTTTGAATCGG	<u>BamHI</u>
<i>RS40-HA<sub>3</sub></i>	AWTU376	F	ATGCGGTACCATGAAGCCAGTCTTCTGTGG	<u>KpnI</u>
	AWTU377	R	ATGCGGATCCCTCGTCAGCTGGTGCGA	<u>BamHI</u>
<i>RS41-HA<sub>3</sub></i>	ES248	F	ATGCGGTACCATGAAGCCTGTCTTTGCGG	<u>KpnI</u>
	ES249	R	ATGCGGATCCTTCCTCTGCTGGCGG	<u>BamHI</u>
<i>HA-RS41</i>	ES206	F	<b>TCCAGATTACGCT</b> ATGAAGCCTGTCTTTGCGG	<b>Partial HA</b>
	ES207	R	ccccGTCGACTTCATTCTCTGCTGGCGG	<u>Sall</u>
	ES208	F	ATGCGGATCCATGT <b>TACCCATACGATGTTCCAGATTACGCT</b>	<u>BamHI</u> <b>HA</b>
<i>RS31 reporter</i>	JS186	F	gatcGGTACCAATGTACCCATGATGGTATGA	<u>KpnI</u>
	JS208	R	gatcGCTAGCAAAGGAAAATTGTCGAGTTT	<u>NheI</u>

**Supplemental Table 6:** Oligonucleotides used to generate CRISPR constructs.

Gene	Primer ID	F / R	Sequence	Details
<i>RS31</i>	JS82 (DT1-BsF)	F	atatatGGTCTCGATTGgtgaacgtggcaggcctcgGTT	<u>Bsal</u> , <b>sgRNA</b>
	JS83 (DT1-F0)	F	TGgtgaacgtggcaggcctcgGTTTTAGAGCTAGAAATAGC	
<i>RS31a</i>	JS80 (DT2-R0)	R	AACACGGATTGCATCTTCAGCACAAATCTCTTAGTCGACTCTAC	<u>Bsal</u> , <b>sgRNA</b>
	JS81 (DT2-BsR)	R	attattGGTCTCGAAACACGGATTGCATCTTCAGCACAA	
<i>RS40</i>	JS86 (DT1-BSF)	F	atatatGGTCTCGATTGTTGAGTATGATGCGCGCGAGTT	<u>Bsal</u> , <b>sgRNA</b>
	JS87 (DT1-F0)	F	TGTTGAGTATGATGCGCGCGAGTTTTAGAGCTAGAAATAGC	
<i>RS41</i>	JS88 (DT2-R0)	R	AACGTGCGACCATATTCAAAGCCAATCTCTTAGTCGACTCTAC	<u>Bsal</u> , <b>sgRNA</b>
	JS89 (DT2-BsR)	R	attattGGTCTCGAAACGTGCGACCATATTCAAAGCCAA	

**Supplemental Table 7:** Oligonucleotides used for genotyping of T-DNA mutants.

Gene	Primer ID	F / R	Sequence	Product size [bp]	Details
RS31	TW107	F	GATAGGGTTGTTCCGTGGA	400	<i>rs31-1<sub>t</sub></i> T-DNA specific
	GD30	R	GAACTGCTTCTTCTTTTAC		
	JS29	F	TCGAAATGGTGGTCGTAGC	389	RS31-1 WT specific
	TW091	R	GGCGTCCAAGTCCAGATT		
RS31	AWHD60	F	TTCATAACCAATCTCGATACAC	300	<i>rs31-2<sub>t</sub></i> T-DNA specific
	TW091	R	GGCGTCCAAGTCCAGATT		
	TW093	F	GGCGTCCAAGTCCAGATT	339	RS31-2 WT specific
	TW091	R	GGCGTCCAAGTCCAGATT		
RS40	GD30	F	GAACTGCTTCTTCTTTTAC	600	<i>rs40-1<sub>t</sub></i> T-DNA specific
	TW082	R	ACCAGATCTTTTATCACCTCCAC		
	TW086	F	TCAGGAAATACGGCAAGGTTG	1050	RS40-1 WT specific
	TW082	R	ACCAGATCTTTTATCACCTCCAC		
RS41	AWHD60	F	TTCATAACCAATCTCGATACAC	1300	<i>rs41-1<sub>t</sub></i> T-DNA specific
	TW090	R	TATCAGGTGACCTATCACGCC		
	TW089	F	ACTCAACATTTGATTTTGGCG	780	RS41-1 WT specific
	LH34	R	CTCGAACCACCTGATCTTCC		
RRC1	LH247	F	GGAATGGACGAGGAACAAAG	765	<i>rrc1-2</i> T-DNA specific
	AW92	R	TGGTTCACGTAGTGGGCCATCG		
	LH247	F	GGAATGGACGAGGAACAAAG	653	RRC1-2 WT specific
	LH248	R	GATTTCTGTTGCCCTCGT		
RRC1	AW92	F	TGGTTCACGTAGTGGGCCATCG	649	<i>rrc1-3</i> T-DNA specific
	LH248	R	GATTTCTGTTGCCCTCGT		
	LH258	F	ATACCAATCCCACAGCCT	869	RRC1-3 WT specific
	LH248	R	GATTTCTGTTGCCCTCGT		

**Supplemental Table 8:** Oligonucleotides used for genotyping of CRISPR mutants. Corresponding PCR products were then used for sequencing.

Gene	Primer ID	F / R	Sequence	Product size [bp]
RS31	JS134	F	TGCTTTCTTTTGTTCAGGA	440
	JS135	R	TTGAGTAGCTTCAAGGGCT	
RS31a	JS136	F	TCTCTAGGTGAAAAGGTGTC	487
	JS137	R	GCAAAATTGCGCCTCATGC	
RS40	JS126	F	TTTAACTGATTTGGAGCTCG	463
	JS127	R	ATGAAGACGAGAGTGGATTT	
RS41	JS129	F	GTCACAGTAAGTAGTAAAGG	473
	JS130	R	AAAGTGCCTCTCCAAGTC	
Cas9	JS99	F	CTGTTTCGTGAGCAGCACAAGCATT	502
	JS103	R	TTCCAATGCCATAATACTCAAACCTCAG	

**Supplemental Table 9:** Oligonucleotides used for genotyping of *RS* OE lines.

Gene	Primer ID	F / R	Sequence	Product size [bp]	Details
<i>RS31</i>	AWS1	F	CAAGACCCTTCCTCTATA	809	Transgene specific
	JS7	R	GGTCATAACCAGGGCTCCTTT		
	LH133	F	CGTCGTCGTCTAGGGTTTGT	755	WT specific
	TW092	R	AGTGGAGGAGTTCAGATATGG		
<i>RS31</i>	AWS1	F	CAAGACCCTTCCTCTATA	772	Transgene specific
	JS9	R	GTCATAGCCCGGACTCCTAG		
	JS27	F	GTCGTCTCTTCAGATTCTTC	1025	WT specific
	JS28	R	TCTTCAGCATCGCGCTCAT		
<i>RS40</i>	AWS1	F	CAAGACCCTTCCTCTATA	1054	Transgene specific
	JS11	R	TGCACCATCATAACCCACCAT		
	JS30	F	ATCTAAATCGTACCTAACTCTG	703	WT specific
	JS31	R	ATCTAAATCGTACCTAACTCTG		
<i>RS41</i>	AWS1	F	CAAGACCCTTCCTCTATA	866	Transgene T-DNA specific
	JS13	R	CACCACGTCCTTTTCTTGGG		
	LH33	F	CGGTACGATTTTTCAACTGC	1792	WT specific
	TW083	R	GTCCACTCAACACGGAGTCT		

**Supplemental Table 10:** Oligonucleotides used for RT-qPCR analyses.

Gene	Primer ID	F / R	Sequence	Product size [bp]	Details
<i>RS31</i>	JS6	F	GTCGTGCTCGAAGCCCA	123	All isoforms
	JS7	R	GGTCATAACCAGGGCTCCTTT		
	JS227	F	AGTGGACATGAAATCTGGATAT	126	Coding isoform specific
	JS234	R	GCCATTCAACTGATAACCTGC		
<i>RS31a</i>	JS8	F	CAGGTACAAGGGTCCTGCTC	103	All isoforms
	JS9	R	GTCATAGCCCGGACTCCTAG		
	JS235	F	GTTGATATGAAGTCTGGTTATG	114	Coding isoform specific
	JS236	R	TGATAACTTGCGTCGCCAT		
<i>RS40</i>	JS10	F	GAAGTTGAAAGTCCCATTGAAAGG	117	All isoforms
	JS11	R	TGCACCATCATAACCCACCAT		
	JS231	F	GGTTGATATGAAAGCTGGGTT	97	Coding isoform specific
	JS232	R	TTCAACACGAAGTCTGCGTC		
<i>RS41</i>	JS12	F	GCCAGGCTTAGCCAGAT	106	All isoforms
	JS13	R	CACCACGTCCTTTTCTTGGG		
	JS231	F	GGTTGATATGAAAGCTGGGTT	114	Coding isoform specific
	JS233	R	CGGAGTCTGCGTCCTGTG		
<i>SR30.1</i>	LH50	F	GCAAGAGCAGGAGTGTGTCA	108	
	LH51	R	TTGATCTTGATTGGGACCTTG		
<i>SR30.2</i>	LH52	F	TCACCTGCTAGATCCATTTC	99	
	LH53	R	CCCAGCTCGTAGCAGTGAG		
<i>RRC1.1</i>	LH302	F	CCTAAGGTTGATTCTGAAGGTGA	94	
	LH303	R	GTGGTGGTGAAGGAAAGAG		
<i>RRC1.2</i>	LH304	F	CCTAAGGTTGATTCTGAAGGTATG	106	
	LH305	R	CTTCCCTAGGCCTCTCCTC		
<i>PPD2.1</i>	LH527	F	AGTAAAGAGAAGATGGTGGAGCT	92	
	LH528	R	TTTCTGTTGCGCTGACCCTC		

<i>PPD2</i>	LH529	F	TGTCCAATTTTGAAGGAGGCA	104
2	LH530	R	CACGAGGCATCTGTAGACACA	
<i>MYBD</i>	JS148	F	CGTGAACGCAAACGAGGAAC	103
.1	JS149	R	TTCTAGAGATTCCTCTCCAATC	
<i>MYBD</i>	JS150	F	CCAAATCTCATCTCTGTTTTTG	104
.2	JS151	R	CAGTAAGAAACAATCTATGTTCT	
<i>PPL1</i>	JS152	F	GTAGAGCTCCATTATCATTTGC	101
1	JS153	R	CTGCCAACCAAATGGATAGAG	
<i>PPL1</i>	JS154	F	AGTAGAGCTCCATTATCATAAAG	93
2	JS153	R	CTGCCAACCAAATGGATAGAG	
<i>SAUR-AC1</i>	JS170	F	TGTGGTGCCGGTTTCATACT	100
	JS171	R	TGTTAAGCCGCCATTGGAT	
<i>BAS1</i>	JS174	F	CGGCGAAGGATTTGTTGGGA	99
	JS175	R	TCTGTTTCCCGGCGAAGAAA	
<i>EXPA</i>	JS182	F	TGTGGTGCTTGCTTCGAGAT	105
1	JS183	R	TAAGGCGTTGTTAGGAGGGC	
<i>PIF3</i>	JS237	F	CACATTTCTTACGCCCTGCA	96
	JS238	R	GAAACACATTTGGCGGGCTT	
<i>PIF4</i>	JS243	F	ATGGCGAGATGGACAAGTGG	101
	JS244	R	AGGTGCTGGATCTTAGGGCT	
<i>COP1</i>	JS241	F	TGGCCACATGAGAAGAACCA	107
	JS242	R	TGTGCCTTCCCCTCTACCTT	
<i>PP2A</i>	DNA28	F	CTATGTTCTTCCTCTGTCCA	102
	DNA29	R	CCACAACCGCTTGGTCG	

**Supplemental Table 11:** Oligonucleotides used for co-amplification PCR.

Gene	Primer ID	F / R	Sequence	Product sizes [bp]	Details
<i>SR30</i>	LH4	F	GTCACCTGCTAGATCCATTTCC	.1: 200	
	LH5	R	AGCCTGAGAAGCTTGAGACG	.2: 550	
<i>RRC1</i>	LH246	F	ACTTTTGTTCGAGGTGGG	.1: 103	
	LH229	R	TGGTGGAAGGAAAGAGGGA	.2: 83	
<i>PPD2</i>	LH319	F	CGGTGGTTGGGCAAATGA	.1: 260	
	LH320	R	ACTTTTCTGTTTCGCCTGAC	.2: 574	
<i>MYBD</i>	LH336	F	TCAAACCTCCTGATCCCAACC	.1: 120	
	LH363	R	CTATGTTCTTCCTCTGTCCA	.2: 200	
<i>PPL1</i>	LH321	F	GTGTTGTTGCTCCTTGGAT	.1: 175	
	LH322	R	AGGCTCAATCACATCTTTG	.2: 185	
<i>RS31</i>	LH133	F	CGTCGTCGTCTAGGGTTTGT	.1: 542	
	LH134	R	CAACCCTATCCAATATTTTGCTC	.2: 931	
					.3: 1037
<i>RS31-EGFP</i>	LH484	F	ACCGAGTGGACATGAAAT	.1: 240	<i>RS31</i> splicing reporter
	AWHD153	R	TGAACTTCAGGGTCAGCTTG	.2: 633	

## Chapter IV: Draft manuscript 3





## **Subcellular and organ localization of RS proteins is controlled in a light-dependent manner in Arabidopsis seedlings**

Jennifer Saile<sup>1,2</sup>, Moritz Paul Denecke<sup>1</sup>, Laura Sophie Schütz<sup>1</sup>, and Andreas Wachter<sup>1,2,\*</sup>

<sup>1</sup>Institute for Molecular Physiology (imP), University of Mainz, Hanns-Dieter-Hüsch-Weg 17, 55128 Mainz, Germany

<sup>2</sup>Center for Plant Molecular Biology (ZMBP), University of Tübingen, Auf der Morgenstelle 32, 72076 Tübingen, Germany

\*Corresponding author: [wachter@uni-mainz.de](mailto:wachter@uni-mainz.de)

### **Contributions**

35S::RS-EGFP constructs and transgenic lines were generated by myself. Furthermore, I performed all microscopy studies shown in Figure 1, Figure 2, and Supplemental Figure 1.

RS-TurboID constructs and transgenic lines were generated by Moritz Denecke and Laura Schütz, under my supervision. Confocal microscopy studies shown in Figure 3 were performed by Moritz Denecke and myself. In addition, Moritz Denecke performed the biotin assay, shown in Figure 4.

Data analysis and figure design were done by myself. Moreover, I wrote the manuscript with contributions from Andreas Wachter.

## Introduction

Pre-mRNA splicing is catalysed by a large ribonucleoprotein complex, that is composed of five small nuclear ribonucleoprotein particles (U1, U2, U4/U6, U5 snRNPs) and additional non-snRNP proteins such as splicing regulators (Will & Lührmann, 2011). Non-snRNP proteins include serine/arginine-rich (SR) proteins that are characterized by one or two N-terminal RNA recognition motifs (RRMs) and a C-terminal arginine/serine-rich (RS) domain (Barta et al., 2010). The RS domain of SR proteins was found to be completely disordered (Haynes & Iakoucheva, 2006) and crucial for the speckle localization (Tillemans et al., 2005). As SR proteins play an essential role in constitutive and alternative pre-mRNA splicing, they interact with both, RNA, and proteins (Reddy, 2004). Previous studies revealed that SR proteins localize to the nucleoplasm but also accumulate in nuclear speckles that are interchromatin granule clusters (Ali et al., 2003; Chen et al., 2013; Chen et al., 2015; Lorković et al., 2004; Tillemans et al., 2005; Yan et al., 2017). Speckle localization is strongly affected by the phosphorylation status of SR proteins that in turn impacts pre-mRNA splicing by changing their protein-protein and protein-RNA interactions (Ali et al., 2003; Docquier et al., 2004; Misteli, 2000; Tillemans et al., 2006). As the nuclear distribution of SR proteins is highly dynamic, it is assumed that interactors differ spatially and temporally. However, to date many protein-protein interaction methods fail to identify proteins that only transiently or weakly interact with the target protein. Recently, proximity labeling (PL) techniques have been developed to overcome these difficulties. PL involves a biotin ligase that is fused to the target protein. The enzyme catalyses the biotinylation of the target protein, as well as proteins that are in close proximity, by covalently attaching biotin. Using streptavidin-coupled beads, biotinylated interactors are specifically purified and identified by mass spectrometry (MS) (Mair & Bergmann, 2022).

In this study we show that RS proteins exhibit an organ-specific localization that is controlled in a light-dependent manner. Furthermore, subcellular localization analyses showed that RS fusion proteins exclusively localize to the nucleus. We found transgenic RS31 and RS31a proteins to be uniformly distributed within the nucleoplasm but also concentrated in nuclear speckles, whereas RS40 and RS41 fusion proteins were mainly localized to the nucleoplasm in etiolated *Arabidopsis* seedlings. Interestingly, light and sugar treatment triggered a re-localization of RS40

and RS41 fusion proteins from the nucleoplasm into nuclear speckles. Hence, we propose that RS interaction partners may differ depending on the metabolic state. To identify RS interactors, we generated transgenic Arabidopsis lines, expressing RS-TurbID (TbID) fusion proteins. An initial PL experiment revealed that RS-TbID proteins can biotinylate proteins in Arabidopsis seedlings. Further establishing and optimizing RS-TbID PL in Arabidopsis seedlings will help to increase our insights into RS interactors and hence, RS function.

## Results

### RS proteins show a light-dependent localization in cotyledons

Given that the upregulation of *RS* genes results in cotyledon opening and hypocotyl growth repression in etiolated Arabidopsis seedlings (see Chapter III), we asked whether RS proteins display an organ- and light-dependent localization. Therefore, we generated transgenic lines expressing the cds of either *RS31*, *RS31a* or *RS41* that were tagged with EGFP at the region corresponding to the C-terminus. Due to a cloning artefact, the RS41 construct contains a double insert, and hence, corresponding lines are designated as RS41-RS41-EGFP. Furthermore, we used the 35S promoter to drive the expression of the fusion proteins. A former study showed that the 35S promoter activity is not significantly altered in darkness vs. light (Zhai et al., 2019). Moreover, we included a 35S::EGFP line as control. When transgenic seedlings were grown in constant darkness, we observed an uniformly distributed EGFP expression in all organs of the 35S::EGFP control line (Supplemental Figure 1). On the contrary, RS localization was strongly detectable in cotyledons and roots of the *RS*-EGFP lines, whereas we detected no or only a weak EGFP signal in the hypocotyl (Figure 1A to C). The RS-EGFP signal was concentrated into dots, indicating that RS proteins localize in nuclei (Figure 1A to C).

To monitor RS localization in the presence of light, we grew transgenic seedlings under continuous red-light conditions. Fluorescence microscopy revealed that RS localization was drastically affected by light, as the EGFP signal was no longer detectable in cotyledons (Figure 1D to F). On the contrary, the control line displayed an EGFP signal in all organs, however, the signal was weaker in cotyledons, compared to the hypocotyl (Supplemental Figure 1). Although, *RS* expression was driven by the 35S promoter, we observed organ-specific localization under dark and light conditions, suggesting a post-translational regulation of RS proteins. Furthermore, our findings implicate

specific functions of RS proteins in cotyledon development, as their distribution in cotyledons was drastically affected in response to light. Future studies are needed to confirm this hypothesis and should include additional transgenic lines, such as plants expressing the *RS* genes under control of the endogenous promoter.

### **RS proteins localize in the nucleoplasm and nuclear speckles**

To examine the subcellular localization of RS proteins, we performed confocal microscopy studies. Consistent with previous reports (Chen et al., 2013; Chen et al., 2015; Docquier et al., 2004; Lorković et al., 2004; Tillemans et al., 2005), we observed a nuclear localization of RS fusion proteins in etiolated *Arabidopsis* seedlings (Figure 2). Confocal microscopy revealed that RS31 and RS31a fusion proteins localize to the nucleoplasm but are also accumulated in nuclear speckles (Figure 2). Speckles are membraneless organelles, present in the interchromatin region of the nucleoplasm and are enriched in splicing regulators (Spector & Lamond, 2011). On the contrary, the RS41 fusion protein was mainly localized in the nucleoplasm in etiolated *Arabidopsis* seedlings (Figure 2).

To analyse whether light affects RS nuclear distribution, we examined RS subcellular localization in light-grown *Arabidopsis* seedlings. RS31 and RS31a localization was not drastically affected by light. Accordingly, RS31 and RS31a fusion proteins were diffusely distributed within the nucleoplasm but also concentrated in nuclear speckles (Figure 2). In contrast, speckle localization of RS41 fusion proteins was strongly increased in light-grown seedlings (Figure 2). Similar findings were obtained, when RS41-RS41-EGFP transgenic seedlings were grown in the presence of sucrose (Figure 2), suggesting that light and sucrose affect RS41 localization, by inducing a re-localization into nuclear speckles.

The nuclear as well as speckle localization of SR proteins was found to be mediated by the RS domain that includes a nuclear localization signal (NLS) (Tillemans et al., 2005). Furthermore, the RS domain contains intrinsically disordered regions (IDRs) that were previously identified to be critical for the formation of membraneless condensates, including nuclear speckles (Boeynaems et al., 2018). To examine the IDRs of RS proteins, we used the Mobi database (Piovesan et al., 2021). All RS proteins were enriched in IDRs, with 37.5% and 32.4% present in RS31 and RS31a (Supplemental Figure 2), respectively, and 58.9% and 58.7% in RS40 and RS41 (Supplemental Figure 3), respectively. To investigate whether RS proteins undergo a

transition from a soluble to a condensed state upon sugar/light exposure, we generated transgenic lines, expressing RS/Dummy-YFP-TbID<sub>NLS</sub> fusion proteins. Those proteins were expressed under the ubiquitous UBIQUITIN10 (UBQ10) promoter and tagged with a myc-tag at the region corresponding to the N-terminus. 6-d-old etiolated RS40-YFP-TbID<sub>NLS</sub> seedlings were then treated with 2% sucrose for 2-3 h. After sugar treatment, we observed RS40 fusion proteins both in the nucleoplasm and in nuclear speckles (Figure 3). In contrast, no speckle localization was observed after mannitol treatment (Figure 3). A dummy construct was included as additional control that showed nucleoplasm localization only upon sucrose treatment (Figure 3). As phosphorylation was found to control the intranuclear distribution of SR proteins (Ali et al., 2003; Docquier et al., 2004; Misteli, 2000; Tillemans et al., 2006), we propose a functional relationship between sugar- and light-induced RS40 and RS41 phosphorylation and intranuclear re-localization.

### **RS-TbID<sub>NLS</sub> fusion proteins can biotinylate proteins in Arabidopsis seedlings**

Based on the findings that the organ distribution as well as subcellular localization of RS proteins was altered in response to light and sugar signals, we propose that RS interaction partners may differ spatially and/or temporally. To increase the insights into RS function, we aimed at identifying RS interactors by using PL. As TbID was previously shown to work well in *N. benthamiana* and Arabidopsis plants (Mair et al., 2019), we used our generated transgenic RS-TbID lines (without YFP-tag) for PL experiments. Upon establishing PL using RS-TbID<sub>NLS</sub> fusion proteins in *N. benthamiana* (see BSc. thesis Laura Schütz (2021), MSc. thesis Moritz Denecke (2021)), we performed a first PL experiment in 6-d-old etiolated transgenic Arabidopsis seedlings that were either further kept in darkness or transferred to white light and treated with biotin for the indicated time points. Subsequently, we performed total protein extraction and used streptavidin immunoblots to detect biotinylated proteins and myc immunoblots for the detection of the fusion proteins. Under mock conditions we already observed a 'background' labeling (Figure 4), possibly caused by the endogenous biotin that accumulates in cells (Alban et al., 2000). However, labeling was enhanced by the application of biotin, demonstrated by the strong self-labeling of RS-TbID<sub>NLS</sub> fusion proteins (Figure 4). Furthermore, specific biotinylated proteins were identified in RS-TbID<sub>NLS</sub> seedlings that were absent from biotin-treated WT seedlings (Figure 4). These findings suggest that our system is working in Arabidopsis and hence, RS-TbID<sub>NLS</sub> fusion proteins induce the biotinylation of proteins. Furthermore,

the intensities of some signals changed in a light-dependent manner (Figure 4). Future studies are required to further establish PL by RS-TbID<sub>NLS</sub> proteins in Arabidopsis. Hence, labeling conditions, including labeling time, temperature and biotin concentration need to be further optimized in Arabidopsis seedlings prior to the identification of biotinylated proteins by streptavidin pulldown followed by MS.

## Discussion

Here we show that RS fusion proteins exclusively localize to the nucleus in Arabidopsis seedlings, which is in line with previous publications (Chen et al., 2013; Chen et al., 2015; Docquier et al., 2004; Lorković et al., 2004; Tillemans et al., 2005). We found RS31 and RS31a to be present in the nucleoplasm but also in nuclear speckles, whereas RS40 and RS41 were mainly distributed within the nucleoplasm in dark grown Arabidopsis seedlings. However, light and sugar treatment induced a re-localization of RS40 and RS41 from the nucleoplasm into nuclear speckles. Speckles are known as membraneless bodies that contain proteins and RNAs and are described as possible storage and modification site of splicing regulators (Spector & Lamond, 2011). As SR splicing regulators rapidly change between the nucleoplasm and nuclear speckles (Ali et al., 2003; Docquier et al., 2004; Fang et al., 2004; Reddy et al., 2012), it is proposed that the formation of speckles involves liquid-liquid phase separation (LLPS). LLPS describes a special form of phase separation where a homogenous solution of biomolecules spontaneously demixes into two liquid phases, a dense and a diluted phase (Boeynaems et al., 2018). Hence, biomolecules are spatially concentrated in membraneless compartments. Hallmarks of molecules that undergo phase separation include the formation of spherical droplets that can fuse with each other, and the fluorescence recovery after photobleaching (FRAP) (Bergeron-Sandoval et al., 2016). Furthermore, it was shown that proteins containing IDRs phase separate, as those regions are flexible and dynamic and mediate interactions, involving protein-protein and protein-RNA (Boeynaems et al., 2018).

As RS proteins are highly enriched in IDRs and re-localize into condensates upon light and sugar treatment, we propose that RS proteins phase separate. In line with this hypothesis is the observation that the IDRs present in SR proteins, including RS31, RSZ22 and SR45 were found to be required for speckle formation *in vivo* (Ali & Reddy, 2006; Tillemans et al., 2005). Furthermore, FRAP studies demonstrated that

photobleaching of RS31, SR34 and SR45 rapidly recovered (Ali & Reddy, 2006; Fang et al., 2004; Tillemans et al., 2005).

Phase separation was also identified to be controlled by post-translational modifications (PTMs), as PTMs can either promote or repress interactions and hence, facilitate or prevent phase separation (Xu et al., 2021). Studies in *Arabidopsis* revealed that the inhibition of phosphorylation increases the speckle size (Ali & Reddy, 2006; Docquier et al., 2004; Tillemans et al., 2005; Tillemans et al., 2006) and further, reduces the mobility of splicing regulators (Ali & Reddy, 2006; Tillemans et al., 2006). On the contrary, Mori et al. reported that the speckle formation of SR30 in onion epidermal cells is suppressed upon dephosphorylation. These contrasting findings suggest that both, dephosphorylation and phosphorylation of SR proteins can trigger speckle localization, possibly involving phase separation.

As RS40 and RS41 undergo a rapid phosphorylation as well as nuclear re-localization in response to light and sugar, we propose a functional relationship between these two processes that may be involved in adjusting the splicing response. This hypothesis is consistent with recent findings, showing that the phosphorylation in the IDRs of the splicing regulator glycine-rich RNA binding protein7 (GRP7) affects GRP7 phase separation and hence, the adaptation to fluctuating temperatures (Xu et al., 2022). To date, studies on phase separation of plant splicing regulators are limited (Xu et al., 2021). Interestingly, a recent study proposed a model for the splicing reaction that takes place at the nuclear speckle interface where exons are pulled into nuclear speckles by SR proteins and introns retained in the nucleoplasm by hnRNP binding. Subsequently, the splice site motif is positioned at the speckle interface and accessible to the spliceosome that catalyses the splicing reaction (Liao & Regev, 2021). However, the fact that speckles have not been identified in some organisms, including yeast (Potashkin et al., 1990), question this model.

Furthermore, it seems also possible that speckles can concentrate, store, modify but also hide proteins, suggesting that the concentration/aggregation of splicing regulators in speckles might affect the splicing activity. The fact, that not all splicing regulators concentrate in nuclear speckles (Stauffer et al., 2010), however, argues against this hypothesis. In addition, we lack studies reporting a direct link between the localization of splicing regulators and the splicing activity. So far, it has been shown that protein isoforms can differ in their speckle size and further, exhibit altered splicing patterns

(Zhang & Mount, 2009), but a direct link has not yet been demonstrated. In line with these findings, reports in mammalian cells demonstrated that phase separation of IDR-containing splicing regulators contributes to AS regulation and hence, human diseases (Gueroussov et al., 2017; Li et al., 2020). However, it remains unclear whether the speckle localization contributes to the splicing reaction, as speckles were not observed in all cell types, despite the described activity of those splicing regulators in every cell (Gueroussov et al., 2017).

Therefore, future analyses are required to elucidate the potential relationship between the localization and splicing activity of splicing regulators. Furthermore, future work will be needed to study whether RS proteins phase separate. We propose that RS proteins undergo phosphorylation induced phase separation to respond to metabolic variations, by adjusting the splicing decision (Figure 5).

## Material and Methods

### Generation of constructs

To generate 35S::RS-EGFP lines, cds of *RS31*, *RS31a* and *RS41* were amplified from plasmid DNA using Herculase II Fusion DNA Polymerase (Agilent Technologies, Santa Clara, CA, US) with JS14/ES233 (*RS31*), JS15/AWTU375 (*RS31a*) and JS17/ES249 (*RS41*). Generated inserts were digested with *Bam*HI and cloned into *Bam*HI-restricted pBinAR-EGFP.

RS-TurboID constructs were cloned using the GoldenGate system (Binder et al., 2014). First, LI modules were generated. Therefore, cds of *RS40* and *RS41* were amplified from plasmid DNA using Q5 High-Fidelity DNA Polymerase (NEB, Ipswich, MA, US) with JS188/189 (*RS40*) and JS190/191 (*RS41*). Generated inserts were A-tailed and ligated into pGEM-T vector (Promega, Madison, WI, US). YFP-TurboID<sub>NLS</sub> and TurboID<sub>NLS</sub> were amplified from pMCD7-11 plasmid using Q5 High-Fidelity DNA Polymerase (NEB, Ipswich, MA, US) with JS192/193 (*YFP-TurboID<sub>NLS</sub>*) and JS195/193 (*TurboID<sub>NLS</sub>*) and directly cloned into pJET1.2 (Thermo Fisher Scientific, Waltham, MA, US).

To generate final GoldenGate LII constructs, concentration of LI modules was adjusted to 100 ng/μl and used for *Bsa*I cut ligation [Σ 15 μl: 1 μl of each LI module, 1.5 μl buffer, 0.75 μl T4 Ligase (Thermo Fisher Scientific, Waltham, MA, US) and 0.5 μl *Bsa*I (Thermo Fisher Scientific, Waltham, MA, US)]. The reaction was incubated in a



thermocycler at 37 °C for 2 min, followed by 16 °C for 5 min. These two steps were repeated 25 x. Subsequently, GoldenGate reactions were further incubated at 37 °C for 5 min, 50 °C for 5 min and 80 °C for 5 min, before cooling down to 16 °C. Since pGEM-T and pJET1.2 vector backbones contained internal *Bsal* sites, 1 µl of T4 DNA ligase was added after the GoldenGate reaction and an additional ligation step was performed at 37 °C for 1 h.

Final 35S::RS-EGFP and RS-(YFP)-TurboID<sub>NLS</sub> constructs were transformed into *Agrobacterium tumefaciens* strain C58C1 and used for transforming *A. thaliana* Col-0 wild-type or *rs40 rs41<sub>c</sub>* mutant plants via floral dipping (Clough & Bent, 1998).

Detailed information about oligonucleotides and generated LII constructs can be found in Supplemental Table 1 and 2, respectively.

### Fluorescence microscopy

Tissue specific localization of RS fusion proteins was analysed in 6-d-old seedlings that were either grown in constant darkness or under continuous red light (8 µmol\*m<sup>-2</sup>\*s<sup>-1</sup>), by using the fluorescence stereomicroscope Leica MS05 FCA; excitation at 470 nm.

Subcellular localization of RS fusion proteins was analysed by confocal microscopy using Leica SP8. EGFP-fusion proteins were excited at 488 nm (settings for emission: 495 – 573 nm) and YFP-fusion proteins at 514 nm (settings for emission: 520 – 579 nm).

Image processing was done using the Leica Application Suite X (LasX) software.

### Biotin assay in Arabidopsis seedlings

Arabidopsis seeds were surfaced sterilized using 3.75% NaClO and 0.01% Triton X-100 and transferred into liquid ½ strength Murashige and Skoog (MS) medium (Duchefa, Haarlem, Netherlands), pH 5.7 – 5.8. After stratification (2 d at 4 °C), germination was induced by a 2 h light treatment (~100 µmol\*m<sup>-2</sup>\*s<sup>-1</sup>), followed by 6 d of growth in darkness. Biotin treatment was performed in dark, by adding 50 µM biotin (B4639, Sigma-Aldrich, St. Louis, MO, US) to the MS media. After 30 min of incubation, plates were either kept in darkness or transferred to white light for further 30 and 90 min, respectively. Subsequently, plant material was dried on the surface using a paper towel and flash frozen.

**Protein extraction and immunoblot analyses**

Protein extraction was performed using a urea buffer [50 mM Tris-HCl pH 7.5, 200 mM NaCl, 4 M Urea, 0.1% Triton X-100, 5 mM DTT, Complete Protease Inhibitor Mixture (Roche)]. Plant debris was collected at 10.000 g for 10 min, 4 °C and proteins were denatured at 95 °C for 5 min. Subsequently, 7.5 µg total protein per sample was loaded onto a 10% SDS-PAGE and finally, transferred onto Nitrocellulose membrane, using wet transfer. Immunoblotting was performed using Streptavidin-horseradish peroxidase conjugate (S911, Thermo Fisher Scientific, Waltham, MA, US) and  $\alpha$ -myc (9E1, 9e1-100, ChromoTek, Planegg-Martinsried, Germany). Tubulin (AS10 680, Agrisera, Vännäs, Sweden) served as loading control. Chemiluminescence was imaged using the Fusion Fx system (Vilber, Collégien, France).

**Conflict of interests**

The authors declare that they have no conflict of interest.

**Author contributions**

J.S. and A.W. designed the research. J.S. generated 35S::RS-EGFP constructs and performed fluorescence microscopy studies. M.P.D. and L.S.S. generated TurbolD constructs and performed establishment experiments in *N. benthamiana* under supervision of J.S. Furthermore, M.P.D. performed the first PL experiment in Arabidopsis. J.S. wrote the manuscript with contributions from A.W.

**Acknowledgments**

We thank Claudia Oecking and Thomas Lahaye for sharing GoldenGate modules with us. Moreover, we are grateful to Claudia Oecking for her support and helpful comments regarding the TurbolD construct generation. This work was supported by the German Research Foundation (Deutsche Forschungsgemeinschaft – DFG: SFB1101/C03).

## References

- Alban, C., Job, D., & Douce, R. (2000). Biotin metabolism in plants. *ANNUAL REVIEW of PLANT PHYSIOLOGY and PLANT MOLECULAR BIOLOGY*, 51, 17–47.
- Ali, G. S., Golovkin, M., & Reddy, A. S. N. (2003). Nuclear localization and in vivo dynamics of a plant-specific serine/arginine-rich protein. *The Plant Journal : For Cell and Molecular Biology*, 36(6), 883–893. <https://doi.org/10.1046/j.1365-313x.2003.01932.x>
- Ali, G. S., & Reddy, A. S. N. (2006). ATP, phosphorylation and transcription regulate the mobility of plant splicing factors. *JOURNAL of CELL SCIENCE*, 119(17), 3527–3538. <https://doi.org/10.1242/jcs.03144>
- Barta, A, Kalyna, M., & Reddy, A. S. N. (2010). Implementing a rational and consistent nomenclature for serine/arginine-rich protein splicing factors (SR proteins) in plants. *The Plant Cell*, 22(9), 2926–2929. <https://doi.org/10.1105/tpc.110.078352>
- Bergeron-Sandoval, L.-P., Safaee, N., & Michnick, S. W. (2016). Mechanisms and Consequences of Macromolecular Phase Separation. *Cell*, 165(5), 1067–1079. <https://doi.org/10.1016/j.cell.2016.05.026>
- Binder, A., Lambert, J., Morbitzer, R., Popp, C., Ott, T., Lahaye, T., & Parniske, M. (2014). A modular plasmid assembly kit for multigene expression, gene silencing and silencing rescue in plants. *PloS One*, 9(2), e88218. <https://doi.org/10.1371/journal.pone.0088218>
- Boeynaems, S., Alberti, S., Fawzi, N. L., Mittag, T., Polymenidou, M., Rousseau, F., Schymkowitz, J., Shorter, J., Wolozin, B., van den Bosch, L., Tompa, P., & Fuxreiter, M. (2018). Protein Phase Separation: A New Phase in Cell Biology. *TRENDS in CELL BIOLOGY*, 28(6), 420–435. <https://doi.org/10.1016/j.tcb.2018.02.004>
- Chen, T., Cui, P., Chen, H., Ali, S., Zhang, S., & Xiong, L. (2013). A KH-Domain RNA-Binding Protein Interacts with FIERY2/CTD Phosphatase-Like 1 and Splicing Factors and Is Important for Pre-mRNA Splicing in Arabidopsis. *PLoS Genetics*, 9(10). <https://doi.org/10.1371/journal.pgen.1003875>

- Chen, T., Cui, P., & Xiong, L. (2015). The RNA-binding protein HOS5 and serine/arginine-rich proteins RS40 and RS41 participate in miRNA biogenesis in *Arabidopsis*. *Nucleic Acids Research*, *43*(17), 8283–8298. <https://doi.org/10.1093/nar/gkv751>
- Clough, S. J., & Bent, A. F. (1998). Floral dip: A simplified method for *Agrobacterium*-mediated transformation of *Arabidopsis thaliana*. *The Plant Journal : For Cell and Molecular Biology*, *16*(6), 735–743. <https://doi.org/10.1046/j.1365-313x.1998.00343.x>
- Docquier, S., Tillemans, V., Deltour, R., & Motte, P. (2004). Nuclear bodies and compartmentalization of pre-mRNA splicing factors in higher plants. *Chromosoma*, *112*(5), 255–266. <https://doi.org/10.1007/s00412-003-0271-3>
- Fang, Y. D., Hearn, S., & Spector, D. L. (2004). Tissue-specific expression and dynamic organization of SR splicing factors in *Arabidopsis*. *Molecular Biology of the Cell*, *15*(6), 2664–2673. <https://doi.org/10.1091/mbc.E04-02-0100>
- Gueroussov, S., Weatheritt, R. J., O'Hanlon, D., Lin, Z.-Y., Narula, A., Gingras, A.-C., & Blencowe, B. J. (2017). Regulatory Expansion in Mammals of Multivalent hnRNP Assemblies that Globally Control Alternative Splicing. *Cell*, *170*(2), 324–+. <https://doi.org/10.1016/j.cell.2017.06.037>
- Haynes, C., & Iakoucheva, L. M. (2006). Serine/arginine-rich splicing factors belong to a class of intrinsically disordered proteins. *Nucleic Acids Research*, *34*(1), 305–312. <https://doi.org/10.1093/nar/gkj424>
- Li, W., Hu, J., Shi, B., Palomba, F., Digman, M. A., Gratton, E., & Jiang, H. (2020). Biophysical properties of AKAP95 protein condensates regulate splicing and tumorigenesis. *NATURE CELL BIOLOGY*, *22*(8), 960–+. <https://doi.org/10.1038/s41556-020-0550-8>
- Liao, S. E., & Regev, O. (2021). Splicing at the phase-separated nuclear speckle interface: a model. *Nucleic Acids Research*, *49*(2). <https://doi.org/10.1093/nar/gkaa1209>
- Lorković, Z. J., Hilscher, J., & Barta, A. (2004). Use of fluorescent protein tags to study nuclear organization of the spliceosomal machinery in transiently transformed

- living plant cells. *Molecular Biology of the Cell*, 15(7), 3233–3243. <https://doi.org/10.1091/mbc.e04-01-0055>
- Mair, A., & Bergmann, D. C. (2022). Advances in enzyme-mediated proximity labeling and its potential for plant research. *Plant Physiology*, 188(2), 756–768. <https://doi.org/10.1093/plphys/kiab479>
- Mair, A., Xu, S.-L., Branon, T. C., Ting, A. Y., & Bergmann, D. C. (2019). Proximity labeling of protein complexes and cell-type-specific organellar proteomes in Arabidopsis enabled by TurboID. *ELife*, 8. <https://doi.org/10.7554/eLife.47864>
- Misteli, T. (2000). Cell biology of transcription and pre-mRNA splicing: nuclear architecture meets nuclear function. *JOURNAL of CELL SCIENCE*, 113(11), 1841–1849.
- Piovesan, D., Necci, M., Escobedo, N., Monzon, A. M., Hatos, A., Micetic, I., Quaglia, F., Paladin, L., Ramasamy, P., Dosztanyi, Z., Vranken, W. F., Davey, N. E., Parisi, G., Fuxreiter, M., & Tosatto, S. C. E. (2021). MobiDB: intrinsically disordered proteins in 2021. *Nucleic Acids Research*, 49(D1), D361-D367. <https://doi.org/10.1093/nar/gkaa1058>
- Potashkin, J. A., Derby, R. J., & Spector, D. L. (1990). Differential distribution of factors involved in pre-mRNA processing in the yeast cell nucleus. *Molecular and Cellular Biology*, 10(7), 3524–3534. <https://doi.org/10.1128/mcb.10.7.3524-3534.1990>
- Reddy, A. S. N. (2004). Plant serine/arginine-rich proteins and their role in pre-mRNA splicing. *Trends in Plant Science*, 9(11), 541–547. <https://doi.org/10.1016/j.tplants.2004.09.007>
- Reddy, A. S. N., Day, I. S., Goehring, J., & Barta, A. (2012). Localization and Dynamics of Nuclear Speckles in Plants. *Plant Physiology*, 158(1), 67–77. <https://doi.org/10.1104/pp.111.186700>
- Spector, D. L., & Lamond, A. I. (2011). Nuclear Speckles. *COLD SPRING HARBOR PERSPECTIVES in BIOLOGY*, 3(2). <https://doi.org/10.1101/cshperspect.a000646>
- Stauffer, E., Westermann, A., Wagner, G., & Wachter, A. (2010). Polypyrimidine tract-binding protein homologues from Arabidopsis underlie regulatory circuits based

- on alternative splicing and downstream control. *The Plant Journal : For Cell and Molecular Biology*, 64(2), 243–255. <https://doi.org/10.1111/j.1365-313X.2010.04321.x>
- Tillemans, V., Dispa, L., Remacle, C., Collinge, M., & Motte, P. (2005). Functional distribution and dynamics of Arabidopsis SR splicing factors in living plant cells. *The Plant Journal : For Cell and Molecular Biology*, 41(4), 567–582. <https://doi.org/10.1111/j.1365-313X.2004.02321.x>
- Tillemans, V., Leponce, I., Rausin, G., Dispa, L., & Motte, P. (2006). Insights into nuclear organization in plants as revealed by the dynamic distribution of Arabidopsis SR splicing factors. *The Plant Cell*, 18(11), 3218–3234. <https://doi.org/10.1105/tpc.106.044529>
- Will, C. L., & Lührmann, R. (2011). Spliceosome structure and function. *COLD SPRING HARBOR PERSPECTIVES in BIOLOGY*, 3(7). <https://doi.org/10.1101/cshperspect.a003707>
- Xu, F., Wang, L., Li, Y., Shi, J., Staiger, D., Chen, W., Wang, L., & Yu, F. (2022). *The Receptor Kinase FER Mediates Phase Separation of Glycine-Rich RNA-Binding Protein 7 to Confer Temperature Resilience in Arabidopsis*. <https://doi.org/10.1101/2022.03.06.483201>
- Xu, X., Zheng, C., Lu, D., Song, C.-P., & Zhang, L. (2021). Phase separation in plants: New insights into cellular compartmentalization. *JOURNAL of INTEGRATIVE PLANT BIOLOGY*, 63(11), 1835–1855. <https://doi.org/10.1111/jipb.13152>
- Yan, Q., Xia, X., Sun, Z., & Fang, Y. (2017). Depletion of Arabidopsis SC35 and SC35-like serine/arginine-rich proteins affects the transcription and splicing of a subset of genes. *PLoS Genetics*, 13(3), e1006663. <https://doi.org/10.1371/journal.pgen.1006663>
- Zhai, Y., Peng, H., Neff, M. M., & Pappu, H. R. (2019). Putative Auxin and Light Responsive Promoter Elements From the Tomato spotted wilt tospovirus Genome, When Expressed as cDNA, Are Functional in Arabidopsis. *FRONTIERS in PLANT SCIENCE*, 10. <https://doi.org/10.3389/fpls.2019.00804>

Zhang, X.-N., & Mount, S. M. (2009). Two alternatively spliced isoforms of the Arabidopsis SR45 protein have distinct roles during normal plant development. *Plant Physiology*, 150(3), 1450–1458. <https://doi.org/10.1104/pp.109.138180>

### **Theses**

Schütz, Laura Sophie (2021): Establishment of proximity labeling to identify RS protein interaction partners *in planta*. Bachelor thesis.

Denecke, Moritz Paul (2021): Proximity labelling for the identification of RS protein interactors *in planta*. Master thesis.

## Main figures

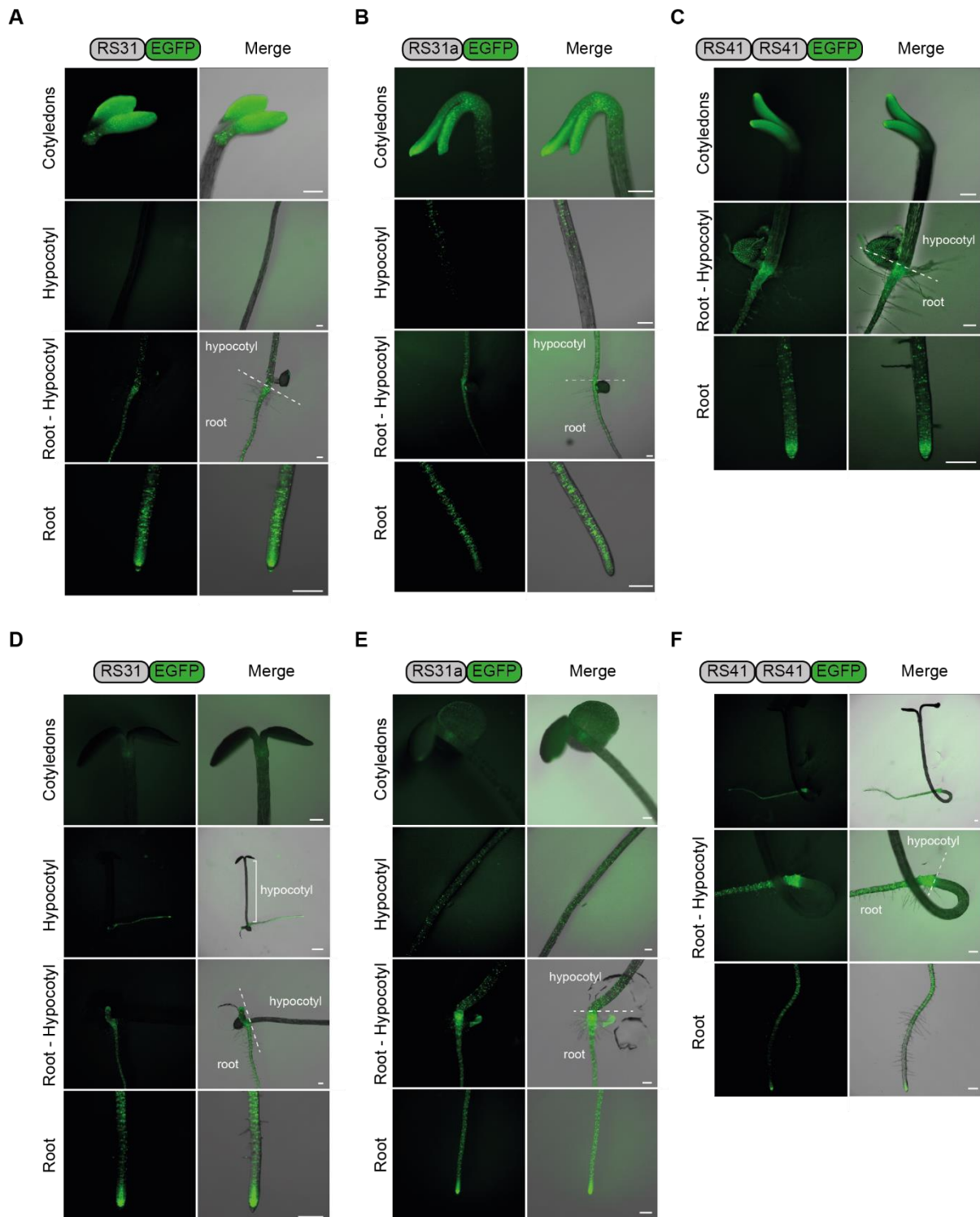


**Figure 1: Organ-specific localization of RS proteins.** Arabidopsis seedlings were grown in darkness (**A to C**) and continuous red light ( $8 \mu\text{mol}\cdot\text{m}^{-2}\cdot\text{s}^{-1}$ ) (**D to F**) for 6 d. The expression of RS fusion proteins was driven by the 35S promoter. Images were taken with Thunder fluorescence stereomicroscope. Scale bar: 200  $\mu\text{m}$ , except for hypocotyl picture in (D), representing 1 mm.



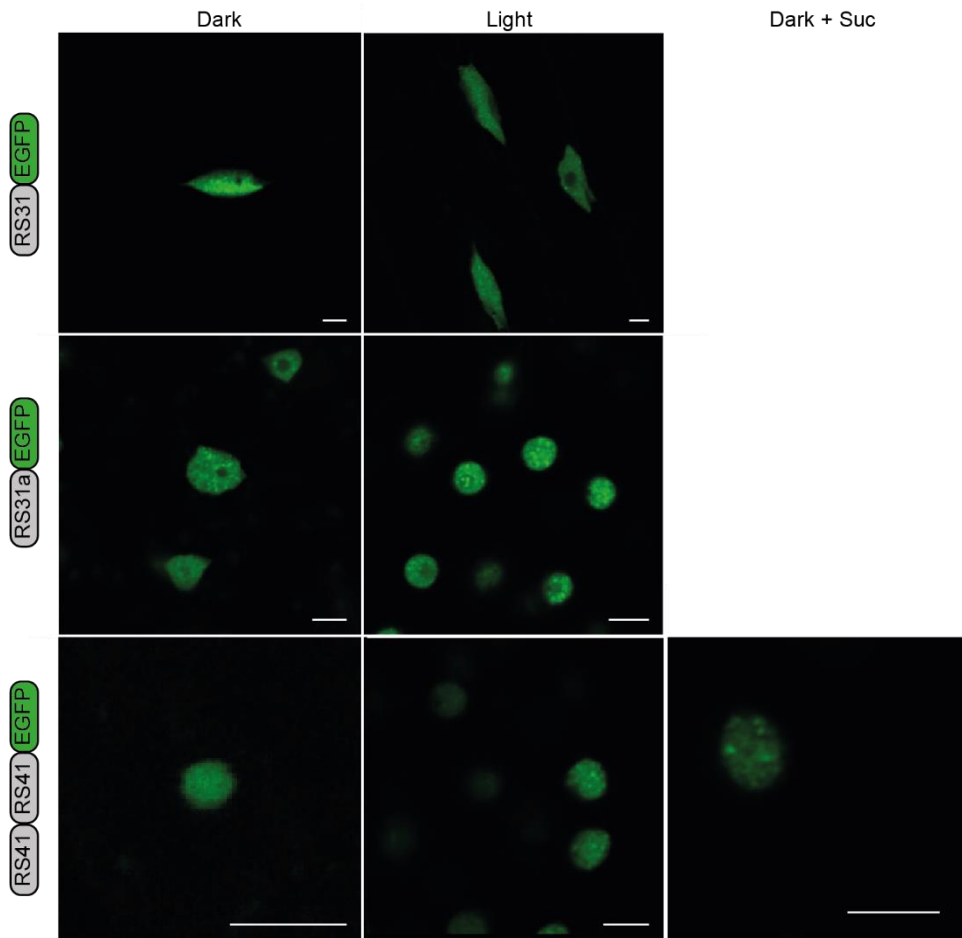


**Figure 2: RS proteins localize in nuclear speckles.** Seedlings were grown in darkness (**left**), under long day conditions with white light at  $\sim 100 \mu\text{mol} \cdot \text{m}^{-2} \cdot \text{s}^{-1}$  (**middle**) or in the presence of 2% sucrose (suc) and darkness (**right**) for 6 d. Expression was driven by the 35S promoter. Images were taken from the elongation zone (for RS31) and tip (for RS31a and RS41) of Arabidopsis roots. Scale bar: 5  $\mu\text{m}$ .

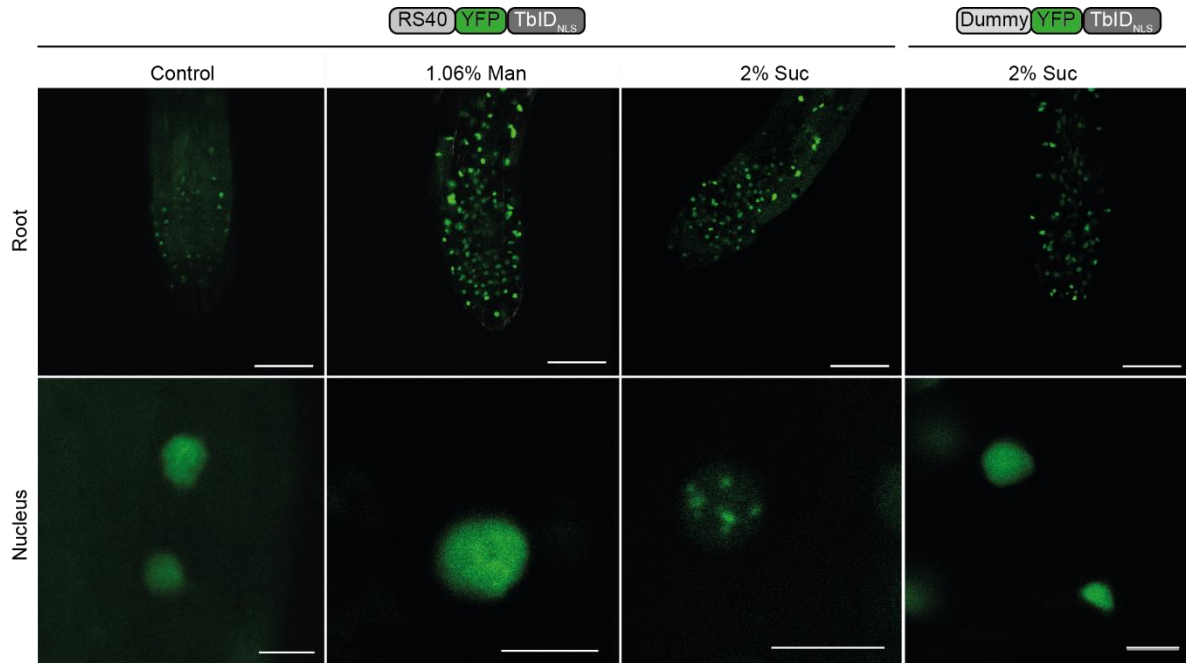


**Figure 3: Sucrose induces RS40-YFP-TbID<sub>NLS</sub> re-localization into nuclear speckles.** Subcellular localization of YFP-TbID<sub>NLS</sub> fusion proteins in nuclei from roots of 6-d-old etiolated *Arabidopsis rs40 rs41<sub>c</sub>* seedlings that were either treated with 1.06% mannitol (Man) or 2% sucrose (Suc) for 2-3 h. Seedlings without further treatment served as control. Expression was driven by the UBI10 promoter. Scale bar in root images: 50 μm, in nucleus pictures: 5 μm.

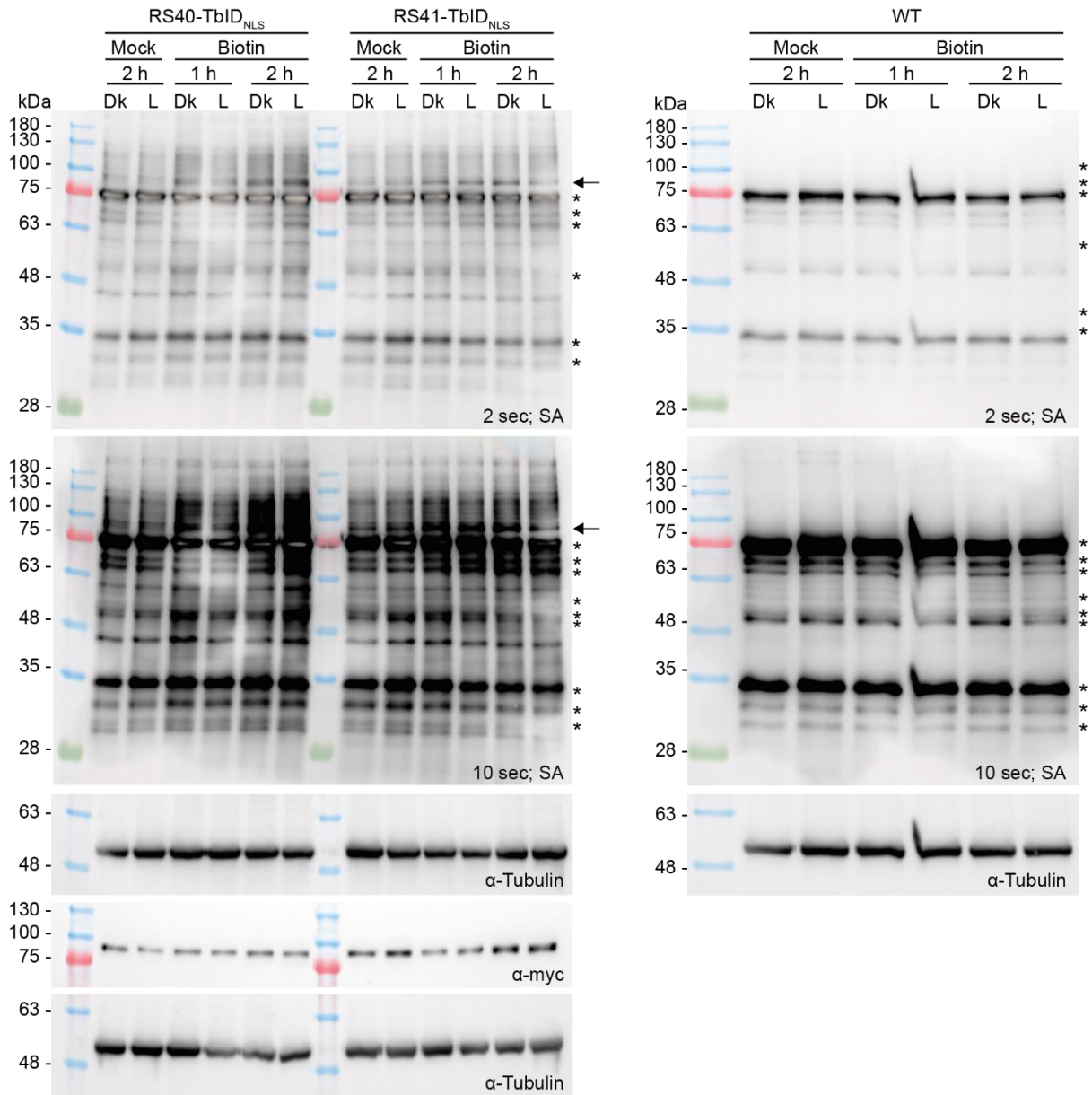


**Figure 4: RS-TbID<sub>NLS</sub> fusion proteins induce biotinylation in Arabidopsis seedlings.** 6-d-old etiolated Arabidopsis seedlings were either kept in darkness or transferred to white light and subjected to a biotin treatment using 50  $\mu$ M biotin for the indicated time points. Corresponding mock treatments served as control. Western blot was performed using Streptavidin-HRP (SA) to detect biotinylated proteins (two different exposure times are shown), and anti-myc for the detection of TbID-fusion proteins. Tubulin served as loading control. Arrows mark the self-labeling of the TbID-fusion proteins and asterisks indicate naturally biotinylated proteins.

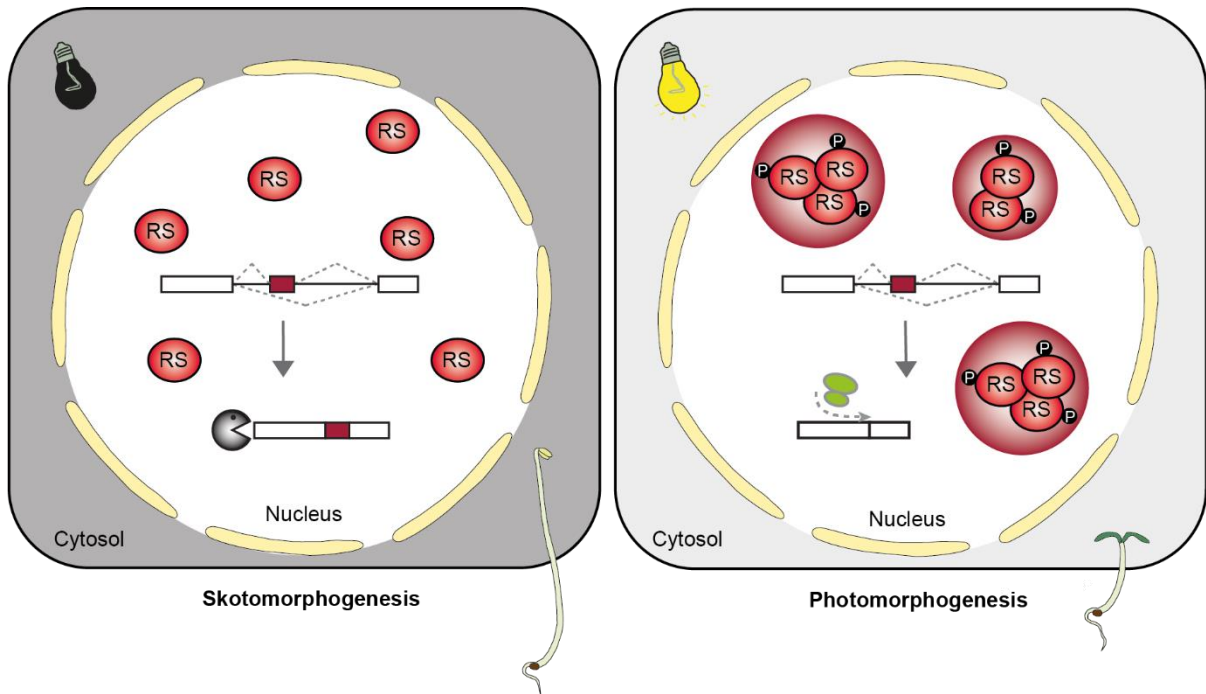


**Figure 5: Proposed model on RS phase separation.** Under dark conditions, RS proteins are mainly distributed within the nucleoplasm where they contribute to the AS decision. In response to light, RS proteins get rapidly phosphorylated, thus triggering RS re-localization into nuclear speckles. Phosphorylated RS proteins are altered in their activity which affects the AS response.

## Supplemental information

### **Subcellular and organ localization of RS proteins is controlled in a light-dependent manner in Arabidopsis seedlings**

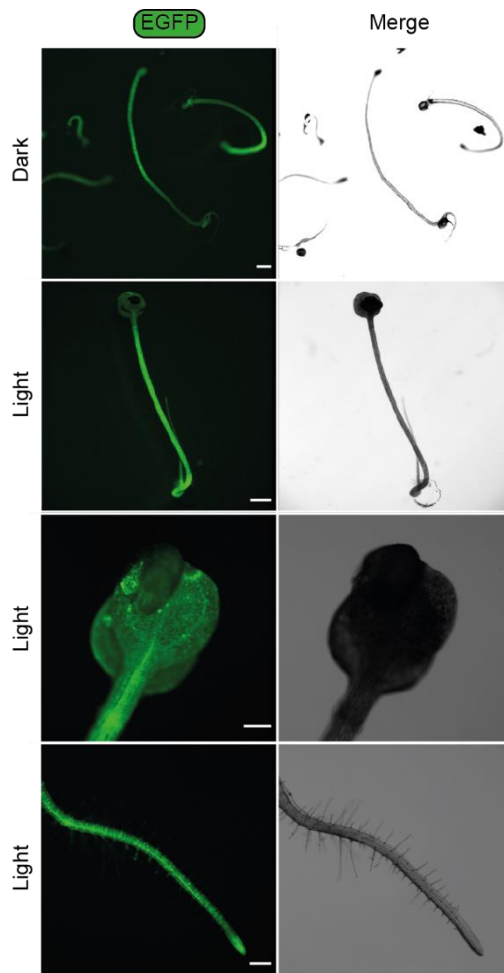
Jennifer Saile<sup>1,2</sup>, Moritz Paul Denecke<sup>1</sup>, Laura Sophie Schütz<sup>1</sup>, and Andreas Wachter<sup>1,2,\*</sup>

<sup>1</sup>Institute for Molecular Physiology (imP), University of Mainz, Hanns-Dieter-Hüschen-Weg 17, 55128 Mainz, Germany

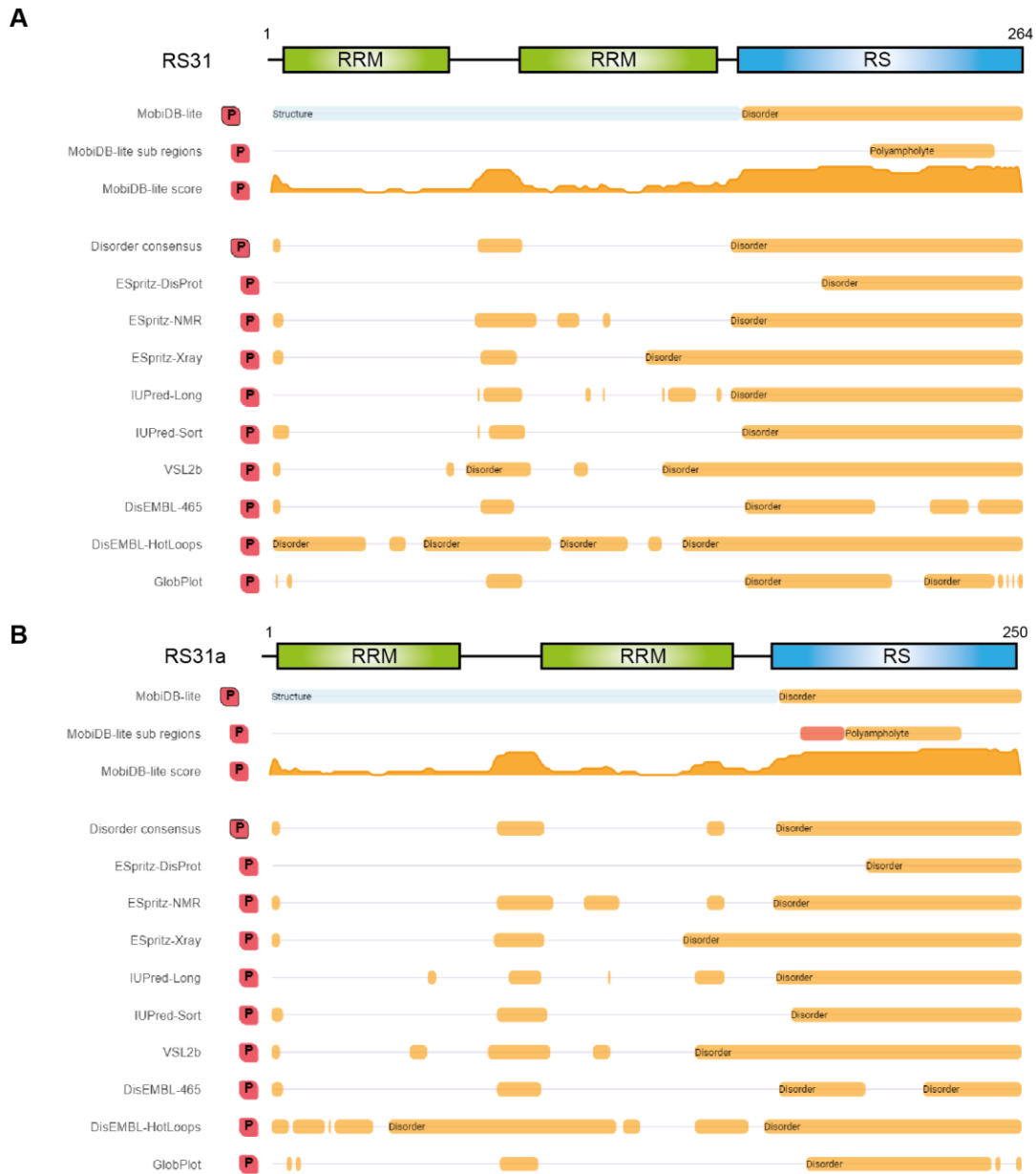
<sup>2</sup>Center for Plant Molecular Biology (ZMBP), University of Tübingen, Auf der Morgenstelle 32, 72076 Tübingen, Germany

\*Corresponding author: [wachter@uni-mainz.de](mailto:wachter@uni-mainz.de)

## SUPPLEMENTAL FIGURES



**Supplemental Figure 1: EGFP expression in Arabidopsis seedlings of a reporter control line.** Arabidopsis seedlings were grown in darkness (first row) and continuous red light ( $8 \mu\text{mol}\cdot\text{m}^{-2}\cdot\text{s}^{-1}$ ) (other panels) for 6 d. The expression of EGFP was driven by the 35S promoter. Images were taken with Thunder fluorescence stereomicroscope. Scale bar in whole seedling images: 1mm, in cotyledon and root image: 200  $\mu\text{m}$ .



**Supplemental Figure 2: Domain structure and predicted intrinsically disordered regions (IDRs) in RS31 and RS31a.** RS proteins contain two N-terminal RNA recognition motifs (RRMs) and a C-terminal arginine/serine (RS)-rich domain. MobiDB database was used for IDR predictions (URL: <https://mobidb.org/>).



**Supplemental Figure 3: Domain structure and predicted intrinsically disordered regions (IDRs) in RS40 and RS41.** RS proteins contain two N-terminal RNA recognition motifs (RRMs) and a C-terminal arginine/serine (RS)-rich domain. MobiDB database was used for IDR predictions (URL: <https://mobidb.org/>).



## SUPPLEMENTAL TABLES

Supplemental Table 1: Oligonucleotides used for construct cloning.

Gene	Primer ID	F		Sequence	Details
		/	R		
RS31	JS14	F		<i>gatc</i> <u>GGATCC</u> atgaggccagtgttcgt	<u>BamHI</u>
	ES233	R		ATGCGGATCCAGGTCTTCCTCTTGGGA	
RS31a	JS15	F		<i>gatc</i> <u>GGATCC</u> ATGAGACATGTGTACGTTGGG	<u>BamHI</u>
	AWTU375	R		ATGCGGATCCACCTCTTGCTCTTTGAATCGG	
RS41	JS17	F		<i>gatc</i> <u>GGATCC</u> ATGAAGCCTGTCTTTTGC	<u>BamHI</u>
	ES249	R		ATGCGGATCCCTTCCTCTGCTGGCGG	
RS40 (LI)	JS188	F		<i>gatc</i> <u>GGTCTC</u> <b>CACACC</b> ATGAAGCCAGTCTTCTGTGG	<u>Bsal</u> , C- <b>OH*</b>
	JS189	R		<i>gatc</i> <u>GGTCTC</u> <b>CACCTT</b> CTCGTCAGCTGGTGGCGA	<u>Bsal</u> , D- <b>OH</b>
RS41 (LI)	JS190	F		<i>gatc</i> <u>GGTCTC</u> <b>CACACC</b> ATGAAGCCTGTCTTTTGC	<u>Bsal</u> , C- <b>OH</b>
	JS191	R		<i>gatc</i> <u>GGTCTC</u> <b>CACCTT</b> TTCTCTGCTGGCGGCGA	<u>Bsal</u> , D- <b>OH</b>
YFP-Turbo ID <sub>NLS</sub> (LI)	JS192	F		<i>gatc</i> <u>GGTCTC</u> <b>AAAGG</b> GAATGGTGAGCAAGGGCGA	<u>Bsal</u> , D <b>OH</b>
	JS193	R		<b>gatc</b> <u>GGTCTC</u> <b>CAGATT</b> CTAGCCTCTTGACGTTTGCGTCC ACCCAATTCTCCATCGTGACGGTCACGCGGACGCTTTG GCCCTTTTCGGCAGACCGCAGA	<u>Bsal</u> , E- <b>OH</b> , NLS
Turbo ID <sub>NLS</sub> (LI)	JS195	F		<i>gatc</i> <u>GGTCTC</u> <b>AAAGG</b> GAAAAGACAATACTGTGCCTCTG	<u>Bsal</u> , D- <b>OH</b>
	JS193	R		<i>gatc</i> <u>GGTCTC</u> <b>CAGATT</b> CTAGCCTCTTGACGTTTGCGTCC ACCCAATTCTCCATCGTGACGGTCACGCGGACGCTTTG GCCCTTTTCGGCAGACCGCAGA	<u>Bsal</u> , E- <b>OH</b> NLS

\*OH: overhang

**Supplemental Table 2:** GoldenGate final constructs.

Name	Lab ID (#)	Type	Reference
<b>BB10_LS01</b>	<b>1750</b>		
G007	1654	LI-B pUbi	Binder et al. 2014
G069	1656	LI B-C c-MYC	Binder et al. 2014
pGEM-T_RS40	1740	RS40 cds	Generated in this study
pJET_YFP-TurboID <sub>NLS</sub>	1743	YFP-TurboID <sub>NLS</sub>	Generated in this study
G006	1657	LI E-F nos-T	Binder et al. 2014
G095	1658	LI F-G Hygro	Binder et al. 2014
BB10	1661	BB10	Binder et al. 2014
<b>BB10_LS02</b>	<b>1751</b>		
G007	1654	LI-B pUbi	Binder et al. 2014
G069	1656	LI B-C c-MYC	Binder et al. 2014
pGEM-T_RS40	1740	RS40 cds	Generated in this study
pJET_TurboID <sub>NLS</sub>	1742	TurboID <sub>NLS</sub>	Generated in this study
G006	1657	LI E-F nos-T	Binder et al. 2014
G095	1658	LI F-G Hygro	Binder et al. 2014
BB10	1661	BB10	Binder et al. 2014
<b>BB10_LS03</b>	<b>1752</b>		
G007	1654	LI-B pUbi	Binder et al. 2014
G069	1656	LI B-C c-MYC	Binder et al. 2014
pGEM-T_RS41	1741	RS41 cds	Generated in this study
pJET_YFP-TurboID <sub>NLS</sub>	1743	YFP-TurboID <sub>NLS</sub>	Generated in this study
G006	1657	LI E-F nos-T	Binder et al. 2014
G095	1658	LI F-G Hygro	Binder et al. 2014
BB10	1661	BB10	Binder et al. 2014

<b>BB10_LS04</b>	<b>1753</b>		
G007	1654	LI-B pUbi	Binder et al. 2014
G069	1656	LI B-C c-MYC	Binder et al. 2014
pGEM-T_RS41	1741	RS41 cds	Generated in this study
pJET_TurboID <sub>NLS</sub>	1742	TurboID <sub>NLS</sub>	Generated in this study
G006	1657	LI E-F nos-T	Binder et al. 2014
G095	1658	LI F-G Hygro	Binder et al. 2014
BB10	1661	BB10	Binder et al. 2014
<b>BB10_LS05</b>	<b>1754</b>		
G007	1654	LI-B pUbi	Binder et al. 2014
G069	1656	LI B-C c-MYC	Binder et al. 2014
B007	1660	LI C-D dy	Binder et al. 2014
pJET_YFP-TurboID <sub>NLS</sub>	1743	YFP-TurboID <sub>NLS</sub>	Generated in this study
G006	1657	LI E-F nos-T	Binder et al. 2014
G095	1658	LI F-G Hygro	Binder et al. 2014
BB10	1661	BB10	Binder et al. 2014
<b>BB10_LS06</b>	<b>1755</b>		
G007	1654	LI-B pUbi	Binder et al. 2014
G069	1656	LI B-C c-MYC	Binder et al. 2014
B007	1660	LI C-D dy	Binder et al. 2014
pJET_TurboID <sub>NLS</sub>	1742	TurboID <sub>NLS</sub>	Generated in this study
G006	1657	LI E-F nos-T	Binder et al. 2014
G095	1658	LI F-G Hygro	Binder et al. 2014
BB10	1661	BB10	Binder et al. 2014

## Chapter V: Conclusion and perspectives



Alternative pre-mRNA splicing (AS) is a crucial mechanism for regulating gene expression in higher eukaryotes. AS uses alternative splice sites to generate more than one mRNA isoform from a single gene, thus contributing to transcriptome and proteome complexity (Chaudhary et al., 2019). Previous transcriptome-wide studies revealed that more than 95% of human genes (Pan et al., 2008) and at least 60% of genes in *Arabidopsis* (Marquez et al., 2015) undergo AS. Remarkably, AS was linked to developmental processes in humans (Baralle & Giudice, 2017) but also plays a crucial role in plant growth and development in response to changing environmental conditions (Staiger & Brown, 2013; Szakonyi & Duque, 2018). Light is an important environmental cue that induces switching from skoto- to photomorphogenesis which is accompanied by organ-specific developmental changes (Gommers & Monte, 2018). In recent years, genome-wide RNA-seq studies demonstrated that light affects AS in etiolated *Arabidopsis* seedlings (Hartmann et al., 2016; Shikata et al., 2014) and light-grown *Arabidopsis* plants (Mancini et al., 2016). Several reports suggested photoreceptors as major players in light-mediated AS regulation (Shikata et al., 2014; Wu et al., 2014), whereas others reported also the existence of a photoreceptor-independent pathway (Hartmann et al., 2016; Mancini et al., 2016; Petrillo et al., 2014). Our group has previously shown that sucrose treatment induces similar AS changes as observed upon illumination and further, that the inhibition of kinase signaling similarly alters the splicing response (Hartmann et al., 2016). Hence, we propose that metabolic and kinase signaling play a major role in changing AS patterns in young *Arabidopsis* seedlings, by affecting the activity and subcellular localization of splicing regulators. To shed more light on upstream regulators controlling AS decisions in response to light, the current work aimed at identifying novel factors participating in the light-dependent AS control.

### **SnRK1, TOR and RS proteins control pre-mRNA splicing of light-regulated AS events to promote photomorphogenesis**

As the SNF1-RELATED KINASE1 (SnRK1) and TARGET OF RAPAMYCIN (TOR) are the major kinases that function as energy sensors, we tested the contribution of SnRK1 and TOR in the AS control. Using inducible ami-RNAs we found that SnRK1 and TOR regulate AS of light-mediated AS events in a similar manner to control skoto- and photomorphogenic development. However, the underlying mechanism of how SnRK1 and TOR signaling affects the AS regulation remains elusive. Based on a

phosphoproteomic study, showing that TOR affects the phosphorylation state of several RNA binding proteins (Scarpin et al., 2020), we propose that TOR and SnRK1 can directly phosphorylate splicing regulators to mediate AS in response to altered metabolic signaling. Hence, phosphoproteome data of wildtype (WT) and kinase mutants might help at identifying splicing regulators that are targets of SnRK1 and TOR, respectively.

Our preliminary phosphoproteomic study in etiolated WT seedlings revealed a rapid and specific phosphorylation of RS40 and RS41 in response to light and sugar, thus making the RS subfamily to a prime candidate in regulating light-mediated AS. Generating higher order *rs* mutants revealed that RS proteins can regulate light-controlled AS events in darkness, whereas AS pattern were comparable to WT in response to white light. As *rs* mutants display altered photomorphogenic phenotypes under red light conditions, we propose that RS proteins play a specific role in phyB signaling. Hence, unaffected light-induced AS responses in *rs* mutants might be caused by some kind of compensation under white light conditions. In recent years, several splicing regulators have been identified to control pre-mRNA splicing in a phytochrome-dependent manner during photomorphogenesis. These splicing regulators include SPLICING FACTOR FOR PHYTOCHROME SIGNALING (SFPS), REDUCED RED-LIGHT RESPONSE IN CRY1CRY2 BACKGROUND 1 (RRC1) and SUPPRESSOR-OF-WHITE-APRICOT/SURP RNA-BINDING DOMAIN-CONTAINING PROTEIN1 (SWAP1) that form a tetrameric complex to regulate common and specific AS events in darkness but also in response to red light (Kathare et al., 2022; Xin et al., 2017; Xin et al., 2019). To examine whether RS proteins are part of this complex, proximity labeling (PL) experiments will help to study RS protein interaction networks in light vs. dark. Moreover, transcriptome-wide RNA-seq studies are crucial to analyse gene expression and AS changes in etiolated *rs* mutants that are exposed to light and/or sugar. These experiments will be of utmost importance to identify splicing networks as well as potential targets of RS proteins that can be further validated by commonly used techniques, including individual nucleotide resolution crosslinking and immunoprecipitation (iCLIP)-seq (Meyer et al., 2017) or non-crosslinking methods, like targets of RNA-binding proteins identified by editing (TRIBE) (McMahon et al., 2016). In conclusion, identifying RS interactors, target pre-mRNAs and binding sites will help to increase our insights into the mechanism by which RS proteins regulate light-mediated AS in order to control photomorphogenesis.

**Phase separation might play a major role in RS controlled light-mediated AS**

Preliminary results showed that light and sugar affect the subcellular localization of RS proteins, by inducing a nuclear re-localization from the nucleoplasm into membraneless condensates. As RS proteins are enriched in intrinsically disordered regions (IDRs), which are subjected to heavy phosphorylation, and further contain two RNA recognition motifs (RRMs), we propose that phase separation may be an intrinsic feature of RS proteins, e.g., induced by their phosphorylation, causing speckle formation, and altered interactions with RNAs and proteins. As a consequence, AS patterns are altered which contributes to the fine-tuning of gene expression to adjust early seedling development.

Despite growing evidence of phase separation in the formation of membraneless organelles, there has only been little demonstrations of phase separation-induced splicing changes (Gueroussov et al., 2017; Li et al., 2020; Xu et al., 2022). Interestingly, a recent study proposed a model for pre-mRNA splicing that takes place at the phase-separated interface of nuclear speckles (Liao & Regev, 2021). Whether phase separation plays a role in RS-mediated AS control during early seedling development remains to be determined. To this end, RS proteins were recently expressed in bacteria to study RS phase separation behaviour *in vitro* (Hobe et al., unpublished). RS proteins were linked to the His<sub>6</sub>-maltose binding protein (MBP) via a TEV-cleavable linker, allowing RS purification by immobilized metal affinity chromatography and the release of the MBP by TEV cleavage, respectively. Preliminary experiments revealed an increased turbidity of RS41 after TEV-mediated MBP release, indicating that RS41 phase separates *in vitro* (Hobe et al., unpublished). Future work is required to increase our insights into the mechanism of RS phase separation that might contribute to light-mediated AS and plant development. Therefore, future studies combining *in vitro* and *in vivo* approaches will address the dynamics of RS proteins, as well as the contribution of distinct domains and phosphorylation sites on RS phase separation, that are required for RS speckle localization, splicing activity, and plant development.

## References

- Baralle, F. E., & Giudice, J. (2017). Alternative splicing as a regulator of development and tissue identity. *Nature Reviews. Molecular Cell Biology*, *18*(7), 437–451. <https://doi.org/10.1038/nrm.2017.27>
- Chaudhary, S., Khokhar, W., Jabre, I., Reddy, A. S. N., Byrne, L. J., Wilson, C. M., & Syed, N. H. (2019). Alternative Splicing and Protein Diversity: Plants Versus Animals. *Frontiers in Plant Science*, *10*, 708. <https://doi.org/10.3389/fpls.2019.00708>
- Gommers, C. M. M., & Monte, E. (2018). Seedling Establishment: A Dimmer Switch-Regulated Process between Dark and Light Signaling. *PLANT PHYSIOLOGY*, *176*(2), 1061–1074. <https://doi.org/10.1104/pp.17.01460>
- Gueroussov, S., Weatheritt, R. J., O'Hanlon, D., Lin, Z.-Y., Narula, A., Gingras, A.-C., & Blencowe, B. J. (2017). Regulatory Expansion in Mammals of Multivalent hnRNP Assemblies that Globally Control Alternative Splicing. *Cell*, *170*(2), 324–+. <https://doi.org/10.1016/j.cell.2017.06.037>
- Hartmann, L., Drewe-Boß, P., Wießner, T., Wagner, G., Geue, S., Lee, H.-C., Obermüller, D. M., Kahles, A., Behr, J., Sinz, F. H., Rättsch, G., & Wachter, A. (2016). Alternative Splicing Substantially Diversifies the Transcriptome during Early Photomorphogenesis and Correlates with the Energy Availability in Arabidopsis. *The Plant Cell*, *28*(11), 2715–2734. <https://doi.org/10.1105/tpc.16.00508>
- Kathare, P. K., Xin, R., Ganesan, A. S., June, V. M., Reddy, A. S. N., & Huq, E. (2022). SWAP1-SFPS-RRC1 splicing factor complex modulates pre-mRNA splicing to promote photomorphogenesis in Arabidopsis. *BioRxiv*, 2022.04.26.489584. <https://doi.org/10.1101/2022.04.26.489584>
- Li, W., Hu, J., Shi, B., Palomba, F., Digman, M. A., Gratton, E., & Jiang, H. (2020). Biophysical properties of AKAP95 protein condensates regulate splicing and tumorigenesis. *NATURE CELL BIOLOGY*, *22*(8), 960–+. <https://doi.org/10.1038/s41556-020-0550-8>



- Liao, S. E., & Regev, O. (2021). Splicing at the phase-separated nuclear speckle interface: a model. *Nucleic Acids Research*, 49(2). <https://doi.org/10.1093/nar/gkaa1209>
- Mancini, E., Sanchez, S. E., Romanowski, A., Schlaen, R. G., Sanchez-Lamas, M., Cerdán, P. D., & Yanovsky, M. J. (2016). Acute Effects of Light on Alternative Splicing in Light-Grown Plants. *Photochemistry and Photobiology*, 92(1), 126–133. <https://doi.org/10.1111/php.12550>
- Marquez, Y., Hoepfler, M., Ayatollahi, Z., Barta, A., & Kalyna, M. (2015). Unmasking alternative splicing inside Protein-coding exons defines exitrans and their role in proteome plasticity. *GENOME RESEARCH*, 25(7), 995–1007. <https://doi.org/10.1101/gr.186585.114>
- McMahon, A. C., Rahman, R., Jin, H., Shen, J. L., Fieldsend, A., Luo, W., & Rosbash, M. (2016). TRIBE: Hijacking an RNA-Editing Enzyme to Identify Cell-Specific Targets of RNA-Binding Proteins. *Cell*, 165(3), 742–753. <https://doi.org/10.1016/j.cell.2016.03.007>
- Meyer, K., Koester, T., Nolte, C., Weinholdt, C., Lewinski, M., Grosse, I., & Staiger, D. (2017). Adaptation of iCLIP to plants determines the binding landscape of the clock-regulated RNA-binding protein AtGRP7. *Genome Biology*, 18. <https://doi.org/10.1186/s13059-017-1332-x>
- Pan, Q., Shai, O., Lee, L. J., Frey, J., & Blencowe, B. J. (2008). Deep surveying of alternative splicing complexity in the human transcriptome by high-throughput sequencing. *NATURE GENETICS*, 40(12), 1413–1415. <https://doi.org/10.1038/ng.259>
- Petrillo, E., Godoy Herz, M. A., Fuchs, A., Reifer, D., Fuller, J., Yanovsky, M. J., Simpson, C., Brown, J. W. S., Barta, A., Kalyna, M., & Kornblihtt, A. R. (2014). A chloroplast retrograde signal regulates nuclear alternative splicing. *Science (New York, N.Y.)*, 344(6182), 427–430. <https://doi.org/10.1126/science.1250322>
- Scarpin, M. R., Leiboff, S., & Brunkard, J. O. (2020). Parallel global profiling of plant TOR dynamics reveals a conserved role for LARP1 in translation. *ELife*, 9. <https://doi.org/10.7554/eLife.58795>

- Shikata, H., Hanada, K., Ushijima, T., Nakashima, M., Suzuki, Y., & Matsushita, T. (2014). Phytochrome controls alternative splicing to mediate light responses in *Arabidopsis*. *Proceedings of the National Academy of Sciences of the United States of America*, *111*(52), 18781–18786. <https://doi.org/10.1073/pnas.1407147112>
- Staiger, D., & Brown, J. W. S. (2013). Alternative splicing at the intersection of biological timing, development, and stress responses. *PLANT CELL*, *25*(10), 3640–3656. <https://doi.org/10.1105/tpc.113.113803>
- Szakonyi, D., & Duque, P. (2018). Alternative Splicing as a Regulator of Early Plant Development. *Frontiers in Plant Science*, *9*, 1174. <https://doi.org/10.3389/fpls.2018.01174>
- Wu, H.-P., Su, Y.-S., Chen, H.-C., Chen, Y.-R., Wu, C.-C., Lin, W.-D., & Tu, S.-L. (2014). Genome-wide analysis of light-regulated alternative splicing mediated by photoreceptors in *Physcomitrella patens*. *Genome Biology*, *15*(1), R10. <https://doi.org/10.1186/gb-2014-15-1-r10>
- Xin, R., Kathare, P. K., & Huq, E. (2019). Coordinated Regulation of Pre-mRNA Splicing by the SFPS-RRC1 Complex to Promote Photomorphogenesis. *The Plant Cell*, *31*(9), 2052–2069. <https://doi.org/10.1105/tpc.18.00786>
- Xin, R., Zhu, L., Salomé, P. A., Mancini, E., Marshall, C. M., Harmon, F. G., Yanovsky, M. J., Weigel, D., & Huq, E. (2017). Spf45-related splicing factor for phytochrome signaling promotes photomorphogenesis by regulating pre-mRNA splicing in *Arabidopsis*. *Proceedings of the National Academy of Sciences of the United States of America*, *114*(33), E7018-E7027. <https://doi.org/10.1073/pnas.1706379114>
- Xu, F., Wang, L., Li, Y., Shi, J., Staiger, D., Chen, W., Wang, L., & Yu, F. (2022). The Receptor Kinase FER Mediates Phase Separation of Glycine-Rich RNA-Binding Protein 7 to Confer Temperature Resilience in *Arabidopsis*. <https://doi.org/10.1101/2022.03.06.483201>